ISSN 1007-9327 (print)
ISSN 2219-2840 (online)

World Journal of *Gastroenterology*

World J Gastroenterol 2022 September 28; 28(36): 5240-5382

Published by Baishideng Publishing Group Inc

World Journal of Gastroenterology

Contents

Weekly Volume 28 Number 36 September 28, 2022

EDITORIAL

5240 SARS-CoV-2 and the pancreas: What do we know about acute pancreatitis in COVID-19 positive patients?

Brisinda G, Chiarello MM, Tropeano G, Altieri G, Puccioni C, Fransvea P, Bianchi V

REVIEW

5250 Deciphering the role of transforming growth factor-beta 1 as a diagnostic-prognostic-therapeutic candidate against hepatocellular carcinoma

Devan AR, Pavithran K, Nair B, Murali M, Nath LR

5265 P2X7 receptor as the regulator of T-cell function in intestinal barrier disruption

Jiang ZF, Wu W, Hu HB, Li ZY, Zhong M, Zhang L

5280 Liver-specific drug delivery platforms: Applications for the treatment of alcohol-associated liver disease

Warner JB, Guenthner SC, Hardesty JE, McClain CJ, Warner DR, Kirpich IA

MINIREVIEWS

5300 Histopathological assessment of the microscopic activity in inflammatory bowel diseases: What are we looking for?

Fabian O, Bajer L

ORIGINAL ARTICLE

Basic Study

5313 Esophageal magnetic compression anastomosis in dogs

Xu XH, Lv Y, Liu SQ, Cui XH, Suo RY

Retrospective Cohort Study

5324 Impact of sarcopenia on tumor response and survival outcomes in patients with hepatocellular carcinoma treated by trans-arterial (chemo)-embolization

Roth G, Teyssier Y, Benhamou M, Abousalihac M, Caruso S, Sengel C, Seror O, Ghelfi J, Seigneurin A, Ganne-Carrie N, Gigante E, Blaise L, Sutter O, Decaens T, Nault JC

5338 Machine learning-based gray-level co-occurrence matrix signature for predicting lymph node metastasis in undifferentiated-type early gastric cancer

Wei X, Yan XJ, Guo YY, Zhang J, Wang GR, Fayyaz A, Yu J

Observational Study

5351 Early extrahepatic recurrence as a pivotal factor for survival after hepatocellular carcinoma resection: A 15-year observational study

Yoon JH, Choi SK, Cho SB, Kim HJ, Ko YS, Jun CH

5364 Atherogenic index of plasma combined with waist circumference and body mass index to predict metabolic-associated fatty liver disease

Duan SJ, Ren ZY, Zheng T, Peng HY, Niu ZH, Xia H, Chen JL, Zhou YC, Wang RR, Yao SK

LETTER TO THE EDITOR

5380 Nonalcoholic steatohepatitis and hepatocellular carcinoma: Beyond the boundaries of the liver

Gupta T

ABOUT COVER

AIMS AND SCOPE

The primary aim of *World Journal of Gastroenterology* (*WJG*, *World J Gastroenterol*) is to provide scholars and readers from various fields of gastroenterology and hepatology with a platform to publish high-quality basic and clinical research articles and communicate their research findings online. *WJG* mainly publishes articles reporting research results and findings obtained in the field of gastroenterology and hepatology and covering a wide range of topics including gastroenterology, hepatology, gastrointestinal endoscopy, gastrointestinal surgery, gastrointestinal oncology, and pediatric gastroenterology.

INDEXING/ABSTRACTING

The *WJG* is now abstracted and indexed in Science Citation Index Expanded (SCIE, also known as SciSearch®), Current Contents/Clinical Medicine, Journal Citation Reports, Index Medicus, MEDLINE, PubMed, PubMed Central, Scopus, Reference Citation Analysis, China National Knowledge Infrastructure, China Science and Technology Journal Database, and Superstar Journals Database. The 2022 edition of Journal Citation Reports® cites the 2021 impact factor (IF) for *WJG* as 5.374; IF without journal self cites: 5.187; 5-year IF: 5.715; Journal Citation Indicator: 0.84; Ranking: 31 among 93 journals in gastroenterology and hepatology; and Quartile category: Q2. The *WJG*'s CiteScore for 2021 is 8.1 and Scopus CiteScore rank 2021: Gastroenterology is 18/149.

RESPONSIBLE EDITORS FOR THIS ISSUE

Production Editor: *Yu-Xi Chen*; **Production Department Director:** *Xu Guo*; **Editorial Office Director:** *Jia-Ru Fan*.

NAME OF JOURNAL
World Journal of Gastroenterology

ISSN
ISSN 1007-9327 (print) ISSN 2219-2840 (online)

LAUNCH DATE
October 1, 1995

FREQUENCY
Weekly

EDITORS-IN-CHIEF
Andrzej S Tarnawski

EDITORIAL BOARD MEMBERS
http://www.wjgnet.com/1007-9327/editorialboard.htm

PUBLICATION DATE
September 28, 2022

INSTRUCTIONS TO AUTHORS
https://www.wjgnet.com/bpg/gerinfo/204

GUIDELINES FOR ETHICS DOCUMENTS
https://www.wjgnet.com/bpg/GerInfo/287

GUIDELINES FOR NON-NATIVE SPEAKERS OF ENGLISH
https://www.wjgnet.com/bpg/gerinfo/240

PUBLICATION ETHICS
https://www.wjgnet.com/bpg/GerInfo/288

PUBLICATION MISCONDUCT
https://www.wjgnet.com/bpg/gerinfo/208

ARTICLE PROCESSING CHARGE
https://www.wjgnet.com/bpg/gerinfo/242

STEPS FOR SUBMITTING MANUSCRIPTS
https://www.wjgnet.com/bpg/GerInfo/239

ONLINE SUBMISSION
https://www.f6publishing.com

World Journal of Gastroenterology

Submit a Manuscript: https://www.f6publishing.com

World J Gastroenterol 2022 September 28; 28(36): 5240-5249

DOI: 10.3748/wjg.v28.i36.5240

ISSN 1007-9327 (print) ISSN 2219-2840 (online)

EDITORIAL

SARS-CoV-2 and the pancreas: What do we know about acute pancreatitis in COVID-19 positive patients?

Giuseppe Brisinda, Maria Michela Chiarello, Giuseppe Tropeano, Gaia Altieri, Caterina Puccioni, Pietro Fransvea, Valentina Bianchi

Specialty type: Gastroenterology and hepatology

Provenance and peer review: Unsolicited article; Externally peer reviewed.

Peer-review model: Single blind

Peer-review report's scientific quality classification

Grade A (Excellent): A
Grade B (Very good): B
Grade C (Good): 0
Grade D (Fair): 0
Grade E (Poor): 0

P-Reviewer: Cai J, China; Gonçalves TN, Portugal

Received: May 17, 2022
Peer-review started: May 17, 2022
First decision: June 19, 2022
Revised: June 23, 2022
Accepted: September 8, 2022
Article in press: September 8, 2022
Published online: September 28, 2022

Giuseppe Brisinda, Department of Medical and Surgical Sciences, Fondazione Policlinico Universitario A Gemelli IRCCS, Rome 00168, Italy

Giuseppe Brisinda, Department of Medicine and Surgery, Università Cattolica del Sacro Cuore, Rome 00168, Italy

Maria Michela Chiarello, Department of Surgery, Azienda Sanitaria Provinciale di Cosenza, Cosenza 87100, Italy

Giuseppe Tropeano, Gaia Altieri, Caterina Puccioni, Pietro Fransvea, Valentina Bianchi, Emergency Surgery and Trauma Center, Fondazione Policlinico Universitario A Gemelli IRCCS, Rome 00168, Italy

Corresponding author: Giuseppe Brisinda, MD, Professor, Surgeon, Department of Medical and Surgical Sciences, Fondazione Policlinico Universitario A Gemelli IRCCS, Largo Agostino Gemelli 8, Rome 00168, Italy. gbrisin@tin.it

Abstract

Severe acute respiratory syndrome coronavirus 2 (SARS-CoV-2) can cause pancreatic damage, both directly to the pancreas *via* angiotensin-converting enzyme 2 receptors (the transmembrane proteins required for SARS-CoV-2 entry, which are highly expressed by pancreatic cells) and indirectly through locoregional vasculitis and thrombosis. Despite that, there is no clear evidence that SARS-CoV-2 is an etiological agent of acute pancreatitis. Acute pancreatitis in coronavirus disease 2019 (COVID-19) positive patients often recognizes biliary or alcoholic etiology. The prevalence of acute pancreatitis in COVID-19 positive patients is not exactly known. However, COVID-19 positive patients with acute pancreatitis have a higher mortality and an increased risk of intensive care unit admission and necrosis compared to COVID-19 negative patients. Acute respiratory distress syndrome is the most frequent cause of death in COVID-19 positive patients and concomitant acute pancreatitis. In this article, we reported recent evidence on the correlation between COVID-19 infection and acute pancreatitis.

Key Words: Acute pancreatitis; SARS-CoV-2; Severe acute pancreatitis; Multiparametric scores; Infected necrosis; Step-up approach

Core Tip: The outbreak of severe acute respiratory syndrome coronavirus 2 (SARS-CoV-2), causing a severe acute respiratory syndrome, has rapidly spread from China all over the world, affecting millions of people. Whereas typical presentations of this infection (such as fever, cough, myalgia, fatigue and pneumonia) are well recognized, several studies report a low incidence of gastrointestinal symptoms. The relationship between SARS-CoV-2 infection and acute pancreatitis is controversial. Acute pancreatitis is not specifically caused by SARS-CoV-2. Furthermore, coronavirus disease 2019 positive patients are more likely to develop severe acute pancreatitis and multiple organ failure.

Citation: Brisinda G, Chiarello MM, Tropeano G, Altieri G, Puccioni C, Fransvea P, Bianchi V. SARS-CoV-2 and the pancreas: What do we know about acute pancreatitis in COVID-19 positive patients? *World J Gastroenterol* 2022; 28(36): 5240-5249

URL: https://www.wjgnet.com/1007-9327/full/v28/i36/5240.htm

DOI: https://dx.doi.org/10.3748/wjg.v28.i36.5240

INTRODUCTION

Severe acute respiratory syndrome coronavirus 2 (SARS-CoV-2) secondary to coronavirus disease 2019 (COVID-19) has spread rapidly from China. The disease has affected millions of people[1]. Whereas typical presentations of this infection (such as fever, cough, myalgia, fatigue and pneumonia) are well recognized, few studies reported the incidence of atypical gastrointestinal symptoms[2-5]. COVID-19 is linked to organ damage including lungs, heart and kidneys and can lead to multiple organ failure. Evidence shows that SARS-CoV-2 has a strong tropism for the gastrointestinal tract[6,7]. Moreover, pancreatic injury in COVID-19 has not been common.

Acute pancreatitis is an inflammatory process that originates from the glandular parenchyma, causing damage and/or destruction to the acinar component first and then extending to the surrounding tissues[8-11]. There are several etiological factors contributing to its onset. However, it is possible to ascribe most of the episodes to two main causes, namely gallbladder lithiasis and alcohol abuse. Pharmacological, iatrogenic and viral causes must also be taken into account[12].

The severity of acute pancreatitis does not always correlate with pancreatic structural changes. It is possible to distinguish interstitial pancreatitis when the organ is locally or wholly increased in volume due to the presence of interstitial edema and necrotizing pancreatitis (10%-20% of all cases)[10,13,14]. It is unclear why COVID-19 starts with exclusively gastrointestinal symptoms, albeit in a low percentage of cases. However, acute pancreatic involvement induced by COVID-19 is severe and can develop rapidly. Close monitoring and admission are necessary to offer proper treatment. The following sections of this editorial discuss some of the recent findings and the approaches for a more effective clinical diagnosis and treatment of acute pancreatitis in patients with SARS-CoV-2 infection.

COVID-19 AND THE PANCREAS

Viral RNA has been found in the stools of COVID-19 patients[1,2,15-17]. High replication of the virus has been documented in both the small and large intestines by electron microscopy studies on tissues derived from biopsies and/or autopsy material[7,18,19]. Additionally, fecal-oral transmission has been documented for SARS-CoV-2[20]. Some molecules are receptors for the virus. These determine a specific tropism for different tissues and organs. SARS-CoV-2 uses its surface envelope called the spike glycoprotein. By means of this protein, SARS-CoV-2 interacts and enters host cells. The virus enters the cell *via* the angiotensin-converting enzyme 2 (ACE2) receptor. As such, the spike glycoprotein-ACE2 binding is the determinant for virus entry and propagation and for the transmissibility of COVID-19-related disease. ACE2 is expressed in human pancreatic cells and pancreatic islets and highly represented in pancreas microvasculature pericytes[6,21,22]. As ACE2 is internalized by SARS-CoV-2 binding, an imbalance of the RAS peptides can be established with a rise of angiotensin II and a decrease in angiotensin 1-7. The latter exerts anti-thrombogenic, anti-inflammatory and pro-resolving actions[23]. Laboratory abnormalities, suggesting pancreatic injury, have been noted in 8.0%-17.5% of cases in several studies[24,25], with 7.0% displaying significant pancreatic changes on computed tomography.

The etiopathogenesis of pancreatic injury in SARS-CoV-2 patients is still unclear. Both pancreatic ACE2 expression and drugs taken before the hospitalization might be involved[26]. The inflammation that occurs in the intestine causes the release of cytokines and bacteria. Both cytokines and bacteria can

reach and enter the lung through the bloodstream. At this level, a direct influence on the immune response and inflammation is observed[27-29]. The gut-liver axis is also strongly influenced by damage to the intestinal mucosa and bacterial imbalance[30]. The host and the microbial metabolites present in the intestine are transferred to the liver through the mesenteric-portal circulation; these affect liver function. The liver releases bile acids and bioactive media into the biliary and systemic circulation in order to transport them to the intestine. This could lead to pancreatic function damage in patients and may also explain the abnormality of pancreatic function indicators in COVID-19 patients. It is important not to consider each COVID-19 patient with increased serum amylase level as affected by acute pancreatitis[31]. Elevated levels of pancreatic enzymes may occur during kidney failure or diarrhea in the course of COVID-19[32]. It could be useful to find some criteria that can guide clinical suspicion.

WHAT DO WE KNOW ABOUT ACUTE PANCREATITIS IN COVID-19 POSITIVE PATIENTS?

Available literature is not able to determine whether the tissue damage leading to acute pancreatitis occurs as a result of direct SARS-CoV-2 infection or as a results of systemic multiple organ dysfunction with increased levels of amylase and lipase[33,34]. Only a few COVID-19 positive patients also have acute pancreatitis; the association between the two pathologies is infrequent. Only 10% of COVID-19 positive patients show abdominal symptoms exclusively[35]: Usually, these patients have the most severe forms of COVID-19 infections. Furthermore, it has not been demonstrated that an increased incidence of acute pancreatitis occurred during the COVID-19 pandemic period[36]. SARS-CoV-2 cannot be said to be an etiological agent of acute pancreatitis[33,37]. Acute pancreatitis in COVID-19 positive patients is idiopathic in most cases[37], and there is no sufficient evidence showing that COVID-19 can cause acute pancreatitis or negatively impact its prognosis.

The involvement of the pancreatic gland appears possible, in consideration of the fact that ACE2 receptors are present both on exocrine cells and on pancreatic islets[23]. In addition, the ACE2 receptor is expressed more in the pancreatic tissue than in the lungs. Furthermore, SARS-CoV-2 induces the onset of endotheliitis, which results in ischemic damage and that can also occur in the pancreas[38].

In the COVID PAN study, it was documented that acute pancreatitis is more severe in COVID-19 positive patients than in COVID-19 negative patients. In them, the onset of multiple organ failure can be linked to factors other than acute pancreatitis[39]. A greater severity of acute pancreatitis, an increased risk of necrosis, intensive care unit admission, persistent organ failure and the need for mechanical ventilation were observed in COVID-19 positive patients with acute pancreatitis. In this same study, 30-d overall mortality from acute pancreatitis was statistically higher in COVID-19 positive (14.7%) than in COVID-19 negative patients (2.6%, $P < 0.04$)[39]. Furthermore, necrosectomy was more likely to be performed in SARS-CoV-2 positive patients, occurring in 5% compared with 1.3% in the control group ($P < 0.001$).

The predominant organ dysfunction was respiratory failure in the majority of COVID-19 positive patients. In addition, acute pancreatitis with concomitant SARS-CoV-2 was more likely to have poorer outcomes due to double pulmonary damage[40]. Lung involvement is common in severe acute pancreatitis. This involvement can progress to full blown acute respiratory distress syndrome[40]. At present, it could be difficult to stratify the severity of symptoms and the degree of lung involvement. Acute respiratory distress syndrome due to acute pancreatitis can worsen lung injury related to COVID-19 pneumonia. Moreover, changes in the gastrointestinal flora affect the respiratory tract through the common mucosal immune system, the so-called "gut-lung axis"[27,29]. COVID-19 positive patients with gastrointestinal symptoms are more likely to be complicated with acute respiratory distress and pancreatic damage. In these patients the prognosis is poorer. In COVID-19 positive patients with gastrointestinal symptoms, attention should be paid to the patient's gastrointestinal symptoms in the diagnosis and treatment process. It also appears essential to prevent the transmission of the virus *via* the fecal-oral route. In a retrospective cohort study, Inamdar *et al*[37] concluded that pancreatitis should be included in the list of gastrointestinal manifestations of COVID-19.

There are few studies in the literature that investigate the relationship between COVID-19 infection and acute pancreatitis. In their experience, Inamdar *et al*[37] documented 189 cases of acute pancreatitis in 48012 hospitalized patients (0.39%). Thirty-two (17%) of these 189 patients were COVID-19 positive, with a prevalence of 0.27% of acute pancreatitis among the patients hospitalized for COVID-19. Idiopathic forms were more frequent (69%) in this patient group than in COVID-19 negative patients (21%, $P < 0.0001$). Wang *et al*[41] found that of 52 COVID-19 patients enrolled, 17% had pancreatic injury, defined as an abnormal increase of amylase and lipase serum levels. Stephens *et al*[31] showed that COVID-19 patients had an amylase serum peak not always related with acute pancreatitis. They enrolled 234 patients, 158 of which had a serum amylase level three times greater than the normal upper limit, but only 1.7% of the studied population met the revised criteria of Atlanta for diagnosis of acute pancreatitis[31].

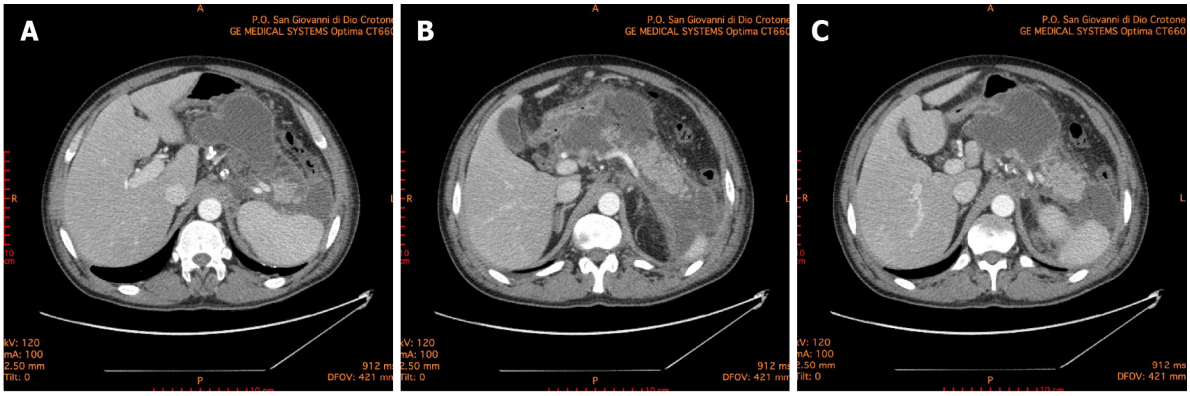

DOI: 10.3748/wjg.v28.i36.5240 **Copyright** ©The Author(s) 2022.

Figure 1 Abdominal computed tomography 10 d after the onset of acute pancreatitis. A: Necrotic collection, with a noticeable wall, dislocating stomach; B: Necrotic collection occupying the majority of pancreatic head and compressing the duodenum; C: Multiple collections of fluid and necrosis involving the cephalad portion of the pancreas, multiple peripancreatic collections around the spleen and the left paracolic gutter.

COVID-19 VACCINE AND PANCREATITIS

Vaccines are considered one of the most important public health achievements of the last century. Many vaccines have side effects. One of these adverse events is the onset of pancreatitis. In these cases, it is believed that acute pancreatitis is secondary to an immunologically induced phenomenon as demonstrated by reports in the literature after the administration of vaccines against the hepatitis virus or other viruses[42-44]. The vaccine BNT162b1 developed by Pfizer-BioNTech is a nucleoside-modified mRNA that encodes the receptor binding domain of the SARS-CoV-2 spike protein. The vaccine RNA is formulated in lipid nanoparticles for an efficient delivery into cells after injections[45].

In the literature there are several cases reporting acute pancreatitis after mRNA-based vaccine[46-50]. Although the vaccine has been proven to be effective and safe, vaccine-induced side effects have been observed. There are nausea, diarrhea, decreased appetite, abdominal pain, vomiting, heartburn and constipation among the most frequently reported gastrointestinal side effects. Most of the cases describe mild acute pancreatitis, however Ozaka *et al*[46] and Walter *et al*[47] reported a single case of necrotizing pancreatitis. According to Pfizer's data, 1 case of pancreatitis and 1 case of obstructive pancreatitis as adverse reactions were observed during the phase II/clinical trial of the COVID-19 mRNA vaccine. The trial included about 38000 participants, indicating that such a link between vaccination and pancreatitis is a very rare adverse event[51]. Between December 9, 2020 and July 21, 2021, information obtained from the United Kingdom database showed 275820 adverse reaction reports, which included 18 cases of mild acute pancreatitis and 1 case of necrotizing pancreatitis[52]. In France, out of a total of 42523573 doses, the Agence Nationale de Securité du Medicament et des Produits de Santé reported 57 cases of acute pancreatitis[53]. VigiBase, the World Health Organization global database of individual case safety reports, included 298 cases of acute pancreatitis and 17 cases of necrotizing pancreatitis[54]. The Agenzia Italiana del Farmaco reported 497 gastrointestinal adverse events equal to 14.1% of the total observations in 1 year. The document does not specify the number of cases of acute pancreatitis[55]. Although it is difficult to make conclusions about the likelihood of the vaccine being the etiologic factor of pancreatitis, it is essential to continue monitoring it for possible under-reported side effects until we have extensive long-term data available in post-marketing surveillance for long-term and rare side effects. Surveillance is also necessary because there are currently no conclusive data on the severity of pancreatitis in the population of subjects vaccinated against COVID-19 compared to patients who have not undergone vaccination. Preliminary results would document a reduced incidence of severe forms of acute pancreatitis in subjects vaccinated against SARS-CoV-2.

DO WE NEED TO CHANGE THE DIAGNOSTIC AND THERAPEUTIC APPROACH?

Since pancreatitis in COVID-19 positive patients occurs more frequently in severe forms, treatment must be intensive and prompt. It is crucial to define and stratify the severity of illness in patients with acute pancreatitis because of the extreme range of potential clinical courses due to the wide range of organs and tissues that may become involved. It is also fundamental to identify patients with potentially severe pancreatitis who require a multidisciplinary approach and an earlier and more aggressive treatment[56, 57]. Suspected acute pancreatitis can be confirmed with laboratory and instrumental investigations. Increased pancreatic enzymes levels are associated with a poor prognosis in COVID-19 patients. Recent findings show that the increment of pancreatic enzymes are significant in critical COVID-19 patients, but only a few of them progress to acute pancreatitis[58]. The rapid response of C-reactive protein to

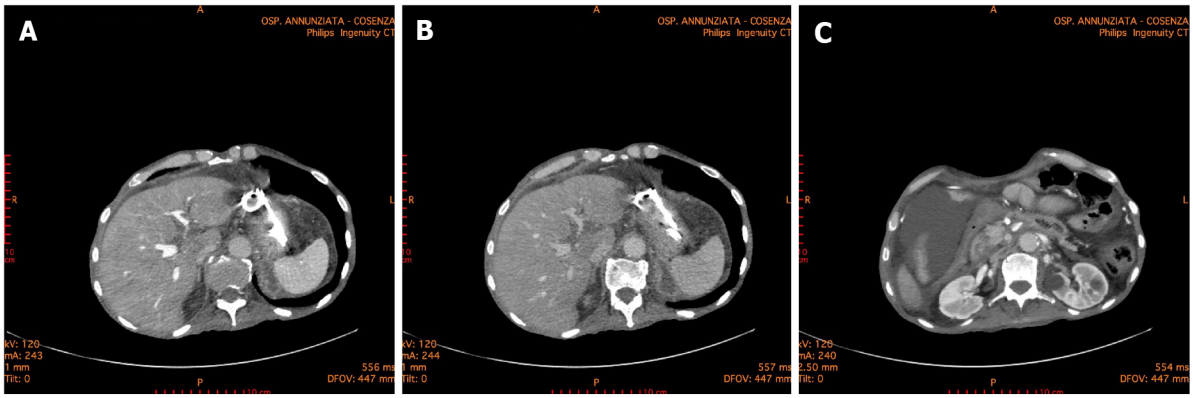

DOI: 10.3748/wjg.v28.i36.5240 **Copyright** ©The Author(s) 2022.

Figure 2 Abdominal computed tomography 6 mo after the onset of acute pancreatitis. A and B: The double pigtail stents positioned during the endoscopic necrosectomy through the stomach is highlighted. Endoscopic necrosectomy through the stomach was performed 4 mo prior; C: A necrotic collection is evident in the lower right quadrant of the abdomen.

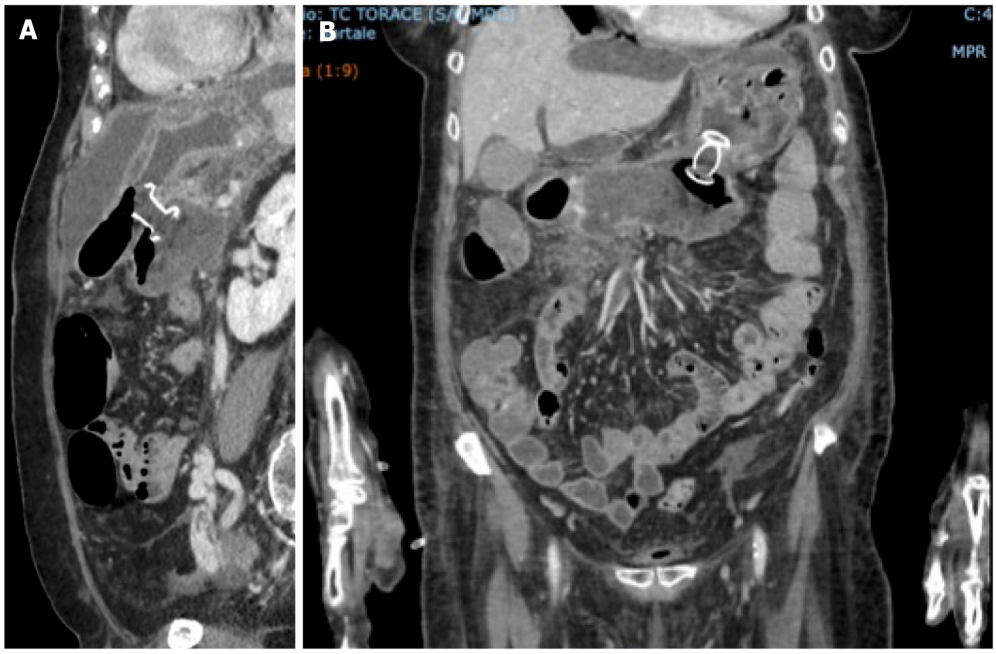

DOI: 10.3748/wjg.v28.i36.5240 **Copyright** ©The Author(s) 2022.

Figure 3 Abdominal computed tomography scan documenting correct placement of lumen-apposing metal stents for the treatment of walled-off necrosis in coronavirus disease 2019 positive patient. A: Sagittal scan; B: Front scan.

changes in the inflammatory process intensity has also suggested its use in the management and monitoring of acute pancreatitis. C-reactive protein is not specific, and although it is correlated with severity, it cannot be used to predict clinical evolution. Serum procalcitonin is also one of the parameters used in predicting the development of severe acute pancreatitis. Its continuous increase correlates with a bacterial superinfection of pancreatic necrosis[59]. In all patients with or without SARS-CoV-2 illness contrast-enhanced computed tomography scan is the gold standard for the diagnosis of acute pancreatitis to evaluate both pancreatic and extrapancreatic alterations (Figure 1).

The revised Atlanta classification provides a good clinical distinction between mild, moderate and severe acute pancreatitis, and it is used in most COVID-19 positive patients with acute pancreatitis[8]. Several scoring systems have been developed to predict the severity of acute pancreatitis; however, none of them represents a gold standard. The scoring systems are without clinical relevance because of their low predictive value[56]. The bedside index for severity in acute pancreatitis failed to identify the severity of acute pancreatitis in COVID-19 positive patients[37].

Early fluid resuscitation is recommended in order to improve tissue perfusion[60], and the maintenance of microcirculation may be associated with resolution of multiple organ failure[61], especially in patients with COVID-19 and acute pancreatitis. Enteral nutrition is safe during acute pancreatitis[62]. Moreover, supplementation of enteral nutrition with probiotics may decrease septic

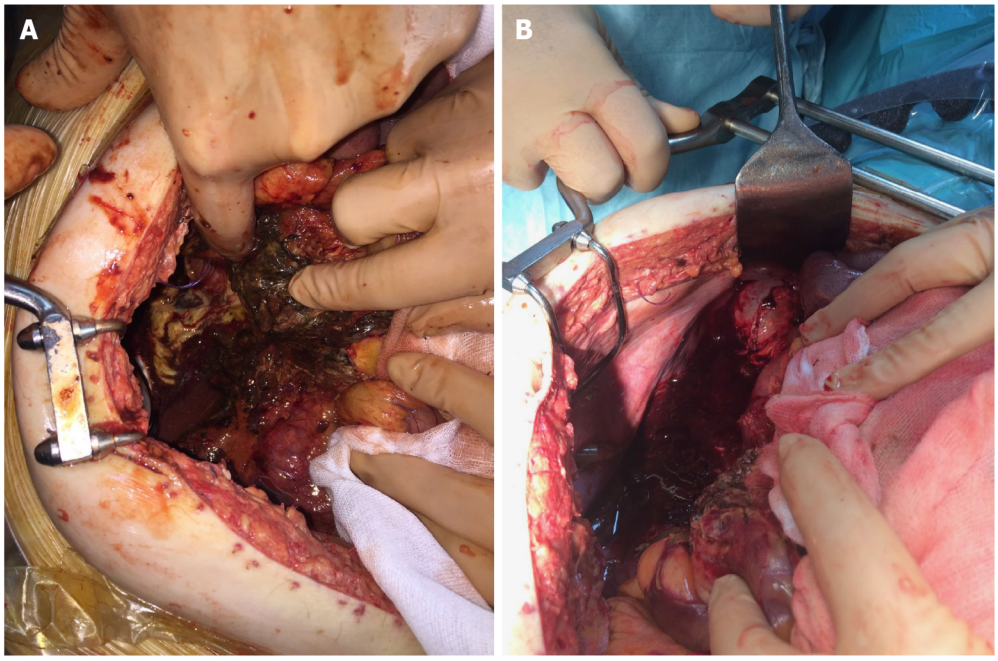

DOI: 10.3748/wjg.v28.i36.5240

Figure 4 Intraoperative photos. A: Surgery was performed for severe abdominal hypertension due to acute pancreatitis with necrotic collections in the retroduodenal region; B: Surgery was performed for severe abdominal hypertension due to acute pancreatitis with necrotic collections along the paracolic gutter.

complications. In patients with COVID-19 requiring mechanical ventilation, early enteral nutrition is associated with earlier liberation from ventilator support, shorter intensive care unit and hospital stay and decreased cost[63,64].

Most patients with sterile necrosis can be managed without invasive treatments. Walled off necrotic collections or pseudocysts may cause mechanical obstruction and a step-up approach is indicated. Percutaneous or transmural endoscopic drainage are both appropriate first-line approaches in managing these patients (Figure 2). However, endoscopic drainage is preferred as it avoids the risk of forming a pancreatocutaneous fistula. In the earlier phase of the pandemic, patients with COVID-19, especially with severe pneumonia and considered highly contagious, did not undergo endoscopic ultrasound or endoscopic treatments. In the later stages, patients with COVID-19 and acute pancreatitis were subjected, with necessary precautions, to percutaneous and endoscopic treatments similar to the COVID-19 negative patients (Figure 3).

The step-up approach might reduce the rates of complications and death by minimizing surgical trauma in already critically ill patients[65,66]. Currently, there is general agreement that surgery in severe acute pancreatitis should be performed as late as possible[67]. In the management of necrotizing acute pancreatitis, open operative debridement (Figure 4) maintains a role in cases not amenable to less invasive endoscopic and/or laparoscopic procedures. Open operative debridement was performed in patients with COVID-19 related lung symptoms and lesions.

CONCLUSION

In pandemic times, clinical conditions could be worsened by COVID-19 infection. SARS-CoV-2 cannot be said to be an etiological agent of acute pancreatitis. Acute pancreatitis in COVID-19 positive patients is idiopathic in most cases, and there is no sufficient evidence showing that SARS-CoV-2 can negatively impact prognosis. On the other hand, acute pancreatitis with concomitant SARS-CoV-2 is more likely to have worse outcomes due to double lung damage and greater pancreatic severity. The multiparametric scores could not recognize and stratify the severity of pancreatic diseases and concomitant COVID-19 infection. In these patients, computed tomography is the gold standard for the diagnosis. Management of COVID-19 positive patients with pancreatitis is complex, and it is optimally provided by a multidisciplinary team. Operative treatments should be modulated, preferably, from the least to the most invasive option. Thus, surgical necrosectomy is relegated to the role of "last resort", remembering that necrotizing pancreatitis is a heterogeneous disease with marked variations in extent and course. This also means that one size treatment does not fit all.

FOOTNOTES

Author contributions: Brisinda G and Chiarello MM equally contributed to the drafting of the manuscript and must both be considered first author; Chiarello MM and Brisinda G conceived the original idea; Tropeano G, Alteri G, Puccioni C, Fransvea P and Bianchi V performed a comprehensive review of all available literature and summarized the data; Brisinda G and Chiarello MM meet the criteria for authorship established by the International Committee of Medical Journal Editors and verify the validity of the results reported; and all authors read and approved the final manuscript.

Conflict-of-interest statement: All the authors report no relevant conflicts of interest for this article.

Country/Territory of origin: Italy

ORCID number: Giuseppe Brisinda 0000-0001-8820-9471; Maria Michela Chiarello 0000-0003-3455-0062; Giuseppe Tropeano 0000-0001-9006-5040; Gaia Altieri 0000-0002-0324-2430; Caterina Puccioni 0000-0001-6092-7957; Pietro Fransvea 0000-0003-4969-3373; Valentina Bianchi 0000-0002-8817-3760.

S-Editor: Wang JJ
L-Editor: Filipodia
P-Editor: Wang JJ

REFERENCES

1 **Guan WJ**, Ni ZY, Hu Y, Liang WH, Ou CQ, He JX, Liu L, Shan H, Lei CL, Hui DSC, Du B, Li LJ, Zeng G, Yuen KY, Chen RC, Tang CL, Wang T, Chen PY, Xiang J, Li SY, Wang JL, Liang ZJ, Peng YX, Wei L, Liu Y, Hu YH, Peng P, Wang JM, Liu JY, Chen Z, Li G, Zheng ZJ, Qiu SQ, Luo J, Ye CJ, Zhu SY, Zhong NS; China Medical Treatment Expert Group for Covid-19. Clinical Characteristics of Coronavirus Disease 2019 in China. *N Engl J Med* 2020; **382**: 1708-1720 [PMID: 32109013 DOI: 10.1056/NEJMoa2002032]

2 **Henry BM**, de Oliveira MHS, Benoit J, Lippi G. Gastrointestinal symptoms associated with severity of coronavirus disease 2019 (COVID-19): a pooled analysis. *Intern Emerg Med* 2020; **15**: 857-859 [PMID: 32303970 DOI: 10.1007/s11739-020-02329-9]

3 **Nobel YR**, Phipps M, Zucker J, Lebwohl B, Wang TC, Sobieszczyk ME, Freedberg DE. Gastrointestinal Symptoms and Coronavirus Disease 2019: A Case-Control Study From the United States. *Gastroenterology* 2020; **159**: 373-375.e2 [PMID: 32294477 DOI: 10.1053/j.gastro.2020.04.017]

4 **Nayar M**, Varghese C, Kanwar A, Siriwardena AK, Haque AR, Awan A, Balakrishnan A, Rawashdeh A, Ivanov B, Parmar C, Halloran CM, Caruana C, Borg CM, Gomez D, Damaskos D, Karavias D, Finch G, Ebied H, Pine JK, Skipworth JRA, Milburn J, Latif J, Apollos J, El Kafsi J, Windsor JA, Roberts K, Wang K, Ravi K, Coats MV, Hollyman M, Phillips M, Okocha M, Wilson MS, Ameer NA, Kumar N, Shah N, Lapolla P, Magee C, Al-Sarireh B, Lunevicius R, Benhmida R, Singhal R, Balachandra S, Demirli Atıcı S, Jaunoo S, Dwerryhouse S, Boyce T, Charalampakis V, Kanakala V, Abbas Z, Tewari N, Pandanaboyana S; COVIDPAN Collborative Group; COVID Pain Collborative Group. SARS-CoV-2 infection is associated with an increased risk of idiopathic acute pancreatitis but not pancreatic exocrine insufficiency or diabetes: long-term results of the COVIDPAN study. *Gut* 2022; **71**: 1444-1447 [PMID: 34764192 DOI: 10.1136/gutjnl-2021-326218]

5 **Troncone E**, Salvatori S, Sena G, De Cristofaro E, Alfieri N, Marafini I, Paganelli C, Argirò R, Giannarelli D, Monteleone G, Del Vecchio Blanco G. Low Frequency of Acute Pancreatitis in Hospitalized COVID-19 Patients. *Pancreas* 2021; **50**: 393-398 [PMID: 33835971 DOI: 10.1097/MPA.0000000000001770]

6 **Akarsu C**, Karabulut M, Aydin H, Sahbaz NA, Dural AC, Yegul D, Peker KD, Ferahman S, Bulut S, Dönmez T, Asar S, Yasar KK, Adas GT. Association between Acute Pancreatitis and COVID-19: Could Pancreatitis Be the Missing Piece of the Puzzle about Increased Mortality Rates? *J Invest Surg* 2022; **35**: 119-125 [PMID: 33138658 DOI: 10.1080/08941939.2020.1833263]

7 **Cholankeril G**, Podboy A, Aivaliotis VI, Pham EA, Spencer SP, Kim D, Ahmed A. Association of Digestive Symptoms and Hospitalization in Patients With SARS-CoV-2 Infection. *Am J Gastroenterol* 2020; **115**: 1129-1132 [PMID: 32618665 DOI: 10.14309/ajg.0000000000000712]

8 **Banks PA**, Bollen TL, Dervenis C, Gooszen HG, Johnson CD, Sarr MG, Tsiotos GG, Vege SS; Acute Pancreatitis Classification Working Group. Classification of acute pancreatitis--2012: revision of the Atlanta classification and definitions by international consensus. *Gut* 2013; **62**: 102-111 [PMID: 23100216 DOI: 10.1136/gutjnl-2012-302779]

9 **Seppänen H**, Puolakkainen P. Classification, Severity Assessment, and Prevention of Recurrences in Acute Pancreatitis. *Scand J Surg* 2020; **109**: 53-58 [PMID: 32192420 DOI: 10.1177/1457496920910007]

10 **Leppäniemi A**, Tolonen M, Tarasconi A, Segovia-Lohse H, Gamberini E, Kirkpatrick AW, Ball CG, Parry N, Sartelli M, Wolbrink D, van Goor H, Baiocchi G, Ansaloni L, Biffl W, Coccolini F, Di Saverio S, Kluger Y, Moore EE, Catena F. Executive summary: WSES Guidelines for the management of severe acute pancreatitis. *J Trauma Acute Care Surg* 2020;

88: 888-890 [PMID: 32459451 DOI: 10.1097/TA.0000000000002691]
11 **Brisinda G**, Vanella S, Crocco A, Mazzari A, Tomaiuolo P, Santullo F, Grossi U, Crucitti A. Severe acute pancreatitis: advances and insights in assessment of severity and management. *Eur J Gastroenterol Hepatol* 2011; **23**: 541-551 [PMID: 21659951 DOI: 10.1097/MEG.0b013e328346e21e]
12 **Rawla P**, Bandaru SS, Vellipuram AR. Review of Infectious Etiology of Acute Pancreatitis. *Gastroenterology Res* 2017; **10**: 153-158 [PMID: 28725301 DOI: 10.14740/gr858w]
13 **van Dijk SM**, Hallensleben NDL, van Santvoort HC, Fockens P, van Goor H, Bruno MJ, Besselink MG; Dutch Pancreatitis Study Group. Acute pancreatitis: recent advances through randomised trials. *Gut* 2017; **66**: 2024-2032 [PMID: 28838972 DOI: 10.1136/gutjnl-2016-313595]
14 **Brisinda G**, Crocco A, Giustacchini P. Classification of the severity of acute pancreatitis: how much is really needed for a new classification? *Ann Surg* 2015; **261**: e101-e102 [PMID: 24577326 DOI: 10.1097/SLA.0000000000000625]
15 **Du M**, Cai G, Chen F, Christiani DC, Zhang Z, Wang M. Multiomics Evaluation of Gastrointestinal and Other Clinical Characteristics of COVID-19. *Gastroenterology* 2020; **158**: 2298-2301.e7 [PMID: 32234303 DOI: 10.1053/j.gastro.2020.03.045]
16 **Correia de Sá T**, Soares C, Rocha M. Acute pancreatitis and COVID-19: A literature review. *World J Gastrointest Surg* 2021; **13**: 574-584 [PMID: 34194615 DOI: 10.4240/wjgs.v13.i6.574]
17 **Rubin R**. SARS-CoV-2 RNA Can Persist in Stool Months After Respiratory Tract Clears Virus. *JAMA* 2022; **327**: 2175-2176 [PMID: 35583898 DOI: 10.1001/jama.2022.7892]
18 **Hanley B**, Naresh KN, Roufosse C, Nicholson AG, Weir J, Cooke GS, Thursz M, Manousou P, Corbett R, Goldin R, Al-Sarraj S, Abdolrasouli A, Swann OC, Baillon L, Penn R, Barclay WS, Viola P, Osborn M. Histopathological findings and viral tropism in UK patients with severe fatal COVID-19: a post-mortem study. *Lancet Microbe* 2020; **1**: e245-e253 [PMID: 32844161 DOI: 10.1016/S2666-5247(20)30115-4]
19 **Chmielik E**, Jazowiecka-Rakus J, Dyduch G, Nasierowska-Guttmejer A, Michalowski L, Sochanik A, Ulatowska-Bialas M. COVID-19 Autopsies: A Case Series from Poland. *Pathobiology* 2021; **88**: 78-87 [PMID: 33254171 DOI: 10.1159/000512768]
20 **Gu J**, Han B, Wang J. COVID-19: Gastrointestinal Manifestations and Potential Fecal-Oral Transmission. *Gastroenterology* 2020; **158**: 1518-1519 [PMID: 32142785 DOI: 10.1053/j.gastro.2020.02.054]
21 **Dalan R**, Bornstein SR, El-Armouche A, Rodionov RN, Markov A, Wielockx B, Beuschlein F, Boehm BO. The ACE-2 in COVID-19: Foe or Friend? *Horm Metab Res* 2020; **52**: 257-263 [PMID: 32340044 DOI: 10.1055/a-1155-0501]
22 **Shaharuddin SH**, Wang V, Santos RS, Gross A, Wang Y, Jawanda H, Zhang Y, Hasan W, Garcia G Jr, Arumugaswami V, Sareen D. Deleterious Effects of SARS-CoV-2 Infection on Human Pancreatic Cells. *Front Cell Infect Microbiol* 2021; **11**: 678482 [PMID: 34282405 DOI: 10.3389/fcimb.2021.678482]
23 **Liu F**, Long X, Zhang B, Zhang W, Chen X, Zhang Z. ACE2 Expression in Pancreas May Cause Pancreatic Damage After SARS-CoV-2 Infection. *Clin Gastroenterol Hepatol* 2020; **18**: 2128-2130.e2 [PMID: 32334082 DOI: 10.1016/j.cgh.2020.04.040]
24 **Zhou Z**, Zhao N, Shu Y, Han S, Chen B, Shu X. Effect of Gastrointestinal Symptoms in Patients With COVID-19. *Gastroenterology* 2020; **158**: 2294-2297 [PMID: 32199880 DOI: 10.1053/j.gastro.2020.03.020]
25 **Aloysius MM**, Thatti A, Gupta A, Sharma N, Bansal P, Goyal H. COVID-19 presenting as acute pancreatitis. *Pancreatology* 2020; **20**: 1026-1027 [PMID: 32444169 DOI: 10.1016/j.pan.2020.05.003]
26 **Annunziata A**, Coppola A, Andreozzi P, Lanza M, Simioli F, Carannante N, Di Somma C, Di Micco P, Fiorentino G. Acute Pancreatitis and COVID-19: A Single-Center Experience. *J Multidiscip Healthc* 2021; **14**: 2857-2861 [PMID: 34675533 DOI: 10.2147/JMDH.S334835]
27 **Aktas B**, Aslim B. Gut-lung axis and dysbiosis in COVID-19. *Turk J Biol* 2020; **44**: 265-272 [PMID: 32595361 DOI: 10.3906/biy-2005-102]
28 **Dang AT**, Marsland BJ. Microbes, metabolites, and the gut-lung axis. *Mucosal Immunol* 2019; **12**: 843-850 [PMID: 30976087 DOI: 10.1038/s41385-019-0160-6]
29 **Marsland BJ**, Trompette A, Gollwitzer ES. The Gut-Lung Axis in Respiratory Disease. *Ann Am Thorac Soc* 2015; **12** Suppl 2: S150-S156 [PMID: 26595731 DOI: 10.1513/AnnalsATS.201503-133AW]
30 **Albillos A**, de Gottardi A, Rescigno M. The gut-liver axis in liver disease: Pathophysiological basis for therapy. *J Hepatol* 2020; **72**: 558-577 [PMID: 31622696 DOI: 10.1016/j.jhep.2019.10.003]
31 **Stephens JR**, Wong JLC, Broomhead R, Stümpfle R, Waheed U, Patel P, Brett SJ, Soni S. Raised serum amylase in patients with COVID-19 may not be associated with pancreatitis. *Br J Surg* 2021; **108**: e152-e153 [PMID: 33793756 DOI: 10.1093/bjs/znaa168]
32 **Abramczyk U**, Nowaczyński M, Słomczyński A, Wojnicz P, Zatyka P, Kuzan A. Consequences of COVID-19 for the Pancreas. *Int J Mol Sci* 2022; **23** [PMID: 35055050 DOI: 10.3390/ijms23020864]
33 **de-Madaria E**, Capurso G. COVID-19 and acute pancreatitis: examining the causality. *Nat Rev Gastroenterol Hepatol* 2021; **18**: 3-4 [PMID: 33203968 DOI: 10.1038/s41575-020-00389-y]
34 **Suchman K**, Raphael KL, Liu Y, Wee D, Trindade AJ; Northwell COVID-19 Research Consortium. Acute pancreatitis in children hospitalized with COVID-19. *Pancreatology* 2021; **21**: 31-33 [PMID: 33309015 DOI: 10.1016/j.pan.2020.12.005]
35 **Mao R**, Qiu Y, He JS, Tan JY, Li XH, Liang J, Shen J, Zhu LR, Chen Y, Iacucci M, Ng SC, Ghosh S, Chen MH. Manifestations and prognosis of gastrointestinal and liver involvement in patients with COVID-19: a systematic review and meta-analysis. *Lancet Gastroenterol Hepatol* 2020; **5**: 667-678 [PMID: 32405603 DOI: 10.1016/S2468-1253(20)30126-6]
36 **Miró Ò**, Llorens P, Jiménez S, Piñera P, Burillo-Putze G, Martín A, Martín-Sánchez FJ, González Del Castillo J; Spanish Investigators in Emergency Situations TeAm (SIESTA) network. Frequency of five unusual presentations in patients with COVID-19: results of the UMC-19-S_1. *Epidemiol Infect* 2020; **148**: e189 [PMID: 32843127 DOI: 10.1017/S0950268820001910]
37 **Inamdar S**, Benias PC, Liu Y, Sejpal DV, Satapathy SK, Trindade AJ; Northwell COVID-19 Research Consortium. Prevalence, Risk Factors, and Outcomes of Hospitalized Patients With Coronavirus Disease 2019 Presenting as Acute Pancreatitis. *Gastroenterology* 2020; **159**: 2226-2228.e2 [PMID: 32860787 DOI: 10.1053/j.gastro.2020.08.044]

38 **Pons S**, Fodil S, Azoulay E, Zafrani L. The vascular endothelium: the cornerstone of organ dysfunction in severe SARS-CoV-2 infection. *Crit Care* 2020; **24**: 353 [PMID: 32546188 DOI: 10.1186/s13054-020-03062-7]

39 **Pandanaboyana S**, Moir J, Leeds JS, Oppong K, Kanwar A, Marzouk A, Belgaumkar A, Gupta A, Siriwardena AK, Haque AR, Awan A, Balakrishnan A, Rawashdeh A, Ivanov B, Parmar C, M Halloran C, Caruana C, Borg CM, Gomez D, Damaskos D, Karavias D, Finch G, Ebied H, K Pine J, R A Skipworth J, Milburn J, Latif J, Ratnam Apollos J, El Kafsi J, Windsor JA, Roberts K, Wang K, Ravi K, V Coats M, Hollyman M, Phillips M, Okocha M, Sj Wilson M, A Ameer N, Kumar N, Shah N, Lapolla P, Magee C, Al-Sarireh B, Lunevicius R, Benhmida R, Singhal R, Balachandra S, Demirli Atıcı S, Jaunoo S, Dwerryhouse S, Boyce T, Charalampakis V, Kanakala V, Abbas Z, Nayar M; COVID PAN collaborative group. SARS-CoV-2 infection in acute pancreatitis increases disease severity and 30-day mortality: COVID PAN collaborative study. *Gut* 2021; **70**: 1061-1069 [PMID: 33547182 DOI: 10.1136/gutjnl-2020-323364]

40 **Chiarello MM**, Cariati M, Brisinda G. Assessment of severity of acute pancreatitis in a Sars-CoV-2 pandemia. *Br J Surg* 2020; **107**: e379 [PMID: 32779743 DOI: 10.1002/bjs.11818]

41 **Wang K**, Luo J, Tan F, Liu J, Ni Z, Liu D, Tian P, Li W. Acute Pancreatitis as the Initial Manifestation in 2 Cases of COVID-19 in Wuhan, China. *Open Forum Infect Dis* 2020; **7**: ofaa324 [PMID: 32959016 DOI: 10.1093/ofid/ofaa324]

42 **Shlomovitz E**, Davies W, Cairns E, Brintnell WC, Goldszmidt M, Dresser GK. Severe necrotizing pancreatitis following combined hepatitis A and B vaccination. *CMAJ* 2007; **176**: 339-342 [PMID: 17261831 DOI: 10.1503/cmaj.060360]

43 **Adler JB**, Mazzotta SA, Barkin JS. Pancreatitis caused by measles, mumps, and rubella vaccine. *Pancreas* 1991; **6**: 489-490 [PMID: 1876605 DOI: 10.1097/00006676-199107000-00018]

44 **Haviv YS**, Sharkia M, Galun E, Safadi R. Pancreatitis following hepatitis A vaccination. *Eur J Med Res* 2000; **5**: 229-230 [PMID: 10806126]

45 **Sahin U**, Muik A, Derhovanessian E, Vogler I, Kranz LM, Vormehr M, Baum A, Pascal K, Quandt J, Maurus D, Brachtendorf S, Lörks V, Sikorski J, Hilker R, Becker D, Eller AK, Grützner J, Boesler C, Rosenbaum C, Kühnle MC, Luxemburger U, Kemmer-Brück A, Langer D, Bexon M, Bolte S, Karikó K, Palanche T, Fischer B, Schultz A, Shi PY, Fontes-Garfias C, Perez JL, Swanson KA, Loschko J, Scully IL, Cutler M, Kalina W, Kyratsous CA, Cooper D, Dormitzer PR, Jansen KU, Türeci Ö. COVID-19 vaccine BNT162b1 elicits human antibody and T_H1 T cell responses. *Nature* 2020; **586**: 594-599 [PMID: 32998157 DOI: 10.1038/s41586-020-2814-7]

46 **Ozaka S**, Kodera T, Ariki S, Kobayashi T, Murakami K. Acute pancreatitis soon after COVID-19 vaccination: A case report. *Medicine (Baltimore)* 2022; **101**: e28471 [PMID: 35029194 DOI: 10.1097/MD.0000000000028471]

47 **Walter T**, Connor S, Stedman C, Doogue M. A case of acute necrotising pancreatitis following the second dose of Pfizer-BioNTech COVID-19 mRNA vaccine. *Br J Clin Pharmacol* 2022; **88**: 1385-1386 [PMID: 34423463 DOI: 10.1111/bcp.15039]

48 **Meo SA**, Bukhari IA, Akram J, Meo AS, Klonoff DC. COVID-19 vaccines: comparison of biological, pharmacological characteristics and adverse effects of Pfizer/BioNTech and Moderna Vaccines. *Eur Rev Med Pharmacol Sci* 2021; **25**: 1663-1669 [PMID: 33629336 DOI: 10.26355/eurrev_202102_24877]

49 **Rosenblum HG**, Hadler SC, Moulia D, Shimabukuro TT, Su JR, Tepper NK, Ess KC, Woo EJ, Mba-Jonas A, Alimchandani M, Nair N, Klein NP, Hanson KE, Markowitz LE, Wharton M, McNally VV, Romero JR, Talbot HK, Lee GM, Daley MF, Mbaeyi SA, Oliver SE. Use of COVID-19 Vaccines After Reports of Adverse Events Among Adult Recipients of Janssen (Johnson & Johnson) and mRNA COVID-19 Vaccines (Pfizer-BioNTech and Moderna): Update from the Advisory Committee on Immunization Practices - United States, July 2021. *MMWR Morb Mortal Wkly Rep* 2021; **70**: 1094-1099 [PMID: 34383735 DOI: 10.15585/mmwr.mm7032e4]

50 **Parkash O**, Sharko A, Farooqi A, Ying GW, Sura P. Acute Pancreatitis: A Possible Side Effect of COVID-19 Vaccine. *Cureus* 2021; **13**: e14741 [PMID: 34084669 DOI: 10.7759/cureus.14741]

51 **Pfizer**. Pfizer-BioNTech COVID-19 vaccine (BNT162, PF-07302048). Vaccines and related biological products advisory committee. [cited 13 April 2022]. Available from: https://www.fda.gov/media/144246/download

52 COVID-19 mRNA Pfizer-BioNTech vaccine analysis print. All UK spontaneous reports received between 9 December 2020 and 30 June 2021 for mRNA Pfizer/BioNTech vaccine analysis print. 2021. [cited 13 April 2022]. Available from: https://assets.publishing.service.gov.uk/government/uploads/system/uploads/attachment_data/file/1009453/COVID-19_mRNA_Pfizer-BioNTech_Vaccine_Analysis_Print_DPL_28.07.2021

53 **ANSM**. Point de situation sur la surveillance des vaccins contre la COVID-19. [cited 13 April 2022]. Available from: https://ansm.sante.fr/actualites/point-de-situation-sur-la-surveillance-des-vaccins-contre-la-covid-19-7

54 **World Health Organization**. VigiAccess. [cited 13 April 2022]. Available from: http://www.vigiaccess.org

55 **FEDAIISF**. Rapporto annuale sulla sicurezza dei vaccini anti-COVID-19. [cited 13 April 2022]. Available from: https://www.fedaiisf.it/aifa-rapporto-annuale-sulla-sicurezza-dei-vaccini-anti-covid-19/

56 **Boxhoorn L**, Voermans RP, Bouwense SA, Bruno MJ, Verdonk RC, Boermeester MA, van Santvoort HC, Besselink MG. Acute pancreatitis. *Lancet* 2020; **396**: 726-734 [PMID: 32891214 DOI: 10.1016/S0140-6736(20)31310-6]

57 **Bulthuis MC**, Boxhoorn L, Beudel M, Elbers PWG, Kop MPM, van Wanrooij RLJ, Besselink MG, Voermans RP. Acute pancreatitis in COVID-19 patients: true risk? *Scand J Gastroenterol* 2021; **56**: 585-587 [PMID: 33715577 DOI: 10.1080/00365521.2021.1896776]

58 **Ding P**, Song B, Liu X, Fang X, Cai H, Zhang D, Zheng X. Elevated Pancreatic Enzymes in ICU Patients With COVID-19 in Wuhan, China: A Retrospective Study. *Front Med (Lausanne)* 2021; **8**: 663646 [PMID: 34485322 DOI: 10.3389/fmed.2021.663646]

59 **Huang HL**, Nie X, Cai B, Tang JT, He Y, Miao Q, Song HL, Luo TX, Gao BX, Wang LL, Li GX. Procalcitonin levels predict acute kidney injury and prognosis in acute pancreatitis: a prospective study. *PLoS One* 2013; **8**: e82250 [PMID: 24349237 DOI: 10.1371/journal.pone.0082250]

60 **Sarr MG**. Early fluid "resuscitation/therapy" in acute pancreatitis: which fluid? *Ann Surg* 2013; **257**: 189-190 [PMID: 23291660 DOI: 10.1097/SLA.0b013e318280e19e]

61 **Bortolotti P**, Saulnier F, Colling D, Redheuil A, Preau S. New tools for optimizing fluid resuscitation in acute pancreatitis. *World J Gastroenterol* 2014; **20**: 16113-16122 [PMID: 25473163 DOI: 10.3748/wjg.v20.i43.16113]

62 **Arvanitakis M**, Ockenga J, Bezmarevic M, Gianotti L, Krznarić Ž, Lobo DN, Löser C, Madl C, Meier R, Phillips M,

Rasmussen HH, Van Hooft JE, Bischoff SC. ESPEN guideline on clinical nutrition in acute and chronic pancreatitis. *Clin Nutr* 2020; **39**: 612-631 [PMID: 32008871 DOI: 10.1016/j.clnu.2020.01.004]

63 **Haines K**, Parker V, Ohnuma T, Krishnamoorthy V, Raghunathan K, Sulo S, Kerr KW, Besecker BY, Cassady BA, Wischmeyer PE. Role of Early Enteral Nutrition in Mechanically Ventilated COVID-19 Patients. *Crit Care Explor* 2022; **4**: e0683 [PMID: 35464756 DOI: 10.1097/CCE.0000000000000683]

64 **Compher C**, Bingham AL, McCall M, Patel J, Rice TW, Braunschweig C, McKeever L. Guidelines for the provision of nutrition support therapy in the adult critically ill patient: The American Society for Parenteral and Enteral Nutrition. *JPEN J Parenter Enteral Nutr* 2022; **46**: 12-41 [PMID: 34784064 DOI: 10.1002/jpen.2267]

65 **Besselink MG**, van Santvoort HC, Nieuwenhuijs VB, Boermeester MA, Bollen TL, Buskens E, Dejong CH, van Eijck CH, van Goor H, Hofker SS, Lameris JS, van Leeuwen MS, Ploeg RJ, van Ramshorst B, Schaapherder AF, Cuesta MA, Consten EC, Gouma DJ, van der Harst E, Hesselink EJ, Houdijk LP, Karsten TM, van Laarhoven CJ, Pierie JP, Rosman C, Bilgen EJ, Timmer R, van der Tweel I, de Wit RJ, Witteman BJ, Gooszen HG; Dutch Acute Pancreatitis Study Group. Minimally invasive 'step-up approach' *vs* maximal necrosectomy in patients with acute necrotising pancreatitis (PANTER trial): design and rationale of a randomised controlled multicenter trial [ISRCTN13975868]. *BMC Surg* 2006; **6**: 6 [PMID: 16606471 DOI: 10.1186/1471-2482-6-6]

66 **Hollemans RA**, Bakker OJ, Boermeester MA, Bollen TL, Bosscha K, Bruno MJ, Buskens E, Dejong CH, van Duijvendijk P, van Eijck CH, Fockens P, van Goor H, van Grevenstein WM, van der Harst E, Heisterkamp J, Hesselink EJ, Hofker S, Houdijk AP, Karsten T, Kruyt PM, van Laarhoven CJ, Laméris JS, van Leeuwen MS, Manusama ER, Molenaar IQ, Nieuwenhuijs VB, van Ramshorst B, Roos D, Rosman C, Schaapherder AF, van der Schelling GP, Timmer R, Verdonk RC, de Wit RJ, Gooszen HG, Besselink MG, van Santvoort HC; Dutch Pancreatitis Study Group. Superiority of Step-up Approach *vs* Open Necrosectomy in Long-term Follow-up of Patients With Necrotizing Pancreatitis. *Gastroenterology* 2019; **156**: 1016-1026 [PMID: 30391468 DOI: 10.1053/j.gastro.2018.10.045]

67 **Boxhoorn L**, van Dijk SM, van Grinsven J, Verdonk RC, Boermeester MA, Bollen TL, Bouwense SAW, Bruno MJ, Cappendijk VC, Dejong CHC, van Duijvendijk P, van Eijck CHJ, Fockens P, Francken MFG, van Goor H, Hadithi M, Hallensleben NDL, Haveman JW, Jacobs MAJM, Jansen JM, Kop MPM, van Lienden KP, Manusama ER, Mieog JSD, Molenaar IQ, Nieuwenhuijs VB, Poen AC, Poley JW, van de Poll M, Quispel R, Römkens TEH, Schwartz MP, Seerden TC, Stommel MWJ, Straathof JWA, Timmerhuis HC, Venneman NG, Voermans RP, van de Vrie W, Witteman BJ, Dijkgraaf MGW, van Santvoort HC, Besselink MG; Dutch Pancreatitis Study Group. Immediate versus Postponed Intervention for Infected Necrotizing Pancreatitis. *N Engl J Med* 2021; **385**: 1372-1381 [PMID: 34614330 DOI: 10.1056/NEJMoa2100826]

World Journal of Gastroenterology

Submit a Manuscript: https://www.f6publishing.com

World J Gastroenterol 2022 September 28; 28(36): 5250-5264

DOI: 10.3748/wjg.v28.i36.5250

ISSN 1007-9327 (print) ISSN 2219-2840 (online)

REVIEW

Deciphering the role of transforming growth factor-beta 1 as a diagnostic-prognostic-therapeutic candidate against hepatocellular carcinoma

Aswathy R Devan, Keechilat Pavithran, Bhagyalakshmi Nair, Maneesha Murali, Lekshmi R Nath

Specialty type: Gastroenterology and hepatology

Provenance and peer review: Invited article; Externally peer reviewed.

Peer-review model: Single blind

Peer-review report's scientific quality classification

Grade A (Excellent): 0
Grade B (Very good): B
Grade C (Good): C
Grade D (Fair): 0
Grade E (Poor): 0

P-Reviewer: Ghazy A, Egypt; Ying HQ, China

Received: March 9, 2022
Peer-review started: March 9, 2022
First decision: April 11, 2022
Revised: April 30, 2022
Accepted: August 16, 2022
Article in press: August 16, 2022
Published online: September 28, 2022

Aswathy R Devan, Bhagyalakshmi Nair, Maneesha Murali, Lekshmi R Nath, Department of Pharmacognosy, Amrita School of Pharmacy, Amrita Vishwa Vidyapeetham, AIMS Health Science Campus, Kochi 682041, Kerala, India

Keechilat Pavithran, Department of Medical Oncology and Hematology, Amrita Institute of Medical Sciences and Research Centre, Amrita Vishwa Vidyapeetham, Kochi 682041, Kerala, India

Corresponding author: Lekshmi R Nath, PhD, Assistant Professor, Department of Pharmacognosy, Amrita School of Pharmacy, Amrita Vishwa Vidyapeetham, AIMS Health Science Campus, Ponekkara, Kochi 682041, Kerala, India. lekshmirnath@aims.amrita.edu

Abstract

Transforming growth factor-beta (TGF-β) is a multifunctional cytokine that performs a dual role as a tumor suppressor and tumor promoter during cancer progression. Among different ligands of the TGF-β family, TGF-β1 modulates most of its biological outcomes. Despite the abundant expression of TGF-β1 in the liver, steatosis to hepatocellular carcinoma (HCC) progression triggers elevated TGF-β1 levels, contributing to poor prognosis and survival. Additionally, elevated TGF-β1 levels in the tumor microenvironment create an immunosuppressive stage *via* various mechanisms. TGF-β1 has a prime role as a diagnostic and prognostic biomarker in HCC. Moreover, TGF-β1 is widely studied as a therapeutic target either as monotherapy or combined with immune checkpoint inhibitors. This review provides clinical relevance and up-to-date information regarding the potential of TGF-β1 in diagnosis, prognosis, and therapy against HCC.

Key Words: Transforming growth factor-beta 1; Inflammation; Immunosuppression; Fibrogenesis; Hepatocellular carcinoma; Biomarker; Immunotherapy

Core Tip: Transforming growth factor-beta 1 (TGF-β1) exhibits a progressive elevation throughout hepatic dysfunction starting from hepatitis to hepatocellular carcinoma (HCC) as an inflammatory cytokine, pro-fibrogenic marker, immunosuppressive agent and pro-carcinogenic growth factor. Aberrant TGF-β1 activation in HCC is associated with poor prognosis and survival. TGF-β1 mediated immunosuppression disturbs the anticancer surveillance and the efficacy of the immunotherapeutic agent. This pleiotropic effect of TGF-β1 in the context of HCC makes it ideal as a diagnostic, prognostic, and therapeutic candidate in HCC.

Citation: Devan AR, Pavithran K, Nair B, Murali M, Nath LR. Deciphering the role of transforming growth factor-beta 1 as a diagnostic-prognostic-therapeutic candidate against hepatocellular carcinoma. *World J Gastroenterol* 2022; 28(36): 5250-5264
URL: https://www.wjgnet.com/1007-9327/full/v28/i36/5250.htm
DOI: https://dx.doi.org/10.3748/wjg.v28.i36.5250

INTRODUCTION

Hepatocellular carcinoma, an aggressive and refractory cold tumor

Liver cancer, specifically hepatocellular carcinoma (HCC) is often recognized as an aggressive malignancy, ranking 6th in incidence and 3rd in terms of mortality in 2020, where mortality rates are roughly equivalent to incidence rate[1]. As it develops in the background of chronic inflammation starting from the fatty liver, HCC remains undiagnosed for years until it worsens. The progressive transformation from cirrhosis to HCC also creates longer delays in diagnosis[2]. HCC is commonly diagnosed by liver imaging techniques such as ultrasound, computed tomography and magnetic resonance imaging. Blood biomarkers such as alpha fetoprotein (AFP), protein induced by vitamin K absence or antagonist II levels, and liver biopsy are also used to diagnose HCC[3,4]. Even though the recent guidelines recommend HCC surveillance biannually and antiviral vaccination, the lack of effective surveillance programs significantly contributes to HCC progression to the advanced stage, particularly in high-risk individuals. Once established, HCC cells rapidly proliferate and spread to the extrahepatic site, such as the lungs, portal vein, and lymph nodes. In such cases, in an advanced stage, curative interventions such as liver transplantation, resection, percutaneous ablation, and chemoembolization were not responsive. Systemic drug therapy remains the primary treatment modality[5,6], where immunotherapy and tyrosine kinase inhibitors are the approved treatment options[7]. However, limited response to therapy, the emergence of multidrug resistance, immunosuppressive tumor microenvironment, and lack of validated diagnostic and prognostic biomarkers pose significant obstacles in establishing effective treatment against HCC[8,9].

Transforming growth factor-beta (TGF-β) is a critical homeostasis regulator, which is aberrantly activated during inflammation, fibrosis and carcinogenesis[10]. Among the three isoforms, TGF-β1 is superior in TGF-β signal transduction, especially those related to chronic liver diseases. Since HCC is an inflammation-induced-immunosuppressed malignancy, the role of TGF-β1 signaling in HCC has been extensively evaluated recently[11]. This review presents the potential of the TGF-β superfamily of ligands, specifically TGF-β1, to develop as a therapeutic and prognostic-diagnostic marker candidate against HCC.

TGF-β1 signaling in HCC

TGF-β superfamily of ligands is a dimeric peptide growth factor with more than 30 members in humans, mainly TGF-βs, activins, inhibins, and bone morphogenetic proteins. TGF-βs are categorized into three different isoforms TGF-β1, TGF-β2, and TGF-β3. Of the three isoforms, TGF-β1 is the most evaluated and abundant, found in epithelial, endothelial, hematopoietic, and connective tissue. TGF-β 2 is expressed in epithelial and neuronal cells, while TGF-β3 is found in mesenchymal cells[12]. TGF-βs are implicated in diverse physiological processes, including cell homeostasis and embryonic development[13]. It is a pleiotropic factor that regulates inflammation, fibrogenesis, cell differentiation, proliferation, epithelial-mesenchymal transition (EMT), extracellular matrix (ECM) formation, tumor-suppressive and pro-tumor effect in a cell-context dependent manner[14].

The three isoforms of TGF-β have structural similarity and functional redundancy[15]. However, TGF-β1 is often considered a potent and superior isoform with significant physiological and pathological importance[16]. Importantly, TGF-β1 exerts a cell-context dependent effect in the liver[17,18]. Normal to activated TGF-β1 signature confers a protective effect by inhibiting hepatocyte proliferation and hepatic stellate cells (HSCs) activation, apoptosis induction, preventing fibrosis and improving liver function. While, aberrantly activated TGF-β1 signature manifests as HSC activation and worsening fibrosis to HCC, where tumor cells lose their sensitivity toward the inhibitory effect of TGF-β1[19-21]. Exposure of hepatocytes to various causative factors such as viruses, alcohol, toxicants and

other metabolic disorders leads to the release of TGF-β1. Also, other pro-inflammatory cytokines such as tumor necrosis factor-α and growth factors from non-parenchymal liver cells switch on inflammation, production of ECM, and accumulation of fibrous material that eventually progress to cirrhosis[22,23]. A simultaneous increase in integrins, a vital cell adhesion molecule, is observed as the fibrogenesis continues. These integrins interact with TGF-β1 and other ECM proteins, altering signal transduction pathways[24]. Along with the accumulation of genetic mutations, HSC induces TGF-β and β-catenin-dependent EMT, leading to tumor growth in the liver. TGF-β1 continues to increase, promoting neo-angiogenesis by interacting with other pathways and mediating stromal-tumor cell interaction, conferring aggressive phenotype and metastasis[25] (Figure 1). Wang *et al*[26] demonstrated that both TGF-β1 and TGFβR1 have a crucial role in regulating proliferation, invasion, metastasis and immune response in HCC cells.

TGF-β1 exerts biological and pathological effects *via* Smad and non-Smad pathways. TGF-βs are synthesized in the inactivated form and exist as latent TGF-β complex (LTC) by binding with latency-associated protein. Later, LTC is converted to large latent complex (LLC) by interacting with latent TGF-β binding protein in ECM. Integrin signaling plays a significant role in the activation and subsequent release of TGF-β1 from LLC. It is also mediated by other factors such as pH, protease enzyme *etc.*[27]. In the canonical Smad pathway, activated TGF-β first binds with the extracellular domain of TGF-β receptor type II, which triggers the cross phosphorylation of the kinase domain of TGF-β receptor type I. TGF-β R1 activation leads to the phosphorylation of Smad proteins, Smad 2 and Smad 3. Later Smad-2 and 3 complex bind with the co-Smad, Smad-4 to form a ternary complex. This ternary complex is then translocated into the nucleus, binds to Smad binding elements in DNA, and activates the transcription of TGF-β-dependent genes[28]. Binding of inhibitory Smad, Smad-7 will shut down the activated pathway[29]. In addition to the Canonical Smad pathway, TGF-β can exert biological functions by activating other diverse signalings such as P38, JNK, PI3K/AKT, RAS-ERK, and RHO-ROCK, which constitute the non-Smad pathway of TGF-β signal transduction[30] (Figure 2).

Smad pathway of TGF-β signal transduction also enhances the transcription of FoxP3, predominantly present in T regulatory (Treg) cells[31,32]. A high amount of tumor-infiltrating Treg cells and FoxP3 positive Treg cells in blood is reported in HCC patients, leading to the deterioration of effector T cells such as CD4+ and CD+ cytotoxic T cells lymphocytes, which are pillars of anticancer immunity[33,34]. Together, TGF-β inhibits natural killer (NK) cells, blocks interferon (IFN)-γ secretion, and prevents effector immune cells recruitment to tumor tissue[35,36]. Additionally, TGF-β inhibits IFN-γ secretion by interacting with the activating transcription factor 1[37]. Likewise, TGF-β-RUNX3 transcription factor interaction and co-expression of programmed death ligand 1 (PD-L1) and interleukin-10 promote the transformation of naïve B cells to immunoglobulin A producing B cells, which are crucial in HCC development from non-alcoholic fatty liver[38]. Elevated TGF-β can directly enhance the transcription of PD-1 in HCC. The interaction of PD-1 with PD-L1 causes significant immunosuppression by T cell exhaustion, which manifests as inhibition of T cell activation, proliferation, and cytotoxic action[39,40]. In a recent study, Bao *et al*[41] reported that TGF-β1 trigger the expression of immune checkpoints such as PD-1 and CTLA4 on HCC cells and attenuates T-cell-mediated anti-tumor immune surveillance. Therefore, up-regulated TGF-β mainly isoforms 1 directly affect immune checkpoint inhibition, and it works as an indicator of T cell exhaustion. This evidence suggests the potential of TGF-β1 targeted immunotherapies against HCC. The pivotal role of the TGF-β1 signature in hepatic dysfunction and HCC extends its potential as a biomarker molecule for diagnosis and prognostic prediction and a therapeutic target.

Clinical utility of TGF-β1 as diagnostic marker of HCC

As an inflammatory-fibrogenic cytokine molecule, the involvement of TGF-β1 in all stages of liver injury, starting from fatty liver, steatosis, fibrosis to cirrhosis, and HCC, is evident. Intergromic analysis of TGF-β gene alterations among the 33 cancer types in the TGCA dataset revealed 39% alterations. Gastrointestinal cancers and HCC exhibited prominent mutation compared with other cancer types[42]. Later, in an HCC-specific transcriptomic analysis, 40% of HCC samples were found with mutations in genes of the TGF-β pathway[43]. Higher TGF-β1 levels in HCC correlate with the high rate of extrahepatic metastasis (EHM), poor prognosis, and low survival rate[44]. After acute/chronic liver injury, liver sinusoidal endothelial cells and HSCs secrete TGF-β1 and up-regulate TGF-β receptors[45,46]. Elevated TGF-β1 level was found in viral and alcohol-induced fibrosis[47]. Thus, TGF-β levels can be used to track the response to therapy so that the decrease in TGF-β 1 level followed by IFN treatment in hepatitis B virus (HBV) patients is associated with improved treatment outcomes. Apart from HSC-triggered TGF-β secretion, hepatitis C virus (HCV) infection can also induce TGF-β1 production in hepatocytes[48]. Likewise, proteomic and phospho-proteomic characterization of 110 tumor and non-tumor tissues of early-stage HBV-associated HCC found an increased expression of TGF-β genes compared with the non-tumor tissue[49]. However, the dichromatic role of TGF-β1 on cancer growth *i.e.*, tumor suppressive in early-stage or oncogenic effect in late-stage, is a matter of concern. Another study indicated a comparative functional genomic approach and illustrated the link between TGF-β expression signature and HCC subtypes. The study shows that TGF-β positive HCC clusters can be categorized into two. HCC with early TGF-β signature exhibit physiological responses while HCC associated with late TGF-β signature showed metastasis and poor survival[50]. N-2-fluorenylacetamide-

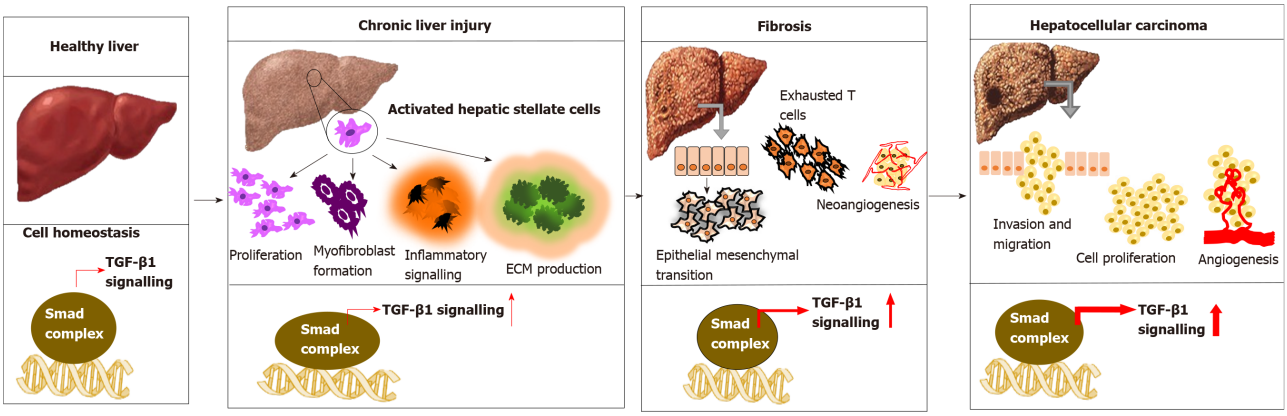

DOI: 10.3748/wjg.v28.i36.5250 **Copyright** ©The Author(s) 2022.

Figure 1 Involvement of transforming growth factor-beta 1 in various stages of liver dysfunction. Transforming growth factor-beta (TGF-β) regulates cell homeostasis in normal physiological conditions. As an inflammatory-fibrogenic cytokine molecule, the involvement of TGF-β1 in all phases of liver injury, from fatty liver, steatosis, fibrosis to cirrhosis, and hepatocellular carcinoma, is evident. Causative agents like viral infection, alcohol and co-morbidities like diabetes and obesity trigger the release of a pro-inflammatory cytokine such as TGF-β1, which stimulates inflammation, extracellular matrix (ECM) production, and accumulation of fibrous material that eventually progress to cirrhosis. As the fibrosis continues, the interaction of overexpressed TGF-β1 with integrins and other ECM proteins can alter signaling, accumulate gene mutation, and induce epithelial-mesenchymal transition and hepatocarcinogenesis. TGF: Transforming growth factor; ECM: Extracellular matrix; HCC: Hepatocellular carcinoma.

induced rat hepatoma model is used to investigate the association of TGF-β1 expression with different stages of hepatocarcinogenesis and a progressive elevation of hepatic TGF-β1 and TGF-β1 mRNA was found during the transformation of hepatocytes to malignant cells[51]. Another study indicates that elevated plasma TGF-β1 level was found in 89.5% of HCC patients, and interestingly, among these patients, 93.3% had an AFP level less than 400 μg/L[52]. This suggested that TGF-β1 expression can be a more accurate and sensitive biomarker for early diagnosis of HCC for monitoring the disease progression.

The diagnostic importance of TGF-β1 is established significantly earlier itself. In 1997, Tsai *et al*[53] investigated the correlation of urine TGF-β1 level with HCC. They found a significant increase in TGF-β 1 level in HCC patients compared with other healthy control groups, cirrhotic chronic hepatitis patients. They also reported the association of TGF-β 1 levels with poor prognosis and shorter survival[53]. Later, the same team compared the study with another important tumor marker, AFP, and found that disease progression from cirrhosis to HCC is characterized by a typical elevation in both urinary TGF-β1 and serum AFP with a diagnostic accuracy of about 90%[54,55]. These collective data suggest the potential of TGF-β1 be used along with AFP as a complementary tumor marker to differentiate HCC from cirrhosis correctly. Another study investigated the rationale for parallel determination of TGF-β1 and AFP to diagnose HCC. They found that the TGF-β1 level exhibited a stage-dependent increase in all liver diseases where AFP showed HCC-specific elevation[56]. As TGF-β1 estimation tracks the disease progression pattern, TGF-β can be considered a more sensitive diagnostic marker of HCC. Its specificity is higher when it is analyzed along with AFP. To diagnose and select patients for galunisertib (TGF-β inhibitor) therapy, Cao *et al*[57] in 2017 performed next-generation sequencing-based analysis in HCC samples and found that m RNA levels of TGF-β1 along with SKIL and PMEPA1 could be better diagnostic markers as well as to select patients who are more likely to respond with galunisertib.

Another study investigated the association of serum TGF-β1 with disease severity in HCC using 180 subjects in different stages of HCC. Group of cirrhotic patients, as well as healthy control, was also maintained. Consistent with the previous reports, this study also found a significant increase in TGF-β1 level in HCC (1687.47 ± 1462.81 pg/mL) as compared with cirrhotic patients (487.98 ± 344.23 pg/mL) and control (250.16 ± 284.16 pg/mL). Additionally, the serum level of TGF-β1 showed exponential elevation as the disease progressed from early to advanced, *i.e.*, during progression from Barcelona Clinic Liver Cancer stage A to D, TGF-β 1 level increased from 652.83-1668.78 pg/mL[56]. The best cut-off value of TGF-β1 detection was determined as 301.9 pg/mL, comparable with the value (370 pg/mL) reported by Shehata *et al*[58] (Table 1).

Background inflammation and indolent transformation are the critical factors that create a waiting time paradox in diagnosing HCC, making the tumor more aggressive and refractory. Since TGF-β, specifically TGF-β1 plays an essential function from the initial hepatic injury to hepatocarcinogenesis, it holds immense potential to validate as a diagnostic marker of HCC. Though the dual functioning of TGF-β1 is still debatable, the diagnostic relevance of TGF-β1 is well evident, and thus, it warrants further investigations and clinical validation.

Table 1 Research progress on the clinical utility of transforming growth factor-beta 1 as diagnostic marker against hepatocellular carcinoma

Ref.	Sample size HCC/control	Assay type	TGF-β1 level	Sample type	Outcome of the study
[60, 61]	26/20	ELISA	Control: 1.4 ± 0.8 ng/mL HCC: 19.3 ± 1.95 ng/mL (P < 0.05)	Plasma	TGF-β1 level showed a progressive elevation from cirrhotic to HCC patients to normal subjects. No significant association was found between plasma TGF-β1 and serum AFP levels
[62, 63]	70	ELISA	Control: 2.7 ± 0.7 ng/mL HCC: 7.3 ± 4.3 ng/mL (P < 0.05)	Plasma	Elevated plasma TGF-β1 levels in HCC patients are associated with increased tumor size, overexpression of tissue inhibitor of metalloproteinase-1 and tumor severity
[54, 55]	94/50	^{125}I-Radio Immuno Assay Kit	Control: 1.5-33.6 μg-^{1} creatinine Cirrhotic: 4.3-52.5 μg^{-1} creatinine HCC: 3.5-184 μg^{-1} creatinine (P < 0.0001)	Urine	Urinary TGF-β1 and serum AFP levels were higher in HCC than in cirrhotic patients. The study suggested that both TGF-β and AFP can be used as complementary biomarkers to distinguish between HCC and cirrhosis
[64]	54/30	ELISA	TGF-β1 score Control: 0.6 ± 0.2 HCC: 1.6 ± 0.5	Serum	The study team calculated the serum concentration score based on the cut-off limit of 74 pg/mL and 637 pg/mL for TGF-β1 and sFas, respectively. TGF-β1 levels were higher than the cut off value in 23% HCC patients with negative AFP values, suggesting its diagnostic potential in AFP negative HCC
[65]	38/23	ELISA	Control: 300 pg/mL HCC: 954.9 pg/mL (P < 0.0001)	Plasma	Elevated plasma TGF-β1 level can be a useful diagnostic marker in detecting small HCC, with higher sensitivity than AFP
[66]	70/32	ELISA	Control: 2 ng/mL HCC: 7.5 ng/mL (P < 0.0001)	Plasma	Higher circulating TGF-β1 in HCC patients is associated with suppression of anti-tumor immunity and disease progression
[52]	50/30	ELISA	Control: 0.67 ± 0.1 μg/mL HCC: 2.21 ± 1.1 μg/mL (sensitivity = 89.5%, specificity = 94%)	Serum	Aberrant TGF-β1 expression in HCC is associated with differentiation and worsening of HBV infection
		RT-PCR	Overexpression TGF-β1 mRNA in HCC patients, P < 0.0001		Circulating TGF-β1 level and TGF-β1 mRNA expression can be used as sensitive biomarkers for diagnosing HBV induced HCC
[56]	23/40	ELISA	Control: 14.35 ± 8.76 ng/mL HCC: 64.35 ± 33.68 ng/mL (P < 0.05)	Serum	TGF-β1 is a sensitive diagnostic marker for HCC than AFP. Specificity can be increased with combined evaluation of TGF-β1 and AFP levels
[67]	54/30	ELISA	Control: 39.5 ± 9.8 pg/mL HCC: 1194 ± 331 pg/mL (P < 0.0001)	Serum	The study suggested elevated TGF-β1 and EGFR levels as reliable diagnostic markers for HCC induced, AFP negative HCC
[68]	120/30	ELISA	Control: 250.16 ± 284.61 pg/mL Cirrhotic: 487.98 ± 344.23 pg/mL HCC: 1687.47 ± 1642 pg/mL (P < 0.0001)	Serum	TGF-β1 showed progressive elevation during various stages of liver dysfunction. Higher TGF-β1 level in HCC is associated with tumor grade, pathological stage and invasiveness
[69]	100/36	ELISA	Control: 57.29 ± 11.70 ng/mL HCC: 225.82 ± 48.93 ng/mL (P < 0.0001)	Serum	Serum levels of TGF-β were significantly higher in HCC patients than in normal controls

ELISA: Enzyme-linked immunosorbent assay; RT-PCR: Reverse transcription-polymerase chain reaction; HCC: Hepatocellular carcinoma; TGF-β: Transforming growth factor-beta; AFP: Alpha fetoprotein; HBV: Hepatitis B virus; EGFR: Epidermal growth factor receptor.

The clinical utility of TGF-β1 as a prognostic marker of HCC

Poor prognostic characteristics of HCC contribute to late detection, aggressiveness and failure of therapeutic interventions[70]. Molecular pathways of hepato-carcinogenesis are still confusing because of the involvement of diverse molecular pathways, genetic alterations and evolution of malignant cells. Thus, this ultimately results in the worst prognosis within the early stage itself[71]. The expression of TGF-β1 is remarkably increased at the advanced stages of HCC and is involved in initiating EMT, regulating tumor proliferation, and promoting immunosuppressive tumor microenvironment during HCC progression under the challenges like liver cirrhosis, HBV and HCV infections. This warrants screening TGF-β1 levels from the early stages of HCC as a tool for evaluating the clinical outcomes. Depending upon the expression profile of TGF-β1, it is effortless to estimate the clinical impact of therapeutic strategies[72].

A research study conducted by Giannelli *et al*[73] proposed that TGF-β1 promotes EMT by stimulating homologous proteins like snail and slug. Secretion of TGF-β1 by HCC invasive cell lines, especially cell lines with α3β1-integrin expression, is significantly higher than in non-invasive and cirrhotic cell lines. The patients at the initial and advanced stages of HCC with a higher profile of TGF-β 1 possess a poor prognostic ratio with lower overall survival (OS) and disease-free survival rate (DFS) [73,74]. Likewise, another notable experimental study by Lee *et al*[75] demonstrated that plasma TGF-β1 is positively correlated with critical conditions like EHM, portal vein thrombosis, EHM, and regional lymph node involvement. Statistical studies involving the detailed examination of overall and cumulative survival rates of HCC patients showed that candidates with abundant levels of plasma TGF-β1 manifested remarkably lower survival rates than the candidates with lower expression of TGF-β1. This evidence points to the usefulness of TGF-β1 as a prognostic marker in HCC.

Wang *et al*[76] elucidated the crucial involvement of TGF-β1 in tumor progression. A total of 180 patients with HCC were selected for the study, and out of 180 HCC patients, 105 patients were found with a solid expression of TGF-β1. This study showed a positive correlation between TGF-β1 and Treg cells. The increased secretion of TGF-β1 at the starting stage of HCC indicates that the tumor may be one of the most critical sources of TGF-β1 in HCC patients. Earlier studies also provided evidence that TGF-β1 promotes the regulatory phenotype and modulates the biological functions of Tregs. By Kaplan-Meier evaluation, HCC patients overexpressing TGF-β1 in neoplastic tissues had a considerably shorter OS and a greater recurrence rate than patients with lower expression[76]. A meta-analysis study conducted by Peng *et al*[77] reported that TGF-β1 implements an unfavorable prognosis on OS rates of HCC patients with a hazard ratio of about 1.71 and 2.29 from both univariate and multivariate analysis. Additionally, the study indicates the worst prognosis of TGF-β1 upon DFS, relapse-free survival and progression-free survival of 1422 patients *via* COX univariate analysis with a hazard ratio of about 1.60. In summary, the results from these studies draw out the negative prognostic impact of high TGF-β1 expression on the OS in HCC patients.

TGF-β1 possesses a dual functional role in malignancy; initially, it acts by blocking epidermal growth and promoting tumor suppression, but in later stages, it appears to be involved in the up-gradation of advanced tumors[78]. Embryonic liver fodrin (ELF), a novel form of β-spectrin is involved as a Smad3/4 adaptor in TGF-β mediated tumor suppression signaling pathway. Miscolocalization of Smad3 and Smad4 caused by the dysregulation of ELF resulted in the disruption of TGF- β signaling pathways[79]. A research study conducted by Ji *et al*[80] investigated the predictive value of both TGF-β1 and ELF in HCC patients after hepatic resection. The expression of TGF-β1 is significantly higher in HCC tissues than in normal liver tissues, while the incidence of ELF is higher in normal liver tissue in contrast with HCC samples. The reports of post-operative survival rates of HCC patients with lower expressions of TGF-β1 showed that DFS and OS rates of HCC patients over 1 (79.4%), 3 (73.5%), and 5 (62.0%) years were significantly higher than the patients with higher expression of TGF-β1 (28.0%, 12.0%, and 12.0%). The study also showed a negative correlation between TGF-β1 and ELF levels. The study also indicates that DFS rates of HCC patients with higher expression of ELF and lower TGF-β1 levels are remarkably more elevated than the HCC patients with low expression of ELF and higher TGF-β1 levels for 1, 3, and 5 years (75.0%, 60.0%, and 57.5% *vs* 25.0%, 15.9%, and 10.2%, respectively), with *P*-value less than 0.001. Data from clinicopathological examination exhibited that TGF-β1 positively relates with hepatitis B surface antigen, tumor size, tumor number, TNM, and recurrence, while ELF is negatively correlated with all metastatic characteristics suggesting that ELF is associated with tumor suppressing features. This research study indicates that both TGF-β1and ELF can be included in the category of relevant biomarkers as prognostic agents for evaluating clinical results after hepatic resection[80].

An experimental approach described the correlation and the possibility of Fibroblast growth factor (FGF) receptor 4 (FGFR4) and TGF-β1 as prognostic biomarkers in HCC. FGFR4 is the most predominant isoform of the FGFRs family and is actively involved in various biological activities, including metastasis, differentiation, embryonic development, proliferation, apoptosis and angiogenesis [81]. Multiple studies showed that FGFR4 plays a clear-cut role in the pathogenesis of HCC and the up-regulation of FGFR4 possesses resistance to various targeted therapies[82]. A clinicopathological examination conducted by Chen *et al*[83] showed that elevated expression of both TGF-β1 and FGFR4 enhances tumors' invasiveness and metastatic nature. Clinicopathologic characteristics revealed that HCC patients at advanced stages with high TGF-β1 and FGFR4 expression were more likely to be at a higher TNM stage. Statistical data showed that the OS of patients over five-year survival rate is about

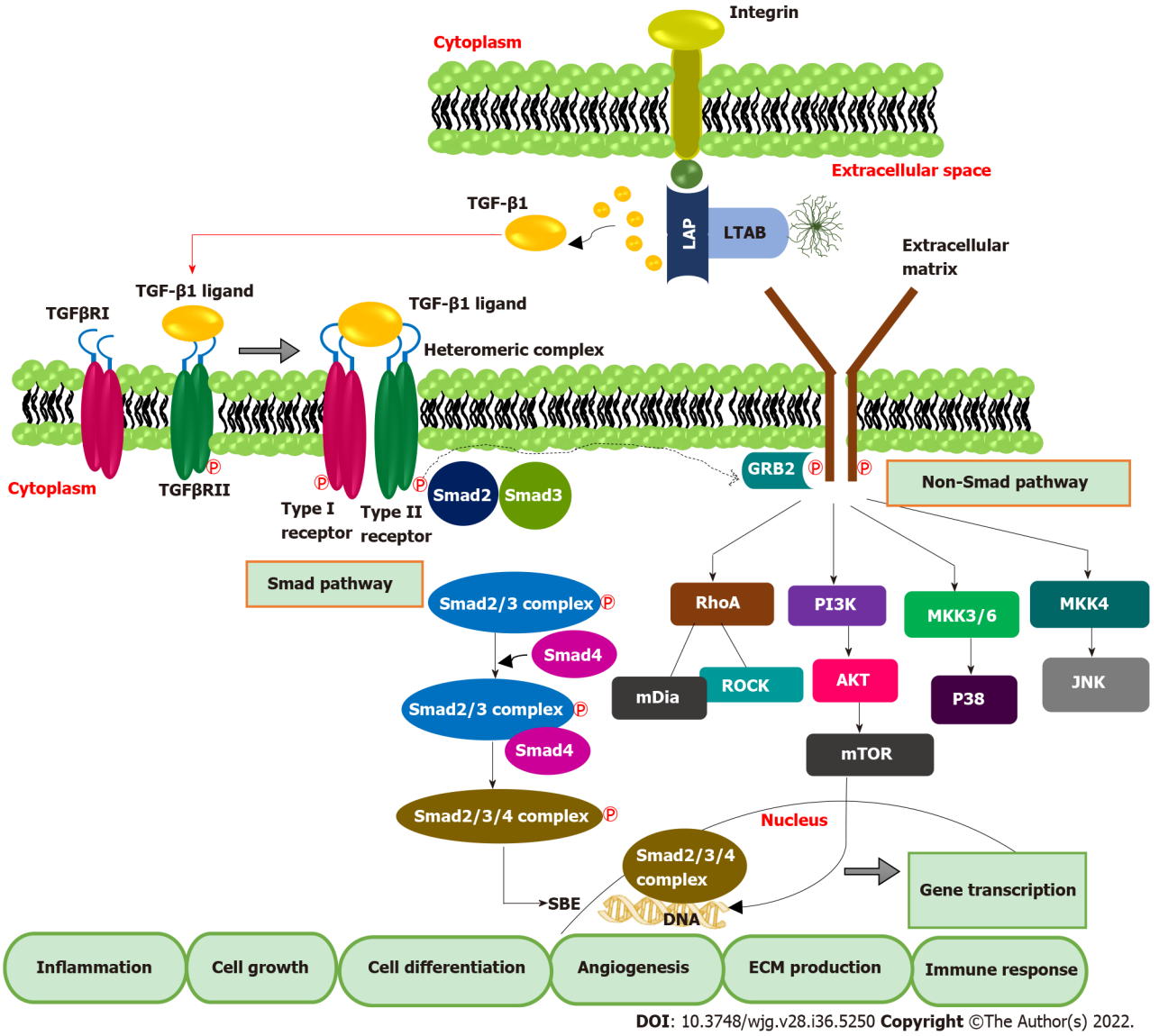

DOI: 10.3748/wjg.v28.i36.5250 **Copyright** ©The Author(s) 2022.

Figure 2 Transforming growth factor-beta 1 signaling pathway. Smad and non-Smad pathways mainly regulate transforming growth factor-beta 1 (TGF-β 1) signal transduction. Integrin signaling triggers the activation and release of TGF-β1 from LCC (large latent complex). Activated TGF-β1 binds TGF-β type II receptor, leading to phosphorylation of TGF-β type I receptor and associated Smad proteins, mainly Smad-2 and Smad-3. Phosphorylated Smad-2 and 3, complex with the co-Smad, Smad-7, form a ternary complex. This ternary complex then translocates into the nucleus, binds to Smad binding elements and regulates the transcription of TGF-β-related genes. TGF: Transforming growth factor; LAP: Latency associated protein; LTAB: Latent transforming growth factor-beta binding protein; SBE: Smad binding elements; ECM: Extracellular matrix; mTOR: Mammalian target of Rapamycin; PI3K: Phosphoinositide 3-kinase; AKT: AKT serine/threonine kinase 1; MKK: Mitogen-activated protein kinase kinase; JNK: C-Jun N-terminal kinase.

8.5%, and the median survival duration is 32.3 mo in case of TGF-β1 positive cases. In contrast, in TGF-β 1 negative expression cases, the OS of the patient is about 45.6% and the median survival rate is 50.4 mo. Candidates with high TGF-β1 expression had a short OS rate in contrast to those with negative TGF-β1 expression profiles. Likewise in cases of high levels of FGFR4, the OS rate of patients is very low, that is five-year survival rate is only about 8.3%, and median survival rate is 29.4 mo while in the condition of impeded FGFR4 expression, the five-year survival rate is about 70.1% and the median survival period is 51.2 mo. This study showed a positive correlation between TGF-β1 and FGFR4 as prognostic markers in HCC. Additionally, the results from univariate and multivariate analyses showed that both TGF-β1 and FGFR4 are independent and reliable prognostic factors in HCCs for evaluating the therapeutic response in HCC patients, especially after post-operative procedures[83]. The strong correlation between TGF-β1 expression and survival rates of HCC patients suggests its potential as a prognostic biomarker for HCC (Table 2). In addition to the role of TGF-β1 as an effective prognostic marker, it can also be used for targeted therapeutic strategies.

The clinical utility of TGF-β1 as therapeutic target in HCC

Tyrosine kinase inhibitor, Sorafenib was the first approved first-line therapy for advanced HCC. Sorafenib was the first-line therapy for ten years until another tyrosine kinase inhibitor, Levatinib was

Table 2 Research progress on the clinical utility of transforming growth factor-beta 1 as a prognostic marker against hepatocellular carcinoma

Ref.	Sample size HCC/control	Sample and assay type	TGF-β1 level	Survival rate (%), (patients with higher TGF-β1 *vs* patients with lower TGF-β1)	Outcome of the study
[75]	571/551	Plasma ELISA	Control: 3.58 ± 0.17 $\log_{10}$ pg/mL Cirrhotic: 3.20 ± 0.37 $\log_{10}$ pg/mL HCC: 3.83 ± 0.31 $\log_{10}$ pg/mL	1 yr survival (47 *vs* 60) 3 yr survival (28 *vs* 36) $P < 0.05$	Plasma TGF-β1 levels showed a positive correlation with tumor size, invasion and extrahepatic metastasis and inversely correlated with survival rates in HCC patients
[83]	126	Tumor tissue Immunohistochemistry	84% samples (106/126) showed high intra-tumoral TGF-β1 expression 64.3% samples (81/126) showed high peri-tumoral TGF-β1 expression	5 yr survival (8.5 *vs* 45.6)	TGF-β1 and FGFR4 were positively correlated in HCC tumor tissues and showed a significant association with shorter survival rates in patients
[80]	84/20	Tumor tissue Immunohistochemistry	TGF-β1 overexpression found in 59.5% samples (50/84) than that of normal liver tissue	1 yr survival (28 *vs* 79.4) 5 yr survival (12 *vs* 62.6)	TGF-β1 expression was dominant, whereas ELF expression was suppressed in HCC tissues Patients with high TGF-β1 and lower ELF expression are associated with poor overall survival and post-operative disease free survival compared with low TGF-β1 and high ELF group
[76]	184/30	Plasma and tumor tissue ELISA and immunohistochemistry	Elevated plasma TGF-β1 level TGF-β1 was strongly stained in tumor tissue	2 yr survival (51 *vs* 77) 3 yr survival (4 *vs* 68), $P < 0.05$	Higher TGF-β1 expression in tumor tissues triggers Treg cells mediated immunosuppression in tumor microenvironment and contribute to poor prognosis in HCC
[84]	40	Serum ELISA	Before RFA: 63.22 ± 23.61 ng/mL After RFA: 56.33 ± 24.24 ng/mL	NA	Radiofrequency ablation lowered TGF-β1 and AFP L3% expression in HCC patients Low TGF-β1 and AFP L3% levels were observed in the no recurrence group, suggesting its potential as prognostic markers for HCC

ELISA: Enzyme-linked immunosorbent assay; HCC: Hepatocellular carcinoma; TGF-β: Transforming growth factor-beta; AFP: Alpha feto protein; ELF: Embryonic liver fodrin; FGFR: Fibroblast growth factor receptor 4.

approved in 2018. Even though tyrosine kinase inhibitors dominated HCC therapy as first-line or second-line options, the efficacy was only modest, with limited treatment outcome, the emergence of drug resistance, and also relapse[85]. Recently treatment strategies adopted a paradigm shift to immunotherapeutic approaches because of the importance of the immune microenvironment in carcinogenesis.

The liver is the most extensive reticuloendothelial system and peripheral immunomodulatory organ in the human body. Immunotherapy is being extensively evaluated in liver cancer[86]. The liver constitutes a vast repository of immune cells including NK cells, kupffer cells, sinusoidal endothelial cells, and innate T cells[87]. Aberrant immune checkpoint activation makes HCC a cold tumor, where anti-tumor immune surveillance is completely abolished[88]. Combination of immune checkpoint inhibitors (ICIs) such as Nivolumab (PD-1 inhibitor) + Ipilimumab (CTLA4 inhibitor) and Atezolizumab (PD-L1 inhibitor) + Bevacizumab [vascular endothelial growth factor (VEGF) inhibitor] got approval as first-line therapy for various cancer such as non-small cell lung cancer (NSCLC), HCC in 2020[89]. Though ICIs exerted a superior effect to tyrosine inhibitors, current immunotherapeutic drugs failed to establish an effective anticancer immunity against HCC. Though the immunotherapeutic approaches modify effector immune cells functions to elicit anti-tumor immune response, the immunosuppressive tumor microenvironment neutralizes the effects of immunotherapy[90].

Analysis of the TGF-β profile of HCC samples in the TGCA data set revealed four categories with typical TGF-β expression[91]. The cluster with a highly activated TGF-β signature, which accounts for 14.5% of samples, exhibited prominent immune exhaustion and poor prognosis. ICIs may not work well in this cluster. Additionally, anti-inflammatory/anti-fibrotic agents targeting TGF-β can improve the

Table 3 Clinical trials of transforming growth factor-beta 1 blockade with Galunisertib in hepatocellular carcinoma and other cancers

Drug	Title of the study	Treatment	Phase	Status	Trial ID
Galunisertib	A study of Galunisertib on the immune system in participants with cancer	Monotherapy	Phase I	Completed	NCT02304419
Galunisertib	Galunisertib (LY2157299) and stereotactic body radiotherapy in advanced hepatocellular carcinoma	Combination with radiotherapy	Phase I	Completed	NCT02906397
Galunisertib	A study of LY2157299 in participants with unresectable hepatocellular cancer	Combination with Nivolumab	Phase II	Completed	NCT02423343
Galunisertib	A study of LY2157299 in participants with unresectable hepatocellular cancer	Combination with Sorafenib	Phase I	Completed	NCT02240433
Galunisertib	A study of LY2157299 in participants with advanced hepatocellular carcinoma	Combination with Sorafenib	Phase II	Completed	NCT02178358
Galunisertib	A study of LY2157299 in participants with hepatocellular carcinoma	Combination with Sorafenib/Ramucirumumab	Phase II	Completed	NCT01246986
Galunisertib	Galunisertib and Capecitabine in advanced resistant TGF-beta activated colorectal cancer (EORTC1615)	Combination with Capecitabine	Phase II	Withdrawn	NCT03470350
Galunisertib	A study of LY2157299 in participants with pancreatic cancer (advanced or has spread to another part of the body)	Combination with Gemcitabine	Phase I	Completed	NCT02154646
Galunisertib	A study of Galunisertib (LY2157299) and Durvalumab (MEDI4736) in participants with metastatic pancreatic cancer	Combination with Durvalumab	Phase I	Completed	NCT02734160

TGF: Transforming growth factor.

immune milieu[92,93]. The majority of HCC samples belong to a cluster of activated TGF-β signature (45%) and showed a low level of an immune response. Hence, combining a TGF-β inhibitor with an immune checkpoint inhibitor can exert a synergistic effect. 30% of HCC samples showed a normal TGF-β signature associated with active immune surveillance; therefore, immunotherapy will be most suitable for this cluster. The fourth cluster is a minor population (9.9%) that exhibits inactivated TGF-β signature with poor immune cell activation and response[94]. With this evidence, it is clear that TGF-β1 signature can be used to decide the suitable therapy or predict the outcome of immunotherapy.

Several specific and non-specific inhibitors of TGF-β, mainly TGF-β1 and 2 inhibitors, are being developed and evaluated against various tumors, including HCC. Regarding non-specific inhibitors, as the primary molecular target is different, its ability to block the TGF-β pathway offers additional benefits as anticancer agents. One such example is Halofuginone, an alkaloid coccidiostat with reported preclinical activity against HCC. In addition to the prominent inhibition of collagen synthesis, Halofuginone also blocks TGF-β1, inhibits ECM formation and fibroblast proliferation, increases IFN-γ and anti-tumor immune response[95,96]. The effect of Halofuginone against advanced progressive solid tumor has been evaluated in phase I clinical trial (NCT00027677), and in 2000, United States Food and Drug Administration gave orphan drug approval status to Halofuginone for treatment of scleroderma [97]. Histone deacetylase exerts epigenetic regulation of TGF-β1 mediated fibrosis and carcinogenesis [98]. Studies indicate that histone deacetylase inhibitors such as Panobinostat have shown effectiveness in HCC animal models and phase I human trials combined with sorafenib (NCT00823290)[99]. Apart from the non-specific inhibitors, recent preclinical interventions combined TGF-β1 targeting antibodies or TGF-βR1 inhibitor with PD-L1 inhibitors and obtained prominent cytotoxic effect and anticancer immune surveillance in various solid tumors[100,101]. Likewise, M7824 is a bifunctional fusion protein with dual targeting of PD-L1 and TGF-β, which has been evaluated in animal models of various cancers either alone or in combination with vaccines[102]. M7824 exerted a significant inhibitory effect on TGF-β 1[103]. Among the different TGF-β inhibitors, LY2109761 is an orally bioavailable TGF-β receptor type I inhibitor, which exhibited an antitumor effect in various HCC animal models[104]. LY2109761 inhibited TGF-β1 induced migration, invasion, and anoikis in HCC cells[105,106]. Another study suggested the anti-angiogenic potential of LY2109761, which was superior to the typical VEGF inhibitor, Bevacizumab, and the effect was mediated by suppression of VEGF through inhibition of Smad dependent TGF-β1 signaling[107,108]. In addition to this, anti-TGF-β agents targeting other isoforms are also developed. AP-12009 is a TGF-β2 specific antisense oligonucleotide in a clinical trial to treat glioma and anaplastic astrocytoma[109,110]. Likewise, TGF-β1 directed mRNA was developed as AP-11011, which is evaluated against NSCLC, colon cancer in preclinical models[111]. Lordelimumab is a TGF-β2 specific monoclonal antibody with an anti-fibrotic effect[112]. Many preclinical studies investigated different TGF-β inhibitors, yet, Galunisertib (LY2157299), a kinase inhibitor of TGF-β1, is only the one in current clinical trials[113]. Several clinical trials of Galunisertib are ongoing or completed either alone or combined with Sorafenib, ICIs, and alkylating agents (Table 3).

CONCLUSION

TGF-β1 exerts a unique regulatory power on inflammation, fibrogenesis, and immune response in HCC. Among other TGF-β isoforms, significant and progressive expression of TGF-β1 during the entire course of HCC pathogenesis, starting from chronic hepatitis to HCC makes it a sensitive and accurate diagnostic marker of HCC. The specificity and sensitivity of TGF-β1 based diagnosis of HCC by parallel estimation of serum AFP. Even after establishing HCC, TGF-β1 continues to elevate as HCC progresses and is associated with poor prognosis and shorter survival. Since TGF-β1 is the master regulator of the immunosuppressive tumor milieu in HCC, TGF-β1 inhibition could sensitize ICI, tyrosine kinase inhibitors, and other systemic or curative interventions. HCC remains the deadliest-refractory tumor predominantly due to its delayed diagnosis. In that context, TGF-β1 is relevant for early diagnosis, prognosis, and therapy. Even though a plethora of supporting evidence is available, still TGF-β1 is not much studied and evaluated compared with other markers such as AFP. Notably, the dichotomic nature of TGF-β signaling in HCC needs to be defined accurately to establish the clinical utility of TGF-β1. Thus, proper and careful determination of the TGF-β1 profile of patients is necessary to choose the suitable patients for TGF-β1 targeted therapy.

FOOTNOTES

Author contributions: Nath LR conceptualized, designed the review content and revised the draft; Devan AR wrote the draft; Pavithran K revised and proofread; Nair B and Murali M collected the data; and all authors have read and approved the final manuscript.

Supported by the Amrita Vishwa Vidyapeetham SEED grant (K-PHAR-22-662).

Conflict-of-interest statement: All the authors report no relevant conflicts of interest for this article.

Country/Territory of origin: India

ORCID number: Aswathy R Devan 0000-0001-8928-8191; Keechilat Pavithran 0000-0002-6129-5709; Bhagyalakshmi Nair 0000-0002-0364-881X; Maneesha Murali 0000-0003-2772-3930; Lekshmi R Nath 0000-0002-7726-7219.

S-Editor: Wang JJ
L-Editor: A
P-Editor: Wang JJ

REFERENCES

1 **McGlynn KA**, Petrick JL, El-Serag HB. Epidemiology of Hepatocellular Carcinoma. *Hepatology* 2021; **73** Suppl 1: 4-13 [PMID: 32319693 DOI: 10.1002/hep.31288]
2 **Patel N**, Yopp AC, Singal AG. Diagnostic delays are common among patients with hepatocellular carcinoma. *J Natl Compr Canc Netw* 2015; **13**: 543-549 [PMID: 25964640 DOI: 10.6004/jnccn.2015.0074]
3 **Bialecki ES**, Di Bisceglie AM. Diagnosis of hepatocellular carcinoma. *HPB (Oxford)* 2005; **7**: 26-34 [PMID: 18333158 DOI: 10.1080/13651820410024049]
4 **Cervello M**, McCubrey JA, Cusimano A, Lampiasi N, Azzolina A, Montalto G. Targeted therapy for hepatocellular carcinoma: novel agents on the horizon. *Oncotarget* 2012; **3**: 236-260 [PMID: 22470194 DOI: 10.18632/oncotarget.466]
5 **Suresh D**, Srinivas AN, Kumar DP. Etiology of Hepatocellular Carcinoma: Special Focus on Fatty Liver Disease. *Front Oncol* 2020; **10**: 601710 [PMID: 33330100 DOI: 10.3389/fonc.2020.601710]
6 **Llovet JM**, Kelley RK, Villanueva A, Singal AG, Pikarsky E, Roayaie S, Lencioni R, Koike K, Zucman-Rossi J, Finn RS. Hepatocellular carcinoma. *Nat Rev Dis Primers* 2021; **7**: 6 [PMID: 33479224 DOI: 10.1038/s41572-020-00240-3]
7 **Kumari R**, Sahu MK, Tripathy A, Uthansingh K, Behera M. Hepatocellular carcinoma treatment: hurdles, advances and prospects. *Hepat Oncol* 2018; **5**: HEP08 [PMID: 31293776 DOI: 10.2217/hep-2018-0002]
8 **Cuestas ML**, Oubina JR, Mathet VL. Hepatocellular carcinoma and multidrug resistance: Past, present and new challenges for therapy improvement. *World J Pharmacol* 2015; **4**: 96-116 [DOI: 10.5497/wjp.v4.i1.96]
9 **Devan AR**, Kumar AR, Nair B, Anto NP, Muraleedharan A, Mathew B, Kim H, Nath LR. Insights into an Immunotherapeutic Approach to Combat Multidrug Resistance in Hepatocellular Carcinoma. *Pharmaceuticals (Basel)* 2021; **14** [PMID: 34358082 DOI: 10.3390/ph14070656]
10 **Prud'homme GJ**. Pathobiology of transforming growth factor beta in cancer, fibrosis and immunologic disease, and

therapeutic considerations. *Lab Invest* 2007; **87**: 1077-1091 [PMID: 17724448 DOI: 10.1038/Labinvest.3700669]
11 **Fabregat I**, Moreno-Càceres J, Sánchez A, Dooley S, Dewidar B, Giannelli G, Ten Dijke P; IT-LIVER Consortium. TGF-β signalling and liver disease. *FEBS J* 2016; **283**: 2219-2232 [PMID: 26807763 DOI: 10.1111/febs.13665]
12 **Katz LH**, Likhter M, Jogunoori W, Belkin M, Ohshiro K, Mishra L. TGF-β signaling in liver and gastrointestinal cancers. *Cancer Lett* 2016; **379**: 166-172 [PMID: 27039259 DOI: 10.1016/j.canlet.2016.03.033]
13 **Ikushima H**, Miyazono K. TGFbeta signalling: a complex web in cancer progression. *Nat Rev Cancer* 2010; **10**: 415-424 [PMID: 20495575 DOI: 10.1038/nrc2853]
14 **Li MO**, Flavell RA. TGF-beta: a master of all T cell trades. *Cell* 2008; **134**: 392-404 [PMID: 18692464 DOI: 10.1016/j.cell.2008.07.025]
15 **Huang J**, Qiu M, Wan L, Wang G, Huang T, Chen Z, Jiang S, Li X, Xie L, Cai L. TGF-β1 Promotes Hepatocellular Carcinoma Invasion and Metastasis *via* ERK Pathway-Mediated FGFR4 Expression. *Cell Physiol Biochem* 2018; **45**: 1690-1699 [PMID: 29490293 DOI: 10.1159/000487737]
16 **Yang AT**, Hu DD, Wang P, Cong M, Liu TH, Zhang D, Sun YM, Zhao WS, Jia JD, You H. TGF-β1 Induces the Dual Regulation of Hepatic Progenitor Cells with Both Anti- and Proliver Fibrosis. *Stem Cells Int* 2016; **2016**: 1492694 [PMID: 26839553 DOI: 10.1155/2016/1492694]
17 **Nair B**, Nath LR. Inevitable role of TGF-β1 in progression of nonalcoholic fatty liver disease. *J Recept Signal Transduct Res* 2020; **40**: 195-200 [PMID: 32054379 DOI: 10.1080/10799893.2020.1726952]
18 **Siegel PM**, Massagué J. Cytostatic and apoptotic actions of TGF-beta in homeostasis and cancer. *Nat Rev Cancer* 2003; **3**: 807-821 [PMID: 14557817 DOI: 10.1038/nrc1208]
19 **Caja L**, Ortiz C, Bertran E, Murillo MM, Miró-Obradors MJ, Palacios E, Fabregat I. Differential intracellular signalling induced by TGF-beta in rat adult hepatocytes and hepatoma cells: implications in liver carcinogenesis. *Cell Signal* 2007; **19**: 683-694 [PMID: 17055226 DOI: 10.1016/j.cellsig.2006.09.002]
20 **Bedossa P**, Peltier E, Terris B, Franco D, Poynard T. Transforming growth factor-beta 1 (TGF-beta 1) and TGF-beta 1 receptors in normal, cirrhotic, and neoplastic human livers. *Hepatology* 1995; **21**: 760-766 [PMID: 7875675 DOI: 10.1002/hep.1840210325]
21 **Zhu T**, Zhang L, Li C, Tan X, Liu J, Huiqin Li, Fan Q, Zhang Z, Zhan M, Fu L, Luo J, Geng J, Wu Y, Zou X, Liang B. The S100 calcium binding protein A11 promotes liver fibrogenesis by targeting TGF-β signaling. *J Genet Genomics* 2022; **49**: 338-349 [PMID: 35240304 DOI: 10.1016/j.jgg.2022.02.013]
22 **Inagaki Y**, Okazaki I. Emerging insights into Transforming growth factor beta Smad signal in hepatic fibrogenesis. *Gut* 2007; **56**: 284-292 [PMID: 17303605 DOI: 10.1136/gut.2005.088690]
23 **Friedman SL**. Mechanisms of hepatic fibrogenesis. *Gastroenterology* 2008; **134**: 1655-1669 [PMID: 18471545 DOI: 10.1053/j.gastro.2008.03.003]
24 **Levine D**, Rockey DC, Milner TA, Breuss JM, Fallon JT, Schnapp LM. Expression of the integrin alpha8beta1 during pulmonary and hepatic fibrosis. *Am J Pathol* 2000; **156**: 1927-1935 [PMID: 10854216 DOI: 10.1016/s0002-9440(10)65066-3]
25 **Mikula M**, Proell V, Fischer AN, Mikulits W. Activated hepatic stellate cells induce tumor progression of neoplastic hepatocytes in a TGF-beta dependent fashion. *J Cell Physiol* 2006; **209**: 560-567 [PMID: 16883581 DOI: 10.1002/jcp.20772]
26 **Wang J**, Xiang H, Lu Y, Wu T. Role and clinical significance of TGFβ1 and TGFβR1 in malignant tumors (Review). *Int J Mol Med* 2021; **47** [PMID: 33604683 DOI: 10.3892/ijmm.2021.4888]
27 **Padua D**, Massagué J. Roles of TGFbeta in metastasis. *Cell Res* 2009; **19**: 89-102 [PMID: 19050696 DOI: 10.1038/cr.2008.316]
28 **Heldin CH**, Moustakas A. Role of Smads in TGFβ signaling. *Cell Tissue Res* 2012; **347**: 21-36 [PMID: 21643690 DOI: 10.1007/s00441-011-1190-x]
29 **Moustakas A**, Heldin CH. Non-Smad TGF-beta signals. *J Cell Sci* 2005; **118**: 3573-3584 [PMID: 16105881 DOI: 10.1242/jcs.02554]
30 **Massagué J**. TGFβ signalling in context. *Nat Rev Mol Cell Biol* 2012; **13**: 616-630 [PMID: 22992590 DOI: 10.1038/nrm3434]
31 **Johnson LD**, Auer R. Commentary on: Jiang B, Zhu F, Cao L, Presley BR, Shen MS, Yang KH. Computational study of fracture characteristics in infant skulls using a simplified finite element model. J Forensic Sci 2017;62(1):39-49. *J Forensic Sci* 2018; **63**: 345-348 [PMID: 29314009 DOI: 10.1111/1556-4029.13706]
32 **Konkel JE**, Zhang D, Zanvit P, Chia C, Zangarle-Murray T, Jin W, Wang S, Chen W. Transforming Growth Factor-β Signaling in Regulatory T Cells Controls T Helper-17 Cells and Tissue-Specific Immune Responses. *Immunity* 2017; **46**: 660-674 [PMID: 28423340 DOI: 10.1016/j.immuni.2017.03.015]
33 **Chen W**, Jin W, Hardegen N, Lei KJ, Li L, Marinos N, McGrady G, Wahl SM. Conversion of peripheral CD4+CD25- naive T cells to CD4+CD25+ regulatory T cells by TGF-beta induction of transcription factor Foxp3. *J Exp Med* 2003; **198**: 1875-1886 [PMID: 14676299 DOI: 10.1084/jem.20030152]
34 **Chen KJ**, Lin SZ, Zhou L, Xie HY, Zhou WH, Taki-Eldin A, Zheng SS. Selective recruitment of regulatory T cell through CCR6-CCL20 in hepatocellular carcinoma fosters tumor progression and predicts poor prognosis. *PLoS One* 2011; **6**: e24671 [PMID: 21935436 DOI: 10.1371/journal.pone.0024671]
35 **David CJ**, Massagué J. Contextual determinants of TGFβ action in development, immunity and cancer. *Nat Rev Mol Cell Biol* 2018; **19**: 419-435 [PMID: 29643418 DOI: 10.1038/s41580-018-0007-0]
36 **de Gramont A**, Faivre S, Raymond E. Novel TGF-**β** inhibitors ready for prime time in onco-immunology. *Oncoimmunology* 2017; **6**: e1257453 [PMID: 28197376 DOI: 10.1080/2162402X.2016.1257453]
37 **Flavell RA**, Sanjabi S, Wrzesinski SH, Licona-Limón P. The polarization of immune cells in the tumour environment by TGFbeta. *Nat Rev Immunol* 2010; **10**: 554-567 [PMID: 20616810 DOI: 10.1038/nri2808]
38 **Shalapour S**, Lin XJ, Bastian IN, Brain J, Burt AD, Aksenov AA, Vrbanac AF, Li W, Perkins A, Matsutani T, Zhong Z, Dhar D, Navas-Molina JA, Xu J, Loomba R, Downes M, Yu RT, Evans RM, Dorrestein PC, Knight R, Benner C, Anstee QM, Karin M. Inflammation-induced IgA+ cells dismantle anti-liver cancer immunity. *Nature* 2017; **551**: 340-345

[PMID: 29144460 DOI: 10.1038/nature24302]

39 **Park BV**, Freeman ZT, Ghasemzadeh A, Chattergoon MA, Rutebemberwa A, Steigner J, Winter ME, Huynh TV, Sebald SM, Lee SJ, Pan F, Pardoll DM, Cox AL. TGFβ1-Mediated SMAD3 Enhances PD-1 Expression on Antigen-Specific T Cells in Cancer. *Cancer Discov* 2016; **6**: 1366-1381 [PMID: 27683557 DOI: 10.1158/2159-8290.CD-15-1347]

40 **Zheng C**, Zheng L, Yoo JK, Guo H, Zhang Y, Guo X, Kang B, Hu R, Huang JY, Zhang Q, Liu Z, Dong M, Hu X, Ouyang W, Peng J, Zhang Z. Landscape of Infiltrating T Cells in Liver Cancer Revealed by Single-Cell Sequencing. *Cell* 2017; **169**: 1342-1356.e16 [PMID: 28622514 DOI: 10.1016/j.cell.2017.05.035]

41 **Bao S**, Jiang X, Jin S, Tu P, Lu J. TGF-β1 Induces Immune Escape by Enhancing PD-1 and CTLA-4 Expression on T Lymphocytes in Hepatocellular Carcinoma. *Front Oncol* 2021; **11**: 694145 [PMID: 34249750 DOI: 10.3389/fonc.2021.694145]

42 **Korkut A**, Zaidi S, Kanchi RS, Rao S, Gough NR, Schultz A, Li X, Lorenzi PL, Berger AC, Robertson G, Kwong LN, Datto M, Roszik J, Ling S, Ravikumar V, Manyam G, Rao A, Shelley S, Liu Y, Ju Z, Hansel D, de Velasco G, Pennathur A, Andersen JB, O'Rourke CJ, Ohshiro K, Jogunoori W, Nguyen BN, Li S, Osmanbeyoglu HU, Ajani JA, Mani SA, Houseman A, Wiznerowicz M, Chen J, Gu S, Ma W, Zhang J, Tong P, Cherniack AD, Deng C, Resar L; Cancer Genome Atlas Research Network, Weinstein JN, Mishra L, Akbani R. A Pan-Cancer Analysis Reveals High-Frequency Genetic Alterations in Mediators of Signaling by the TGF-β Superfamily. *Cell Syst* 2018; **7**: 422-437.e7 [PMID: 30268436 DOI: 10.1016/j.cels.2018.08.010]

43 **Chen J**, Zaidi S, Rao S, Chen JS, Phan L, Farci P, Su X, Shetty K, White J, Zamboni F, Wu X, Rashid A, Pattabiraman N, Mazumder R, Horvath A, Wu RC, Li S, Xiao C, Deng CX, Wheeler DA, Mishra B, Akbani R, Mishra L. Analysis of Genomes and Transcriptomes of Hepatocellular Carcinomas Identifies Mutations and Gene Expression Changes in the Transforming Growth Factor-β Pathway. *Gastroenterology* 2018; **154**: 195-210 [PMID: 28918914 DOI: 10.1053/j.gastro.2017.09.007]

44 **Reichl P**, Haider C, Grubinger M, Mikulits W. TGF-β in epithelial to mesenchymal transition and metastasis of liver carcinoma. *Curr Pharm Des* 2012; **18**: 4135-4147 [PMID: 22630087 DOI: 10.2174/138161212802430477]

45 **Tarantino G**, Conca P, Riccio A, Tarantino M, Di Minno MN, Chianese D, Pasanisi F, Contaldo F, Scopacasa F, Capone D. Enhanced serum concentrations of transforming growth factor-beta1 in simple fatty liver: is it really benign? *J Transl Med* 2008; **6**: 72 [PMID: 19038040 DOI: 10.1186/1479-5876-6-72]

46 **Majumdar A**, Curley SA, Wu X, Brown P, Hwang JP, Shetty K, Yao ZX, He AR, Li S, Katz L, Farci P, Mishra L. Hepatic stem cells and transforming growth factor β in hepatocellular carcinoma. *Nat Rev Gastroenterol Hepatol* 2012; **9**: 530-538 [PMID: 22710573 DOI: 10.1038/nrgastro.2012.114]

47 **Kirmaz C**, Terzioglu E, Topalak O, Bayrak P, Yilmaz O, Ersoz G, Sebik F. Serum tumor growth factor-β1 Levels in patients with cirrhosis, chronic hepatitis B and chronic hepatitis C. *Eur Cytokine Netw* 2004; **15**: 112-116 [DOI: 10.17352/ahr.000019]

48 **Taniguchi H**, Kato N, Otsuka M, Goto T, Yoshida H, Shiratori Y, Omata M. Hepatitis C virus core protein upregulates transforming growth factor-beta 1 transcription. *J Med Virol* 2004; **72**: 52-59 [PMID: 14635011 DOI: 10.1002/jmv.10545]

49 **Jiang Y**, Sun A, Zhao Y, Ying W, Sun H, Yang X, Xing B, Sun W, Ren L, Hu B, Li C, Zhang L, Qin G, Zhang M, Chen N, Huang Y, Zhou J, Liu M, Zhu X, Qiu Y, Sun Y, Huang C, Yan M, Wang M, Liu W, Tian F, Xu H, Wu Z, Shi T, Zhu W, Qin J, Xie L, Fan J, Qian X, He F; Chinese Human Proteome Project (CNHPP) Consortium. Proteomics identifies new therapeutic targets of early-stage hepatocellular carcinoma. *Nature* 2019; **567**: 257-261 [PMID: 30814741 DOI: 10.1038/s41586-019-0987-8]

50 **Coulouarn C**, Factor VM, Thorgeirsson SS. Transforming growth factor-beta gene expression signature in mouse hepatocytes predicts clinical outcome in human cancer. *Hepatology* 2008; **47**: 2059-2067 [PMID: 18506891 DOI: 10.1002/hep.22283]

51 **Dong ZZ**, Yao DF, Zou L, Yao M, Qiu LW, Wu XH, Wu W. [An evaluation of transforming growth factor-beta 1 in diagnosing hepatocellular carcinoma and metastasis]. *Zhonghua Gan Zang Bing Za Zhi* 2007; **15**: 503-508 [PMID: 17669238]

52 **Dong ZZ**, Yao DF, Yao M, Qiu LW, Zong L, Wu W, Wu XH, Yao DB, Meng XY. Clinical impact of plasma TGF-beta1 and circulating TGF-beta1 mRNA in diagnosis of hepatocellular carcinoma. *Hepatobiliary Pancreat Dis Int* 2008; **7**: 288-295 [PMID: 18522884]

53 **Tsai JF**, Chuang LY, Jeng JE, Yang ML, Chang WY, Hsieh MY, Lin ZY, Tsai JH. Clinical relevance of transforming growth factor-beta 1 in the urine of patients with hepatocellular carcinoma. *Medicine (Baltimore)* 1997; **76**: 213-226 [PMID: 9193456 DOI: 10.1097/00005792-199705000-00007]

54 **Tsai JF**, Jeng JE, Chuang LY, Yang ML, Ho MS, Chang WY, Hsieh MY, Lin ZY, Tsai JH. Clinical evaluation of urinary transforming growth factor-beta1 and serum alpha-fetoprotein as tumour markers of hepatocellular carcinoma. *Br J Cancer* 1997; **75**: 1460-1466 [PMID: 9166938 DOI: 10.1038/bjc.1997.250]

55 **Balzarini P**, Benetti A, Invernici G, Cristini S, Zicari S, Caruso A, Gatta LB, Berenzi A, Imberti L, Zanotti C, Portolani N, Giulini SM, Ferrari M, Ciusani E, Navone SE, Canazza A, Parati EA, Alessandri G. Transforming growth factor-beta1 induces microvascular abnormalities through a down-modulation of neural cell adhesion molecule in human hepatocellular carcinoma. *Lab Invest* 2012; **92**: 1297-1309 [PMID: 22732936 DOI: 10.1038/labinvest.2012.94]

56 **Mohd Azamai ES**, Sulaiman S, Mohd Habib SH, Looi ML, Das S, Abdul Hamid NA, Wan Ngah WZ, Mohd Yusof YA. Chlorella vulgaris triggers apoptosis in hepatocarcinogenesis-induced rats. *J Zhejiang Univ Sci B* 2009; **10**: 14-21 [PMID: 19198018 DOI: 10.1631/jzus.B0820168]

57 **Cao Y**, Agarwal R, Dituri F, Lupo L, Trerotoli P, Mancarella S, Winter P, Giannelli G. NGS-based transcriptome profiling reveals biomarkers for companion diagnostics of the TGF-β receptor blocker galunisertib in HCC. *Cell Death Dis* 2017; **8**: e2634 [PMID: 28230858 DOI: 10.1038/cddis.2017.44]

58 **Kohla MA**, Attia A, Darwesh N, Obada M, Taha H, Youssef MF. Association of serum levels of transforming growth factor β1 with disease severity in patients with hepatocellular carcinoma. *Hepatoma Res* 2017; **3**: 294 [DOI: 10.20517/2394-5079.2017.40]

59 **Shehata F**, Abdel Monem N, Sakr M, Kasem S, Balbaa M. Epidermal growth factor, its receptor and transforming growth

factor-β1 in the diagnosis of HCV-induced hepatocellular carcinoma. *Med Oncol* 2013; **30**: 673 [PMID: 23912699 DOI: 10.1007/s12032-013-0673-x]

60 **Shirai Y**, Kawata S, Tamura S, Ito N, Tsushima H, Takaishi K, Kiso S, Matsuzawa Y. Plasma transforming growth factor-β1 in patients with hepatocellular carcinoma. Comparison with chronic liver diseases. *Cancer* 1994; **73**: 2275-2279 [DOI: 10.1002/1097-0142(19940501)73:9<2275::AID-CNCR2820730907>3.0.CO;2-T]

61 **Tu S**, Huang W, Huang C, Luo Z, Yan X. Contextual Regulation of TGF-β Signaling in Liver Cancer. *Cells* 2019; **8** [PMID: 31614569 DOI: 10.3390/cells8101235]

62 **Murawaki Y**, Ikuta Y, Nishimura Y, Koda M, Kawasaki H. Serum markers for fibrosis and plasma transforming growth factor-beta 1 in patients with hepatocellular carcinoma in comparison with patients with liver cirrhosis. *J Gastroenterol Hepatol* 1996; **11**: 443-450 [PMID: 8743916 DOI: 10.1111/j.1440-1746.1996.tb00289.x]

63 **Neuzillet C**, de Gramont A, Tijeras-Raballand A, de Mestier L, Cros J, Faivre S, Raymond E. Perspectives of TGF-β inhibition in pancreatic and hepatocellular carcinomas. *Oncotarget* 2014; **5**: 78-94 [PMID: 24393789 DOI: 10.18632/oncotarget.1569]

64 **Sacco R**, Leuci D, Tortorella C, Fiore G, Marinosci F, Schiraldi O, Antonaci S. Transforming growth factor beta1 and soluble Fas serum levels in hepatocellular carcinoma. *Cytokine* 2000; **12**: 811-814 [PMID: 10843770 DOI: 10.1006/cyto.1999.0650]

65 **Song BC**, Chung YH, Kim JA, Choi WB, Suh DD, Pyo SI, Shin JW, Lee HC, Lee YS, Suh DJ. Transforming growth factor-beta1 as a useful serologic marker of small hepatocellular carcinoma. *Cancer* 2002; **94**: 175-180 [PMID: 11815974 DOI: 10.1002/cncr.10170]

66 **Okumoto K**, Hattori E, Tamura K, Kiso S, Watanabe H, Saito K, Saito T, Togashi H, Kawata S. Possible contribution of circulating transforming growth factor-beta1 to immunity and prognosis in unresectable hepatocellular carcinoma. *Liver Int* 2004; **24**: 21-28 [PMID: 15101997 DOI: 10.1111/j.1478-3231.2004.00882.x]

67 **Divella R**, Daniele A, Gadaleta C, Tufaro A, Venneri MT, Paradiso A, Quaranta M. Circulating transforming growth factor-β and epidermal growth factor receptor as related to virus infection in liver carcinogenesis. *Anticancer Res* 2012; **32**: 141-145 [PMID: 22213299]

68 **Sue SR**, Chari RS, Kong FM, Mills JJ, Fine RL, Jirtle RL, Meyers WC. Transforming growth factor-beta receptors and mannose 6-phosphate/insulin-like growth factor-II receptor expression in human hepatocellular carcinoma. *Ann Surg* 1995; **222**: 171-178 [PMID: 7639583 DOI: 10.1097/00000658-199508000-00009]

69 **An Y**, Gao S, Zhao WC, Qiu BA, Xia NX, Zhang PJ, Fan ZP. Transforming growth factor-β and peripheral regulatory cells are negatively correlated with the overall survival of hepatocellular carcinoma. *World J Gastroenterol* 2018; **24**: 2733-2740 [PMID: 29991878 DOI: 10.3748/wjg.v24.i25.2733]

70 **Llovet JM**, Fuster J, Bruix J. Prognosis of hepatocellular carcinoma. *Hepatogastroenterology* 2002; **49**: 7-11 [PMID: 11941987]

71 **Qin LX**, Tang ZY. The prognostic molecular markers in hepatocellular carcinoma. *World J Gastroenterol* 2002; **8**: 385-392 [PMID: 12046056 DOI: 10.3748/wjg.v8.i3.385]

72 **Matsuzaki K**. Modulation of TGF-beta signaling during progression of chronic liver diseases. *Front Biosci (Landmark Ed)* 2009; **14**: 2923-2934 [PMID: 19273245 DOI: 10.2741/3423]

73 **Giannelli G**, Bergamini C, Fransvea E, Sgarra C, Antonaci S. Laminin-5 with transforming growth factor-beta1 induces epithelial to mesenchymal transition in hepatocellular carcinoma. *Gastroenterology* 2005; **129**: 1375-1383 [PMID: 16285938 DOI: 10.1053/j.gastro.2005.09.055]

74 **Giannelli G**, Fransvea E, Marinosci F, Bergamini C, Colucci S, Schiraldi O, Antonaci S. Transforming growth factor-beta1 triggers hepatocellular carcinoma invasiveness *via* alpha3beta1 integrin. *Am J Pathol* 2002; **161**: 183-193 [PMID: 12107103 DOI: 10.1016/s0002-9440(10)64170-3]

75 **Lee D**, Chung YH, Kim JA, Lee YS, Lee D, Jang MK, Kim KM, Lim YS, Lee HC. Transforming growth factor beta 1 overexpression is closely related to invasiveness of hepatocellular carcinoma. *Oncology* 2012; **82**: 11-18 [PMID: 22269311 DOI: 10.1159/000335605]

76 **Wang Y**, Liu T, Tang W, Deng B, Chen Y, Zhu J, Shen X. Hepatocellular Carcinoma Cells Induce Regulatory T Cells and Lead to Poor Prognosis *via* Production of Transforming Growth Factor-β1. *Cell Physiol Biochem* 2016; **38**: 306-318 [PMID: 26799063 DOI: 10.1159/000438631]

77 **Peng L**, Yuan XQ, Zhang CY, Ye F, Zhou HF, Li WL, Liu ZY, Zhang YQ, Pan X, Li GC. High TGF-β1 expression predicts poor disease prognosis in hepatocellular carcinoma patients. *Oncotarget* 2017; **8**: 34387-34397 [PMID: 28415739 DOI: 10.18632/oncotarget.16166]

78 **Principe DR**, Doll JA, Bauer J, Jung B, Munshi HG, Bartholin L, Pasche B, Lee C, Grippo PJ. TGF-β: duality of function between tumor prevention and carcinogenesis. *J Natl Cancer Inst* 2014; **106**: djt369 [PMID: 24511106 DOI: 10.1093/jnci/djt369]

79 **Wang Z**, Liu F, Tu W, Chang Y, Yao J, Wu W, Jiang X, He X, Lin J, Song Y. Embryonic liver fodrin involved in hepatic stellate cell activation and formation of regenerative nodule in liver cirrhosis. *J Cell Mol Med* 2012; **16**: 118-128 [PMID: 21388516 DOI: 10.1111/j.1582-4934.2011.01290.x]

80 **Ji F**, Fu SJ, Shen SL, Zhang LJ, Cao QH, Li SQ, Peng BG, Liang LJ, Hua YP. The prognostic value of combined TGF-β1 and ELF in hepatocellular carcinoma. *BMC Cancer* 2015; **15**: 116 [PMID: 25880619 DOI: 10.1186/s12885-015-1127-y]

81 **Ho HK**, Pok S, Streit S, Ruhe JE, Hart S, Lim KS, Loo HL, Aung MO, Lim SG, Ullrich A. Fibroblast growth factor receptor 4 regulates proliferation, anti-apoptosis and alpha-fetoprotein secretion during hepatocellular carcinoma progression and represents a potential target for therapeutic intervention. *J Hepatol* 2009; **50**: 118-127 [PMID: 19008009 DOI: 10.1016/j.jhep.2008.08.015]

82 **Lee JJ**, Choo SP. The fibroblast growth factor receptor pathway in hepatocellular carcinoma. *Hepatoma Res* 2018; **4**: 52 [DOI: 10.20517/2394-5079.2018.42]

83 **Chen Z**, Xie B, Zhu Q, Xia Q, Jiang S, Cao R, Shi L, Qi D, Li X, Cai L. FGFR4 and TGF-β1 expression in hepatocellular carcinoma: correlation with clinicopathological features and prognosis. *Int J Med Sci* 2013; **10**: 1868-1875 [PMID: 24324363 DOI: 10.7150/ijms.6868]

84 **El-Ashram S**, Aboelhadid SM, Abdel-Kafy EM, Hashem SA, Mahrous LN, Farghly EM, Kamel AA. Erratum: Saeed, E.-A.; Shawky, M.A.; El-Sayed, M.A.-K.; Shymaa, A.H.; Lilian, N.M.; Eman, M.F.; Asmaa, A.K. Investigation of Pre- and Post-Weaning Mortalities in Rabbits Bred in Egypt, with Reference to Parasitic and Bacterial Causes. *Animals* 2020, *10*, 537. *Animals (Basel)* 2020; **10** [PMID: 32290038 DOI: 10.3390/ani10040650]

85 **Fan G**, Wei X, Xu X. Is the era of sorafenib over? *Ther Adv Med Oncol* 2020; **12**: 1758835920927602 [PMID: 32518599 DOI: 10.1177/1758835920927602]

86 **Giraud J**, Chalopin D, Blanc JF, Saleh M. Hepatocellular Carcinoma Immune Landscape and the Potential of Immunotherapies. *Front Immunol* 2021; **12**: 655697 [PMID: 33815418 DOI: 10.3389/fimmu.2021.655697]

87 **Robinson MW**, Harmon C, O'Farrelly C. Liver immunology and its role in inflammation and homeostasis. *Cell Mol Immunol* 2016; **13**: 267-276 [PMID: 27063467 DOI: 10.1038/cmi.2016.3]

88 **Nishida N**, Kudo M. Immune Phenotype and Immune Checkpoint Inhibitors for the Treatment of Human Hepatocellular Carcinoma. *Cancers (Basel)* 2020; **12** [PMID: 32443599 DOI: 10.3390/cancers12051274]

89 **Xu W**, Liu K, Chen M, Sun JY, McCaughan GW, Lu XJ, Ji J. Immunotherapy for hepatocellular carcinoma: recent advances and future perspectives. *Ther Adv Med Oncol* 2019; **11**: 1758835919862692 [PMID: 31384311 DOI: 10.1177/1758835919862692]

90 **Prieto J**, Melero I, Sangro B. Immunological landscape and immunotherapy of hepatocellular carcinoma. *Nat Rev Gastroenterol Hepatol* 2015; **12**: 681-700 [PMID: 26484443 DOI: 10.1038/nrgastro.2015.173]

91 **Sia D**, Jiao Y, Martinez-Quetglas I, Kuchuk O, Villacorta-Martin C, Castro de Moura M, Putra J, Camprecios G, Bassaganyas L, Akers N, Losic B, Waxman S, Thung SN, Mazzaferro V, Esteller M, Friedman SL, Schwartz M, Villanueva A, Llovet JM. Identification of an Immune-specific Class of Hepatocellular Carcinoma, Based on Molecular Features. *Gastroenterology* 2017; **153**: 812-826 [PMID: 28624577 DOI: 10.1053/j.gastro.2017.06.007]

92 **Chen J**, Gingold JA, Su X. Immunomodulatory TGF-β Signaling in Hepatocellular Carcinoma. *Trends Mol Med* 2019; **25**: 1010-1023 [PMID: 31353124 DOI: 10.1016/j.molmed.2019.06.007]

93 **Pinyol R**, Sia D, Llovet JM. Immune Exclusion-Wnt/CTNNB1 Class Predicts Resistance to Immunotherapies in HCC. *Clin Cancer Res* 2019; **25**: 2021-2023 [PMID: 30617138 DOI: 10.1158/1078-0432.CCR-18-3778]

94 **Meindl-Beinker NM**, Matsuzaki K, Dooley S. TGF-β signaling in onset and progression of hepatocellular carcinoma. *Dig Dis* 2012; **30**: 514-523 [PMID: 23108308 DOI: 10.1159/000341704]

95 **McGaha TL**, Phelps RG, Spiera H, Bona C. Halofuginone, an inhibitor of type-I collagen synthesis and skin sclerosis, blocks transforming-growth-factor-beta-mediated Smad3 activation in fibroblasts. *J Invest Dermatol* 2002; **118**: 461-470 [PMID: 11874485 DOI: 10.1046/j.0022-202x.2001.01690.x]

96 **Taras D**, Blanc JF, Rullier A, Dugot-Senant N, Laurendeau I, Bièche I, Pines M, Rosenbaum J. Halofuginone suppresses the lung metastasis of chemically induced hepatocellular carcinoma in rats through MMP inhibition. *Neoplasia* 2006; **8**: 312-318 [PMID: 16756723 DOI: 10.1593/neo.05796]

97 **Nagler A**, Ohana M, Shibolet O, Shapira MY, Alper R, Vlodavsky I, Pines M, Ilan Y. Suppression of hepatocellular carcinoma growth in mice by the alkaloid coccidiostat halofuginone. *Eur J Cancer* 2004; **40**: 1397-1403 [PMID: 15177499 DOI: 10.1016/j.ejca.2003.11.036]

98 **Glenisson W**, Castronovo V, Waltregny D. Histone deacetylase 4 is required for TGFbeta1-induced myofibroblastic differentiation. *Biochim Biophys Acta* 2007; **1773**: 1572-1582 [PMID: 17610967 DOI: 10.1016/j.bbamcr.2007.05.016]

99 **Di Fazio P**, Schneider-Stock R, Neureiter D, Okamoto K, Wissniowski T, Gahr S, Quint K, Meissnitzer M, Alinger B, Montalbano R, Sass G, Hohenstein B, Hahn EG, Ocker M. The pan-deacetylase inhibitor panobinostat inhibits growth of hepatocellular carcinoma models by alternative pathways of apoptosis. *Cell Oncol* 2010; **32**: 285-300 [PMID: 20208142 DOI: 10.3233/CLO-2010-0511]

100 **Mariathasan S**, Turley SJ, Nickles D, Castiglioni A, Yuen K, Wang Y, Kadel EE III, Koeppen H, Astarita JL, Cubas R, Jhunjhunwala S, Banchereau R, Yang Y, Guan Y, Chalouni C, Ziai J, Şenbabaoğlu Y, Santoro S, Sheinson D, Hung J, Giltnane JM, Pierce AA, Mesh K, Lianoglou S, Riegler J, Carano RAD, Eriksson P, Höglund M, Somarriba L, Halligan DL, van der Heijden MS, Loriot Y, Rosenberg JE, Fong L, Mellman I, Chen DS, Green M, Derleth C, Fine GD, Hegde PS, Bourgon R, Powles T. TGFβ attenuates tumour response to PD-L1 blockade by contributing to exclusion of T cells. *Nature* 2018; **554**: 544-548 [PMID: 29443960 DOI: 10.1038/nature25501]

101 **Tauriello DVF**, Palomo-Ponce S, Stork D, Berenguer-Llergo A, Badia-Ramentol J, Iglesias M, Sevillano M, Ibiza S, Cañellas A, Hernando-Momblona X, Byrom D, Matarin JA, Calon A, Rivas EI, Nebreda AR, Riera A, Attolini CS, Batlle E. TGFβ drives immune evasion in genetically reconstituted colon cancer metastasis. *Nature* 2018; **554**: 538-543 [PMID: 29443964 DOI: 10.1038/nature25492]

102 **Knudson KM**, Hicks KC, Luo X, Chen JQ, Schlom J, Gameiro SR. M7824, a novel bifunctional anti-PD-L1/TGFβ Trap fusion protein, promotes anti-tumor efficacy as monotherapy and in combination with vaccine. *Oncoimmunology* 2018; **7**: e1426519 [PMID: 29721396 DOI: 10.1080/2162402X.2018.1426519]

103 **Lan Y**, Zhang D, Xu C, Hance KW, Marelli B, Qi J, Yu H, Qin G, Sircar A, Hernández VM, Jenkins MH, Fontana RE, Deshpande A, Locke G, Sabzevari H, Radvanyi L, Lo KM. Enhanced preclinical antitumor activity of M7824, a bifunctional fusion protein simultaneously targeting PD-L1 and TGF-β. *Sci Transl Med* 2018; **10** [PMID: 29343622 DOI: 10.1126/scitranslmed.aan5488]

104 **Li HY**, McMillen WT, Heap CR, McCann DJ, Yan L, Campbell RM, Mundla SR, King CH, Dierks EA, Anderson BD, Britt KS, Huss KL, Voss MD, Wang Y, Clawson DK, Yingling JM, Sawyer JS. Optimization of a dihydropyrrolopyrazole series of transforming growth factor-beta type I receptor kinase domain inhibitors: discovery of an orally bioavailable transforming growth factor-beta receptor type I inhibitor as antitumor agent. *J Med Chem* 2008; **51**: 2302-2306 [PMID: 18314943 DOI: 10.1021/jm701199p]

105 **Fransvea E**, Angelotti U, Antonaci S, Giannelli G. Blocking transforming growth factor-beta up-regulates E-cadherin and reduces migration and invasion of hepatocellular carcinoma cells. *Hepatology* 2008; **47**: 1557-1566 [PMID: 18318443 DOI: 10.1002/hep.22201]

106 **Melisi D**, Ishiyama S, Sclabas GM, Fleming JB, Xia Q, Tortora G, Abbruzzese JL, Chiao PJ. LY2109761, a novel transforming growth factor beta receptor type I and type II dual inhibitor, as a therapeutic approach to suppressing

pancreatic cancer metastasis. *Mol Cancer Ther* 2008; **7**: 829-840 [PMID: 18413796 DOI: 10.1158/1535-7163.MCT-07-0337]

107 **Mazzocca A**, Fransvea E, Lavezzari G, Antonaci S, Giannelli G. Inhibition of transforming growth factor beta receptor I kinase blocks hepatocellular carcinoma growth through neo-angiogenesis regulation. *Hepatology* 2009; **50**: 1140-1151 [PMID: 19711426 DOI: 10.1002/hep.23118]

108 **Hau P**, Jachimczak P, Schlingensiepen R, Schulmeyer F, Jauch T, Steinbrecher A, Brawanski A, Proescholdt M, Schlaier J, Buchroithner J, Pichler J, Wurm G, Mehdorn M, Strege R, Schuierer G, Villarrubia V, Fellner F, Jansen O, Straube T, Nohria V, Goldbrunner M, Kunst M, Schmaus S, Stauder G, Bogdahn U, Schlingensiepen KH. Inhibition of TGF-beta2 with AP 12009 in recurrent malignant gliomas: from preclinical to phase I/II studies. *Oligonucleotides* 2007; **17**: 201-212 [PMID: 17638524 DOI: 10.1089/oli.2006.0053]

109 **Vallières L**. Trabedersen, a TGFbeta2-specific antisense oligonucleotide for the treatment of malignant gliomas and other tumors overexpressing TGFbeta2. *IDrugs* 2009; **12**: 445-453 [PMID: 19579166]

110 **Bogdahn U**, Hau P, Stockhammer G, Venkataramana NK, Mahapatra AK, Suri A, Balasubramaniam A, Nair S, Oliushine V, Parfenov V, Poverennova I, Zaaroor M, Jachimczak P, Ludwig S, Schmaus S, Heinrichs H, Schlingensiepen KH; Trabedersen Glioma Study Group. Targeted therapy for high-grade glioma with the TGF-β2 inhibitor trabedersen: results of a randomized and controlled phase IIb study. *Neuro Oncol* 2011; **13**: 132-142 [PMID: 20980335 DOI: 10.1093/neuonc/noq142]

111 **Schlingensiepen KH**, Bischof A, Egger T, Hafner M, Herrmuth H, Jachimczak P, Kielmanowicz M, Niewel M, Zavadova E, Stauder G. The TGF-beta1 antisense oligonucleotide AP 11014 for the treatment of non-small cell lung, colorectal and prostate cancer: Preclinical studies. *J Clin Oncol* 2004; **22**: 3132 [DOI: 10.1200/jco.2004.22.90140.3132]

112 **Mead AL**, Wong TT, Cordeiro MF, Anderson IK, Khaw PT. Evaluation of anti-TGF-beta2 antibody as a new postoperative anti-scarring agent in glaucoma surgery. *Invest Ophthalmol Vis Sci* 2003; **44**: 3394-3401 [PMID: 12882787 DOI: 10.1167/iovs.02-0978]

113 **Rodon J**, Carducci MA, Sepulveda-Sánchez JM, Azaro A, Calvo E, Seoane J, Braña I, Sicart E, Gueorguieva I, Cleverly AL, Pillay NS, Desaiah D, Estrem ST, Paz-Ares L, Holdhoff M, Blakeley J, Lahn MM, Baselga J. First-in-human dose study of the novel transforming growth factor-β receptor I kinase inhibitor LY2157299 monohydrate in patients with advanced cancer and glioma. *Clin Cancer Res* 2015; **21**: 553-560 [PMID: 25424852 DOI: 10.1158/1078-0432.CCR-14-1380]

World Journal of Gastroenterology

Submit a Manuscript: https://www.f6publishing.com

World J Gastroenterol 2022 September 28; 28(36): 5265-5279

DOI: 10.3748/wjg.v28.i36.5265

ISSN 1007-9327 (print) ISSN 2219-2840 (online)

REVIEW

P2X7 receptor as the regulator of T-cell function in intestinal barrier disruption

Zhi-Feng Jiang, Wei Wu, Han-Bing Hu, Zheng-Yang Li, Ming Zhong, Lin Zhang

Specialty type: Critical care medicine

Provenance and peer review: Unsolicited article; Externally peer reviewed.

Peer-review model: Single blind

Peer-review report's scientific quality classification

Grade A (Excellent): A
Grade B (Very good): B, B, B
Grade C (Good): 0
Grade D (Fair): 0
Grade E (Poor): 0

P-Reviewer: Pongcharoen S, Thailand; Zamani M, Iran

Received: March 12, 2022
Peer-review started: March 12, 2022
First decision: June 11, 2022
Revised: June 20, 2022
Accepted: September 1, 2022
Article in press: September 1, 2022
Published online: September 28, 2022

Zhi-Feng Jiang, Han-Bing Hu, Lin Zhang, Center of Emergency & Intensive Care Unit, Jinshan Hospital of Fudan University, Shanghai 201508, China

Wei Wu, Ming Zhong, Department of Critical Care Medicine, Zhongshan Hospital of Fudan University, Shanghai 200032, China

Zheng-Yang Li, Department of Gastroenterology, Jinshan Hospital of Fudan University, Shanghai 201508, China

Corresponding author: Lin Zhang, MD, PhD, Doctor, Center of Emergency & Intensive Care Unit, Jinshan Hospital of Fudan University, No. 1508 Longhang Road, Shanghai 201508, China. linzhang0315@fudan.edu.cn

Abstract

The intestinal mucosa is a highly compartmentalized structure that forms a direct barrier between the host intestine and the environment, and its dysfunction could result in a serious disease. As T cells, which are important components of the mucosal immune system, interact with gut microbiota and maintain intestinal homeostasis, they may be involved in the process of intestinal barrier dysfunction. P2X7 receptor (P2X7R), a member of the P2X receptors family, mediates the effects of extracellular adenosine triphosphate and is expressed by most innate or adaptive immune cells, including T cells. Current evidence has demonstrated that P2X7R is involved in inflammation and mediates the survival and differentiation of T lymphocytes, indicating its potential role in the regulation of T cell function. In this review, we summarize the available research about the regulatory role and mechanism of P2X7R on the intestinal mucosa-derived T cells in the setting of intestinal barrier dysfunction.

Key Words: Intestinal barrier dysfunction; P2X7 receptor; T lymphocyte

Core Tip: Intestinal barrier dysfunction is usually accompanied by inflammation and the death of epithelial cells, which may lead to an elevated concentration of extracellular adenosine triphosphate and the intestinal immune response. Meanwhile, available studies have demonstrated that P2X7 receptor (P2X7R) can be an important regulatory factor in the activation and differentiation of T cells, suggesting that P2X7R may play a key role in intestinal barrier disruption by regulating T cells. Therefore, in this review, we summarized the recent advances regarding the intestinal barrier, the role of P2X7R and T-cells in the pathophysiology of intestinal barrier disruption, and the role of T cell-derived P2X7R in the pathophysiology of intestinal barrier dysfunction.

Citation: Jiang ZF, Wu W, Hu HB, Li ZY, Zhong M, Zhang L. P2X7 receptor as the regulator of T-cell function in intestinal barrier disruption. *World J Gastroenterol* 2022; 28(36): 5265-5279
URL: https://www.wjgnet.com/1007-9327/full/v28/i36/5265.htm
DOI: https://dx.doi.org/10.3748/wjg.v28.i36.5265

INTRODUCTION

The intestinal tract is one of the largest interfaces in the human body that directly contacts the external environment[1]. The intestine, a highly specialized and complex organ, plays an important role in absorbing useful substances and presenting potentially harmful substances[2]. The intestinal barrier also maintains the homeostasis of the inner environment and develops the intestinal immune system[3]. The intestinal barrier is composed of several parts, including the microbiological barrier, the chemical barrier, the physical barrier and the immune barrier[4]. Dysfunction of the intestinal barrier increases intestinal permeability and is related to the pathophysiology of several serious diseases[5]. The intestinal tract is exposed to various commensal bacteria, dietary antigens and pathogens that are related to immune tolerance and defense, showing the importance of the immune system in the intestine [6]. The immune barrier mainly includes the lamina propria lymphocytes, dendritic cells (DCs), mast cells, macrophages and lymphocytes — mainly $CD8^+$ T cells — located among epithelial cells[7]. Considering the involvement of T cells in the oral tolerance and immune defense against pathogens in the intestine, it is not surprising that they have an essential role in the pathology of intestinal barrier dysfunction[8,9].

The purinergic signaling pathway is highly conserved and plays a critical role in immune regulatory response[10]. This signaling pathway is mainly mediated by adenosine triphosphate (ATP) and nicotinamide adenine dinucleotide (NAD^+). Purinergic receptors are a group of transmembrane proteins widely expressed in immune cells[11]. According to their different structural properties, these receptors can be divided into the following three families: P2X receptor, P2Y receptor and P1 receptor[12]. Among them, P2X receptors, a class of ligand-gated, cationic-selective channels, are mainly activated by extracellular ATP (eATP)[13]. P2X7 receptors (P2X7R) have a low affinity for ATP and need to be triggered by high concentrations of ATP[14]. When the concentration of ATP is low, P2X7R can act as ion channels for Na^+, K^+ or Ca^{2+}. However, P2X7R can form nonselective and large-conductance pores in settings with high concentrations of ATP, thereby inducing cell apoptosis[14]. Under normal conditions, the cell membrane is impermeable to ATP and other related substances, and the maintenance of low eATP concentration is achieved by the strong degrading activity of ATPases[15,16]. The leakage of intracellular ATP due to the destruction of cell membrane could result in significant elevation of eATP concentration, thereby inducing the activation of the immune system[17-19]. Indeed, an ultrahigh concentration of eATP can be observed at the inflammatory sites[20]. In the process of acute inflammation, ATP activates P2X7R on the Treg cells, inhibiting their activity and viability[21]. P2X receptor channels on effector T cells are stimulated by eATP, facilitating the activation of nuclear factor of activated T cells and the production of IL-2, which could increase the activation of effector T cells[22,23]. The receptor can also be activated by NAD^+ released from damaged cells or activated T cells[24,25]. This NAD^+-dependent process is associated with ecto-ADP-ribosyltransferase ARTC2.2, which is activated by NAD^+ and induces the ADP-ribosylation of P2X7. In the presence of low micromolar concentrations of extracellular NAD^+, this process finally leads to cell death because of the activated P2X7R, a phenomenon known as NAD^+-induced cell death (NICD)[26,27]. In contrast, NAD^+ may be degraded into hydrolysate in the case of high levels of ATP, which would block the NAD^+-dependent process[28,29] (Figure 1). Intestinal barrier dysfunction is usually accompanied by inflammation and the death of epithelial cells, which may lead to an elevated concentration of eATP and the intestinal immune response[30]. Meanwhile, available studies have demonstrated that P2X7R can be an important regulatory factor in the activation and differentiation of T cells[31], suggesting that P2X7R may play a key role in intestinal barrier disruption by regulating T cells.

Therefore, in this review, we summarized the recent advances regarding the intestinal barrier, the role of P2X7R and T-cells in the pathophysiology of intestinal barrier disruption, and the role of T cell-

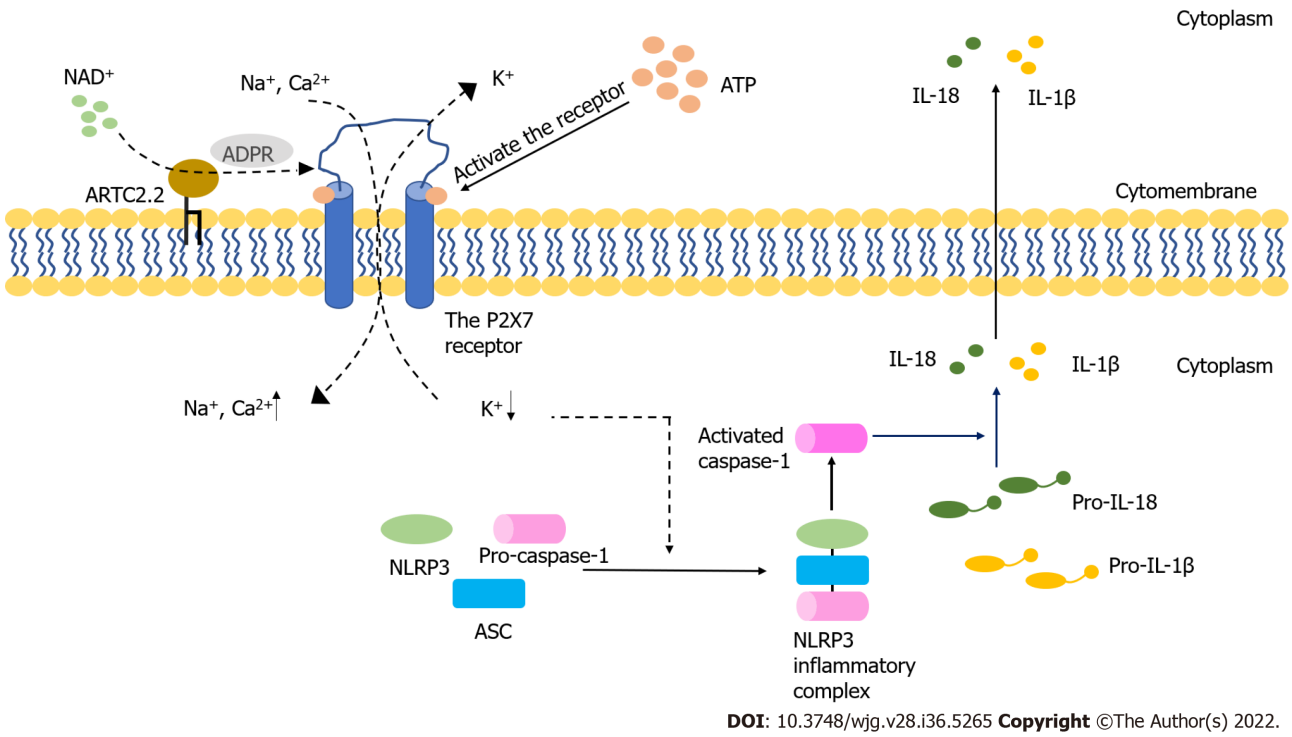

DOI: 10.3748/wjg.v28.i36.5265

Figure 1 The activation of the P2X7 receptor and NLRP3 inflammasome. The P2X7 receptor is activated by extracellular ATP and NAD^+ and serves as an ion channel. It can also form non-selective macropores. The activated P2X7 receptor induces the decreasing of intracellular K^+, which initiates NOD-like receptor family pyrin domain containing 3 (NLRP3) inflammasome activation. The activated process of pro-interleukin (IL)-1β and pro-IL-18 are triggered by the active caspase-1 that results from the formation of NLRP3 inflammasome. Mature inflammatory cytokines are released into extracellular space from cells, which finally results in the cell death. ADPR: ADP-ribose; ARTC2.2: ADP-ribosyltransferase 2.2; ASC: Apoptosis-associated speck-like protein containing a CARD; NLRP3: NOD-like receptor family pyrin domain containing 3; IL-18: Interleukin-18; IL-1β: Interleukin-1β.

derived P2X7R in the pathophysiology of intestinal barrier dysfunction.

THE OVERVIEW OF THE INTESTINAL BARRIER

The intestinal barrier, one of the most important biological barriers in the body, is composed of various extracellular and cellular components. It works as a semipermeable membrane that allows nutrients to pass through while limiting the transport of pathogens and noxious substances. This dual function is regulated by the interaction among the four components of the intestinal barrier (the microbiological barrier, the chemical barrier, the physical barrier and the immunological barrier)[2].

There are over 10^{14} microorganisms and about 10000 bacterial species in the human intestine[32]. The microbiological barrier is formed by symbiotic microorganisms in the outermost position of the mucus layer, which effectively prevents harmful substances from entering intestinal epithelial cells[31,33,34]. The chemical barrier, also known as the inner mucus layer, is composed of macromolecules, including proteins, enzymes, peptides and immunoglobulins[35,36]. Mucin2 secreted by goblet cells is the main mucus protein and it serves as a protective barrier[37]. In intestinal crypts, pluripotent stem cells can differentiate into five different cell types, including enterocytes, goblet cells, Paneth cells, enteroendocrine cells and microfold cells[38]. The physical barrier beneath the mucus layer is composed of intestinal epithelial cells which are critical to the physical features of the intestinal barrier[30].

Beneath the intestinal epithelium, the immunological barrier consists of various immune cells, including T lymphocytes, B lymphocytes, dendritic cells, macrophages and plasma cells. This barrier is involved in innate and adaptive immune responses *via* antigen presentation and the secretion of inflammatory mediators and antibodies[39,40]. In addition to immune cells, substances secreted from these cells are also important in the construction of the intestinal immunological barrier. Secretory IgA, another constituent of the immunological barrier, is mainly found at the intestinal mucosal surface, and it provides antipathogen protection by interacting with bacteria[41].

There are several interactions among different components of the intestinal barrier. The physical barrier and the inner mucus layer separate the microbiological barrier and the intestinal immunological barrier, preventing unnecessary conflict and maintaining intestinal homeostasis[42]. The intestinal microbiota induces the functional maturation of innate and adaptive immunity, and instructs immune response through microbiota-derived metabolites and components (such as lipopolysaccharides and

peptidoglycans)[43,44]. The metabolites maintain intestinal homeostasis and regulate inflammation through immune responses, while the components of the microbiota direct immune responses by activating the intestinal TLR pathway[45-47]. For example, the expression of IL17, an inflammatory cytokine produced by γδ T cells, can be inhibited by propionate, a metabolite of intestinal bacteria[48]. Conversely, intestinal immune cells precisely regulate the microbial community both directly and indirectly, thus establishing a sustainable balance between the immune cells and intestinal microbiota [49-51].

The intestinal barrier should be considered a highly dynamic and complex structure that responds to internal and external stimuli[52,53]. Dysfunction of the intestinal barrier often occurs when the damage of the intestinal mucosa is severe and the components of the intestinal barrier change[54]. Under pathological conditions such as stress[55] and ischemia or hypoxia[56], the intestinal barrier is destroyed and the permeability of the intestine increases, thereby inducing bacterial translocation, electrolyte disorders and inflammatory response[57] (Figure 2). With the increasing permeability of the intestine, locally produced ATP is released into the intestinal microenvironment, followed by the activation of immune cells *via* ATP receptors, including P2X7 purinoceptor. When the intestinal immune system is activated, the inflammatory effects may not be regulated, which may lead to the irreversible destruction of the intestinal barrier[58]. More recently, it has been reported that increased ATP concentrations promote T-cell responses by enhancing the expression of the CD86 costimulatory molecule on antigen-presenting cells, an effect mediated through P2X7 purinergic receptor. Thus, the immune system may be the key player in barrier dysfunction and T cells may be involved in adaptive immune responses.

THE ROLE OF T CELLS IN THE INTEGRITY OF THE INTESTINAL BARRIER

T lymphocytes, which are adaptive immune cells, respond to specific antigens and remain the bacterial diversity by complex mechanisms in the homeostatic condition[2]. In the intestine, invariant NKT (iNKT) cells could either enhance or inhibit the immune response, and they might directly or indirectly regulate the microbiota in the intestine[59-62]. $CD8^+$ T cells are the main intraepithelial lymphocytes that monitor and respond to pathogens[63]. $CD4^+$ T cells and T-helper (Th) cells are mainly located in the intestinal lamina propria, and Th1 and Th17 cells can be found in the intestine[64]. Activated intestinal effector T cells could mount immune responses and influence the gut microbiota, and the excess of these cells might induce advanced inflammatory responses and acute or chronic inflammatory diseases[65-67]. In the intestinal adaptive immune response, dendritic cells ingest antigens and activate T cells, and Th cells are induced to differentiate into three different types of Th cells[68]. When lymphocytes respond to different stimuli, they can be divided into different groups based on their cytokine profile, such as Th1, Th2, or Treg cells, which are regulated by P2X7 purinergic receptor, mechanistically[69]. Activated T cells can modulate immune responses by secreting inflammatory cytokines or by interacting with other cells. The function of Th1 cells is to activate and proliferate cytotoxic T cells, thereby inducing the damage of infected intestinal epithelial cells[70]. Th2 cells can release inflammatory cytokines (IL-4, IL-5, and IL-13) and activate B cells to attack the infected cells[71-73]. Transforming growth factor β is capable of suppressing immunoglobulins M and G and promoting their switch to immunoglobulin A. This cytokine is secreted by T cells in Peyer's patches, suggesting the role of T cells in oral tolerance[74]. When intestinal permeability is damaged, antigens can pass through the intestinal epithelial cells and be taken up by macrophages or dendritic cells. Then, the antigens are presented to T cells in the lamina propria by these antigen-presenting cells, which stimulates T cells and induces their proliferation[75, 76]. Some antigens may be taken up by intestinal epithelial cells *via* endocytosis and then be presented to T cells after intracellular processing. This process is based on the classical and nonclassical histocompatibility molecules[77,78]. T cells use both their receptor and a costimulatory signal to recognize antigens[79].

Intestinal barrier disruption is usually accompanied by intestinal inflammation and pathogen invasion. T cells, the key components of adaptive immunity, can effectively limit the invading bacteria and regulate the inflammatory response together with the innate immune system and cytokines[80]. For example, the T helper cell type (Th)1 immune response is necessary in antipathogen protection and is involved in intestinal inflammation[81,82]. In humans, Th17 cells mainly reside in the intestine, where their polarization occurs. Because of the plasticity of Th17 cells, polarized cells have antipathogenic functions and maintain the intestinal epithelial integrity under normal physiological conditions, but they may turn into proinflammatory cells when exposed to IL-23[83]. Th17 cells can mediate inflammation by secreting a proinflammatory cytokine, IL-17A[70]. Peripheral Th17 cells are produced and migrate to the intestine in the case of oral inflammation, which may cause intestinal inflammation[84]. In addition to suppressing the proliferation of Th cells, Treg cells can protect against bacteria and dietary antigens and can produce anti-inflammatory cytokines to exert their anti-inflammatory function, thereby maintaining the homeostasis of the intestinal epithelium[85-87]. With the development of intestinal inflammation, the balance between Th17 cells and Treg cells may be broken up, biasing the function of Th17 cells[88]. In a recent study, it has been found that tissue-resident memory T cells are important in the development of intestinal inflammation, but the role of these cells in this process is not

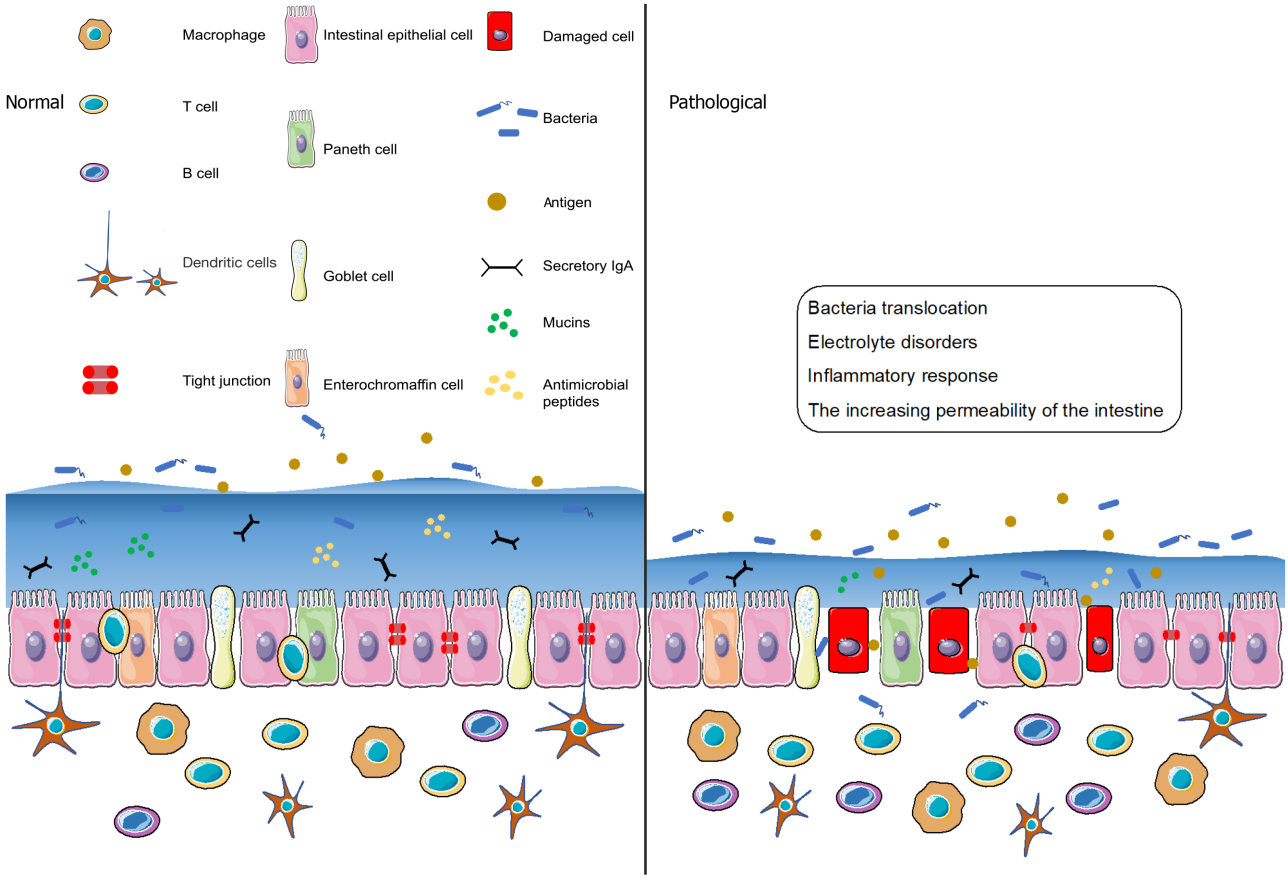

DOI: 10.3748/wjg.v28.i36.5265

Figure 2 Intestinal barrier components and the intestinal barrier dysfunction. The normal intestinal barrier is formed by many layers which includes cytokines, bacteria, cells and secretory IgA. The intestinal barrier dysfunction results in the increasing of the intestinal permeability, which subsequently causes the inflammatory response and bacteria translocation.

clear[89]. In summary, T cells are very likely to become effective regulatory targets in the intestinal barrier, and T cell-associated therapy may be used in clinical settings in the future.

THE ROLE OF P2X7R IN THE INTESTINAL BARRIER DYSFUNCTION

Among the members of P2X receptor family, P2X7R (encoded by p2rx7) is the largest (with 595 amino acids in humans). It has special structural and signaling features because of its long intracellular carboxy-terminal, which helps prevent receptor desensitization[90,91]. The monomeric structure of P2X7R has two intracellular domains (C-terminal and N-terminal) and an extracellular ATP-binding domain that separates two transmembrane domains[92]. There were over 1500 single nucleotide polymorphisms (SNPs) reported in NCBI database, and most of them were missense, intronic or nonsynonymous[93]. In highly polymorphic human P2RX7, SNPs play a critical role in the biological process and function of P2X7R. About 10 loss of function SNPs and 3 gain of function SNPs have been identified[12]. For example, the activity of human P2X7R was reduced when Ala replaced Glu 496[94]. When Asn replaced lle-568, the expression of P2X7R was decreased to approximately 50% of normal, and P2X7R became nonfunctional[95]. The mutation of R307Q located in the ATP-binding pocket impaired the binding of ATP to P2X7R[96]. Genetic variants in P2X7R may be involved in the inflammatory response[97,98]. P2X7R function related SNPs played a regulatory role in inflammatory diseases [32]. Unlike other P2X receptors, the complete activation of P2X7R requires a higher concentration of ATP (range from about 0.1 to 2.5 mmol/L)[99]. When activated by ATP, P2X7R not only mediates the uptake of cations and macromolecules, but also leads to the activation of intracellular signaling pathways[100-102]. It has been demonstrated that the formation of macropores requires pannexin-1 channels, and pannexin-1 antagonists can decrease the formation of these pores[103]. However, recent data have suggested that the formation of macropores may be intrinsic to P2X7R without accessory molecules[104-106]. Moreover, P2X7R is associated with the activation of the signaling pathway and transcription factors, including MAP kinases, the cyclic AMP response element[107,108]. P2X7R is widely expressed in immune cells, which suggests its importance in the regulation of both the innate

and adaptive immunity, especially in the regulation of inflammation[109,110].

ATP is the most important energy molecule and a common extracellular signaling nucleotide that participates in the regulation of cellular proliferation, differentiation and death[111-113]. In a healthy body, eATP is maintained in a low concentration thanks to ATPases in extracellular spaces. ATP can leak from damaged or distressed cells, and can also be released by nonlytic regulated mechanisms, which increase the concentration of eATP16[114-117]. It has been proven that the concentration of eATP is higher in different inflammatory conditions than in normal conditions[118,119].

The intestinal barrier dysfunction induces the inflammatory response and epithelial cell death[120, 121]. In the acute-inflammatory tissue, high amounts of IL-6 are released, thereby inducing the synthesis and release of ATP from Treg cells exposed to IL-6[122]. The concentration of eATP may increase after intestinal barrier dysfunction, which may activate P2X7R. T follicular helper cells enhance germinal center reactions by deleting P2X7, resisting ATP-mediated immune cell death[123]. When the concentration of eATP produced by the intestinal microbiota is high, commensal-specific IgA responses initiated by intestinal lymphoid tissues are inhibited, which influences the composition of intestinal microbiota[124,125]. Moreover, Perruzza *et al*[126] showed that the blockade of P2X7R could decrease proinflammatory cytokines and protect the intestinal barrier function by inhibiting the activation of macrophages. Nucleotide-binding domain, leucine-rich-repeat receptor, pyrin domain-containing NLR family pyrin domain containing 3 (NLRP3) is a multiprotein complex that participates in the occurrence and development of many inflammatory diseases[127]. The inhibition of NLRP3 can reduce intestinal inflammation and enhance the barrier function[128]. Both NLRP3 and P2X7R are expressed in different immune cells, including T cells, B cells and monocytes[99]. Several signaling pathways induced by activated P2X7R may lead to a decrease in intracellular K^+, an increase in Ca^{2+} and the production of reactive oxygen species, which are key steps in NLRP3 activation[129-132] (Figure 1).

THE ROLE OF T CELL-DERIVED P2X7R IN THE INTESTINAL BARRIER DYSFUNCTION

It has been reported that activated P2X7R can affect several of the biological processes of T cells, including activation, differentiation and death[133]. After recognizing antigens, T cells rapidly release ATP through pannexin channels due to the T cell receptor signaling and co-stimulatory molecules[134, 135]. Because of the highly expressed P2X7 in iNKT cells, they were susceptible to P2X7-mediated cell death and regulated by vitamin A, finally influencing the intestinal homeostasis[136]. ATP released from T cells can activate P2X receptor which increases the expression of the *p2rx7* gene[14,135]. Yip *et al* [135] found that the silencing of P2X7R blocked Ca^{2+} influx and inhibited T cell activation in human $CD4^+$ T cells. These findings suggest that activated P2X7R is essential for the activation of T cells. L-selectin (CD62L) is related to the migration of T cells[137,138]. Low expression of L-selectin is necessary for activated or differentiated T cells to egress from the lymph node[139]. P2X7R activated by ATP can trigger CD62L shedding in human naïve T cells[140]. In a lymph node, activated P2X7R also affects the motility of T cells by inducing their calcium waves[141]. When intracellular ATP and NAD^+ nucleotides are released from cells, they can trigger the activation of P2X7R and induce apoptosis or necrosis[142]. In the case of low micromolar concentration of extracellular NAD^+, ADP ribosylation of P2X7R induces cell death because of persistent P2X7R activation[27]. Under the condition of activated P2X7R, there are two independent ways to induce T cell death: one of them depends on the phosphorylation of ERK1/2, and the other is associated with the nonselective pore[143,144]. In addition, CD62L shedding triggered by the activated P2X7R may induce cell death by apoptosis[145,146]. Compared with native T cells, activated T cells are less sensitive to NICD induced by P2X7R[147]. The expression of P2X7R is different in different populations of T cells. For example, Tregs and follicular helper T cells exhibit high expression of the P2X7 receptor, suggesting that they are more susceptible to cell death than other populations of T cells[148,149]. eATP and P2X7R influence the differentiation of T cells and play a significant role in the metabolism, generation, and memory function of $CD8^+$ T cells[150]. It has been shown that the AMP-activated protein kinase signaling pathway may promote constant efflux of intracellular ATP in memory $CD8^+$ T cells, and is involved in the differentiation and maintenance of memory T cells induced by P2X7R[151,152]. In an inflammatory environment, activated P2X7R drives the differentiation from T cells to Th17 cells[153], and the receptor reduces the differentiation of Tr1 cells with a high expression of IL-10 without Foxp3[21,155]. Activated P2X7R can also regulate the plasticity of Th17 cells and induce Th17 cells to differentiate[156]. In addition to acting directly on T cells, P2X7R can regulate the differentiation of T cells by affecting the physiological functions of dendritic cells[157, 158]. Although ATP may not only reduce the DCs-induced Th1 cell differentiation but can also influence the interaction of DCs with T cells, there is little research on the role of P2X7R during this process[159, 160]. Moreover, activated P2X7R regulates the cytokine secretion and polarization of Th17 cells by influencing dendritic cells[161,162] (Figure 3). Myeloid derived suppressor cells were considered as the regulator of immunosuppression *via* affecting the amounts, functions, or phenotypes of T cells, and the ATP/P2X7R signaling axis may be involved in this process[163].

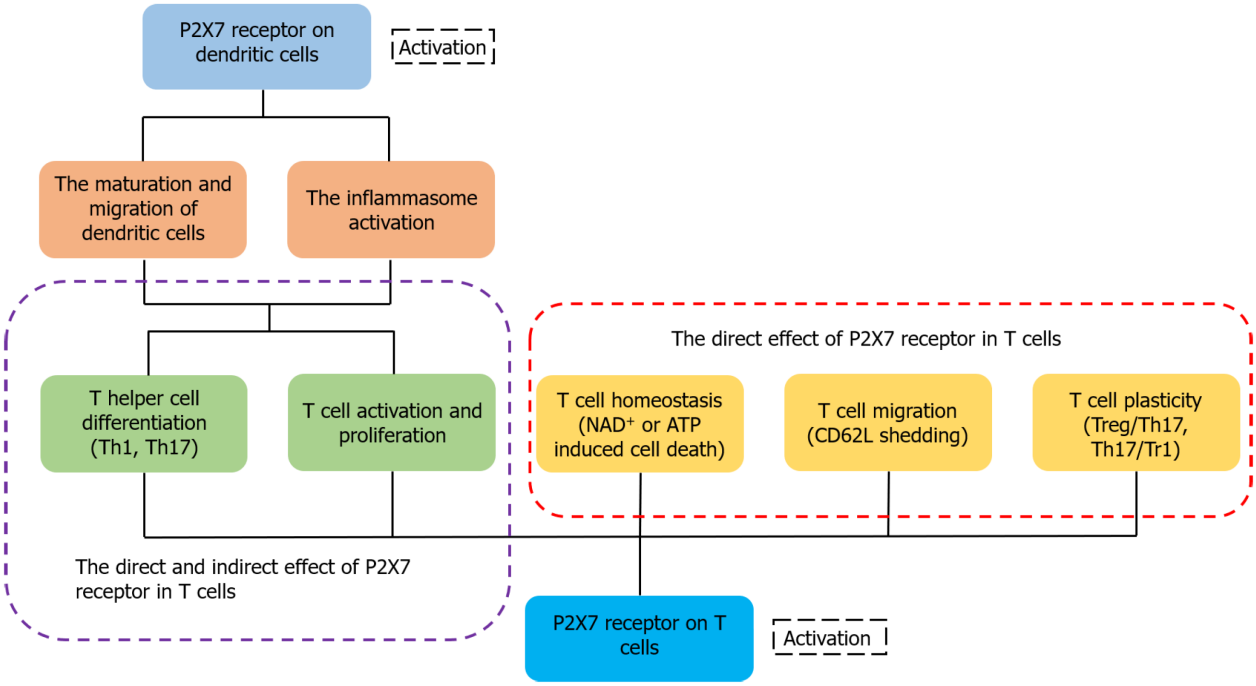

DOI: 10.3748/wjg.v28.i36.5265

Figure 3 P2X7 receptor on dendritic cells and T cells influences the fate of T cells indirectly or directly, respectively. The activation of P2X7 receptor on dendritic cells induces the maturation and migration of cells and promotes the inflammasome activation, affecting the activation and differentiation of T cells finally. The activation of P2X7 receptor in T cells can directly regulate the activation, differentiation, migration and homeostasis of T cells[33].

DISCUSSION

The intestinal barrier dysfunction is a complex and severe pathological condition, which induces the inflammatory response and bacterial invasion. Sepsis is a serious systemic inflammatory disease with high morbidity and mortality in the intensive care unit because it can cause multiple organ failure in patients[164]. Given that the progression and pathogenesis of sepsis have been attributed to intestinal barrier dysfunction, further research on the immune and inflammatory factors of the intestinal barrier dysfunction is necessary[165,166].

According to the above description, T cells are involved in oral tolerance and immune response to antigens in the intestine, and they are the most common lymphocytes that reside in the intestine[167]. Moreover, infiltration by inflammatory T cells is a significant pathological characteristic of intestinal inflammation[168]. Thus, an appropriate number and population of T cells may mitigate the damage of intestinal barrier dysfunction.

P2X7R is widely expressed in T cells and serves as a regulatory factor of their biological processes. Heiss *et al*[169] found that intestinal $CD8^+$ T cells express a high concentration of P2X7R and are highly sensitive to extracellular nucleotides, indicating that P2X7R can regulate intestinal T cell responses. Inflammatory effector T cells can be depleted and intestinal inflammation can be relieved after treatment with NAD^+[170]. P2X7R has been shown to be the trigger for the activation of NLRP3, indicating that this receptor regulates the release of inflammatory cytokines (IL-18, IL-1β) and the initiation of an inflammatory response[171-174]. Therefore, P2X7R may influence inflammation *via* T cells which is indirect. The selectively P2X7 antagonist was proven to significantly inhibit the innate immune cells and upregulate the immunosuppressive-associated T cells, indicating that this antagonist may be a kind of potential treatment[175]. The effect of P2X7-blockade drug has also been demonstrated in the mouse models with advanced tuberculosis[176]. In addition to the above intracellular signaling pathways (MAPK pathway), previous studies verified that P2X7R also regulated MyD88/NF-κB and PI3K/Akt/mTOR signaling pathways in innate and adaptive immune responses, which suggested that the key proteins in these pathways can be considered as novel therapeutic targets[177].

CONCLUSION

In summary, T cells, the key participant in the intestinal barrier dysfunction, are regulated by P2X7R. The roles and mechanisms of P2X7R are associated with T lymphocytes in the intestinal barrier dysfunction and may be a potential research direction, although there have been few studies on this topic (Figure 4). Furthermore, different specific molecules that inhibit the expression of P2X7R may be

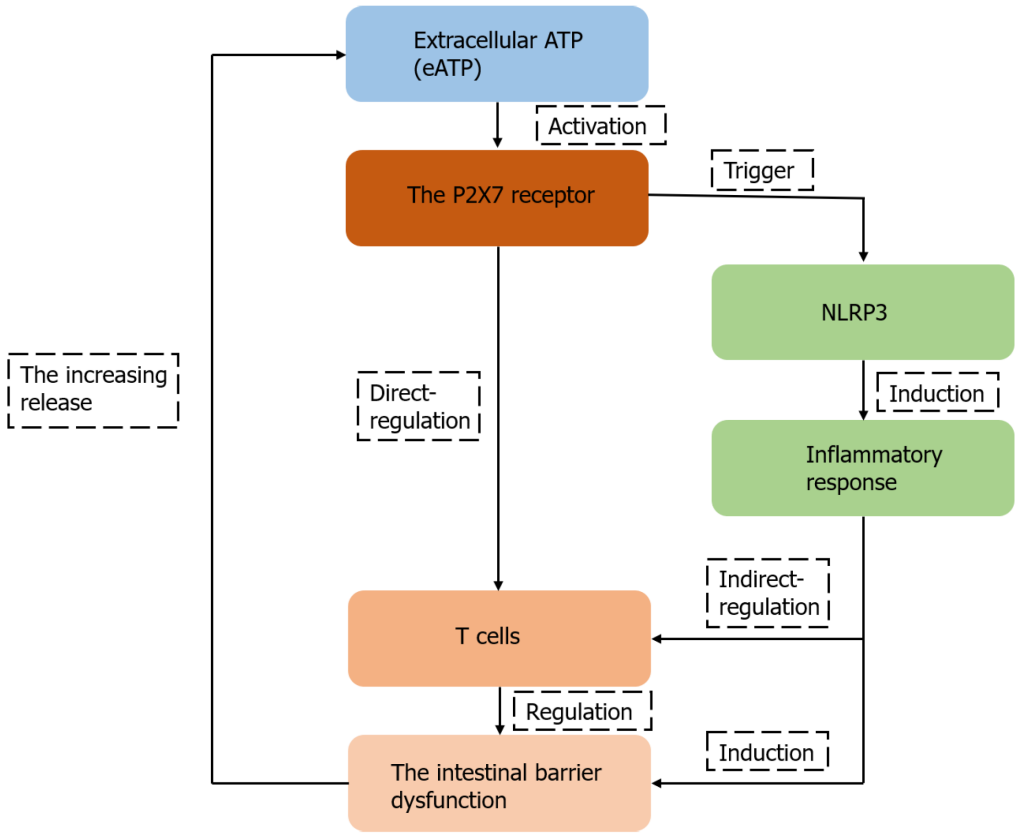

DOI: 10.3748/wjg.v28.i36.5265

Figure 4 The schematic diagram of the hypothesis of the P2X7 receptor as the regulator of T-cell function in intestinal barrier disruption.

potential therapeutic drugs in the future.

FOOTNOTES

Author contributions: Jiang ZF and Wu W contributed equally to this work; Zhong M and Zhang L were co-corresponding authors; Jiang ZF and Wu W wrote the manuscript; Zhang L and Zhong M conceived the topic and reviewed the manuscript; Jiang ZF and Zhang L revised the manuscript; Hu HB and Li ZY reviewed the manuscript; all authors contributed to the article and approved the submitted version.

Supported by The National Natural Science Foundation of China, No. 81801943; Shanghai Pujiang Program, No. 21PJD009; and The Research Grant for Public Health Key Discipline of Shanghai Municipality, China, No. GWV-10.1-XK26.

Conflict-of-interest statement: All the authors report no relevant conflicts of interest for this article.

Country/Territory of origin: China

ORCID number: Zhi-Feng Jiang 0000-0003-0714-3453; Lin Zhang 0000-0002-0950-7145.

S-Editor: Gong ZM
L-Editor: Filipodia
P-Editor: Gong ZM

REFERENCES

1 **Takiishi T**, Fenero CIM, Câmara NOS. Intestinal barrier and gut microbiota: Shaping our immune responses throughout life. *Tissue Barriers* 2017; **5**: e1373208 [PMID: 28956703 DOI: 10.1080/21688370.2017.1373208]
2 **Salvo Romero E**, Alonso Cotoner C, Pardo Camacho C, Casado Bedmar M, Vicario M. The intestinal barrier function and its involvement in digestive disease. *Rev Esp Enferm Dig* 2015; **107**: 686-696 [PMID: 26541659 DOI: 10.17235/reed.2015.3846/2015]
3 **Vancamelbeke M**, Vermeire S. The intestinal barrier: a fundamental role in health and disease. *Expert Rev Gastroenterol Hepatol* 2017; **11**: 821-834 [PMID: 28650209 DOI: 10.1080/17474124.2017.1343143]
4 **Huang Z**, Weng Y, Shen Q, Zhao Y, Jin Y. Microplastic: A potential threat to human and animal health by interfering with the intestinal barrier function and changing the intestinal microenvironment. *Sci Total Environ* 2021; **785**: 147365 [PMID: 33933760 DOI: 10.1016/j.scitotenv.2021.147365]
5 **Cui Y**, Wang Q, Chang R, Zhou X, Xu C. Intestinal Barrier Function-Non-alcoholic Fatty Liver Disease Interactions and Possible Role of Gut Microbiota. *J Agric Food Chem* 2019; **67**: 2754-2762 [PMID: 30798598 DOI: 10.1021/acs.jafc.9b00080]
6 **Izcue A**, Coombes JL, Powrie F. Regulatory T cells suppress systemic and mucosal immune activation to control intestinal inflammation. *Immunol Rev* 2006; **212**: 256-271 [PMID: 16903919 DOI: 10.1111/j.0105-2896.2006.00423.x]
7 **Gill N**, Wlodarska M, Finlay BB. Roadblocks in the gut: barriers to enteric infection. *Cell Microbiol* 2011; **13**: 660-669 [PMID: 21392202 DOI: 10.1111/j.1462-5822.2011.01578.x]
8 **Olivares-Villagómez D**, Van Kaer L. Intestinal Intraepithelial Lymphocytes: Sentinels of the Mucosal Barrier. *Trends Immunol* 2018; **39**: 264-275 [PMID: 29221933 DOI: 10.1016/j.it.2017.11.003]
9 **Cheroutre H**, Lambolez F, Mucida D. The light and dark sides of intestinal intraepithelial lymphocytes. *Nat Rev Immunol* 2011; **11**: 445-456 [PMID: 21681197 DOI: 10.1038/nri3007]
10 **Adinolfi E**, Giuliani AL, De Marchi E, Pegoraro A, Orioli E, Di Virgilio F. The P2X7 receptor: A main player in inflammation. *Biochem Pharmacol* 2018; **151**: 234-244 [PMID: 29288626 DOI: 10.1016/j.bcp.2017.12.021]
11 **Di Virgilio F**, Sarti AC, Falzoni S, De Marchi E, Adinolfi E. Extracellular ATP and P2 purinergic signalling in the tumour microenvironment. *Nat Rev Cancer* 2018; **18**: 601-618 [PMID: 30006588 DOI: 10.1038/s41568-018-0037-0]
12 **Di Virgilio F**, Dal Ben D, Sarti AC, Giuliani AL, Falzoni S. The P2X7 Receptor in Infection and Inflammation. *Immunity* 2017; **47**: 15-31 [PMID: 28723547 DOI: 10.1016/j.immuni.2017.06.020]
13 **Niemi K**, Teirilä L, Lappalainen J, Rajamäki K, Baumann MH, Öörni K, Wolff H, Kovanen PT, Matikainen S, Eklund KK. Serum amyloid A activates the NLRP3 inflammasome *via* P2X7 receptor and a cathepsin B-sensitive pathway. *J Immunol* 2011; **186**: 6119-6128 [PMID: 21508263 DOI: 10.4049/jimmunol.1002843]
14 **Junger WG**. Immune cell regulation by autocrine purinergic signalling. *Nat Rev Immunol* 2011; **11**: 201-212 [PMID: 21331080 DOI: 10.1038/nri2938]
15 **Aliagas E**, Muñoz-Esquerre M, Cuevas E, Careta O, Huertas D, López-Sánchez M, Escobar I, Dorca J, Santos S. Is the purinergic pathway involved in the pathology of COPD? *Respir Res* 2018; **19**: 103 [PMID: 29807526 DOI: 10.1186/s12931-018-0793-0]
16 **Linden J**, Koch-Nolte F, Dahl G. Purine Release, Metabolism, and Signaling in the Inflammatory Response. *Annu Rev Immunol* 2019; **37**: 325-347 [PMID: 30676821 DOI: 10.1146/annurev-immunol-051116-052406]
17 **Burnstock G**, Verkhratsky A. Evolutionary origins of the purinergic signalling system. *Acta Physiol (Oxf)* 2009; **195**: 415-447 [PMID: 19222398 DOI: 10.1111/j.1748-1716.2009.01957.x]
18 **Alarcón-Vila C**, Baroja-Mazo A, de Torre-Minguela C, Martínez CM, Martínez-García JJ, Martínez-Banaclocha H, García-Palenciano C, Pelegrin P. CD14 release induced by P2X7 receptor restricts inflammation and increases survival during sepsis. *Elife* 2020; **9** [PMID: 33135636 DOI: 10.7554/eLife.60849]
19 **Cekic C**, Linden J. Purinergic regulation of the immune system. *Nat Rev Immunol* 2016; **16**: 177-192 [PMID: 26922909 DOI: 10.1038/nri.2016.4]
20 **Pelleg A**. Extracellular adenosine 5'-triphosphate in pulmonary disorders. *Biochem Pharmacol* 2021; **187**: 114319 [PMID: 33161021 DOI: 10.1016/j.bcp.2020.114319]
21 **Schenk U**, Frascoli M, Proietti M, Geffers R, Traggiai E, Buer J, Ricordi C, Westendorf AM, Grassi F. ATP inhibits the generation and function of regulatory T cells through the activation of purinergic P2X receptors. *Sci Signal* 2011; **4**: ra12 [PMID: 21364186 DOI: 10.1126/scisignal.2001270]
22 **Wang L**, Jacobsen SE, Bengtsson A, Erlinge D. P2 receptor mRNA expression profiles in human lymphocytes, monocytes and CD34+ stem and progenitor cells. *BMC Immunol* 2004; **5**: 16 [PMID: 15291969 DOI: 10.1186/1471-2172-5-16]
23 **Romio M**, Reinbeck B, Bongardt S, Hüls S, Burghoff S, Schrader J. Extracellular purine metabolism and signaling of CD73-derived adenosine in murine Treg and Teff cells. *Am J Physiol Cell Physiol* 2011; **301**: C530-C539 [PMID: 21593451 DOI: 10.1152/ajpcell.00385.2010]
24 **Scheuplein F**, Rissiek B, Driver JP, Chen YG, Koch-Nolte F, Serreze DV. A recombinant heavy chain antibody approach blocks ART2 mediated deletion of an iNKT cell population that upon activation inhibits autoimmune diabetes. *J Autoimmun* 2010; **34**: 145-154 [PMID: 19796917 DOI: 10.1016/j.jaut.2009.08.012]
25 **Bao L**, Locovei S, Dahl G. Pannexin membrane channels are mechanosensitive conduits for ATP. *FEBS Lett* 2004; **572**: 65-68 [PMID: 15304325 DOI: 10.1016/j.febslet.2004.07.009]
26 **Adriouch S**, Bannas P, Schwarz N, Fliegert R, Guse AH, Seman M, Haag F, Koch-Nolte F. ADP-ribosylation at R125 gates the P2X7 ion channel by presenting a covalent ligand to its nucleotide binding site. *FASEB J* 2008; **22**: 861-869 [PMID: 17928361 DOI: 10.1096/fj.07-9294com]
27 **Seman M**, Adriouch S, Scheuplein F, Krebs C, Freese D, Glowacki G, Deterre P, Haag F, Koch-Nolte F. NAD-induced T cell death: ADP-ribosylation of cell surface proteins by ART2 activates the cytolytic P2X7 purinoceptor. *Immunity* 2003; **19**: 571-582 [PMID: 14563321 DOI: 10.1016/s1074-7613(03)00266-8]

28 **Lee HC**. Structure and enzymatic functions of human CD38. *Mol Med* 2006; **12**: 317-323 [PMID: 17380198 DOI: 10.2119/2006–00086.Lee]

29 **Rissiek B**, Haag F, Boyer O, Koch-Nolte F, Adriouch S. P2X7 on Mouse T Cells: One Channel, Many Functions. *Front Immunol* 2015; **6**: 204 [PMID: 26042119 DOI: 10.3389/fimmu.2015.00204]

30 **Jiang ZF**, Zhang L. LncRNA: A Potential Research Direction in Intestinal Barrier Function. *Dig Dis Sci* 2021; **66**: 1400-1408 [PMID: 32591966 DOI: 10.1007/s10620-020-06417-w]

31 **Rissiek B**, Haag F, Boyer O, Koch-Nolte F, Adriouch S. ADP-ribosylation of P2X7: a matter of life and death for regulatory T cells and natural killer T cells. *Curr Top Microbiol Immunol* 2015; **384**: 107-126 [PMID: 25048544 DOI: 10.1007/82_2014_420]

32 **Javed I**, Cui X, Wang X, Mortimer M, Andrikopoulos N, Li Y, Davis TP, Zhao Y, Ke PC, Chen C. Implications of the Human Gut-Brain and Gut-Cancer Axes for Future Nanomedicine. *ACS Nano* 2020; **14**: 14391-14416 [PMID: 33138351 DOI: 10.1021/acsnano.0c07258]

33 **Paone P**, Cani PD. Mucus barrier, mucins and gut microbiota: the expected slimy partners? *Gut* 2020; **69**: 2232-2243 [PMID: 32917747 DOI: 10.1136/gutjnl-2020-322260]

34 **Donaldson GP**, Lee SM, Mazmanian SK. Gut biogeography of the bacterial microbiota. *Nat Rev Microbiol* 2016; **14**: 20-32 [PMID: 26499895 DOI: 10.1038/nrmicro3552]

35 **Garrett WS**, Gordon JI, Glimcher LH. Homeostasis and inflammation in the intestine. *Cell* 2010; **140**: 859-870 [PMID: 20303876 DOI: 10.1016/j.cell.2010.01.023]

36 **Singh PK**, Parsek MR, Greenberg EP, Welsh MJ. A component of innate immunity prevents bacterial biofilm development. *Nature* 2002; **417**: 552-555 [PMID: 12037568 DOI: 10.1038/417552a]

37 **Zarepour M**, Bhullar K, Montero M, Ma C, Huang T, Velcich A, Xia L, Vallance BA. The mucin Muc2 limits pathogen burdens and epithelial barrier dysfunction during Salmonella enterica serovar Typhimurium colitis. *Infect Immun* 2013; **81**: 3672-3683 [PMID: 23876803 DOI: 10.1128/IAI.00854-13]

38 **Salim SY**, Söderholm JD. Importance of disrupted intestinal barrier in inflammatory bowel diseases. *Inflamm Bowel Dis* 2011; **17**: 362-381 [PMID: 20725949 DOI: 10.1002/ibd.21403]

39 **Mu Q**, Kirby J, Reilly CM, Luo XM. Leaky Gut As a Danger Signal for Autoimmune Diseases. *Front Immunol* 2017; **8**: 598 [PMID: 28588585 DOI: 10.3389/fimmu.2017.00598]

40 **Berin MC**, Li H, Sperber K. Antibody-mediated antigen sampling across intestinal epithelial barriers. *Ann N Y Acad Sci* 2006; **1072**: 253-261 [PMID: 17057205 DOI: 10.1196/annals.1326.002]

41 **Woof JM**, Russell MW. Structure and function relationships in IgA. *Mucosal Immunol* 2011; **4**: 590-597 [PMID: 21937984 DOI: 10.1038/mi.2011.39]

42 **Kayama H**, Okumura R, Takeda K. Interaction Between the Microbiota, Epithelia, and Immune Cells in the Intestine. *Annu Rev Immunol* 2020; **38**: 23-48 [PMID: 32340570 DOI: 10.1146/annurev-immunol-070119-115104]

43 **Round JL**, Mazmanian SK. The gut microbiota shapes intestinal immune responses during health and disease. *Nat Rev Immunol* 2009; **9**: 313-323 [PMID: 19343057 DOI: 10.1038/nri2515]

44 **Rooks MG**, Garrett WS. Gut microbiota, metabolites and host immunity. *Nat Rev Immunol* 2016; **16**: 341-352 [PMID: 27231050 DOI: 10.1038/nri.2016.42]

45 **Park J**, Kim M, Kang SG, Jannasch AH, Cooper B, Patterson J, Kim CH. Short-chain fatty acids induce both effector and regulatory T cells by suppression of histone deacetylases and regulation of the mTOR-S6K pathway. *Mucosal Immunol* 2015; **8**: 80-93 [PMID: 24917457 DOI: 10.1038/mi.2014.44]

46 **Sun M**, Wu W, Chen L, Yang W, Huang X, Ma C, Chen F, Xiao Y, Zhao Y, Yao S, Carpio VH, Dann SM, Zhao Q, Liu Z, Cong Y. Microbiota-derived short-chain fatty acids promote Th1 cell IL-10 production to maintain intestinal homeostasis. *Nat Commun* 2018; **9**: 3555 [PMID: 30177845 DOI: 10.1038/s41467-018-05901-2]

47 **Diehl GE**, Longman RS, Zhang JX, Breart B, Galan C, Cuesta A, Schwab SR, Littman DR. Microbiota restricts trafficking of bacteria to mesenteric lymph nodes by CX(3)CR1(hi) cells. *Nature* 2013; **494**: 116-120 [PMID: 23334413 DOI: 10.1038/nature11809]

48 **Dupraz L**, Magniez A, Rolhion N, Richard ML, Da Costa G, Touch S, Mayeur C, Planchais J, Agus A, Danne C, Michaudel C, Spatz M, Trottein F, Langella P, Sokol H, Michel ML. Gut microbiota-derived short-chain fatty acids regulate IL-17 production by mouse and human intestinal γδ T cells. *Cell Rep* 2021; **36**: 109332 [PMID: 34233192 DOI: 10.1016/j.celrep.2021.109332]

49 **Levy M**, Kolodziejczyk AA, Thaiss CA, Elinav E. Dysbiosis and the immune system. *Nat Rev Immunol* 2017; **17**: 219-232 [PMID: 28260787 DOI: 10.1038/nri.2017.7]

50 **Hoytema van Konijnenburg DP**, Reis BS, Pedicord VA, Farache J, Victora GD, Mucida D. Intestinal Epithelial and Intraepithelial T Cell Crosstalk Mediates a Dynamic Response to Infection. *Cell* 2017; **171**: 783-794.e13 [PMID: 28942917 DOI: 10.1016/j.cell.2017.08.046]

51 **Kogut MH**, Lee A, Santin E. Microbiome and pathogen interaction with the immune system. *Poult Sci* 2020; **99**: 1906-1913 [PMID: 32241470 DOI: 10.1016/j.psj.2019.12.011]

52 **Lee SH**. Intestinal permeability regulation by tight junction: implication on inflammatory bowel diseases. *Intest Res* 2015; **13**: 11-18 [PMID: 25691839 DOI: 10.5217/ir.2015.13.1.11]

53 **Camilleri M**, Madsen K, Spiller R, Greenwood-Van Meerveld B, Verne GN. Intestinal barrier function in health and gastrointestinal disease. *Neurogastroenterol Motil* 2012; **24**: 503-512 [PMID: 22583600 DOI: 10.1111/j.1365-2982.2012.01921.x]

54 **Nalle SC**, Turner JR. Intestinal barrier loss as a critical pathogenic link between inflammatory bowel disease and graft-versus-host disease. *Mucosal Immunol* 2015; **8**: 720-730 [PMID: 25943273 DOI: 10.1038/mi.2015.40]

55 **Ferrier L**, Mazelin L, Cenac N, Desreumaux P, Janin A, Emilie D, Colombel JF, Garcia-Villar R, Fioramonti J, Bueno L. Stress-induced disruption of colonic epithelial barrier: role of interferon-gamma and myosin light chain kinase in mice. *Gastroenterology* 2003; **125**: 795-804 [PMID: 12949725 DOI: 10.1016/s0016-5085(03)01057-6]

56 **Drewe J**, Beglinger C, Fricker G. Effect of ischemia on intestinal permeability of lipopolysaccharides. *Eur J Clin Invest*

2001; **31**: 138-144 [PMID: 11168452 DOI: 10.1046/j.1365-2362.2001.00792.x]
57 **Pan P**, Song Y, Du X, Bai L, Hua X, Xiao Y, Yu X. Intestinal barrier dysfunction following traumatic brain injury. *Neurol Sci* 2019; **40**: 1105-1110 [PMID: 30771023 DOI: 10.1007/s10072-019-03739-0]
58 **Plichta DR**, Graham DB, Subramanian S, Xavier RJ. Therapeutic Opportunities in Inflammatory Bowel Disease: Mechanistic Dissection of Host-Microbiome Relationships. *Cell* 2019; **178**: 1041-1056 [PMID: 31442399 DOI: 10.1016/j.cell.2019.07.045]
59 **Wingender G**, Kronenberg M. Role of NKT cells in the digestive system. IV. The role of canonical natural killer T cells in mucosal immunity and inflammation. *Am J Physiol Gastrointest Liver Physiol* 2008; **294**: G1-G8 [PMID: 17947447 DOI: 10.1152/ajpgi.00437.2007]
60 **Zeissig S**, Kaser A, Dougan SK, Nieuwenhuis EE, Blumberg RS. Role of NKT cells in the digestive system. III. Role of NKT cells in intestinal immunity. *Am J Physiol Gastrointest Liver Physiol* 2007; **293**: G1101-G1105 [PMID: 17717040 DOI: 10.1152/ajpgi.00342.2007]
61 **Wang Y**, Sedimbi S, Löfbom L, Singh AK, Porcelli SA, Cardell SL. Unique invariant natural killer T cells promote intestinal polyps by suppressing TH1 immunity and promoting regulatory T cells. *Mucosal Immunol* 2018; **11**: 131-143 [PMID: 28401935 DOI: 10.1038/mi.2017.34]
62 **Selvanantham T**, Lin Q, Guo CX, Surendra A, Fieve S, Escalante NK, Guttman DS, Streutker CJ, Robertson SJ, Philpott DJ, Mallevaey T. NKT Cell-Deficient Mice Harbor an Altered Microbiota That Fuels Intestinal Inflammation during Chemically Induced Colitis. *J Immunol* 2016; **197**: 4464-4472 [PMID: 27799307 DOI: 10.4049/jimmunol.1601410]
63 **Alonso C**, Vicario M, Pigrau M, Lobo B, Santos J. Intestinal barrier function and the brain-gut axis. *Adv Exp Med Biol* 2014; **817**: 73-113 [PMID: 24997030 DOI: 10.1007/978-1-4939-0897-4_4]
64 **Maynard CL**, Weaver CT. Intestinal effector T cells in health and disease. *Immunity* 2009; **31**: 389-400 [PMID: 19766082 DOI: 10.1016/j.immuni.2009.08.012]
65 **Marrack P**, Scott-Browne J, MacLeod MK. Terminating the immune response. *Immunol Rev* 2010; **236**: 5-10 [PMID: 20636804 DOI: 10.1111/j.1600-065X.2010.00928.x]
66 **Yang Y**, Torchinsky MB, Gobert M, Xiong H, Xu M, Linehan JL, Alonzo F, Ng C, Chen A, Lin X, Sczesnak A, Liao JJ, Torres VJ, Jenkins MK, Lafaille JJ, Littman DR. Focused specificity of intestinal TH17 cells towards commensal bacterial antigens. *Nature* 2014; **510**: 152-156 [PMID: 24739972 DOI: 10.1038/nature13279]
67 **McKinstry KK**, Strutt TM, Swain SL. Regulation of CD4+ T-cell contraction during pathogen challenge. *Immunol Rev* 2010; **236**: 110-124 [PMID: 20636812 DOI: 10.1111/j.1600-065X.2010.00921.x]
68 **Chen Y**, Cui W, Li X, Yang H. Interaction Between Commensal Bacteria, Immune Response and the Intestinal Barrier in Inflammatory Bowel Disease. *Front Immunol* 2021; **12**: 761981 [PMID: 34858414 DOI: 10.3389/fimmu.2021.761981]
69 **Khor B**, Gardet A, Xavier RJ. Genetics and pathogenesis of inflammatory bowel disease. *Nature* 2011; **474**: 307-317 [PMID: 21677747 DOI: 10.1038/nature10209]
70 **Lee SH**, Kwon JE, Cho ML. Immunological pathogenesis of inflammatory bowel disease. *Intest Res* 2018; **16**: 26-42 [PMID: 29422795 DOI: 10.5217/ir.2018.16.1.26]
71 **Chang JT**. Pathophysiology of Inflammatory Bowel Diseases. *N Engl J Med* 2020; **383**: 2652-2664 [PMID: 33382932 DOI: 10.1056/NEJMra2002697]
72 **Armstrong H**, Alipour M, Valcheva R, Bording-Jorgensen M, Jovel J, Zaidi D, Shah P, Lou Y, Ebeling C, Mason AL, Lafleur D, Jerasi J, Wong GK, Madsen K, Carroll MW, Huynh HQ, Dieleman LA, Wine E. Host immunoglobulin G selectively identifies pathobionts in pediatric inflammatory bowel diseases. *Microbiome* 2019; **7**: 1 [PMID: 30606251 DOI: 10.1186/s40168-018-0604-3]
73 **Romagnani S**. Lymphokine production by human T cells in disease states. *Annu Rev Immunol* 1994; **12**: 227-257 [PMID: 8011282 DOI: 10.1146/annurev.iy.12.040194.001303]
74 **Baumgart DC**, Dignass AU. Intestinal barrier function. *Curr Opin Clin Nutr Metab Care* 2002; **5**: 685-694 [PMID: 12394645 DOI: 10.1097/00075197-200211000-00012]
75 **Elson CO**, Cong Y, Iqbal N, Weaver CT. Immuno-bacterial homeostasis in the gut: new insights into an old enigma. *Semin Immunol* 2001; **13**: 187-194 [PMID: 11394961 DOI: 10.1006/smim.2001.0312]
76 **Rescigno M**, Urbano M, Valzasina B, Francolini M, Rotta G, Bonasio R, Granucci F, Kraehenbuhl JP, Ricciardi-Castagnoli P. Dendritic cells express tight junction proteins and penetrate gut epithelial monolayers to sample bacteria. *Nat Immunol* 2001; **2**: 361-367 [PMID: 11276208 DOI: 10.1038/86373]
77 **Shao L**, Serrano D, Mayer L. The role of epithelial cells in immune regulation in the gut. *Semin Immunol* 2001; **13**: 163-176 [PMID: 11394959 DOI: 10.1006/smim.2000.0311]
78 **Telega GW**, Baumgart DC, Carding SR. Uptake and presentation of antigen to T cells by primary colonic epithelial cells in normal and diseased states. *Gastroenterology* 2000; **119**: 1548-1559 [PMID: 11113076 DOI: 10.1053/gast.2000.20168]
79 **Cario E**, Podolsky DK. Differential alteration in intestinal epithelial cell expression of toll-like receptor 3 (TLR3) and TLR4 in inflammatory bowel disease. *Infect Immun* 2000; **68**: 7010-7017 [PMID: 11083826 DOI: 10.1128/iai.68.12.7010-7017.2000]
80 **Holleran G**, Lopetuso L, Petito V, Graziani C, Ianiro G, McNamara D, Gasbarrini A, Scaldaferri F. The Innate and Adaptive Immune System as Targets for Biologic Therapies in Inflammatory Bowel Disease. *Int J Mol Sci* 2017; **18** [PMID: 28934123 DOI: 10.3390/ijms18102020]
81 **Bagheri N**, Salimzadeh L, Shirzad H. The role of T helper 1-cell response in Helicobacter pylori-infection. *Microb Pathog* 2018; **123**: 1-8 [PMID: 29936093 DOI: 10.1016/j.micpath.2018.06.033]
82 **De Carli M**, D'Elios MM, Zancuoghi G, Romagnani S, Del Prete G. Human Th1 and Th2 cells: functional properties, regulation of development and role in autoimmunity. *Autoimmunity* 1994; **18**: 301-308 [PMID: 7858116 DOI: 10.3109/08916939409009532]
83 **Shao L**, Li M, Zhang B, Chang P. Bacterial dysbiosis incites Th17 cell revolt in irradiated gut. *Biomed Pharmacother* 2020; **131**: 110674 [PMID: 32866810 DOI: 10.1016/j.biopha.2020.110674]
84 **Kitamoto S**, Nagao-Kitamoto H, Jiao Y, Gillilland MG 3rd, Hayashi A, Imai J, Sugihara K, Miyoshi M, Brazil JC, Kuffa

P, Hill BD, Rizvi SM, Wen F, Bishu S, Inohara N, Eaton KA, Nusrat A, Lei YL, Giannobile WV, Kamada N. The Intermucosal Connection between the Mouth and Gut in Commensal Pathobiont-Driven Colitis. *Cell* 2020; **182**: 447-462.e14 [PMID: 32758418 DOI: 10.1016/j.cell.2020.05.048]

85 **O'Garra A**, Vieira P. Regulatory T cells and mechanisms of immune system control. *Nat Med* 2004; **10**: 801-805 [PMID: 15286781 DOI: 10.1038/nm0804-801]

86 **Fernandes C**, Wanderley CWS, Silva CMS, Muniz HA, Teixeira MA, Souza NRP, Cândido AGF, Falcão RB, Souza MHLP, Almeida PRC, Câmara LMC, Lima-Júnior RCP. Role of regulatory T cells in irinotecan-induced intestinal mucositis. *Eur J Pharm Sci* 2018; **115**: 158-166 [PMID: 29307857 DOI: 10.1016/j.ejps.2018.01.006]

87 **Geremia A**, Biancheri P, Allan P, Corazza GR, Di Sabatino A. Innate and adaptive immunity in inflammatory bowel disease. *Autoimmun Rev* 2014; **13**: 3-10 [PMID: 23774107 DOI: 10.1016/j.autrev.2013.06.004]

88 **Ueno A**, Jeffery L, Kobayashi T, Hibi T, Ghosh S, Jijon H. Th17 plasticity and its relevance to inflammatory bowel disease. *J Autoimmun* 2018; **87**: 38-49 [PMID: 29290521 DOI: 10.1016/j.jaut.2017.12.004]

89 **Zundler S**, Becker E, Spocinska M, Slawik M, Parga-Vidal L, Stark R, Wiendl M, Atreya R, Rath T, Leppkes M, Hildner K, López-Posadas R, Lukassen S, Ekici AB, Neufert C, Atreya I, van Gisbergen KPJM, Neurath MF. Hobit- and Blimp-1-driven $CD4^+$ tissue-resident memory T cells control chronic intestinal inflammation. *Nat Immunol* 2019; **20**: 288-300 [PMID: 30692620 DOI: 10.1038/s41590-018-0298-5]

90 **Rassendren F**, Buell GN, Virginio C, Collo G, North RA, Surprenant A. The permeabilizing ATP receptor, P2X7. Cloning and expression of a human cDNA. *J Biol Chem* 1997; **272**: 5482-5486 [PMID: 9038151 DOI: 10.1074/jbc.272.9.5482]

91 **McCarthy AE**, Yoshioka C, Mansoor SE. Full-Length $P2X_7$ Structures Reveal How Palmitoylation Prevents Channel Desensitization. *Cell* 2019; **179**: 659-670.e13 [PMID: 31587896 DOI: 10.1016/j.cell.2019.09.017]

92 **Surprenant A**, Rassendren F, Kawashima E, North RA, Buell G. The cytolytic P2Z receptor for extracellular ATP identified as a P2X receptor (P2X7). *Science* 1996; **272**: 735-738 [PMID: 8614837 DOI: 10.1126/science.272.5262.735]

93 **Zhu X**, Li Q, Song W, Peng X, Zhao R. P2X7 receptor: a critical regulator and potential target for breast cancer. *J Mol Med (Berl)* 2021; **99**: 349-358 [PMID: 33486566 DOI: 10.1007/s00109-021-02041-x]

94 **Gu BJ**, Zhang W, Worthington RA, Sluyter R, Dao-Ung P, Petrou S, Barden JA, Wiley JS. A Glu-496 to Ala polymorphism leads to loss of function of the human P2X7 receptor. *J Biol Chem* 2001; **276**: 11135-11142 [PMID: 11150303 DOI: 10.1074/jbc.M010353200]

95 **Wiley JS**, Dao-Ung LP, Li C, Shemon AN, Gu BJ, Smart ML, Fuller SJ, Barden JA, Petrou S, Sluyter R. An Ile-568 to Asn polymorphism prevents normal trafficking and function of the human P2X7 receptor. *J Biol Chem* 2003; **278**: 17108-17113 [PMID: 12586825 DOI: 10.1074/jbc.M212759200]

96 **Gu BJ**, Sluyter R, Skarratt KK, Shemon AN, Dao-Ung LP, Fuller SJ, Barden JA, Clarke AL, Petrou S, Wiley JS. An Arg307 to Gln polymorphism within the ATP-binding site causes loss of function of the human P2X7 receptor. *J Biol Chem* 2004; **279**: 31287-31295 [PMID: 15123679 DOI: 10.1074/jbc.M313902200]

97 **Wesselius A**, Bours MJ, Arts IC, Theunisz EH, Geusens P, Dagnelie PC. The P2X(7) loss-of-function Glu496Ala polymorphism affects *ex vivo* cytokine release and protects against the cytotoxic effects of high ATP-levels. *BMC Immunol* 2012; **13**: 64 [PMID: 23210974 DOI: 10.1186/1471-2172-13-64]

98 **Ide S**, Nishizawa D, Fukuda K, Kasai S, Hasegawa J, Hayashida M, Minami M, Ikeda K. Haplotypes of P2RX7 gene polymorphisms are associated with both cold pain sensitivity and analgesic effect of fentanyl. *Mol Pain* 2014; **10**: 75 [PMID: 25472448 DOI: 10.1186/1744-8069-10-75]

99 **Tao JH**, Cheng M, Tang JP, Dai XJ, Zhang Y, Li XP, Liu Q, Wang YL. Single nucleotide polymorphisms associated with P2X7R function regulate the onset of gouty arthritis. *PLoS One* 2017; **12**: e0181685 [PMID: 28797095 DOI: 10.1371/journal.pone.0181685]

100 **Pelegrin P**. P2X7 receptor and the NLRP3 inflammasome: Partners in crime. *Biochem Pharmacol* 2021; **187**: 114385 [PMID: 33359010 DOI: 10.1016/j.bcp.2020.114385]

101 **Garcia-Marcos M**, Pérez-Andrés E, Tandel S, Fontanils U, Kumps A, Kabré E, Gómez-Muñoz A, Marino A, Dehaye JP, Pochet S. Coupling of two pools of P2X7 receptors to distinct intracellular signaling pathways in rat submandibular gland. *J Lipid Res* 2006; **47**: 705-714 [PMID: 16415476 DOI: 10.1194/jlr.M500408-JLR200]

102 **North RA**. P2X receptors. *Philos Trans R Soc Lond B Biol Sci* 2016; **371** [PMID: 27377721 DOI: 10.1098/rstb.2015.0427]

103 **Virginio C**, MacKenzie A, North RA, Surprenant A. Kinetics of cell lysis, dye uptake and permeability changes in cells expressing the rat P2X7 receptor. *J Physiol* 1999; **519** Pt 2: 335-346 [PMID: 10457053 DOI: 10.1111/j.1469-7793.1999.0335m.x]

104 **Pelegrin P**, Surprenant A. Pannexin-1 mediates large pore formation and interleukin-1beta release by the ATP-gated P2X7 receptor. *EMBO J* 2006; **25**: 5071-5082 [PMID: 17036048 DOI: 10.1038/sj.emboj.7601378]

105 **Schachter J**, Motta AP, de Souza Zamorano A, da Silva-Souza HA, Guimarães MZ, Persechini PM. ATP-induced P2X7-associated uptake of large molecules involves distinct mechanisms for cations and anions in macrophages. *J Cell Sci* 2008; **121**: 3261-3270 [PMID: 18782864 DOI: 10.1242/jcs.029991]

106 **Browne LE**, Compan V, Bragg L, North RA. P2X7 receptor channels allow direct permeation of nanometer-sized dyes. *J Neurosci* 2013; **33**: 3557-3566 [PMID: 23426683 DOI: 10.1523/JNEUROSCI.2235-12.2013]

107 **Jiang LH**, Rassendren F, Mackenzie A, Zhang YH, Surprenant A, North RA. N-methyl-D-glucamine and propidium dyes utilize different permeation pathways at rat P2X(7) receptors. *Am J Physiol Cell Physiol* 2005; **289**: C1295-C1302 [PMID: 16093280 DOI: 10.1152/ajpcell.00253.2005]

108 **Amstrup J**, Novak I. P2X7 receptor activates extracellular signal-regulated kinases ERK1 and ERK2 independently of Ca2+ influx. *Biochem J* 2003; **374**: 51-61 [PMID: 12747800 DOI: 10.1042/bj20030585]

109 **Gavala ML**, Pfeiffer ZA, Bertics PJ. The nucleotide receptor P2RX7 mediates ATP-induced CREB activation in human and murine monocytic cells. *J Leukoc Biol* 2008; **84**: 1159-1171 [PMID: 18625910 DOI: 10.1189/jlb.0907612]

110 **Di Virgilio F**, Sarti AC, Grassi F. Modulation of innate and adaptive immunity by P2X ion channels. *Curr Opin Immunol* 2018; **52**: 51-59 [PMID: 29631184 DOI: 10.1016/j.coi.2018.03.026]

111 **Alarcón-Vila C**, Pizzuto M, Pelegrín P. Purinergic receptors and the inflammatory response mediated by lipids. *Curr Opin Pharmacol* 2019; **47**: 90-96 [PMID: 30952060 DOI: 10.1016/j.coph.2019.02.004]

112 **Burnstock G**. Purinergic signaling and vascular cell proliferation and death. *Arterioscler Thromb Vasc Biol* 2002; **22**: 364-373 [PMID: 11884276 DOI: 10.1161/hq0302.105360]

113 **Burnstock G**. Physiology and pathophysiology of purinergic neurotransmission. *Physiol Rev* 2007; **87**: 659-797 [PMID: 17429044 DOI: 10.1152/physrev.00043.2006]

114 **Surprenant A**, North RA. Signaling at purinergic P2X receptors. *Annu Rev Physiol* 2009; **71**: 333-359 [PMID: 18851707 DOI: 10.1146/annurev.physiol.70.113006.100630]

115 **Sun X**, Zhou R, Lei Y, Hu J, Li X. The ligand-gated ion channel P2X7 receptor mediates NLRP3/caspase-1-mediated pyroptosis in cerebral cortical neurons of juvenile rats with sepsis. *Brain Res* 2020; **1748**: 147109 [PMID: 32905819 DOI: 10.1016/j.brainres.2020.147109]

116 **Bulanova E**, Bulfone-Paus S. P2 receptor-mediated signaling in mast cell biology. *Purinergic Signal* 2010; **6**: 3-17 [PMID: 19921464 DOI: 10.1007/s11302-009-9173-z]

117 **Ruan Z**, Orozco IJ, Du J, Lü W. Structures of human pannexin 1 reveal ion pathways and mechanism of gating. *Nature* 2020; **584**: 646-651 [PMID: 32494015 DOI: 10.1038/s41586-020-2357-y]

118 **Chekeni FB**, Elliott MR, Sandilos JK, Walk SF, Kinchen JM, Lazarowski ER, Armstrong AJ, Penuela S, Laird DW, Salvesen GS, Isakson BE, Bayliss DA, Ravichandran KS. Pannexin 1 channels mediate 'find-me' signal release and membrane permeability during apoptosis. *Nature* 2010; **467**: 863-867 [PMID: 20944749 DOI: 10.1038/nature09413]

119 **Barberà-Cremades M**, Baroja-Mazo A, Gomez AI, Machado F, Di Virgilio F, Pelegrín P. P2X7 receptor-stimulation causes fever *via* PGE2 and IL-1β release. *FASEB J* 2012; **26**: 2951-2962 [PMID: 22490780 DOI: 10.1096/fj.12-205765]

120 **Amores-Iniesta J**, Barberà-Cremades M, Martínez CM, Pons JA, Revilla-Nuin B, Martínez-Alarcón L, Di Virgilio F, Parrilla P, Baroja-Mazo A, Pelegrín P. Extracellular ATP Activates the NLRP3 Inflammasome and Is an Early Danger Signal of Skin Allograft Rejection. *Cell Rep* 2017; **21**: 3414-3426 [PMID: 29262323 DOI: 10.1016/j.celrep.2017.11.079]

121 **Chen WY**, Wang M, Zhang J, Barve SS, McClain CJ, Joshi-Barve S. Acrolein Disrupts Tight Junction Proteins and Causes Endoplasmic Reticulum Stress-Mediated Epithelial Cell Death Leading to Intestinal Barrier Dysfunction and Permeability. *Am J Pathol* 2017; **187**: 2686-2697 [PMID: 28935573 DOI: 10.1016/j.ajpath.2017.08.015]

122 **Sun S**, Duan Z, Wang X, Chu C, Yang C, Chen F, Wang D, Wang C, Li Q, Ding W. Neutrophil extracellular traps impair intestinal barrier functions in sepsis by regulating TLR9-mediated endoplasmic reticulum stress pathway. *Cell Death Dis* 2021; **12**: 606 [PMID: 34117211 DOI: 10.1038/s41419-021-03896-1]

123 **Piconese S**, Gri G, Tripodo C, Musio S, Gorzanelli A, Frossi B, Pedotti R, Pucillo CE, Colombo MP. Mast cells counteract regulatory T-cell suppression through interleukin-6 and OX40/OX40L axis toward Th17-cell differentiation. *Blood* 2009; **114**: 2639-2648 [PMID: 19643985 DOI: 10.1182/blood-2009-05-220004]

124 **Proietti M**, Cornacchione V, Rezzonico Jost T, Romagnani A, Faliti CE, Perruzza L, Rigoni R, Radaelli E, Caprioli F, Preziuso S, Brannetti B, Thelen M, McCoy KD, Slack E, Traggiai E, Grassi F. ATP-gated ionotropic P2X7 receptor controls follicular T helper cell numbers in Peyer's patches to promote host-microbiota mutualism. *Immunity* 2014; **41**: 789-801 [PMID: 25464855 DOI: 10.1016/j.immuni.2014.10.010]

125 **Proietti M**, Perruzza L, Scribano D, Pellegrini G, D'Antuono R, Strati F, Raffaelli M, Gonzalez SF, Thelen M, Hardt WD, Slack E, Nicoletti M, Grassi F. ATP released by intestinal bacteria limits the generation of protective IgA against enteropathogens. *Nat Commun* 2019; **10**: 250 [PMID: 30651557 DOI: 10.1038/s41467-018-08156-z]

126 **Perruzza L**, Gargari G, Proietti M, Fosso B, D'Erchia AM, Faliti CE, Rezzonico-Jost T, Scribano D, Mauri L, Colombo D, Pellegrini G, Moregola A, Mooser C, Pesole G, Nicoletti M, Norata GD, Geuking MB, McCoy KD, Guglielmetti S, Grassi F. T Follicular Helper Cells Promote a Beneficial Gut Ecosystem for Host Metabolic Homeostasis by Sensing Microbiota-Derived Extracellular ATP. *Cell Rep* 2017; **18**: 2566-2575 [PMID: 28297661 DOI: 10.1016/j.celrep.2017.02.061]

127 **Wu X**, Ren J, Chen G, Wu L, Song X, Li G, Deng Y, Wang G, Gu G, Li J. Systemic blockade of P2X7 receptor protects against sepsis-induced intestinal barrier disruption. *Sci Rep* 2017; **7**: 4364 [PMID: 28663567 DOI: 10.1038/s41598-017-04231-5]

128 **Jiang H**, Gong T, Zhou R. The strategies of targeting the NLRP3 inflammasome to treat inflammatory diseases. *Adv Immunol* 2020; **145**: 55-93 [PMID: 32081200 DOI: 10.1016/bs.ai.2019.11.003]

129 **Li M**, Lv R, Wang C, Ge Q, Du H, Lin S. *Tricholoma matsutake*-derived peptide WFNNAGP protects against DSS-induced colitis by ameliorating oxidative stress and intestinal barrier dysfunction. *Food Funct* 2021; **12**: 11883-11897 [PMID: 34738612 DOI: 10.1039/d1fo02806e]

130 **Lee GS**, Subramanian N, Kim AI, Aksentijevich I, Goldbach-Mansky R, Sacks DB, Germain RN, Kastner DL, Chae JJ. The calcium-sensing receptor regulates the NLRP3 inflammasome through Ca2+ and cAMP. *Nature* 2012; **492**: 123-127 [PMID: 23143333 DOI: 10.1038/nature11588]

131 **Tschopp J**, Schroder K. NLRP3 inflammasome activation: The convergence of multiple signalling pathways on ROS production? *Nat Rev Immunol* 2010; **10**: 210-215 [PMID: 20168318 DOI: 10.1038/nri2725]

132 **Hafner-Bratkovič I**, Pelegrín P. Ion homeostasis and ion channels in NLRP3 inflammasome activation and regulation. *Curr Opin Immunol* 2018; **52**: 8-17 [PMID: 29555598 DOI: 10.1016/j.coi.2018.03.010]

133 **Di A**, Xiong S, Ye Z, Malireddi RKS, Kometani S, Zhong M, Mittal M, Hong Z, Kanneganti TD, Rehman J, Malik AB. The TWIK2 Potassium Efflux Channel in Macrophages Mediates NLRP3 Inflammasome-Induced Inflammation. *Immunity* 2018; **49**: 56-65.e4 [PMID: 29958799 DOI: 10.1016/j.immuni.2018.04.032]

134 **Woehrle T**, Yip L, Elkhal A, Sumi Y, Chen Y, Yao Y, Insel PA, Junger WG. Pannexin-1 hemichannel-mediated ATP release together with P2X1 and P2X4 receptors regulate T-cell activation at the immune synapse. *Blood* 2010; **116**: 3475-3484 [PMID: 20660288 DOI: 10.1182/blood-2010-04-277707]

135 **Yip L**, Woehrle T, Corriden R, Hirsh M, Chen Y, Inoue Y, Ferrari V, Insel PA, Junger WG. Autocrine regulation of T-cell activation by ATP release and P2X7 receptors. *FASEB J* 2009; **23**: 1685-1693 [PMID: 19211924 DOI: 10.1096/fj.08-126458]

136 **Liu Q**, Kim CH. Control of Tissue-Resident Invariant NKT Cells by Vitamin A Metabolites and P2X7-Mediated Cell

Death. *J Immunol* 2019; **203**: 1189-1197 [PMID: 31308092 DOI: 10.4049/jimmunol.1900398]
137 **Arbonés ML**, Ord DC, Ley K, Ratech H, Maynard-Curry C, Otten G, Capon DJ, Tedder TF. Lymphocyte homing and leukocyte rolling and migration are impaired in L-selectin-deficient mice. *Immunity* 1994; **1**: 247-260 [PMID: 7534203 DOI: 10.1016/1074-7613(94)90076-0]
138 **Masopust D**, Schenkel JM. The integration of T cell migration, differentiation and function. *Nat Rev Immunol* 2013; **13**: 309-320 [PMID: 23598650 DOI: 10.1038/nri3442]
139 **Mueller SN**, Gebhardt T, Carbone FR, Heath WR. Memory T cell subsets, migration patterns, and tissue residence. *Annu Rev Immunol* 2013; **31**: 137-161 [PMID: 23215646 DOI: 10.1146/annurev-immunol-032712-095954]
140 **Foster JG**, Carter E, Kilty I, MacKenzie AB, Ward SG. Mitochondrial superoxide generation enhances P2X7R-mediated loss of cell surface CD62L on naive human CD4+ T lymphocytes. *J Immunol* 2013; **190**: 1551-1559 [PMID: 23319734 DOI: 10.4049/jimmunol.1201510]
141 **Grassi F**. The P2X7 Receptor as Regulator of T Cell Development and Function. *Front Immunol* 2020; **11**: 1179 [PMID: 32587592 DOI: 10.3389/fimmu.2020.01179]
142 **Wang CM**, Ploia C, Anselmi F, Sarukhan A, Viola A. Adenosine triphosphate acts as a paracrine signaling molecule to reduce the motility of T cells. *EMBO J* 2014; **33**: 1354-1364 [PMID: 24843045 DOI: 10.15252/embj.201386666]
143 **Sluyter R**. The P2X7 Receptor. *Adv Exp Med Biol* 2017; **1051**: 17-53 [PMID: 28676924 DOI: 10.1007/5584_2017_59]
144 **Tsukimoto M**, Maehata M, Harada H, Ikari A, Takagi K, Degawa M. P2X7 receptor-dependent cell death is modulated during murine T cell maturation and mediated by dual signaling pathways. *J Immunol* 2006; **177**: 2842-2850 [PMID: 16920919 DOI: 10.4049/jimmunol.177.5.2842]
145 **Auger R**, Motta I, Benihoud K, Ojcius DM, Kanellopoulos JM. A role for mitogen-activated protein kinase(Erk1/2) activation and non-selective pore formation in P2X7 receptor-mediated thymocyte death. *J Biol Chem* 2005; **280**: 28142-28151 [PMID: 15937334 DOI: 10.1074/jbc.M501290200]
146 **Scheuplein F**, Schwarz N, Adriouch S, Krebs C, Bannas P, Rissiek B, Seman M, Haag F, Koch-Nolte F. NAD+ and ATP released from injured cells induce P2X7-dependent shedding of CD62L and externalization of phosphatidylserine by murine T cells. *J Immunol* 2009; **182**: 2898-2908 [PMID: 19234185 DOI: 10.4049/jimmunol.0801711]
147 **Le Stunff H**, Auger R, Kanellopoulos J, Raymond MN. The Pro-451 to Leu polymorphism within the C-terminal tail of P2X7 receptor impairs cell death but not phospholipase D activation in murine thymocytes. *J Biol Chem* 2004; **279**: 16918-16926 [PMID: 14761980 DOI: 10.1074/jbc.M313064200]
148 **Adriouch S**, Hubert S, Pechberty S, Koch-Nolte F, Haag F, Seman M. NAD+ released during inflammation participates in T cell homeostasis by inducing ART2-mediated death of naive T cells in vivo. *J Immunol* 2007; **179**: 186-194 [PMID: 17579037 DOI: 10.4049/jimmunol.179.1.186]
149 **Hubert S**, Rissiek B, Klages K, Huehn J, Sparwasser T, Haag F, Koch-Nolte F, Boyer O, Seman M, Adriouch S. Extracellular NAD+ shapes the Foxp3+ regulatory T cell compartment through the ART2-P2X7 pathway. *J Exp Med* 2010; **207**: 2561-2568 [PMID: 20975043 DOI: 10.1084/jem.20091154]
150 **Iyer SS**, Latner DR, Zilliox MJ, McCausland M, Akondy RS, Penaloza-Macmaster P, Hale JS, Ye L, Mohammed AU, Yamaguchi T, Sakaguchi S, Amara RR, Ahmed R. Identification of novel markers for mouse CD4(+) T follicular helper cells. *Eur J Immunol* 2013; **43**: 3219-3232 [PMID: 24030473 DOI: 10.1002/eji.201343469]
151 **Borges da Silva H**, Beura LK, Wang H, Hanse EA, Gore R, Scott MC, Walsh DA, Block KE, Fonseca R, Yan Y, Hippen KL, Blazar BR, Masopust D, Kelekar A, Vulchanova L, Hogquist KA, Jameson SC. The purinergic receptor P2RX7 directs metabolic fitness of long-lived memory CD8$^+$ T cells. *Nature* 2018; **559**: 264-268 [PMID: 29973721 DOI: 10.1038/s41586-018-0282-0]
152 **Wanhainen KM**, Jameson SC, da Silva HB. Self-Regulation of Memory CD8 T Cell Metabolism through Extracellular ATP Signaling. *Immunometabolism* 2019; **1** [PMID: 31428464 DOI: 10.20900/immunometab20190009]
153 **Herzig S**, Shaw RJ. AMPK: guardian of metabolism and mitochondrial homeostasis. *Nat Rev Mol Cell Biol* 2018; **19**: 121-135 [PMID: 28974774 DOI: 10.1038/nrm.2017.95]
154 **Roncarolo MG**, Gregori S, Battaglia M, Bacchetta R, Fleischhauer K, Levings MK. Interleukin-10-secreting type 1 regulatory T cells in rodents and humans. *Immunol Rev* 2006; **212**: 28-50 [PMID: 16903904 DOI: 10.1111/j.0105-2896.2006.00420.x]
155 **Mascanfroni ID**, Takenaka MC, Yeste A, Patel B, Wu Y, Kenison JE, Siddiqui S, Basso AS, Otterbein LE, Pardoll DM, Pan F, Priel A, Clish CB, Robson SC, Quintana FJ. Metabolic control of type 1 regulatory T cell differentiation by AHR and HIF1-α. *Nat Med* 2015; **21**: 638-646 [PMID: 26005855 DOI: 10.1038/nm.3868]
156 **Fernández D**, Flores-Santibáñez F, Neira J, Osorio-Barrios F, Tejón G, Nuñez S, Hidalgo Y, Fuenzalida MJ, Meza D, Ureta G, Lladser A, Pacheco R, Acuña-Castillo C, Guixé V, Quintana FJ, Bono MR, Rosemblatt M, Sauma D. Purinergic Signaling as a Regulator of Th17 Cell Plasticity. *PLoS One* 2016; **11**: e0157889 [PMID: 27322617 DOI: 10.1371/journal.pone.0157889]
157 **Del Prete A**, Scutera S, Sozzani S, Musso T. Role of osteopontin in dendritic cell shaping of immune responses. *Cytokine Growth Factor Rev* 2019; **50**: 19-28 [PMID: 31126876 DOI: 10.1016/j.cytogfr.2019.05.004]
158 **de Jong EC**, Smits HH, Kapsenberg ML. Dendritic cell-mediated T cell polarization. *Springer Semin Immunopathol* 2005; **26**: 289-307 [PMID: 15609003 DOI: 10.1007/s00281-004-0167-1]
159 **la Sala A**, Ferrari D, Corinti S, Cavani A, Di Virgilio F, Girolomoni G. Extracellular ATP induces a distorted maturation of dendritic cells and inhibits their capacity to initiate Th1 responses. *J Immunol* 2001; **166**: 1611-1617 [PMID: 11160202 DOI: 10.4049/jimmunol.166.3.1611]
160 **la Sala A**, Sebastiani S, Ferrari D, Di Virgilio F, Idzko M, Norgauer J, Girolomoni G. Dendritic cells exposed to extracellular adenosine triphosphate acquire the migratory properties of mature cells and show a reduced capacity to attract type 1 T lymphocytes. *Blood* 2002; **99**: 1715-1722 [PMID: 11861288 DOI: 10.1182/blood.v99.5.1715]
161 **Li R**, Wang J, Li R, Zhu F, Xu W, Zha G, He G, Cao H, Wang Y, Yang J. ATP/P2X7-NLRP3 axis of dendritic cells participates in the regulation of airway inflammation and hyper-responsiveness in asthma by mediating HMGB1 expression and secretion. *Exp Cell Res* 2018; **366**: 1-15 [PMID: 29545090 DOI: 10.1016/j.yexcr.2018.03.002]

162 **Atarashi K**, Nishimura J, Shima T, Umesaki Y, Yamamoto M, Onoue M, Yagita H, Ishii N, Evans R, Honda K, Takeda K. ATP drives lamina propria T(H)17 cell differentiation. *Nature* 2008; **455**: 808-812 [PMID: 18716618 DOI: 10.1038/nature07240]

163 **Principi E**, Raffaghello L. The role of the P2X7 receptor in myeloid-derived suppressor cells and immunosuppression. *Curr Opin Pharmacol* 2019; **47**: 82-89 [PMID: 30959357 DOI: 10.1016/j.coph.2019.02.010]

164 **Ayala JC**, Grismaldo A, Aristizabal-Pachon AF, Mikhaylenko EV, Nikolenko VN, Mikhaleva LM, Somasundaram SG, Kirkland CE, Aliev G, Morales L. Mitochondrial Dysfunction in Intensive Care Unit Patients. *Curr Pharm Des* 2021; **27**: 3074-3081 [PMID: 33292115 DOI: 10.2174/1381612826666201207112931]

165 **De Winter BY**, De Man JG. Interplay between inflammation, immune system and neuronal pathways: effect on gastrointestinal motility. *World J Gastroenterol* 2010; **16**: 5523-5535 [PMID: 21105185 DOI: 10.3748/wjg.v16.i44.5523]

166 **Tian X**, Li L, Fu G, Wang J, He Q, Zhang C, Qin B. miR-133a-3p regulates the proliferation and apoptosis of intestinal epithelial cells by modulating the expression of TAGLN2. *Exp Ther Med* 2021; **22**: 824 [PMID: 34149870 DOI: 10.3892/etm.2021.10256]

167 **Preza GC**, Yang OO, Elliott J, Anton PA, Ochoa MT. T lymphocyte density and distribution in human colorectal mucosa, and inefficiency of current cell isolation protocols. *PLoS One* 2015; **10**: e0122723 [PMID: 25856343 DOI: 10.1371/journal.pone.0122723]

168 **Tindemans I**, Joosse ME, Samsom JN. Dissecting the Heterogeneity in T-Cell Mediated Inflammation in IBD. *Cells* 2020; **9** [PMID: 31906479 DOI: 10.3390/cells9010110]

169 **Heiss K**, Jänner N, Mähnss B, Schumacher V, Koch-Nolte F, Haag F, Mittrücker HW. High sensitivity of intestinal CD8+ T cells to nucleotides indicates P2X7 as a regulator for intestinal T cell responses. *J Immunol* 2008; **181**: 3861-3869 [PMID: 18768840 DOI: 10.4049/jimmunol.181.6.3861]

170 **Hashimoto-Hill S**, Friesen L, Kim M, Kim CH. Contraction of intestinal effector T cells by retinoic acid-induced purinergic receptor P2X7. *Mucosal Immunol* 2017; **10**: 912-923 [PMID: 27966552 DOI: 10.1038/mi.2016.109]

171 **Shokoples BG**, Paradis P, Schiffrin EL. P2X7 Receptors: An Untapped Target for the Management of Cardiovascular Disease. *Arterioscler Thromb Vasc Biol* 2021; **41**: 186-199 [PMID: 32998520 DOI: 10.1161/ATVBAHA.120.315116]

172 **Zhou J**, Zhou Z, Liu X, Yin HY, Tang Y, Cao X. P2X7 Receptor-Mediated Inflammation in Cardiovascular Disease. *Front Pharmacol* 2021; **12**: 654425 [PMID: 33995071 DOI: 10.3389/fphar.2021.654425]

173 **Sharma D**, Kanneganti TD. The cell biology of inflammasomes: Mechanisms of inflammasome activation and regulation. *J Cell Biol* 2016; **213**: 617-629 [PMID: 27325789 DOI: 10.1083/jcb.201602089]

174 **Rivas-Yáñez E**, Barrera-Avalos C, Parra-Tello B, Briceño P, Rosemblatt MV, Saavedra-Almarza J, Rosemblatt M, Acuña-Castillo C, Bono MR, Sauma D. P2X7 Receptor at the Crossroads of T Cell Fate. *Int J Mol Sci* 2020; **21** [PMID: 32668623 DOI: 10.3390/ijms21144937]

175 **Raffaghello L**, Principi E, Baratto S, Panicucci C, Pintus S, Antonini F, Del Zotto G, Benzi A, Bruzzone S, Scudieri P, Minetti C, Gazzerro E, Bruno C. P2X7 Receptor Antagonist Reduces Fibrosis and Inflammation in a Mouse Model of Alpha-Sarcoglycan Muscular Dystrophy. *Pharmaceuticals (Basel)* 2022; **15** [PMID: 35056146 DOI: 10.3390/ph15010089]

176 **Santiago-Carvalho I**, de Almeida-Santos G, Bomfim CCB, de Souza PC, Silva JCSE, de Melo BMS, Amaral EP, Cione MVP, Lasunskaia E, Hirata MH, Alves-Filho JCF, Nakaya HI, Alvarez JM, D'Império Lima MR. P2x7 Receptor Signaling Blockade Reduces Lung Inflammation and Necrosis During Severe Experimental Tuberculosis. *Front Cell Infect Microbiol* 2021; **11**: 672472 [PMID: 34026666 DOI: 10.3389/fcimb.2021.672472]

177 **Savio LEB**, de Andrade Mello P, da Silva CG, Coutinho-Silva R. The P2X7 Receptor in Inflammatory Diseases: Angel or Demon? *Front Pharmacol* 2018; **9**: 52 [PMID: 29467654 DOI: 10.3389/fphar.2018.00052]

World Journal of Gastroenterology

Submit a Manuscript: https://www.f6publishing.com

World J Gastroenterol 2022 September 28; 28(36): 5280-5299

DOI: 10.3748/wjg.v28.i36.5280

ISSN 1007-9327 (print) ISSN 2219-2840 (online)

REVIEW

Liver-specific drug delivery platforms: Applications for the treatment of alcohol-associated liver disease

Jeffrey Barr Warner, Steven Corrigan Guenthner, Josiah Everett Hardesty, Craig James McClain, Dennis Ray Warner, Irina Andreyevna Kirpich

Specialty type: Gastroenterology and hepatology

Provenance and peer review: Unsolicited article; Externally peer reviewed.

Peer-review model: Single blind

Peer-review report's scientific quality classification

Grade A (Excellent): 0
Grade B (Very good): B, B, B
Grade C (Good): 0
Grade D (Fair): 0
Grade E (Poor): 0

P-Reviewer: Barisani D, Italy; Li H, China; Senchukova M, Russia

Received: June 24, 2022
Peer-review started: June 24, 2022
First decision: August 6, 2022
Revised: August 16, 2022
Accepted: September 6, 2022
Article in press: September 6, 2022
Published online: September 28, 2022

Jeffrey Barr Warner, Steven Corrigan Guenthner, Josiah Everett Hardesty, Craig James McClain, Dennis Ray Warner, Irina Andreyevna Kirpich, Department of Medicine, Division of Gastroenterology, Hepatology and Nutrition, University of Louisville School of Medicine, Louisville, KY 40202, United States

Jeffrey Barr Warner, Irina Andreyevna Kirpich, Department of Pharmacology and Toxicology, University of Louisville School of Medicine, Louisville, KY 40202, United States

Craig James McClain, Irina Andreyevna Kirpich, Alcohol Research Center, University of Louisville School of Medicine, Louisville, KY 40202, United States

Craig James McClain, Irina Andreyevna Kirpich, Hepatobiology and Toxicology Center, University of Louisville School of Medicine, Louisville, KY 40202, United States

Craig James McClain, Veterans Health Administration, Robley Rex Veterans Medical Center, Louisville, KY 40206, United States

Irina Andreyevna Kirpich, Department of Microbiology and Immunology, University of Louisville School of Medicine, Louisville, KY 40202, United States

Corresponding author: Irina Andreyevna Kirpich, MPH, PhD, Associate Professor, Department of Microbiology and Immunology, University of Louisville School of Medicine, 505 S. Hancock St., Louisville, KY 40202, United States. irina.kirpich@louisville.edu

Abstract

Alcohol-associated liver disease (ALD) is a common chronic liver disease and major contributor to liver disease-related deaths worldwide. Despite its prevalence, there are few effective pharmacological options for the severe stages of this disease. While much pre-clinical research attention is paid to drug development in ALD, many of these experimental therapeutics have limitations such as poor pharmacokinetics, poor efficacy, or off-target side effects due to systemic administration. One means of addressing these limitations is through liver-targeted drug delivery, which can be accomplished with different platforms including liposomes, polymeric nanoparticles, exosomes, bacteria, and adeno-associated viruses, among others. These platforms allow drugs to target the liver passively or actively, thereby reducing systemic circulation and increasing the 'effective dose' in the liver. While many studies, some clinical, have applied targeted delivery systems to other liver diseases such as viral hepatitis or hepato-

cellular carcinoma, only few have investigated their efficacy in ALD. This review provides basic information on these liver-targeting drug delivery platforms, including their benefits and limitations, and summarizes the current research efforts to apply them to the treatment of ALD in rodent models. We also discuss gaps in knowledge in the field, which when addressed, may help to increase the efficacy of novel therapies and better translate them to humans.

Key Words: Liver targeted delivery; Nanoparticles; Liposomes; Polymeric nanoparticles; Precision medicine; Alcohol associated liver disease

Core Tip: Alcohol-associated liver disease (ALD) is a common chronic liver disease and global healthcare burden. While a great deal of pre-clinical research attention is paid to ALD, many experimental therapeutics which are administered systemically suffer from poor pharmacokinetics or poor efficacy. Liver-targeted delivery may address these drawbacks while avoiding extra-hepatic side effects. This article reviews literature applying liver-targeted drug delivery platforms such as liposomes, exosomes, polymeric nanoparticles, viruses, and bioengineered bacteria to the treatment of ALD.

Citation: Warner JB, Guenthner SC, Hardesty JE, McClain CJ, Warner DR, Kirpich IA. Liver-specific drug delivery platforms: Applications for the treatment of alcohol-associated liver disease. *World J Gastroenterol* 2022; 28(36): 5280-5299
URL: https://www.wjgnet.com/1007-9327/full/v28/i36/5280.htm
DOI: https://dx.doi.org/10.3748/wjg.v28.i36.5280

INTRODUCTION

Pathogenesis and pharmacological management of alcohol-associated liver disease

Alcohol-associated liver disease (ALD) is a common chronic liver disease and contributes to the global healthcare burden caused by excess alcohol consumption, which is defined as more than 1 or 2 standard drinks of alcohol per day for females and males, respectively. Globally, nearly half of liver cirrhosis deaths are attributed to alcohol abuse[1]. The pathogenesis of ALD follows a well-described pattern of disease stages beginning with simple liver steatosis progressing to steatohepatitis (steatosis with inflammation), cirrhosis (advanced liver fibrosis), and in some severe cases, hepatocellular carcinoma (HCC) [2] (Figure 1A). In individuals who chronically consume alcohol, binge-drinking episodes may cause acute alcohol-associated hepatitis (AH), a life-threatening condition with high short-term mortality due to infection, severe inflammation, and multi-organ failure[3]. The pathophysiology of ALD is multifactorial and involves a variety of effects of alcohol on multiple organs, including the liver and the gut (Figure 1B). For example, alcohol-induced intestinal permeability and subsequent translocation of gut bacteria and bacteria-derived products into the portal circulation may contribute to inflammation, hepatic stellate cell (HSC) activation, and fibrosis in the liver. Further, direct effects of alcohol on the liver may result in dysregulated lipid signaling, hepatocyte cell death, and production of reactive oxygen species leading to steatosis as well as further inflammation, fibrosis, and ultimately liver cancer (these concepts have been reviewed in detail previously[2]). Most patients with early-to-mid-stage ALD (*i.e.*, hepatic steatosis or mild steatohepatitis) are asymptomatic, therefore a diagnosis of ALD is often not made until later stages of the disease. In those individuals where a diagnosis is made, abstinence and nutrition are key, and indeed, some stages of the disease (*e.g.*, steatosis) are reversible upon alcohol cessation. Limited pharmacological options exist for patients with alcohol-related late-stage liver disease (*e.g.*, cirrhosis or AH), including prednisolone (a corticosteroid) and pentoxifylline (a phosphodiesterase inhibitor used in patients for which corticosteroids are contraindicated or not effective), but importantly, these drugs only reduce short-term mortality[4,5]. There is much research attention being given to drug development in ALD using animal models. These therapies target various pathogenic mechanisms in ALD including oxidative stress (*e.g.*, S-adenosylmethionine, betaine, natural antioxidants), inflammation [*e.g.*, anti-tumor necrosis factor (TNF) therapy, interleukin (IL)-22, glucocorticoids, steroids, IL-1R inhibitors, granulocyte-colony stimulating factor], fibrosis (*e.g.*, transforming growth factor-β inhibitors, phosphodiesterase inhibitors, PPAR agonists), gut barrier dysfunction and microbial dysbiosis (*e.g.*, probiotics and antibiotics), and other processes (these drugs and others are thoroughly reviewed in[6]).

Overview of liver-specific drug delivery systems

While much pre-clinical research attention is given to new drug development for liver diseases,

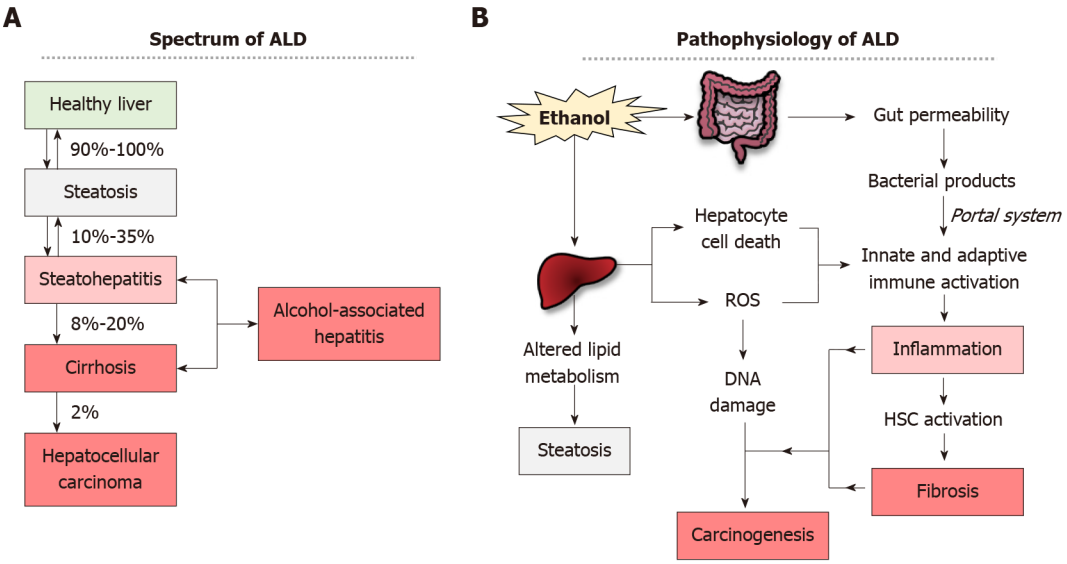

DOI: 10.3748/wjg.v28.i36.5280 **Copyright** ©The Author(s) 2022.

Figure 1 Spectrum and pathophysiology of alcohol-associated liver disease. A: Schematic diagram describing the spectrum of disease stages in alcohol-associated liver disease (ALD). Percentages represent proportion of chronic drinkers who progress to the indicated disease stage; B: Schematic diagram depicting the pathophysiology of ALD. Ethanol affects both the gut and liver to induce changes in lipid metabolism, generation of reactive oxygen species and hepatocyte cell death, gut permeability, and downstream consequences including inflammation, hepatic stellate cell activation, fibrosis, DNA damage, and carcinogenesis. ALD: Alcohol-associated liver disease; ROS: Reactive oxygen species; HSC: Hepatic stellate cell.

including ALD, many experimental therapeutics relying on systemic drug administration suffer from drawbacks including poor pharmacokinetics or a low margin of safety due to off-target effects in other organs. An example of an early attempt to address some of these drawbacks is covalent conjugation of polyethylene glycol (PEG) to drug molecules (termed 'PEGylation'), a strategy that has been used for many years to lengthen half-life, improve water solubility, and decrease immunogenicity[7]. For instance, PEGylated interferon-α has been the first line treatment for chronic hepatitis B since 2005[8]. However, since that time, advances in nanomedicine have produced numerous liver-specific drug delivery platforms based on lipid vesicles, inorganic nanoparticles, and biological systems which allow: (1) Improved pharmacokinetics for drugs with poor solubility, low bioavailability, rapid metabolism, *etc*.; (2) Reduced systemic side effects by delivering drugs to the liver while avoiding other organs; and (3) Improved efficacy of drugs intended to act in the liver by increasing the 'effective dose'.

There are several types of liver-targeting drug delivery platforms which can be broadly categorized by their composition, including: lipid-based particles (*e.g*., micelles, liposomes, and exosomes, Figure 2A), non-lipid-based particles [*e.g*., polymeric nanoparticles (PNPs), metallic nanoparticles, and ceramic nanoparticles, Figure 2B], and bacterial and viral platforms (*e.g*., bioengineered bacteria and adeno-associated viruses, Figure 2C). These systems are either synthetic or derived from living systems, and have distinct advantages and disadvantages based on their efficacy, pharmacokinetics, and side effects (summarized in Table 1). Briefly, lipid-based particles are composed of endogenous lipids which keep the risk of immunogenicity and toxicity low. Metallic, ceramic, and some PNPs are non-biodegradable and sometimes cytotoxic, but can be modified to reduce toxicity and have additional uses in medical imaging and diagnostics[9]. Bacterial and viral drug delivery platforms benefit from the natural tropism of certain bacteria or viruses for a particular organ or niche but are also potentially immunogenic. These liver-targeting approaches have been used for the treatment of various liver diseases including HCC (*e.g*., liposomal, PEGylated, or PNP-encapsulated anti-cancer compounds[10-12]), viral hepatitis (*e.g*., metal nanoparticles[13] and PEGylated interferon[8]), and liver fibrosis (*e.g*., liposomal vitamin A[14]) with some reaching full FDA approval (*e.g*., Pegasys, Miriplatin, and others)[15].

Biodistribution of liver-targeted drug delivery platforms

The benefits of the liver specific drug delivery platforms stem from their unique ability to biodistribute to the liver while avoiding accumulation in other organs. To better understand the *in vivo* pharmacokinetics of these platforms, a knowledge of the structural organization of the liver and distribution of liver cell types is necessary. A graphical representation of liver structure and cell types can be found in Figure 3. The well-accepted lobular model of liver architecture describes the organ as being divided into discrete hexagonal anatomical units called lobules (Figure 3A)[16]. Surrounding the perimeter of the lobule at each vertex is a portal triad — a vascular bundle composed of a hepatic artery, portal vein, and bile duct. Portal blood and arterial blood fill fenestrated hepatic sinusoids and drain toward the central vein, providing oxygen and nutrients (as well as drugs and nanoparticles) to liver tissue. With regard to

Table 1 Summary of liver-specific drug delivery platforms, including molecular composition, potential modifications, benefits, and limitations

Platform	Composition	Origin	Benefits	Limitations
Lipid-based				
Liposomes	Lipids	Synthetic	Non-immunogenic, non-toxic, modifiable	High clearance by liver/spleen RES
Exosomes	Lipids	Biological	Endogenous cargo (proteins, nucleic acids, *etc.*), but can add additional cargo	Non-standardized isolation methods, potentially immunogenic
Micelles	Lipids	Biological	Non-immunogenic, non-toxic, modifiable	High clearance by liver/spleen RES
Non-lipid-based				
Polymeric nanoparticles	Polymers	Synthetic	Modifiable, capable of controlled drug release	High clearance by liver/spleen RES, potentially immunogenic
Metallic nanoparticles	Gold, silver, aluminum, zinc, iron, gadolinium, copper, rubidium, palladium, titanium	Synthetic	Modifiable, magnetic (iron), anti-microbial (copper, silver, titanium)	Non-biodegradable and potentially cytotoxic, immunogenic, or allergenic
Ceramic nanoparticles	Carbon, silicon with metallic or non-metallic core	Synthetic	Modifiable, resistant to pH change	Potentially cytotoxic or immunogenic, non-biodegradable or lowly biodegradable
Bacterial and viral				
Bacteria	Bacterial cells	Biological	Self-propulsion, chemotaxis, on-site drug production, transfection	Immunogenicity, infection risk
Viral vectors	AAVs, HSVs	Biological	Active liver tropism	Immunogenicity, toxicity, neutralizing antibodies

RES: Reticuloendothelial system; AAV: Adeno-associated virus; HSV: Herpes simplex virus.

cellular composition, the liver is divided into parenchymal and non-parenchymal cell types. The parenchymal cells of the liver are the hepatocytes, constituting a majority of cells by both number and volume (60% and 80%, respectively, Figure 3B)[17]. The remaining non-parenchymal cells include liver sinusoidal endothelial cells (LSECs), tissue resident macrophages (Kupffer cells, KCs), HSCs, and intra-hepatic lymphocytes (T cells, B cells, natural killer cells, *etc.*). LSECs form a fenestrated endothelium lacking a basal lamina separating liver sinusoids from the liver parenchyma.

The biodistribution of liver-specific drug delivery platforms in the body after systemic administration is based on the physical properties of the particle. For example, before reaching target liver cells, many particles may be opsonized by binding plasma proteins (*e.g.*, albumin, apolipoproteins, antibodies, complement component proteins) and cleared by the reticuloendothelial system (RES) of the liver and spleen, including by LSECs, particularly if the particles are greater than 200 nm in diameter or carry a negative charge[18]. Particle modifications such as PEGylation help avoid RES surveillance by preventing plasma protein binding, thereby improving *in vivo* half-life. Stealth liposomes, for example, are PEGylated phospholipid particles commonly used to improve the pharmacokinetics of a drug with a short half-life[19]. Particles which avoid RES clearance and have favorable size and charge can pass through the liver sinusoidal fenestrae, which are approximately 100-150 nm in diameter[20], to access HSCs in the space of Disse and the liver parenchyma. Accordingly, particles must have roughly the same or smaller diameter than these fenestrae and carry a charge which is not excessively positive or negative, as high charge magnitude is associated with increased plasma clearance[21]. Controlling these physical properties to allow accumulation of particles in the liver is called passive liver targeting, whereas active liver targeting relies on conjugation of a "homing" ligand whose receptor is expressed in the target organ, and in particular, the specific target cell type. For example, carbohydrate receptors such as the asialoglycoprotein receptor can be targeted to deliver therapeutics to hepatocytes with ligands including galactose, lactose, pullulan, and others (more information regarding active targeting has been reviewed by Kang *et al*[22]).

LIVER-SPECIFIC DRUG DELIVERY: IMPLICATIONS FOR ALD

The goal of this review is to summarize pre-clinical research efforts which apply liver-specific drug delivery platforms in various rodent models to prevent or treat ALD, as well as to further discuss the

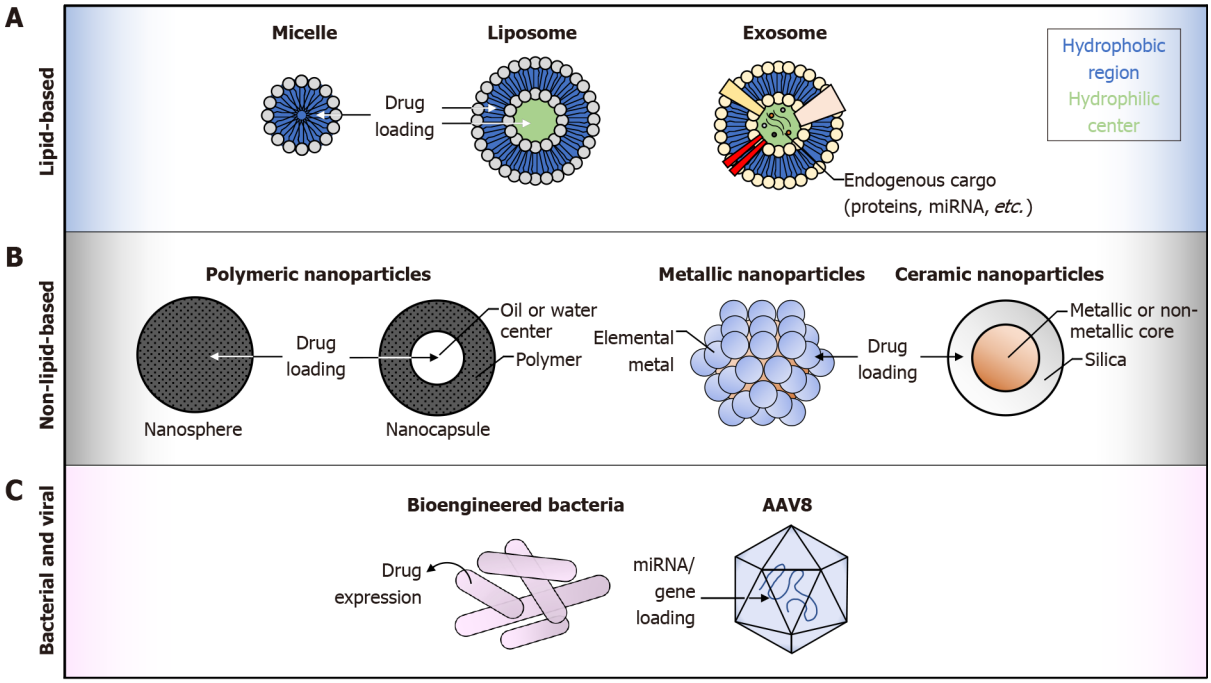

DOI: 10.3748/wjg.v28.i36.5280 **Copyright** ©The Author(s) 2022.

Figure 2 Graphical representation of targeted drug delivery platforms. A: Lipid-based particles, including micelles, liposomes, and exosomes; B: Non-lipid-based particles, including polymeric nanospheres and nanocapsules, metallic nanoparticles, and ceramic nanoparticles; C: Bioengineered bacteria and adeno-associated virus serotype 8. Graphics are not drawn to scale. miRNA: MicroRNA; AAV8: Adeno-associated virus serotype 8.

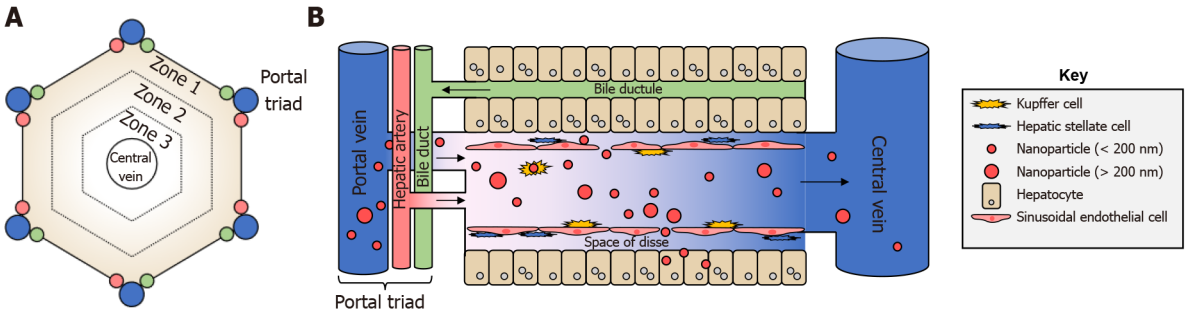

DOI: 10.3748/wjg.v28.i36.5280 **Copyright** ©The Author(s) 2022.

Figure 3 Lobular liver architecture and biodistribution of nanoparticles. A: Top-down view of a liver lobule. Portal triads, consisting of a portal vein, hepatic artery, and bile duct, surround a central vein in a hexagonal shape. Concentric hexagons designate zones 1-3 moving from the outside to the inside. Portal and arterial blood flows from the triads toward the central vein, whereas bile travels the opposite direction; B: Side view. With the portal triad on the left, portal blood brings nanoparticles from the digestive tract to the liver sinusoids where they can interact with Kupffer cells, liver sinusoidal endothelial cells, and others. Nanoparticles of sufficiently small size can pass through the liver fenestrae formed by liver sinusoidal endothelial cells to access the Space of Disse, and subsequently, hepatocytes. Images are not drawn to scale.

drug delivery systems themselves, which include liposomes, exosomes, PNPs, bacteria, and adeno-associated viruses. To this end, we searched the PubMed (https://pubmed.ncbi.nlm.nih.gov), Google Scholar (https://scholar.google.com), and Web of Science (https://www.webofscience.com/wos/woscc/basic-search) databases for studies published up to June 1, 2022 using a combination of text keywords "alcohol liver disease" and the following: "liposome(s)", "liposomal", "nanoparticle(s)", "nanoformulated", "polymersome(s)", "polymeric nanoparticle(s)", "micelle(s)", "exosome(s)", "AAV", "adenovirus", "adeno-associated virus", and "bioengineered bacteria". Our search strategy identified 846 unique results, which were screened individually by title and abstract and were included based on relevance to liver-targeted drug delivery in ALD. Studies were not excluded based on date of publication, model organism, funding source, or drug delivery platform used. Based on these criteria, 16 studies were included, and then categorized by drug delivery platform (n = 7 studies related to liposomes, n = 2 related to exosomes, n = 5 related to PNPs, and n = 2 related to bacterial or viral systems). A graphical summary of the search strategy and study categorization can be found in Figure 4. The 16 key studies are described in detail in Table 2. The reader is encouraged to refer to this table for

Table 2 Summary of studies employing a liver-specific drug delivery platform in animal models of alcohol-associated liver disease

Ref.	EtOH feeding model	Platform, route of administration (targeting strategy)	Cargo, paradigm (prevention or treatment)	Physical characterization			Empty particle control	Results	Mechanisms	
				Size (nm)	Charge (mV)	EE%			*In vitro*	*In vivo*
Liposomes										
Ponnappa *et al*[24], 2005	Rat chronic (8-10 wk), males	Liposomes, i.v. (passive)	S-ODN, prevention	N/P	N/P	10%-14%	Yes	↓ Liver injury (ALT)	-	↓ Serum and liver TNFα
Rodriguez *et al*[28], 2019	Mouse acute-on-chronic, males	Fusogenic liposomes, i.p. (passive)	Rolipram, treatment	N/P	N/P	N/P	No	↓ Liver injury (ALT and AST); ↓ Steatosis; ↓ Oxidative stress; ↓ ER Stress; ↓ Liver cell apoptosis	-	↑ Hepatic cAMP; ↑ *Sod1* and *Sod2*; ↓ ATF3, *Atf4*, CHOP, and *Gadd34*; ↑ Bcl-xl; ↓ Caspase activation
Zhao *et al*[32], 2016	Mouse chronic (8 wk), males	Liposomes, i.v. (passive)	Puerarin, Prevention	Approximately 182	Approximately -29.4	93.6% ± 1.7%	Yes	↓ Liver injury (ALT and AST)	-	-
Wu *et al*[35], 2019	Mouse EtOH binge (3 wk), males	Liposomes, i.p. or oral (passive)	Astaxanthin, prevention	225.0 ± 58.3	N/P	98%	Yes	↓ Liver injury (ALT and AST); ↓ Liver fibrosis	-	-
Kumar *et al*[36], 2019	Rat chronic (4 wk *via* 2 × daily gavage), males	Liposomes, oral (passive)	Silymarin, treatment	Approximately 146.9	Approximately -47.4	50.50%	No	↓ Liver injury (ALT and AST); ↑ Liver function (albumin); ↓ Oxidative stress; ↓ Liver inflammation	↓ Apoptosis in Chang cells	↑ SOD, GSH, catalase; ↓ TBARS; ↓ IL-6, MPO, nitrite
Yu *et al*[37], 2021	Mouse acute-on-chronic, males	Liposomes, oral (passive)	Saikosaponin D, prevention	61.66 ± 3.89	-37.18 ± 2.89	92.28% ± 0.84%	Yes	↓ Liver injury (ALT and AST); ↓ Steatosis; ↓ Oxidative stress; ↓ Liver inflammation	-	↓ MDA; ↑ GPx, SOD; ↓ Liver TNFα
Jain *et al*[38], 2013	Rat chronic (8 wk), males and females	Liposomes, oral (passive)	Mangiferin, prevention	980 ± 230	N/P	N/A	No	↓ Oxidative stress	-	↓ MDA; ↑ SOD, GSH, catalase
Exosomes										
Gu *et al*[50], 2021	Mouse acute-on-chronic, males	Exosomes, from LGG, oral (passive)	Endogenous cargo, treatment	75 ± 12.7	N/P	N/A	N/A	↓ Liver injury (ALT and AST); ↓ Steatosis	↓ TNFα, *Il-6*, IL-1β, *Mcp1* in RAW264.7 cells; ↑ AhR activity in gut leukocytes; ↑ ZO-1, occludin, claudin-1, Nrf2 in Caco-2 cells	↓ *Tnf* and *Il-1β*; ↑ *Cyp1a1*, IL-22, *Reg3b*, *Reg3g*; ↓ Hepatic bacteria; ↓ Liver endotoxin; ↑ Nrf2
Zhuang *et al*[57], 2015	Mouse acute-on-chronic, males	Exosomes from ginger, oral (passive)	Endogenous cargo, prevention	Approximately 340.4	Approximately -27.2	N/P	N/A	↓ Liver injury (ALT and AST); ↓ Steatosis	-	↑ Nrf2 activation

Polymeric nanoparticles										
Nag *et al*[64], 2020	Mouse chronic drinking water (16 wk), males	Poly(lactic-co-glycolic acid) nanoparticles, i.p. (passive)	Tannic acid/ vitamin e, treatment	127.5 ± 1.6	-21.2 ± 0.39	Tannic acid: 69.7% ± 2.6%; Vitamin E: 63.7% ± 3.2%	No	↓ Liver injury (ALT, AST, ALP); ↓ Steatosis; ↓ Liver fibrosis; ↓ Oxidative stress; ↓ Liver cell apoptosis; ↓ Liver inflammation; ↑ Cell survival	-	↑ HDL ↓ LDL; ↓ ROS; ↑ Catalase, GPx, Nrf2; ↓ Bax, bad, cytochrome C, caspase activation; ↑ Bcl2; ↓ TFGβ, IL-6, TNFα, IL-1β, iNOS, COX2; ↓ EGF, EGFR, AKT, PI3K, and mTOR
Natarajan *et al*[68], 2019	Mouse chronic (4 wk), males	Poly l-lysine-polyethylene glycol copolymer nanoparticles, i.p. (passive)	Superoxide dismutase, treatment	Approximately 44	N/P	N/P	No	↓ Steatosis; ↓ Liver inflammation	↑ SOD1 and ↓ DCF in E47 Hepatoma cells	↓ SREBP1; ↑ ADH1; ↓ *Cd68*, *Ccl2*, *Mmp12*, MCP1, and CCR2; ↑ P-AMPKα
Gopal *et al*[73], 2020	Mouse chronic (4 wk), males	Poly l-lysine-polyethylene glycol copolymer nanoparticles, i.p. (passive)	Superoxide dismutase 1, treatment	Approximately 44	N/P	N/P	No	↓ Liver injury (ALT); ↓ Steatosis	-	↓ Plasma and liver MCP-1; ↑ *Pparα*, *Acox1*, and *Acot1*; ↑ *Mt2*; ↑ SOD1 activity
Zhang *et al*[75], 2022	Mouse chronic (3 wk) + CCL_4, females	Chol-PCX nanoparticles, i.v. (passive)	PCX and anti-miR-155, Treatment	Approximately 70	Approximately 25	N/P	No	↓ Liver injury (ALT); ↓ Liver fibrosis; ↓ Liver inflammation	↓ LPS-induced miR-155 expression in RAW264.7 cells; ↑ CXCR4 antagonism in U20S cells	↓ *Col1a1*, MMPs, TIMPs, HSC activation; ↓ F480+ cells
Wang *et al*[76], 2020	Mouse EtOH binge (4 d), females	*Angelica sinensis* amphipathic cholesteryl hemisuccinate conjugate nanoparticles, i.v. (passive)	Curcumin, prevention	Approximately 208.4	Approximately -20	54.7%-86.1%	Yes	↓ Liver injury (ALT and AST); ↓ Oxidative stress	-	↑ GSH; ↓ ROS (DHE and MDA)
Bacteria and viruses										
Hendrikx *et al*[83], 2019	Mouse acute-on-chronic, male and females	*L. reuteri*, oral (intestine-targeted)	IL-22, prevention	N/A	N/A	N/A	Yes (regular *L. reuteri*)	↓ Liver injury (ALT); ↓ Steatosis (ORO and TG); ↓ Liver inflammation; ↑ Intestinal barrier defense	-	↓ *Cxcl1*, *Cxcl2*; ↑ Small intestine *Reg3g*; ↓ Hepatic bacteria
Satishchandran *et al* [93], 2018	Mouse chronic (5 wk), females	AAV8, i.v. (active)	*pri-MiR122*, treatment	N/A	N/A	N/A	Yes (scrambled miRNA)	↓ Liver injury (ALT); ↓ Steatosis (TG, ORO); ↓ Liver inflammation; ↓ Liver fibrosis (Sirius red)	-	↓ MCP1, IL-1β; ↓ *Col1a1*

Passive targeting denotes a strategy wherein the physical properties of a particle are modified to target the liver, and active targeting denotes a strategy wherein a particle targets the liver through a ligand/receptor interaction.

Treatment paradigm denotes models wherein the drug is administered after liver injury has been established (*e.g.*, half-way through the model, at the end of the model, *etc.*), whereas prevention paradigm denotes models wherein the drug is administered for the entire duration of the model. Changes in results/mechanisms columns are in liver unless otherwise stated. AAV8: Adeno-associated Virus Serotype 8; ADH1: Alcohol dehydrogenase 1; AhR: Aryl hydrocarbon receptor; AKT: Protein kinase B; ALP: Alkaline phosphatase; ALT: Alanine aminotransferase; AST: Aspartate aminotransferase; ATF3: Activating transcription factor 3; cAMP: Cyclic adenosine monophosphate; CCl4: Carbon tetrachloride; CCR2: C-C motif chemokine receptor 2; CHOP: C/EBP homologous protein; COX2: Cyclooxygenase 2; DCF: Dichlorodihydrofluorescein; DHE: Dihydroethidium; EE%: Encapsulation efficiency percent; EGF: Epidermal growth factor; EGFR: Epidermal growth factor receptor; ER: Endoplasmic reticulum; GPx: Glutathione peroxidase; GSH: Glutathione; HDL: High density lipoprotein; HSC: Hepatic stellate cell; i.p.: Intraperitoneal injection; i.v.: Intravenous injection; IL: Interleukin ; iNOS: Inducible nitric oxide synthase; LDL: Low density lipoprotein; LGG: Lactobacillus rhamnosus GG; LPS: Lipopolysaccharide; MCP1: Monocyte chemoattractant protein 1; MDA: Malondialdehyde; miR: Micro-RNA; MMPs: Matrix metalloproteinases; MPO: Myeloperoxidase; mTOR: Mechanistic target of rapamycin; N/A: Not applicable; N/P: Not provided; NRF2: Nuclear factor erythroid 2-related factor 2; ORO: Oil red O; P-AMPKα: Phospho-AMP-activated protein kinase alpha; PCX: Polycationic CXCR4 antagonists; PEG: Polyethylene glycol; PG: Propylene glycol; PI3K: Phosphoinositide 3-kinase; RoA: Route of administration; ROS: Reactive oxygen species; SOD: Superoxide dismutase; S-ODN: Antisense phosphorothioate oligodeoxynucleotide; TBARS: Thiobarbituric acid reactive substances; TG: Triglycerides; TGFβ: Transforming growth factor beta; TIMPs: Tissue inhibitors of metalloproteinases; TNFα: Tumor necrosis factor alpha; ZO1: Zonal occludin 1.

information such as the platform employed, the cargo molecule(s), the physical characterization of the particles used (if provided), and the animal model of ALD used, among other information.

Liposome-mediated drug delivery in ALD

Liposomes are one of the most common targeted drug delivery platforms, and indeed, about a third of the studies reviewed here used liposomal drug delivery in some form. Liposomes are vesicles composed of a phospholipid bilayer consisting of one (unilamellar) or more (multilamellar) concentric spherical layers enclosing an aqueous center (Figure 2A, middle panel)[23]. The presence of both aqueous and lipid compartments allows encapsulation or attachment of large quantities of both hydrophilic and lipophilic drugs, respectively (even simultaneously). Liposomes can be modified in many ways to alter their biodistribution *in vivo*, for example by modifying the lipid composition (saturated *vs* unsaturated, positively charged *vs* negatively charged), controlling size, attaching molecules such as PEG to improve stability, or adding proteins, antibodies, peptides, or carbohydrates to facilitate targeting of a specific cell type. The use of naturally occurring phospholipids gives liposomes the advantage of typically being non-immunogenic and non-pharmacologically active when administered alone. A major challenge in using liposomes to deliver drugs to the liver is opsonization and clearance by KCs and LSECs, as well as by RES components in the liver and other organs including the spleen, kidney, lung, bone marrow, and lymph nodes, although the liver is the primary site of liposome retention[23]. Attaching PEG to the liposome surface is an effective way to improve pharmacokinetics and avoid RES clearance, as PEG prevents attachment of opsonizing molecules and subsequent recognition by macrophages[19]. Controlling liposome size and surface charge can also avoid opsonization, as smaller (approximately 200 nm), more neutral liposomes do not as readily bind plasma proteins as larger, more highly charged liposomes.

An early study by Ponnappa *et al*[24] used pH-sensitive liposomes consisting of phosphatidylethanolamine, cholesterol hemisuccinate, and cholesterol to encapsulate an antisense oligonucleotide against *Tnf* mRNA (termed S-ODN) for delivery to the liver in a passive targeting approach. TNF-α is a pro-inflammatory cytokine elevated in ALD which, at high concentrations, sensitizes hepatocytes to cell death signals[25]. Liver macrophages and monocytes are a large source of liver TNF-α production[26]. Given the ability of liposomes to passively target liver macrophages, liposomes were therefore a natural choice of platform for the authors to employ in order to increase delivery of S-ODN to KCs. Intravenous administration of liposomal S-ODNs in a rat chronic ALD model decreased liver *Tnf* mRNA expression

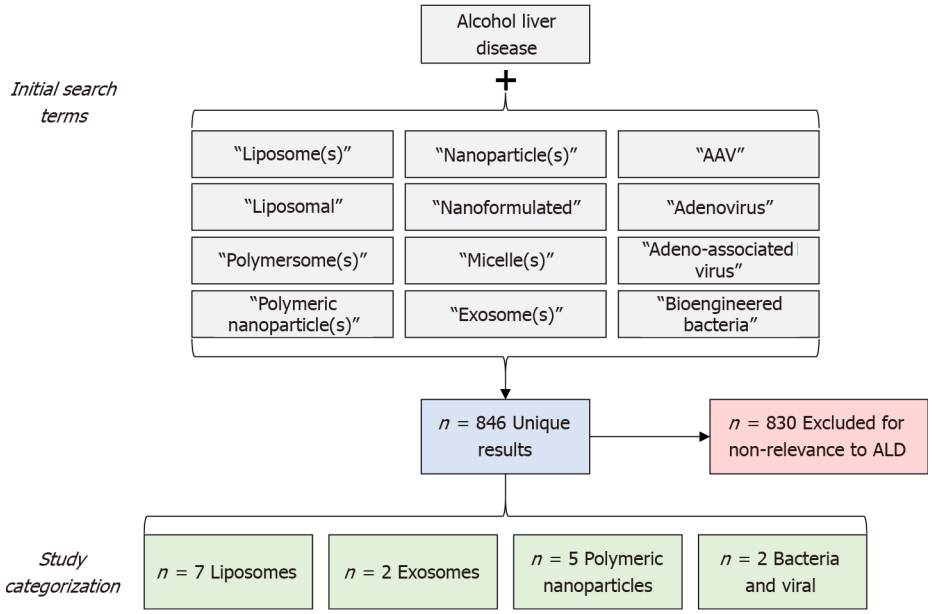

DOI: 10.3748/wjg.v28.i36.5280

Figure 4 Schematic representation of literature search strategy. Initial search terms included "alcohol liver disease" combined with the boxed terms. Eight hundred and forty-six unique results were generated, screened by title and abstract, and excluded based on relevance to the scope of the review. Sixteen studies were included in the review, broken down into four categories based on drug delivery platform. ALD: Alcohol-associated liver disease; AAV: Adeno-associated virus.

as expected, and subsequently prevented liver injury as demonstrated by plasma ALT[24]. The concentration of S-ODN in KCs was confirmed as being 20-fold higher compared to hepatocytes. In that study, liver-targeted delivery of the therapeutic was necessary to prevent side effects, specifically, to avoid the inhibition of blood coagulation associated with systemic administration (a process already perturbed in liver diseases[27]). A study by Rodriguez *et al*[28] also used a liposomal delivery system to avoid the systemic side effects of the hepato-protective drug rolipram, a phosphodiesterase 4 inhibitor. Previous studies demonstrated the beneficial effects of rolipram for ALD and other liver diseases[29]. However, in humans, rolipram causes significant central nervous system and gastrointestinal side effects (headache, vomiting, *etc*.). To this end, Rodriguez *et al*[28] used fusogenic liposomes composed of 1,2-Dioleoyl-sn-glycerol-3-phosphocholine and 1-palmitoyl-2-oleoyl-sn-glycerol-3-phosphate to passively deliver rolipram to the liver. Fusogenic liposomes differ from conventional liposomes because they avoid endocytosis and lysosomal degradation and instead fuse with the target cell membrane to release the drug cargo into the cytoplasm (for hydrophilic drugs) or membrane (for lipophilic drugs)[30]. Since phosphodiesterase 4 is expressed in the cytoplasm and plasma membrane of HSCs, among other liver cell types[31], the fusogenic liposome platform was an obvious choice for rolipram delivery. Indeed, in an acute-on-chronic mouse model of ALD, rolipram-loaded liposomes reduced liver damage (as determined by plasma ALT/AST activity), steatosis, oxidative stress, and endoplasmic reticulum (ER) stress similar to unencapsulated rolipram. However, encapsulated rolipram prevented liver cell death to a greater degree than un-encapsulated rolipram.

In 2016, Zhao *et al*[32] employed a liposome approach to deliver puerarin to the liver. Unlike the previous two studies, liposomal encapsulation in this study was used to improve pharmacokinetics, because puerarin, a plant-derived isoflavin, is rapidly cleared from the blood by the kidneys (with a half-life of less than one hour[33]). Liposomal encapsulation of this hydrophilic drug was achieved with liposomes composed of phosphatidylcholine, cholesterol, and propylene glycol. The authors demonstrated improved pharmacokinetics when administering puerarin liposomes to mice compared to non-encapsulated puerarin. Specifically, plasma area under the curve and half-life improved by 2.37- and 4.16-fold, respectively, and puerarin was detected most highly in the liver compared to other organs in both preparations. Previous studies supported puerarin as a beneficial molecule in a rat ALD model [34], but liposomal encapsulation improved efficacy further with respect to liver injury (decreased plasma ALT and AST levels) and, to a lesser degree, steatosis. In 2019, Wu *et al*[35] similarly employed a liposomal encapsulation technique to improve the pharmacokinetics of a naturally produced anti-inflammatory carotenoid, astaxanthin. Liposomal astaxanthin was administered to mice either orally or by intraperitoneal injection in an intragastric ethanol feeding model of ALD. Oral and intraperitoneal liposomal astaxanthin ameliorated alcohol-induced liver injury and histological signs of fibrosis. Whereas biodistribution of astaxanthin liposomes was not directly characterized in this study, the physical properties of the drug (low bioavailability, poor water solubility) suggest that liposomal encapsulation was necessary for efficacy. Silymarin is another excellent example of a beneficial

compound with poor pharmacokinetics which can be improved by incorporation into liposomes. Kumar *et al*[36] showed that encapsulation of this hepato-protective flavonolignan in phosphatidylcholine and cholesterol liposomes (either un-modified or PEGylated) improved pharmacokinetics and efficacy. Liposomal encapsulation improved the maximum plasma concentration and plasma area under the curve, while also increasing the solubility of the drug. *In vitro*, silymarin liposomes protected Chang Liver (HeLa) cells against ethanol-induced cell death. *In vivo*, in a rat chronic model of ALD, both un-modified and PEGylated silymarin liposomes ameliorated alcohol-induced liver injury while retaining the anti-inflammatory and antioxidant properties of silymarin. Recently, Yu *et al*[37] encapsulated Saikosaponin D, an anti-inflammatory/anti-oxidant plant-derived compound, in liposomes and demonstrated improved pharmacokinetics and efficacy in a mouse model of ALD compared to the nonencapsulated compound.

Lastly, Jain *et al*[38] employed a liposomal encapsulation approach for a plant-derived molecule, mangiferin. Like silymarin, mangiferin is a natural antioxidant with demonstrated benefits in the treatment of ALD and other diseases[39,40], but is not efficacious when used alone due to low bioavailability and metabolism by gut bacteria, as demonstrated by Jain *et al*[38]. To this end, the authors used a so-called 'herbosome' encapsulation strategy for mangiferin to improve the bioavailability of this compound. Herbosomes are defined as plant-derived compounds encapsulated in phospholipid particles, which in this study consisted of phosphatidylcholine and cholesterol. In a chronic rat model of ALD, unencapsulated mangiferin was able to significantly decrease liver injury, and mangiferin-loaded herbosomes further decreased the liver injury. Mechanistically, the authors attributed this protection to the antioxidant effects of mangiferin, as demonstrated by rescued SOD, catalase, and GSH levels and decreased liver MDA.

These studies support liposomal encapsulation as an effective approach not only for targeting drugs to the liver to avoid systemic side effects, but also for increasing the bioavailability of various compounds. The studies cited herein accomplished these goals by using liposomes composed of various glycerophospholipids including phosphatidylethanolamine, phosphatidyl choline, phosphatidic acid, and lecithin. Selection of certain lipids over others influences membrane fluidity/rigidity, which indirectly alters the permeability of the liposomal bilayer[41]. Certain phospholipids can also be chosen over others to impart fusogenic character, wherein liposomal cargoes can be targeted to the cell cytoplasm by fusing with the plasma membrane while avoiding endocytic degradation[30]. Rodriguez *et al*[28] employed this approach by using liposomes composed of 1,2-dioleoyl-sn-glycero-3-phosphocholine and 1-palmitoyl-2-oleoyl-sn-glycero-3-phosphate to target cytosolic phosphodiesterase. Further, most other groups incorporated cholesterol into their formulation, which can alter the release of the drug cargo and prevent unwanted 'leakage', thereby contributing to the overall stability of the nanoparticle[42].

Exosomes in ALD

Exosomes are another type of lipid-based liver-targeting nanoparticle which have been evaluated pre-clinically as potential therapeutics for ALD as well as potential biomarkers of disease progression in AH [43] (Figure 2A, right panel). Exosomes can be derived from bacteria or food, and are often small (approximately 30-150 nm in diameter) compared to synthetic liposomes (150 nm and larger in the studies cited here)[44]. Because they are products of the host cell membrane which are excreted by exocytosis, they are composed of phospholipids and cholesterol. While originally thought to be used by cells for waste removal, more recent evidence has supported a role in cell signaling, antigen presentation, tissue repair and regeneration, among other processes[44]. Unlike liposomes, exosomes contain numerous surface proteins (*e.g.*, CD63 in eukaryotic exosomes[45]) and internal cargo molecules including lipids, proteins, and nucleic acids. Despite the presence of existing cargo, additional molecules including drugs can be added to exosomes after isolation. The surface proteins present on exosomes mediate their cellular uptake, which has been shown to occur mostly in the liver and spleen, but also to some degree in the kidney, lung, and gastrointestinal tract, although pharmacokinetics depend on the source of the exosomes[46]. Liver macrophages are the cell type thought to be most responsible for exosome uptake through recognition of their charge by scavenging receptors, or recognition of surface signals such as sialic acid or phosphatidyl serine[47,48]. Thus, clearance by macrophages is again a drawback when trying to administer drugs to the liver parenchyma. Another significant consideration is standardization of isolation or purification protocols. Some techniques, for example, fail to completely exclude extraneous types of extracellular vesicles, leading to an impure drug product preparation[49]. Lastly, there are many unanswered questions related to how the choice of cell type from which to isolate exosomes impacts immunogenicity and efficacy.

A study from Gu *et al*[50] aimed to use exosomes derived from the beneficial bacteria *Lactobacillus rhamnosus GG* (LGG) to treat ALD. LGG has previously been demonstrated to be beneficial for ALD as a probiotic supplement which prevents gut permeability, thereby ameliorating liver injury[51,52]. The benefits of LGG probiotic supplementation are mediated, in part, by molecules secreted by LGG, as evidenced by the protective effects of LGG cell culture supernatant[53,54]. These soluble mediators are thought to be released from bacteria in exosomes. Gu *et al*[50] showed that orally administered LGG-derived exosomes (termed LDNPs) ameliorated experimental ALD in an acute-on-chronic mouse model. In contrast to previous studies aiming to deliver drugs to the liver, LDNPs in this study were

designed to ameliorate liver injury *via* the gut-liver axis, by targeting intestinal cells. Fluorescent labeled LDNPs were detectable in the intestine to a much larger extent than in the liver. Mice that received LDNPs were protected from the ethanol-associated reduction in intestinal tight junction protein expression and had boosted expression of intestinal anti-microbial peptides (*e.g.*, *Reg3b*, *Reg3g*) and IL-22. As a result, circulating endotoxin levels were decreased in LDNP-treated mice. Consequently, liver injury, steatosis, and inflammation were attenuated, confirming the critical importance of intestinal barrier defense in preventing ALD pathogenesis. Mechanistically, Gu *et al*[50] showed that the beneficial effects of LDNPs were mediated by the aryl hydrocarbon receptor (AhR), suggesting that the cargo molecules responsible for the benefits of LDNPs are likely AhR ligands.

Foods are another excellent source of exosomes with beneficial endogenous cargo molecules which target the intestinal epithelium or translocate to the bloodstream to target various organs including the liver[55]. Fluorescently labelled milk-derived exosomes, for example, have been shown to localize in the liver after oral administration to mice[56]. Food-derived exosomes from ginger, grapefruit, grape, garlic, ginseng, lemon, and others have been shown to be efficacious in the treatment of numerous diseases by nature of their antioxidant, anti-tumor, or anti-inflammatory cargo[55]. To investigate the efficacy of food-derived exosomes in ALD, Zhuang *et al*[57] used exosomes derived from ginger, a food which has been demonstrated to protect against liver injury of multiple etiologies, including alcohol, *via* antioxidant compounds called gingerols[58]. In an acute-on-chronic mouse model of ALD, daily oral ginger-derived exosome delivery decreased liver injury and steatosis. The antioxidant effects of the exosomes were also demonstrated, with increased expression of antioxidant genes in the liver through activation of NRF2. The authors also analyzed the distribution of the exosomes by fluorescent labeling, showing that the liver was the primary site of accumulation, with no detectable signal in lung, spleen, or other organs. Further, co-localization with albumin-positive cells by immunofluorescence showed that the ginger-derived exosomes primarily associated with hepatocytes, indicating cell-specificity. Collectively, these studies show the utility of exosomes as 'pre-packaged' lipid vesicles which can deliver beneficial cargo molecules from various sources to the liver for the treatment of ALD.

PNP-mediated drug delivery in ALD

PNPs are a class of non-lipid-based nanoparticles composed of natural or synthetic polymers that are gaining popularity in numerous applications, including medicinal and non-medicinal (material science, electronics, ecology, *etc*., Figure 2B, left panel)[59]. PNPs are classified as either nanospheres (composed entirely of polymer matrix) or nanocapsules (a polymer shell with a water or oil center) with an approximate size of 100-250 nm, which can be controlled during synthesis. Poly(lactic-co-glycolic acid) (PLGA) and vinyl monomer-based polymers are commonly used in PNP synthesis (*e.g.*, polystyrene, polyalkyl acrylates), although many other polymers can be used including polyesters, polyurethanes, polysaccharides, polypeptides, and biopolymers (*e.g.*, lignin)[60]. Polymer choice can be adjusted to control stability, particle size, and *in vivo* drug release. As with liposomes, surface modifications can also be made to PNPs to alter their pharmacokinetic profile and biodistribution, such as active targeting moieties or hydrophilic molecules that prevent opsonization (*e.g.*, PEG). Surface modifications can also change the intrinsic negative charge of most PNPs to neutral or positive. PEGylation, for example, shifts the charge to neutral, whereas conjugation of other molecules such as chitosan imparts a positive charge [61,62]. After reaching target cells, PNPs are up taken by pinocytosis or clathrin-mediated endocytosis but can escape lysosomal degradation and enter the cell cytoplasm within 10 min[63]. Other benefits of PNPs include low immunogenicity, low toxicity, and large surface area. As with liposomes, one drawback of PNPs is their susceptibility to opsonization in plasma and rapid clearance by the liver and spleen RES.

Several studies have applied PNPs to the treatment of ALD by attaching various cargo molecules. A study by Nag *et al*[64] used PLGA PNPs to deliver tannic acid and vitamin E to the liver in a chronic mouse model of ALD. These two naturally occurring molecules have previously been established to be beneficial for the treatment of ALD through anti-inflammatory and antioxidant mechanisms[65]. PNP formulation is necessary to ensure extended release of these molecules due to intestinal modification, poor absorption, rapid metabolism, and short half-life[66,67]. Nag *et al*[64] demonstrated that tannic acid/vitamin E PLGA PNPs ameliorated ALD as evaluated by multiple endpoints including reduced liver injury, steatosis, fibrosis, inflammation, oxidative stress, and liver cell apoptosis, as well as increased hepatocyte viability. Importantly, *in vitro* pharmacokinetic analysis showed that the PNPs slowed the movement of tannic acid and vitamin E across a semi-permeable membrane compared to free tannic acid and vitamin E, indicating that this formulation may improve the retention time of these compounds in the liver.

Another study targeting oxidative stress in ALD was conducted by Natarajan *et al*[68], who employed a PNP approach to deliver the enzyme superoxide dismutase (SOD) to the liver. Oxidative stress is a key mechanism in ALD pathogenesis[69]. A previous study in rats demonstrated that increasing hepatic SOD expression (*via* gene therapy) alleviated ALD by scavenging superoxide[70]; however, PNP-mediated SOD delivery is a more favorable translational therapy due to clinical issues surrounding the use of gene therapy (hepatotoxicity and generation of anti-adenovirus antibodies, for example)[71]. Further, previous studies suggest that administration of unencapsulated recombinant SOD does not produce effects that are as long-lasting as those by encapsulated SOD[72]. After establishing successful

delivery of functional SOD *in vitro* in E-47 hepatocytes and protection against ethanol and linoleic acid-induced oxidative stress, the authors administered SOD PNPs to mice by intraperitoneal injection in a chronic model of ALD. Compared to ethanol-treated mice, mice which received ethanol and SOD PNPs had decreased liver steatosis and inflammation as quantified by hematoxylin-eosin staining and decreased liver cytokine expression, respectively. Interestingly, the authors could not detect an increase in SOD in SOD PNP-treated mice, although the authors speculate that the time course of the study may not allow proper detection of elevated SOD levels. In a follow up study by the same research group, Gopal *et al*[73] again assessed the efficacy of intraperitoneal administered SOD PNPs in ALD, although in a modified model where mice are fed a high fat diet prior to the beginning of the ethanol feeding paradigm. Unlike the previous study, here the authors were able to show evidence of increased SOD expression and activity in the livers of mice administered SOD PNPs. Ethanol significantly induced liver injury in control mice, but not in mice administered SOD PNPs, as evidenced by plasma ALT levels. Again, ethanol-induced hepatic steatosis and inflammation were attenuated, corroborating the beneficial effects and mechanisms of protection of liver-specific SOD delivery.

Apart from proteins, another group of novel cargo molecules which can be delivered by PNPs are anti-micro RNAs (anti-MIRs), which are designed to inhibit endogenous MIRs, such as MIR-155, which has been previously shown to play a pathogenic role in ALD[74]. Zhang *et al*[75] aimed to not only block the effects of MIR-155, but also to deliver CXCR4 antagonists (collectively termed polycationic CXCR4 antagonists, or PCX, by the authors), which block alcohol-induced liver fibrosis *via* inhibition of HSC activation. Thus, the group administered synthetic cholesterol-modified polyethyleneimine nanoparticles *via* i.v. injection to mice to target HSCs and KCs in a model of alcohol + CCL_4-induced fibrosis. Indeed, compared to nanoparticles harboring a MIR negative control, the anti-MIR-155/PCX-loaded PNPs significantly reduced liver injury, fibrosis, and inflammation when administered in a treatment paradigm. This study supports the idea that numerous therapeutic cargos are compatible with the PNP platform, even when combined in a dual approach.

In contrast to the synthetic PNPs used in the studies mentioned above, a study by Wang *et al*[76]. used PNPs synthesized from a naturally occurring polysaccharide isolated from *Angelica sinensis* root [*Angelica sinensis* polysaccharide (ASP)]. ASP was combined with cholesterol hemisuccinate to prepare self-assembling ASP-cholesterol hemisuccinate PNPs (termed ACNPs), which were loaded with curcumin, a plant-derived compound with antioxidant effects which has previously shown beneficial effects in ALD[77,78]. The authors used PNPs to improve the delivery of curcumin, which is not readily water-soluble and has low bioavailability due to rapid metabolism[79]. In an intragastric feeding mouse model of ALD, the authors demonstrated that curcumin-loaded ACNPs decreased liver oxidative stress, and consequently, liver injury. Mechanistically, curcumin ACNPs increased NRF2 protein, consistent with other studies implicating NRF2 signaling for the beneficial effects of curcumin[77,80]. These studies show that PNPs, in addition to liposomes, are an effective choice of delivery platform to target drugs to the liver, and importantly, improve the bioavailability of compounds such as tannic acid, vitamin E, and curcumin.

Bacteria and adeno-associated virus-mediated liver-specific delivery in ALD

Certain bacteria have long been considered for their therapeutic potential either as whole organisms (probiotics), colonies of many bacterial species (*i.e.*, fecal transplant), or bacterial products[81]. More recently, genetically engineered bacteria have been developed to facilitate delivery of drugs, proteins, enzymes, and genes for the treatment of numerous pathologies[81] (Figure 2C, left panel). Bacteria as drug delivery systems are beneficial in several ways, including that they can provide their own propulsion and taxis *via* flagella or pili in response to external stimuli (*e.g.*, phototaxis, chemotaxis, thermotaxis, *etc.*), they can be designed to seek a certain molecule (*i.e.*, active targeting), they can produce a desired drug 'on-site' by metabolism, and they can even be designed to transfect host cells. These benefits, and numerous others (described in great detail in[81]), come at the cost of potential host immune response. Use of non-pathogenic bacterial strains, commensal bacteria, or genetic modification can decrease immunogenicity, but there is still considerable risk of septic shock which can result in mortality when targeting sterile body compartments (*e.g.*, blood, abdominal cavity, *etc.*)[82]. Hendrikx *et al*[83], for example, used genetically engineered *Lactobacillus reuteri* (*L. reuteri*), a commensal gut microbe, as a means of increasing intestinal IL-22 for the treatment of ALD in an acute-on-chronic mouse model. This approach aimed to ameliorate alcohol-associated changes in both the intestine and the liver. The gut and liver are connected *via* the so-called gut-liver axis, where alcohol-induced gut permeability allows pro-inflammatory bacteria and bacterial products (*e.g.*, endotoxins) to enter the hepatic portal system and exacerbate liver injury[84]. IL-22 is a cytokine which contributes to gut barrier defense and homeostasis[85], which the authors demonstrated to be decreased in the intestines of ethanol-fed mice. Mice which were enterally provided IL-22-expressing *L. reuteri* throughout the feeding protocol had increased expression of the gut anti-microbial peptide, *Reg3g*, decreased translocation of bacteria to the liver, and consequently, decreased liver injury, steatosis, and inflammation. Increased intestinal IL-22 was confirmed, but there was no increase in plasma IL-22, indicating that a localized increase in gut IL-22 was sufficient to restore gut barrier health and ameliorate liver injury. This engineered bacteria approach may be more clinically useful than simply administering recombinant IL-22 protein systemically, as systemic administration is associated with increased risk of tumor

development in chronic liver disease patients[86-88]. Indeed, bacteria serve as a unique drug delivery system with several key advantages, especially given that liver diseases such as ALD can be targeted indirectly *via* the gut-liver axis.

AAVs (adeno-associated virus) vectors are another biological system with the capability to target specific organs (Figure 2C, right). There exist multiple AAV serotypes with differing capsid proteins (13 in total), which confer serotype-specific functional features, including tropism for different organs[89]. AAV serotype 8 (AAV8), for example, exhibits high liver tropism, since the capsid proteins expressed in this serotype interact with the laminin receptor, which is highly expressed in the liver (for this reason, we have defined AAV8 as 'actively' targeting the liver in Table 2)[90]. This natural ability to target the liver comes at the cost of immunogenicity, liver toxicity, and the production of neutralizing antibodies by the host, several key hurdles for clinical AAV8-based therapy[89]. In contrast to the previous nanoparticle- and bacteria-based delivery systems discussed in this review, AAV vectors are used as a gene delivery vehicle, rather than a carrier of natural or synthetic drugs, based on their ability to transfect host cells[91]. This review will discuss one study using AAV8 as a delivery mechanism for a microRNA; for more information regarding gene therapy for the treatment of liver disease the reader is encouraged to read Kattenhorn *et al*[92]. Satishchandran *et al*[93] employed an AAV8 vector to rescue the ethanol-associated loss of microRNA 122 (MIR-122), which was demonstrated in both human ALD patients and mice in a 5-week chronic model of ALD. Previous work showed that loss of liver *Mir122* alone led to hepatic steatosis with spontaneous development of liver fibrosis and even HCC[94], suggesting a beneficial or homeostatic role of this microRNA in the liver. The authors used the AAV8 serotype to transfect hepatocytes with *pri-MiR122* or a scrambled control vector. Compared to controls, mice receiving AAV8-MIR122 had increased mature liver MIR-122 and, importantly, decreased alcohol-induced liver injury, steatosis, inflammation, and fibrosis. The AAV8 vector was shown to specifically target hepatocytes (as liver mononuclear cells had no increase in MIR122), suggesting this platform may be effective in targeting genes, including microRNAs, to not only the liver, but specifically to hepatocytes.

GAPS IN KNOWLEDGE

Research efforts to apply targeted drug delivery systems for the treatment of ALD are growing, but there are still considerable gaps in knowledge and several barriers to address. First is the lack of use of active targeting strategies, where addition of a ligand to a liposome or nanoparticle targets a drug to a particular liver cell type. Targeting a drug to a particular cell type (*e.g.*, targeting an antioxidant to hepatocytes) may increase efficacy, or produce the same beneficial effect with a lower total dose, thereby reducing the possibility of off-target effects. In additional to hepatocytes, other cell types contribute to ALD, including HSCs and both resident (Kupffer cells) and infiltrating macrophages, thus presenting opportunities to target these non-parenchymal liver cells. In this way, such treatments could target various stages of ALD such as hepatic fibrosis, which is largely driven by these cell types in their activated states (*i.e.*, activated HSCs or M1-polarized KCs)[95]. Fifteen of the 16 studies used a passive targeting approach, where the physical properties of the particle (*i.e.*, size and charge) were controlled in such a way that the particles would passively accumulate in the liver. The Satishchandran *et al*[93] study using AAV8 is one example of biological active targeting, where the AAV8 capsid binds to a particular receptor in the liver. Future research should consider ligand conjugation and active targeting of liposomes and PNPs to improve their drug formulations.

Next, with respect to the paradigm in which drug therapies were administered, in the 16 studies reviewed here, only about half used a so-called 'treatment paradigm', where the drug was given after establishment of liver injury (*i.e.*, half-way through the model or later). The remaining half administered their therapeutics in a 'prevention paradigm', where the drug was given at the start (or even prior to the start) of the alcohol feeding model. Studying the efficacy of a drug in a prevention paradigm certainly provides useful insight into whether the drug has any beneficial effect in ALD. However, this paradigm has limited clinical relevance, since most patients with mild to moderate ALD are asymptomatic, and they would not receive a diagnosis nor treatment until after injury has developed. In the case of studies establishing benefits of a liver-targeted drug in ALD in a prevention paradigm, additional studies should be carried out to determine whether administration of that drug formulation later in the feeding model is still effective. Another issue related to the models used in these studies is the lack of knowledge of the efficacy of these therapies in advanced ALD stages such as fibrosis/cirrhosis. Only one study discussed here (Zhang *et al*[75]), employed a model which is known to produce liver fibrosis, in this case by use of a 'second hit' of carbon tetrachloride superimposed on chronic EtOH feeding. While the authors did note reductions in fibrosis as measured by immunohistochemistry, this is only one study. Most of the studies discussed herein employed chronic, acute-on-chronic, or multiple-binge models which typically produce mild ALD characterized by hepatic steatosis, low-level inflammation, and mild liver injury with elevated ALT but no fibrosis[96,97]. Future studies should investigate the efficacy of nanoformulated drugs in experimental models of more advanced ALD which mimic alcohol-associated cirrhosis or severe AH, especially as better models are developed.

Another consideration with significant clinical implications is the route of administration. The studies reviewed here applied oral (gavage) or injection routes of delivery. Clearly, oral delivery is most attractive from a patient compliance perspective due to ease of self-administration and the absence of potential adverse effects from injections (injection site pain, inflammation, and infection). In general, nanoparticle systems tend to improve the pharmacokinetics of a drug to enable oral delivery in cases where this route would be otherwise unfeasible due to enzymatic digestion or poor absorption[98]. Indeed, many of the studies discussed here employed these platforms with this goal in mind, particularly for poorly soluble plant-derived compounds. However, compared to oral delivery, injection allows the highest level of control over the rate of drug delivery and can bypass any issues associated with first-pass metabolism or poor gastrointestinal absorption, resulting in a bioavailability of 100% and a rapid onset of action[99]. Direct injection of the drug solution into circulation does, however, pose a higher risk of adverse reactions and requires a healthcare professional to administer the treatment. This may be most acceptable in cases where drugs are developed for advanced ALD stages such as AH, where patients are already hospitalized. Regardless, authors should justify their chosen route of administration in the context of their future translational goals.

Additionally, in pre-clinical ALD research, it is important to consider sex differences, since men and women consume and metabolize alcohol differently, have different risk factors contributing to ALD, and ultimately, have different susceptibility to developing the disease[100]. Even in mice, there are sex differences in susceptibility to ALD when controlling for alcohol intake, diet, and other factors[101]. Further, evidence suggests biodistribution of nanoparticles may also differ by sex[102], providing an additional rationale for studying nanoparticle systems in ALD in both sexes. Despite these differences, many of the studies reviewed here (14 of 16) used either only male mice or only female mice, and the remaining two which used both sexes did not report the results for each sex separately.

Lastly, keeping in mind the goal of translating effective therapies to humans for the treatment of ALD, there is a lack of knowledge regarding the efficacy of liver-targeted therapies in humans for this disease. Critically, however, nanoparticle platforms have been used for many years for the treatment of other diseases. For example, liposomes have been used in numerous drug formulations for the treatment of various cancers, fungal and viral infection, pain, and other diseases since 1995 with excellent safety and efficacy[103]. Liposomes are also increasing in popularity as an excellent vaccine delivery system with several benefits over conventional vaccines (*e.g.*, liposomes are used in the Moderna and Pfizer/BioNTech COVID-19 mRNA vaccines)[104]. Although less common than liposomes, PNPs have also undergone clinical evaluation for the treatment of head, neck, lung, and breast cancers[105]. Other platforms not discussed in this review, such as N-acetyl-galactosamine (GalNac) conjugate (commonly used to delivery nucleic acids to hepatocytes by binding the asialoglycoprotein receptor[106]), have also been shown to have favorable safety profiles in clinical trials[107]. Clearly, drug delivery platforms with the capability to deliver drugs to the liver have undergone significant clinical evaluation, although not for the treatment of ALD. Future work should build on the growing pre-clinical data supporting the efficacy of particle therapeutics in ALD and the existing clinical data showing the safety of these systems in humans to move these nanomedicines to the clinic.

CONCLUSION

The research efforts reviewed here employed liver-targeted (or intestine-targeted) drug delivery platforms to improve their drug formulations and more effectively develop pharmacological interventions for ALD (summarized in Figure 5). These platforms, including liposomes, PNPs, exosomes, bacteria, and AAV vectors are aimed at improving a drug's pharmacokinetics, efficacy, and safety by reducing off target effects associated with systemic delivery and increasing the concentration of the drug locally in the liver. The authors of these studies used nanomedicine platforms to deliver phosphodiesterase inhibitors, naturally occurring antioxidants, oligonucleotides, miRNAs, enzymes, and anti-inflammatory cytokines in various rodent models of ALD, showing promising results which will move the pace of drug development for this disease forward toward clinical translation. Future studies should continue to apply and characterize targeted delivery platforms, as well as consider active targeting approaches, drug administration paradigms, and sex-specific differences in the pursuit of supporting future clinical trials in this field.

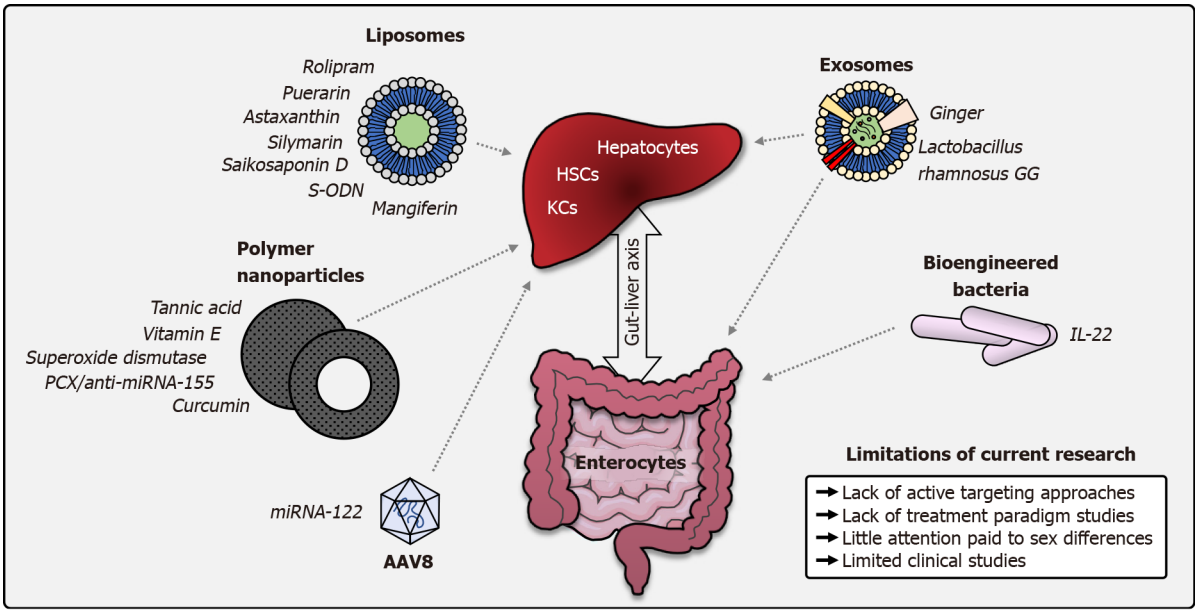

DOI: 10.3748/wjg.v28.i36.5280

Figure 5 Summary of studies applying nanoparticle platforms in alcohol-associated liver disease. A graphical summary of nanoparticle platforms which to date have been applied for the treatment or prevention of alcohol-associated liver disease in rodent models. Arrows represent organ targets of each platform. Example cargoes used in research articles discussed in this review are listed next to each platform. Current limitations of the field are described on the lower right. AAV8: Adeno-associated virus serotype 8; HSCs: Hepatic stellate cells; IL-22: Interleukin 22; KCs: Kupffer cells; miRNA: Micro-RNA; PCX: Polycationic CXCR4 antagonists; S-ODN: Antisense phosphorothioate oligodeoxynucleotide.

ACKNOWLEDGEMENTS

We apologize to and acknowledge any authors whose studies were not identified by our literature search strategy. We also acknowledge Marion McClain for manuscript editing support.

FOOTNOTES

Author contributions: Warner JB and Kirpich IA designed and outlined the review; Warner JB wrote the contents of the review; Warner JB and Guenthner SC designed the figures; Guenthner SC, Hardesty JE, McClain CJ, Warner DR, and Kirpich IA edited the manuscript; all authors have read and approve the final manuscript.

Supported by National Institutes of Health, No. R01AA028905-01A1 (to Kirpich IA), No. 1F31AA028423-01A1 (to Warner JB), No. F32AA027950-01A1 (to Hardesty JE) and No. U01AA026934 (to McClain CJ); Jewish Heritage Fund for Excellence Research Enhancement Grant Program at the University of Louisville, as well as an Institutional Development Award (IDeA) from the National Institute of General Medical Sciences of the National Institutes of Health, No. P20GM113226 (to McClain CJ); and National Institute on Alcohol Abuse and Alcoholism of the National Institutes of Health, No. P50AA024337 (to McClain CJ).

Conflict-of-interest statement: All the authors report no relevant conflicts of interest for this article.

Country/Territory of origin: United States

ORCID number: Jeffrey Barr Warner 0000-0003-2022-7854; Steven Corrigan Guenthner 0000-0003-3561-9607; Josiah Everett Hardesty 0000-0003-1955-3046; Craig James McClain 0000-0002-7219-8939; Dennis Ray Warner 0000-0002-5303-6870; Irina Andreyevna Kirpich 0000-0002-9545-6451.

S-Editor: Gao CC
L-Editor: A
P-Editor: Gao CC

REFERENCES

1 **Rehm J**, Samokhvalov AV, Shield KD. Global burden of alcoholic liver diseases. *J Hepatol* 2013; **59**: 160-168 [PMID: 23511777 DOI: 10.1016/j.jhep.2013.03.007]
2 **Seitz HK**, Bataller R, Cortez-Pinto H, Gao B, Gual A, Lackner C, Mathurin P, Mueller S, Szabo G, Tsukamoto H. Alcoholic liver disease. *Nat Rev Dis Primers* 2018; **4**: 16 [PMID: 30115921 DOI: 10.1038/s41572-018-0014-7]
3 **Lucey MR**, Mathurin P, Morgan TR. Alcoholic hepatitis. *N Engl J Med* 2009; **360**: 2758-2769 [PMID: 19553649 DOI: 10.1056/NEJMra0805786]
4 **European Association for the Study of the Liver**. EASL Clinical Practice Guidelines: Management of alcohol-related liver disease. *J Hepatol* 2018; **69**: 154-181 [PMID: 29628280 DOI: 10.1016/j.jhep.2018.03.018]
5 **Akriviadis E**, Botla R, Briggs W, Han S, Reynolds T, Shakil O. Pentoxifylline improves short-term survival in severe acute alcoholic hepatitis: a double-blind, placebo-controlled trial. *Gastroenterology* 2000; **119**: 1637-1648 [PMID: 11113085 DOI: 10.1053/gast.2000.20189]
6 **Singh S**, Osna NA, Kharbanda KK. Treatment options for alcoholic and non-alcoholic fatty liver disease: A review. *World J Gastroenterol* 2017; **23**: 6549-6570 [PMID: 29085205 DOI: 10.3748/wjg.v23.i36.6549]
7 **Veronese FM**, Mero A. The impact of PEGylation on biological therapies. *BioDrugs* 2008; **22**: 315-329 [PMID: 18778113 DOI: 10.2165/00063030-200822050-00004]
8 **Woo ASJ**, Kwok R, Ahmed T. Alpha-interferon treatment in hepatitis B. *Ann Transl Med* 2017; **5**: 159 [PMID: 28480195 DOI: 10.21037/atm.2017.03.69]
9 **Mody VV**, Siwale R, Singh A, Mody HR. Introduction to metallic nanoparticles. *J Pharm Bioallied Sci* 2010; **2**: 282-289 [PMID: 21180459 DOI: 10.4103/0975-7406.72127]
10 **Onxeo**. Efficacy and Safety Doxorubicin Transdrug Study in Patients Suffering From Advanced Hepatocellular Carcinoma. [accessed 2022 June 1]. In: ClinicalTrials.gov [Internet]. Canton (OH): U.S. National Library of Medicine. Available from: https://clinicaltrials.gov/ct2/show/study/NCT01655693 ClinicalTrials.gov Identifier: NCT01655693
11 **Zhang L**, Liu M, Jamil S, Han R, Xu G, Ni Y. PEGylation and pharmacological characterization of a potential anti-tumor drug, an engineered arginine deiminase originated from Pseudomonas plecoglossicida. *Cancer Lett* 2015; **357**: 346-354 [PMID: 25462857 DOI: 10.1016/j.canlet.2014.11.042]
12 **Dicerna Pharmaceuticals**. Phase Ib/2, Multicenter, Dose Escalation Study of DCR-MYC in Patients With Hepatocellular Carcinoma. [accessed 2022 June 1]. In: ClinicalTrials.gov [Internet]. Scottsdale (AZ): U.S. National Library of Medicine. Available from: https://clinicaltrials.gov/ct2/show/NCT02314052 ClinicalTrials.gov Identifier: NCT02314052
13 **Li SW**, Zhao Q, Wu T, Chen S, Zhang J, Xia NS. The development of a recombinant hepatitis E vaccine HEV 239. *Hum Vaccin Immunother* 2015; **11**: 908-914 [PMID: 25714510 DOI: 10.1080/21645515.2015.1008870]
14 **Lawitz E**, Tanaka Y, Poordad F, Gutierrez JA, Carr K, Ying WB, Niitsu Y, Maruyama K. Safety, Pharmacokinetics, and Biologic Activity of ND-L02-s0201, a Novel Targeted Lipid-Nanoparticle to Deliver HSP47 siRNA for the Treatment of Patients with Advanced Liver Fibrosis: Interim Results from Clinical Phase 1b/2 Studies. *Hepatology* 2015; **62**: 909a
15 **Ivanenkov YA**, Maklakova SY, Beloglazkina EK, Zyk NV, Nazarenko AG, Tonevitsky AG, Kotelianski VE, Majouga AG. Development of liver cell-targeted drug delivery systems: experimental approaches. *Russian Chem Rev* 2017; **86**
16 **Ben-Moshe S**, Itzkovitz S. Spatial heterogeneity in the mammalian liver. *Nat Rev Gastroenterol Hepatol* 2019; **16**: 395-410 [PMID: 30936469 DOI: 10.1038/s41575-019-0134-x]
17 **Vekemans K**, Braet F. Structural and functional aspects of the liver and liver sinusoidal cells in relation to colon carcinoma metastasis. *World J Gastroenterol* 2005; **11**: 5095-5102 [PMID: 16127736 DOI: 10.3748/wjg.v11.i33.5095]
18 **Shilpi S**, Shivvedi R, Gurnany E, Dixit S, Khatri K, Dwivedi D. Drug targeting strategies for liver cancer and other liver diseases. *Drug Des Devel Ther* 2018; **2**: 171-177 [DOI: 10.15406/mojddt.2018.02.00044]
19 **Immordino ML**, Dosio F, Cattel L. Stealth liposomes: review of the basic science, rationale, and clinical applications, existing and potential. *Int J Nanomedicine* 2006; **1**: 297-315 [PMID: 17717971]
20 **Wisse E**, Jacobs F, Topal B, Frederik P, De Geest B. The size of endothelial fenestrae in human liver sinusoids: implications for hepatocyte-directed gene transfer. *Gene Ther* 2008; **15**: 1193-1199 [PMID: 18401434 DOI: 10.1038/gt.2008.60]
21 **Arvizo RR**, Miranda OR, Moyano DF, Walden CA, Giri K, Bhattacharya R, Robertson JD, Rotello VM, Reid JM, Mukherjee P. Modulating pharmacokinetics, tumor uptake and biodistribution by engineered nanoparticles. *PLoS One* 2011; **6**: e24374 [PMID: 21931696 DOI: 10.1371/journal.pone.0024374]
22 **Kang JH**, Toita R, Murata M. Liver cell-targeted delivery of therapeutic molecules. *Crit Rev Biotechnol* 2016; **36**: 132-143 [PMID: 25025274 DOI: 10.3109/07388551.2014.930017]
23 **Sercombe L**, Veerati T, Moheimani F, Wu SY, Sood AK, Hua S. Advances and Challenges of Liposome Assisted Drug Delivery. *Front Pharmacol* 2015; **6**: 286 [PMID: 26648870 DOI: 10.3389/fphar.2015.00286]
24 **Ponnappa BC**, Israel Y, Aini M, Zhou F, Russ R, Cao QN, Hu Y, Rubin R. Inhibition of tumor necrosis factor alpha secretion and prevention of liver injury in ethanol-fed rats by antisense oligonucleotides. *Biochem Pharmacol* 2005; **69**: 569-577 [PMID: 15670576 DOI: 10.1016/j.bcp.2004.11.011]
25 **Lopetuso LR**, Mocci G, Marzo M, D'Aversa F, Rapaccini GL, Guidi L, Armuzzi A, Gasbarrini A, Papa A. Harmful Effects and Potential Benefits of Anti-Tumor Necrosis Factor (TNF)-α on the Liver. *Int J Mol Sci* 2018; **19** [PMID: 30060508 DOI: 10.3390/ijms19082199]
26 **Yang YM**, Seki E. TNFα in liver fibrosis. *Curr Pathobiol Rep* 2015; **3**: 253-261 [PMID: 26726307 DOI: 10.1007/s40139-015-0093-z]
27 **Lisman T**, Porte RJ. Rebalanced hemostasis in patients with liver disease: evidence and clinical consequences. *Blood* 2010; **116**: 878-885 [PMID: 20400681 DOI: 10.1182/blood-2010-02-261891]
28 **Rodriguez WE**, Wahlang B, Wang Y, Zhang J, Vadhanam MV, Joshi-Barve S, Bauer P, Cannon R, Ahmadi AR, Sun Z, Cameron A, Barve S, Maldonado C, McClain C, Gobejishvili L. Phosphodiesterase 4 Inhibition as a Therapeutic Target

for Alcoholic Liver Disease: From Bedside to Bench. *Hepatology* 2019; **70**: 1958-1971 [PMID: 31081957 DOI: 10.1002/hep.30761]

29 **Wahlang B**, McClain C, Barve S, Gobejishvili L. Role of cAMP and phosphodiesterase signaling in liver health and disease. *Cell Signal* 2018; **49**: 105-115 [PMID: 29902522 DOI: 10.1016/j.cellsig.2018.06.005]

30 **Kube S**, Hersch N, Naumovska E, Gensch T, Hendriks J, Franzen A, Landvogt L, Siebrasse JP, Kubitscheck U, Hoffmann B, Merkel R, Csiszár A. Fusogenic Liposomes as Nanocarriers for the Delivery of Intracellular Proteins. *Langmuir* 2017; **33**: 1051-1059 [PMID: 28059515 DOI: 10.1021/acs.langmuir.6b04304]

31 **Thul PJ**, Åkesson L, Wiking M, Mahdessian D, Geladaki A, Ait Blal H, Alm T, Asplund A, Björk L, Breckels LM, Bäckström A, Danielsson F, Fagerberg L, Fall J, Gatto L, Gnann C, Hober S, Hjelmare M, Johansson F, Lee S, Lindskog C, Mulder J, Mulvey CM, Nilsson P, Oksvold P, Rockberg J, Schutten R, Schwenk JM, Sivertsson Å, Sjöstedt E, Skogs M, Stadler C, Sullivan DP, Tegel H, Winsnes C, Zhang C, Zwahlen M, Mardinoglu A, Pontén F, von Feilitzen K, Lilley KS, Uhlén M, Lundberg E. A subcellular map of the human proteome. *Science* 2017; **356** [PMID: 28495876 DOI: 10.1126/science.aal3321]

32 **Zhao YZ**, Zhang L, Gupta PK, Tian FR, Mao KL, Qiu KY, Yang W, Lv CZ, Lu CT. Using PG-Liposome-Based System to Enhance Puerarin Liver-Targeted Therapy for Alcohol-Induced Liver Disease. *AAPS PharmSciTech* 2016; **17**: 1376-1382 [PMID: 26753818 DOI: 10.1208/s12249-015-0427-5]

33 **Li Y**, Pan WS, Chen SL, Xu HX, Yang DJ, Chan AS. Pharmacokinetic, tissue distribution, and excretion of puerarin and puerarin-phospholipid complex in rats. *Drug Dev Ind Pharm* 2006; **32**: 413-422 [PMID: 16638679 DOI: 10.1080/03639040600559123]

34 **Zhao M**, Du YQ, Yuan L, Wang NN. Protective effect of puerarin on acute alcoholic liver injury. *Am J Chin Med* 2010; **38**: 241-249 [PMID: 20387222 DOI: 10.1142/S0192415X10007816]

35 **Wu YC**, Huang HH, Wu YJ, Manousakas I, Yang CC, Kuo SM. Therapeutic and Protective Effects of Liposomal Encapsulation of Astaxanthin in Mice with Alcoholic Liver Fibrosis. *Int J Mol Sci* 2019; **20** [PMID: 31434227 DOI: 10.3390/ijms20164057]

36 **Kumar N**, Rai A, Reddy ND, Shenoy RR, Mudgal J, Bansal P, Mudgal PP, Arumugam K, Udupa N, Sharma N, Rao CM. Improved *in vitro* and *in vivo* hepatoprotective effects of liposomal silymarin in alcohol-induced hepatotoxicity in Wistar rats. *Pharmacol Rep* 2019; **71**: 703-712 [PMID: 31207432 DOI: 10.1016/j.pharep.2019.03.013]

37 **Yu X**, Pan J, Shen N, Zhang H, Zou L, Miao H, Xing L. Development of Saikosaponin D Liposome Nanocarrier with Increased Hepatoprotective Effect Against Alcoholic Hepatitis Mice. *J Biomed Nanotechnol* 2021; **17**: 627-639 [PMID: 35057889 DOI: 10.1166/jbn.2021.3054]

38 **Jain PK**, Kharya M, Gajbhiye A. Pharmacological evaluation of mangiferin herbosomes for antioxidant and hepatoprotection potential against ethanol induced hepatic damage. *Drug Dev Ind Pharm* 2013; **39**: 1840-1850 [PMID: 23167243 DOI: 10.3109/03639045.2012.738685]

39 **Yoshikawa M**, Ninomiya K, Shimoda H, Nishida N, Matsuda H. Hepatoprotective and antioxidative properties of Salacia reticulata: preventive effects of phenolic constituents on CCl4-induced liver injury in mice. *Biol Pharm Bull* 2002; **25**: 72-76 [PMID: 11824561 DOI: 10.1248/bpb.25.72]

40 **Miura T**, Ichiki H, Hashimoto I, Iwamoto N, Kato M, Kubo M, Ishihara E, Komatsu Y, Okada M, Ishida T, Tanigawa K. Antidiabetic activity of a xanthone compound, mangiferin. *Phytomedicine* 2001; **8**: 85-87 [PMID: 11315760 DOI: 10.1078/0944-7113-00009]

41 **Akbarzadeh A**, Rezaei-Sadabady R, Davaran S, Joo SW, Zarghami N, Hanifehpour Y, Samiei M, Kouhi M, Nejati-Koshki K. Liposome: classification, preparation, and applications. *Nanoscale Res Lett* 2013; **8**: 102 [PMID: 23432972 DOI: 10.1186/1556-276X-8-102]

42 **Ahmed KS**, Hussein SA, Ali AH, Korma SA, Lipeng Q, Jinghua C. Liposome: composition, characterisation, preparation, and recent innovation in clinical applications. *J Drug Target* 2019; **27**: 742-761 [PMID: 30239255 DOI: 10.1080/1061186X.2018.1527337]

43 **Momen-Heravi F**, Saha B, Kodys K, Catalano D, Satishchandran A, Szabo G. Increased number of circulating exosomes and their microRNA cargos are potential novel biomarkers in alcoholic hepatitis. *J Transl Med* 2015; **13**: 261 [PMID: 26264599 DOI: 10.1186/s12967-015-0623-9]

44 **Doyle LM**, Wang MZ. Overview of Extracellular Vesicles, Their Origin, Composition, Purpose, and Methods for Exosome Isolation and Analysis. *Cells* 2019; **8** [PMID: 31311206 DOI: 10.3390/cells8070727]

45 **Kowal J**, Arras G, Colombo M, Jouve M, Morath JP, Primdal-Bengtson B, Dingli F, Loew D, Tkach M, Théry C. Proteomic comparison defines novel markers to characterize heterogeneous populations of extracellular vesicle subtypes. *Proc Natl Acad Sci U S A* 2016; **113**: E968-E977 [PMID: 26858453 DOI: 10.1073/pnas.1521230113]

46 **Morishita M**, Takahashi Y, Nishikawa M, Takakura Y. Pharmacokinetics of Exosomes-An Important Factor for Elucidating the Biological Roles of Exosomes and for the Development of Exosome-Based Therapeutics. *J Pharm Sci* 2017; **106**: 2265-2269 [PMID: 28283433 DOI: 10.1016/j.xphs.2017.02.030]

47 **Matsumoto A**, Takahashi Y, Nishikawa M, Sano K, Morishita M, Charoenviriyakul C, Saji H, Takakura Y. Role of Phosphatidylserine-Derived Negative Surface Charges in the Recognition and Uptake of Intravenously Injected B16BL6-Derived Exosomes by Macrophages. *J Pharm Sci* 2017; **106**: 168-175 [PMID: 27649887 DOI: 10.1016/j.xphs.2016.07.022]

48 **Parada N**, Romero-Trujillo A, Georges N, Alcayaga-Miranda F. Camouflage strategies for therapeutic exosomes evasion from phagocytosis. *J Adv Res* 2021; **31**: 61-74 [PMID: 34194832 DOI: 10.1016/j.jare.2021.01.001]

49 **Li X**, Corbett AL, Taatizadeh E, Tasnim N, Little JP, Garnis C, Daugaard M, Guns E, Hoorfar M, Li ITS. Challenges and opportunities in exosome research-Perspectives from biology, engineering, and cancer therapy. *APL Bioeng* 2019; **3**: 011503 [PMID: 31069333 DOI: 10.1063/1.5087122]

50 **Gu Z**, Li F, Liu Y, Jiang M, Zhang L, He L, Wilkey DW, Merchant M, Zhang X, Deng ZB, Chen SY, Barve S, McClain CJ, Feng W. Exosome-Like Nanoparticles From *Lactobacillus rhamnosus*GG Protect Against Alcohol-Associated Liver Disease Through Intestinal Aryl Hydrocarbon Receptor in Mice. *Hepatol Commun* 2021; **5**: 846-864 [PMID: 34027273 DOI: 10.1002/hep4.1679]

51 **Bruch-Bertani JP**, Uribe-Cruz C, Pasqualotto A, Longo L, Ayres R, Beskow CB, Barth AL, Lima-Morales D, Meurer F, Tayguara Silveira Guerreiro G, da Silveira TR, Álvares-da-Silva MR, Dall'Alba V. Hepatoprotective Effect of Probiotic *Lactobacillus rhamnosus* GG Through the Modulation of Gut Permeability and Inflammasomes in a Model of Alcoholic Liver Disease in Zebrafish. *J Am Coll Nutr* 2020; **39**: 163-170 [PMID: 31241423 DOI: 10.1080/07315724.2019.1627955]

52 **Wang Y**, Kirpich I, Liu Y, Ma Z, Barve S, McClain CJ, Feng W. Lactobacillus rhamnosus GG treatment potentiates intestinal hypoxia-inducible factor, promotes intestinal integrity and ameliorates alcohol-induced liver injury. *Am J Pathol* 2011; **179**: 2866-2875 [PMID: 22093263 DOI: 10.1016/j.ajpath.2011.08.039]

53 **Zhao H**, Zhao C, Dong Y, Zhang M, Wang Y, Li F, Li X, McClain C, Yang S, Feng W. Inhibition of miR122a by Lactobacillus rhamnosus GG culture supernatant increases intestinal occludin expression and protects mice from alcoholic liver disease. *Toxicol Lett* 2015; **234**: 194-200 [PMID: 25746479 DOI: 10.1016/j.toxlet.2015.03.002]

54 **Wang Y**, Liu Y, Sidhu A, Ma Z, McClain C, Feng W. Lactobacillus rhamnosus GG culture supernatant ameliorates acute alcohol-induced intestinal permeability and liver injury. *Am J Physiol Gastrointest Liver Physiol* 2012; **303**: G32-G41 [PMID: 22538402 DOI: 10.1152/ajpgi.00024.2012]

55 **Munir J**, Lee M, Ryu S. Exosomes in Food: Health Benefits and Clinical Relevance in Diseases. *Adv Nutr* 2020; **11**: 687-696 [PMID: 31796948 DOI: 10.1093/advances/nmz123]

56 **Manca S**, Upadhyaya B, Mutai E, Desaulniers AT, Cederberg RA, White BR, Zempleni J. Milk exosomes are bioavailable and distinct microRNA cargos have unique tissue distribution patterns. *Sci Rep* 2018; **8**: 11321 [PMID: 30054561 DOI: 10.1038/s41598-018-29780-1]

57 **Zhuang X**, Deng ZB, Mu J, Zhang L, Yan J, Miller D, Feng W, McClain CJ, Zhang HG. Ginger-derived nanoparticles protect against alcohol-induced liver damage. *J Extracell Vesicles* 2015; **4**: 28713 [PMID: 26610593 DOI: 10.3402/jev.v4.28713]

58 **Mu J**, Zhuang X, Wang Q, Jiang H, Deng ZB, Wang B, Zhang L, Kakar S, Jun Y, Miller D, Zhang HG. Interspecies communication between plant and mouse gut host cells through edible plant derived exosome-like nanoparticles. *Mol Nutr Food Res* 2014; **58**: 1561-1573 [PMID: 24842810 DOI: 10.1002/mnfr.201300729]

59 **Rao JP**, Geckeler KE. Polymer nanoparticles: Preparation techniques and size-control parameters. *Prog Polym Sci* 2011; **36**: 887-913 [DOI: 10.1016/j.progpolymsci.2011.01.001]

60 **Danhier F**, Ansorena E, Silva JM, Coco R, Le Breton A, Préat V. PLGA-based nanoparticles: an overview of biomedical applications. *J Control Release* 2012; **161**: 505-522 [PMID: 22353619 DOI: 10.1016/j.jconrel.2012.01.043]

61 **Danhier F**, Feron O, Préat V. To exploit the tumor microenvironment: Passive and active tumor targeting of nanocarriers for anti-cancer drug delivery. *J Control Release* 2010; **148**: 135-146 [PMID: 20797419 DOI: 10.1016/j.jconrel.2010.08.027]

62 **Tahara K**, Sakai T, Yamamoto H, Takeuchi H, Hirashima N, Kawashima Y. Improved cellular uptake of chitosan-modified PLGA nanospheres by A549 cells. *Int J Pharm* 2009; **382**: 198-204 [PMID: 19646519 DOI: 10.1016/j.ijpharm.2009.07.023]

63 **Vasir JK**, Labhasetwar V. Biodegradable nanoparticles for cytosolic delivery of therapeutics. *Adv Drug Deliv Rev* 2007; **59**: 718-728 [PMID: 17683826 DOI: 10.1016/j.addr.2007.06.003]

64 **Nag S**, Manna K, Saha M, Das Saha K. Tannic acid and vitamin E loaded PLGA nanoparticles ameliorate hepatic injury in a chronic alcoholic liver damage model *via* EGFR-AKT-STAT3 pathway. *Nanomedicine (Lond)* 2020; **15**: 235-257 [PMID: 31789102 DOI: 10.2217/nnm-2019-0340]

65 **Adewusi EA**, Afolayan AJ. Effect of Pelargonium reniforme roots on alcohol-induced liver damage and oxidative stress. *Pharm Biol* 2010; **48**: 980-987 [PMID: 20731548 DOI: 10.3109/13880200903410354]

66 **Carbonaro M**, Grant G, Pusztai A. Evaluation of polyphenol bioavailability in rat small intestine. *Eur J Nutr* 2001; **40**: 84-90 [PMID: 11518204 DOI: 10.1007/s003940170020]

67 **D'Archivio M**, Filesi C, Varì R, Scazzocchio B, Masella R. Bioavailability of the polyphenols: status and controversies. *Int J Mol Sci* 2010; **11**: 1321-1342 [PMID: 20480022 DOI: 10.3390/ijms11041321]

68 **Natarajan G**, Perriotte-Olson C, Casey CA, Donohue TM Jr, Talmon GA, Harris EN, Kabanov AV, Saraswathi V. Effect of nanoformulated copper/zinc superoxide dismutase on chronic ethanol-induced alterations in liver and adipose tissue. *Alcohol* 2019; **79**: 71-79 [PMID: 30611703 DOI: 10.1016/j.alcohol.2018.12.005]

69 **Tan HK**, Yates E, Lilly K, Dhanda AD. Oxidative stress in alcohol-related liver disease. *World J Hepatol* 2020; **12**: 332-349 [PMID: 32821333 DOI: 10.4254/wjh.v12.i7.332]

70 **Wheeler MD**, Kono H, Yin M, Rusyn I, Froh M, Connor HD, Mason RP, Samulski RJ, Thurman RG. Delivery of the Cu/Zn-superoxide dismutase gene with adenovirus reduces early alcohol-induced liver injury in rats. *Gastroenterology* 2001; **120**: 1241-1250 [PMID: 11266387 DOI: 10.1053/gast.2001.23253]

71 **Eto Y**, Yoshioka Y, Mukai Y, Okada N, Nakagawa S. Development of PEGylated adenovirus vector with targeting ligand. *Int J Pharm* 2008; **354**: 3-8 [PMID: 17904316 DOI: 10.1016/j.ijpharm.2007.08.025]

72 **Laursen JB**, Rajagopalan S, Galis Z, Tarpey M, Freeman BA, Harrison DG. Role of superoxide in angiotensin II-induced but not catecholamine-induced hypertension. *Circulation* 1997; **95**: 588-593 [PMID: 9024144 DOI: 10.1161/01.cir.95.3.588]

73 **Gopal T**, Kumar N, Perriotte-Olson C, Casey CA, Donohue TM Jr, Harris EN, Talmon G, Kabanov AV, Saraswathi V. Nanoformulated SOD1 ameliorates the combined NASH and alcohol-associated liver disease partly *via* regulating CYP2E1 expression in adipose tissue and liver. *Am J Physiol Gastrointest Liver Physiol* 2020; **318**: G428-G438 [PMID: 31928222 DOI: 10.1152/ajpgi.00217.2019]

74 **Bala S**, Csak T, Saha B, Zatsiorsky J, Kodys K, Catalano D, Satishchandran A, Szabo G. The pro-inflammatory effects of miR-155 promote liver fibrosis and alcohol-induced steatohepatitis. *J Hepatol* 2016; **64**: 1378-1387 [PMID: 26867493 DOI: 10.1016/j.jhep.2016.01.035]

75 **Zhang C**, Hang Y, Tang W, Sil D, Jensen-Smith HC, Bennett RG, McVicker BL, Oupický D. Dually Active Polycation/miRNA Nanoparticles for the Treatment of Fibrosis in Alcohol-Associated Liver Disease. *Pharmaceutics* 2022; **14** [PMID: 35336043 DOI: 10.3390/pharmaceutics14030669]

76 **Wang K**, Xu J, Liu Y, Cui Z, He Z, Zheng Z, Huang X, Zhang Y. Self-assembled Angelica sinensis polysaccharide

nanoparticles with an instinctive liver-targeting ability as a drug carrier for acute alcoholic liver damage protection. *Int J Pharm* 2020; **577**: 118996 [PMID: 31904402 DOI: 10.1016/j.ijpharm.2019.118996]

77 **Lu C**, Xu W, Zhang F, Shao J, Zheng S. Nrf2 Knockdown Disrupts the Protective Effect of Curcumin on Alcohol-Induced Hepatocyte Necroptosis. *Mol Pharm* 2016; **13**: 4043-4053 [PMID: 27764939 DOI: 10.1021/acs.molpharmaceut.6b00562]

78 **Varatharajalu R**, Garige M, Leckey LC, Reyes-Gordillo K, Shah R, Lakshman MR. Protective Role of Dietary Curcumin in the Prevention of the Oxidative Stress Induced by Chronic Alcohol with respect to Hepatic Injury and Antiatherogenic Markers. *Oxid Med Cell Longev* 2016; **2016**: 5017460 [PMID: 26881029 DOI: 10.1155/2016/5017460]

79 **Yen FL**, Wu TH, Tzeng CW, Lin LT, Lin CC. Curcumin nanoparticles improve the physicochemical properties of curcumin and effectively enhance its antioxidant and antihepatoma activities. *J Agric Food Chem* 2010; **58**: 7376-7382 [PMID: 20486686 DOI: 10.1021/jf100135h]

80 **Ashrafizadeh M**, Ahmadi Z, Mohammadinejad R, Farkhondeh T, Samarghandian S. Curcumin Activates the Nrf2 Pathway and Induces Cellular Protection Against Oxidative Injury. *Curr Mol Med* 2020; **20**: 116-133 [PMID: 31622191 DOI: 10.2174/1566524019666191016150757]

81 **Hosseinidoust Z**, Mostaghaci B, Yasa O, Park BW, Singh AV, Sitti M. Bioengineered and biohybrid bacteria-based systems for drug delivery. *Adv Drug Deliv Rev* 2016; **106**: 27-44 [PMID: 27641944 DOI: 10.1016/j.addr.2016.09.007]

82 **Pawelek JM**, Low KB, Bermudes D. Bacteria as tumour-targeting vectors. *Lancet Oncol* 2003; **4**: 548-556 [PMID: 12965276 DOI: 10.1016/s1470-2045(03)01194-x]

83 **Hendrikx T**, Duan Y, Wang Y, Oh JH, Alexander LM, Huang W, Stärkel P, Ho SB, Gao B, Fiehn O, Emond P, Sokol H, van Pijkeren JP, Schnabl B. Bacteria engineered to produce IL-22 in intestine induce expression of REG3G to reduce ethanol-induced liver disease in mice. *Gut* 2019; **68**: 1504-1515 [PMID: 30448775 DOI: 10.1136/gutjnl-2018-317232]

84 **Szabo G**. Gut-liver axis in alcoholic liver disease. *Gastroenterology* 2015; **148**: 30-36 [PMID: 25447847 DOI: 10.1053/j.gastro.2014.10.042]

85 **Sonnenberg GF**, Fouser LA, Artis D. Border patrol: regulation of immunity, inflammation and tissue homeostasis at barrier surfaces by IL-22. *Nat Immunol* 2011; **12**: 383-390 [PMID: 21502992 DOI: 10.1038/ni.2025]

86 **Park O**, Wang H, Weng H, Feigenbaum L, Li H, Yin S, Ki SH, Yoo SH, Dooley S, Wang FS, Young HA, Gao B. In vivo consequences of liver-specific interleukin-22 expression in mice: Implications for human liver disease progression. *Hepatology* 2011; **54**: 252-261 [PMID: 21465510 DOI: 10.1002/hep.24339]

87 **Waidmann O**, Kronenberger B, Scheiermann P, Köberle V, Mühl H, Piiper A. Interleukin-22 serum levels are a negative prognostic indicator in patients with hepatocellular carcinoma. *Hepatology* 2014; **59**: 1207 [PMID: 23729376 DOI: 10.1002/hep.26528]

88 **Jiang R**, Tan Z, Deng L, Chen Y, Xia Y, Gao Y, Wang X, Sun B. Interleukin-22 promotes human hepatocellular carcinoma by activation of STAT3. *Hepatology* 2011; **54**: 900-909 [PMID: 21674558 DOI: 10.1002/hep.24486]

89 **Pipe S**, Leebeek FWG, Ferreira V, Sawyer EK, Pasi J. Clinical Considerations for Capsid Choice in the Development of Liver-Targeted AAV-Based Gene Transfer. *Mol Ther Methods Clin Dev* 2019; **15**: 170-178 [PMID: 31660419 DOI: 10.1016/j.omtm.2019.08.015]

90 **Akache B**, Grimm D, Pandey K, Yant SR, Xu H, Kay MA. The 37/67-kilodalton laminin receptor is a receptor for adeno-associated virus serotypes 8, 2, 3, and 9. *J Virol* 2006; **80**: 9831-9836 [PMID: 16973587 DOI: 10.1128/JVI.00878-06]

91 **Wang D**, Tai PWL, Gao G. Adeno-associated virus vector as a platform for gene therapy delivery. *Nat Rev Drug Discov* 2019; **18**: 358-378 [PMID: 30710128 DOI: 10.1038/s41573-019-0012-9]

92 **Kattenhorn LM**, Tipper CH, Stoica L, Geraghty DS, Wright TL, Clark KR, Wadsworth SC. Adeno-Associated Virus Gene Therapy for Liver Disease. *Hum Gene Ther* 2016; **27**: 947-961 [PMID: 27897038 DOI: 10.1089/hum.2016.160]

93 **Satishchandran A**, Ambade A, Rao S, Hsueh YC, Iracheta-Vellve A, Tornai D, Lowe P, Gyongyosi B, Li J, Catalano D, Zhong L, Kodys K, Xie J, Bala S, Gao G, Szabo G. MicroRNA 122, Regulated by GRLH2, Protects Livers of Mice and Patients From Ethanol-Induced Liver Disease. *Gastroenterology* 2018; **154**: 238-252.e7 [PMID: 28987423 DOI: 10.1053/j.gastro.2017.09.022]

94 **Hsu SH**, Wang B, Kota J, Yu J, Costinean S, Kutay H, Yu L, Bai S, La Perle K, Chivukula RR, Mao H, Wei M, Clark KR, Mendell JR, Caligiuri MA, Jacob ST, Mendell JT, Ghoshal K. Essential metabolic, anti-inflammatory, and anti-tumorigenic functions of miR-122 in liver. *J Clin Invest* 2012; **122**: 2871-2883 [PMID: 22820288 DOI: 10.1172/JCI63539]

95 **Zhang CY**, Yuan WG, He P, Lei JH, Wang CX. Liver fibrosis and hepatic stellate cells: Etiology, pathological hallmarks and therapeutic targets. *World J Gastroenterol* 2016; **22**: 10512-10522 [PMID: 28082803 DOI: 10.3748/wjg.v22.i48.10512]

96 **Lamas-Paz A**, Hao F, Nelson LJ, Vázquez MT, Canals S, Gómez Del Moral M, Martínez-Naves E, Nevzorova YA, Cubero FJ. Alcoholic liver disease: Utility of animal models. *World J Gastroenterol* 2018; **24**: 5063-5075 [PMID: 30568384 DOI: 10.3748/wjg.v24.i45.5063]

97 **Ghosh Dastidar S**, Warner JB, Warner DR, McClain CJ, Kirpich IA. Rodent Models of Alcoholic Liver Disease: Role of Binge Ethanol Administration. *Biomolecules* 2018; **8** [PMID: 29342874 DOI: 10.3390/biom8010003]

98 **Agrawal U**, Sharma R, Gupta M, Vyas SP. Is nanotechnology a boon for oral drug delivery? *Drug Discov Today* 2014; **19**: 1530-1546 [PMID: 24786464 DOI: 10.1016/j.drudis.2014.04.011]

99 **Chenthamara D**, Subramaniam S, Ramakrishnan SG, Krishnaswamy S, Essa MM, Lin FH, Qoronfleh MW. Therapeutic efficacy of nanoparticles and routes of administration. *Biomater Res* 2019; **23**: 20 [PMID: 31832232 DOI: 10.1186/s40824-019-0166-x]

100 **Kezer CA**, Simonetto DA, Shah VH. Sex Differences in Alcohol Consumption and Alcohol-Associated Liver Disease. *Mayo Clin Proc* 2021; **96**: 1006-1016 [PMID: 33714602 DOI: 10.1016/j.mayocp.2020.08.020]

101 **Wagnerberger S**, Fiederlein L, Kanuri G, Stahl C, Millonig G, Mueller S, Bischoff SC, Bergheim I. Sex-specific differences in the development of acute alcohol-induced liver steatosis in mice. *Alcohol Alcohol* 2013; **48**: 648-656 [PMID: 23969550 DOI: 10.1093/alcalc/agt138]

102 **Hajipour MJ**, Aghaverdi H, Serpooshan V, Vali H, Sheibani S, Mahmoudi M. Sex as an important factor in nanomedicine. *Nat Commun* 2021; **12**: 2984 [PMID: 34017011 DOI: 10.1038/s41467-021-23230-9]

103 **Bulbake U**, Doppalapudi S, Kommineni N, Khan W. Liposomal Formulations in Clinical Use: An Updated Review. *Pharmaceutics* 2017; **9** [PMID: 28346375 DOI: 10.3390/pharmaceutics9020012]

104 **Wang N**, Chen M, Wang T. Liposomes used as a vaccine adjuvant-delivery system: From basics to clinical immunization. *J Control Release* 2019; **303**: 130-150 [PMID: 31022431 DOI: 10.1016/j.jconrel.2019.04.025]

105 **Anselmo AC**, Mitragotri S. Nanoparticles in the clinic: An update. *Bioeng Transl Med* 2019; **4**: e10143 [PMID: 31572799 DOI: 10.1002/btm2.10143]

106 **Springer AD**, Dowdy SF. GalNAc-siRNA Conjugates: Leading the Way for Delivery of RNAi Therapeutics. *Nucleic Acid Ther* 2018; **28**: 109-118 [PMID: 29792572 DOI: 10.1089/nat.2018.0736]

107 **Debacker AJ**, Voutila J, Catley M, Blakey D, Habib N. Delivery of Oligonucleotides to the Liver with GalNAc: From Research to Registered Therapeutic Drug. *Mol Ther* 2020; **28**: 1759-1771 [PMID: 32592692 DOI: 10.1016/j.ymthe.2020.06.015]

World Journal of Gastroenterology

Submit a Manuscript: https://www.f6publishing.com

World J Gastroenterol 2022 September 28; 28(36): 5300-5312

DOI: 10.3748/wjg.v28.i36.5300

ISSN 1007-9327 (print) ISSN 2219-2840 (online)

MINIREVIEWS

Histopathological assessment of the microscopic activity in inflammatory bowel diseases: What are we looking for?

Ondrej Fabian, Lukas Bajer

Specialty type: Gastroenterology and hepatology

Provenance and peer review: Invited article; Externally peer reviewed.

Peer-review model: Single blind

Peer-review report's scientific quality classification

Grade A (Excellent): 0
Grade B (Very good): B
Grade C (Good): C
Grade D (Fair): 0
Grade E (Poor): 0

P-Reviewer: Iizuka M, Japan; Qian N, China

Received: July 1, 2022
Peer-review started: July 1, 2022
First decision: August 1, 2022
Revised: August 11, 2022
Accepted: September 8, 2022
Article in press: September 8, 2022
Published online: September 28, 2022

Ondrej Fabian, Clinical and Transplant Pathology Centre, Institute for Clinical and Experimental Medicine, Prague 14021, Czech Republic

Ondrej Fabian, Department of Pathology and Molecular Medicine, 3rd Faculty of Medicine, Charles University and Thomayer Hospital, Prague 14059, Czech Republic

Lukas Bajer, Hepatogastroenterology Department, Institute for Clinical and Experimental Medicine, Prague 14021, Czech Republic

Lukas Bajer, Institute of Microbiology, Czech Academy of Sciences, Prague 14220, Czech Republic

Corresponding author: Ondrej Fabian, MD, PhD, Assistant Professor, Postdoc, Clinical and Transplant Pathology Centre, Institute for Clinical and Experimental Medicine, Videnska 1958/9, Prague 14021, Czech Republic. ondrej.fabian@ikem.cz

Abstract

Advances in diagnostics of inflammatory bowel diseases (IBD) and improved treatment strategies allowed the establishment of new therapeutic endpoints. Currently, it is desirable not only to cease clinical symptoms, but mainly to achieve endoscopic remission, a macroscopic normalization of the bowel mucosa. However, up to one-third of IBD patients in remission exhibit persisting microscopic activity of the disease. The evidence suggests a better predictive value of histology for the development of clinical complications such as clinical relapse, surgical intervention, need for therapy escalation, or development of colorectal cancer. The proper assessment of microscopic inflammatory activity thus became an important part of the overall histopathological evaluation of colonic biopsies and many histopathological scoring indices have been established. Nonetheless, a majority of them have not been validated and no scoring index became a part of the routine bioptic practice. This review summarizes a predictive value of microscopic disease activity assessment for the subsequent clinical course of IBD, describes the most commonly used scoring indices for Crohn's disease and ulcerative colitis, and comments on current limitations and unresolved issues.

Key Words: Crohn's disease; Microscopy; Predictor; Score; Ulcerative colitis

Core Tip: Approximately one third of the patients with inflammatory bowel diseases in endoscopic remission show persisting signs of microscopic disease activity. Histology seems to have a predictive value for development of severe clinical complications. Proper assessment of the microscopic activity of the disease using respective scoring indices is thus necessary. This review summarizes the most widely used histological scoring indices, discusses their advantages and limitations and comments persisting unresolved issues from the perspective of gastrointestinal pathologists.

Citation: Fabian O, Bajer L. Histopathological assessment of the microscopic activity in inflammatory bowel diseases: What are we looking for? *World J Gastroenterol* 2022; 28(36): 5300-5312
URL: https://www.wjgnet.com/1007-9327/full/v28/i36/5300.htm
DOI: https://dx.doi.org/10.3748/wjg.v28.i36.5300

INTRODUCTION

The first description of inflammatory bowel disease (IBD) dates back to 1932, when Burrill Bernard Crohn published the article "Regional ileitis: A pathologic and clinical entity"[1]. In the following decades, our understanding of IBD has evolved. Currently, we perceive both Crohn's disease (CD) and ulcerative colitis (UC) as systemic inflammatory conditions showing predilection to the gastrointestinal (GI) tract[2-4]. Despite persisting ominous etiology and poorly understood pathogenesis, substantial advances in diagnostics and therapy of IBD have been made, allowing new therapeutic endpoints to be laid out. At present, we strive not only to cease all clinical symptoms, but mainly to reach the endoscopic remission, defined as normalization of endoscopic mucosal appearance[5,6]. However, normal endoscopic finding does not necessarily reflect normal histology. Correlation between endoscopy and histology is poor and up to 1/3 of both CD and UC patients in endoscopic remission show signs of persisting histological activity[7-10]. There is increasing evidence that histological activity of the disease may be a better predictor of important clinical endpoints such as hospitalization rate, risk of clinical relapse, need for systemic corticosteroid use, or development of colorectal cancer when compared to sole endoscopy[11-16]. This is even more important for certain IBD subtypes such as IBD associated with primary sclerosing cholangitis, currently considered a distinct phenotype of IBD entailing a four times higher risk of a colorectal cancer development compared to conventional IBD[17, 18]. The evaluation of the histological disease activity by reliable scoring indices thus represents an important part of the overall microscopic assessment. Nonetheless, a majority of them lack proper validation and none of them have been established in routine clinical practice. Endoscopy remains a gold standard for the assessment of luminal activity of the disease[5].

The aim of this review is to provide a summary of the most commonly used scoring indices for CD and UC, highlight clinical benefits of the microscopic disease activity assessment and comment on current limitations and unresolved issues from the pathologists' perspective.

BASIC PRINCIPLES OF IBD HISTOPATHOLOGY

To better conceive microscopic features included in histopathological scoring indices, it seems convenient to briefly summarize a basic IBD pathology first. UC is characterized by a continuous inflammation affecting a rectum and progressing towards the proximal colon and terminal ileum. The inflammatory infiltrate is usually confined to the mucosa. Submucosa may be affected in case of severe colitis, but transmural inflammation is not a feature of UC. As far as CD is concerned, the inflammation displays a discontinuous pattern on both macroscopic and microscopic levels. Any part of the GI tract from the oral cavity to the anal region may be affected, while the terminal ileum is the most frequent site of the disease. The inflammation is typically transmural, infiltrating deeper layers of the bowel wall. In both IBD subtypes, the infiltrate is mainly mononuclear, with a predominance of lymphocytes and plasmacytes. The presence of neutrophils is a sign of the disease activity. In case of mildly active disease, they are scarce and confined to lamina propria. With an increasing degree of activity, they tend to infiltrate surface epithelium and colonic crypts (defined as cryptitis). Later on, the crypt walls are disrupted and neutrophils exudate into their lumina forming crypt abscesses. The most severe grade of activity is usually characterized by the presence of erosions and ulcerations. Erosions were traditionally defined as defects confined to the mucosa, whilst ulcerations penetrated deeper into the submucosa, but there is no strict adherence to this criterion in pathological practice. Currently, ulcerations are often recognized rather by the presence of granulation tissue and erosions by fibrinopurulent exudate covering the defect[4,19,20]. The inflammatory infiltrate is often accompanied by numerous eosinophils. However, their proper assessment remains challenging due to the lack of a clearly defined cut-off value for their pathological increase[21]. Their numbers also vary among bowel segments being more

prevalent in the right-sided colon[22] and several studies document their substantial seasonal and geographic oscillation[23,24]. Other characteristic features of IBD are basal plasmacytosis and disrupted mucosal architecture. Basal plasmacytosis is defined as an increased number of plasmacytes between the base of the crypts and muscularis mucosae. It is a strong indicator of IBD and also one of the earliest signs of chronicity[25]. Disrupted mucosal architecture refers to any distortion of the physiological appearance of the crypts. Normally, colonic crypts are straight, parallel, and evenly spaced. In IBD, they show changes such as branching, angulation, dilatation, shortening, or dropout[26]. A hallmark of CD diagnosis is the presence of non-caseating epithelioid granulomas. Although a differential diagnosis of granulomatous colitis is broad, the presence of immune granuloma in IBD patients excludes the diagnosis of UC. Their incidence ranges from 15% to 85% according to various studies[26]. They are more closely tied to an ileocolic form of CD or CD with upper GI involvement[27] and seem to be almost twice as frequent in pediatric CD[28].

A PREDICTIVE VALUE OF MICROSCOPIC DISEASE ACTIVITY FOR THE DEVELOPMENT OF CLINICAL COMPLICATIONS

According to a recent meta-analysis by Gupta *et al*[8] performed on 2677 UC patients in endoscopic remission, the presence of persisting microscopic activity is associated with an increased risk of clinical relapse [odds ratio (OR) 2.41; 95% confidence interval (CI): 1.91-3.04]. These findings are supported by another meta-analysis by Yoon *et al*[29], which showed similar results based on the analysis of 757 UC patients in endoscopic remission. In their cohort, an absence of histological activity of the disease was associated with a 63% lower risk of clinical relapse (risk ratio 0.37; 95%CI: 0.24-0.56). In the study by Hefti *et al*[30], the authors evaluated 561 UC patients with a median follow-up of 21.4 years since the onset of the disease. According to both univariate and multivariate analyses, a mean histological inflammatory activity showed to be a significant predictor of colectomy ($P < 0.001$). Azad *et al*[31] showed that the presence of mucosal neutrophils and eosinophils in clinically and endoscopically quiescent UC was associated with an increased risk of clinical relapse over 12 mo ($P < 0.01$). Last but not least, Bryant *et al*[12] performed a study on 91 UC patients assessing a prognostic value of endoscopic and histological remission for the prediction of corticosteroid use, hospitalization and colectomy in a median 6-year follow-up. In their analysis, a histological remission was a predictor of colectomy and development of an acute severe colitis, in contrast to endoscopy (OR 0.42, 95%CI: 0.2-0.9, $P = 0.02$; OR 0.21, 95%CI: 0.1-0.7, $P = 0.02$ respectively). These results suggest that persisting histological activity of the disease seems to be associated with an adverse clinical course in UC patients.

Studies documenting a prognostic value of histology in CD are still limited in number. However, Christensen *et al*[14] demonstrated that the absence of histologic activity in patients with ileal CD is associated with a lower risk of clinical relapse [hazard ratio (HR) 2.05; 95%CI: 1.07-3.94; $P = 0.031$], corticosteroid use (HR 2.44; 95 % CI 1.17 - 5.09; $P = 0.018$) and medical escalation (HR 2.17; 95%CI: 1.2-3.96; $P = 0.011$) in a 21-mo follow-up. In the study by Brennan *et al*[32], the absence of histological activity was associated with a lower percentage of disease flares at both 12 mo (2.4% *vs* 25.5%, $P = 0.03$) and 24 mo (10.5% *vs* 37.8%, $P = 0.05$) of follow-up, in contrast to endoscopy, where no significant difference between an endoscopically active and an inactive disease was found. On the other hand, the aforementioned meta-analysis by Gupta *et al*[8], which analyzed the predictive value of histology in 2677 UC patients, did not confirm the results, which were displayed by the group of 129 CD patients.

A predictive value of histology for the development of colorectal dysplasia and cancer is of no less importance. A meta-analysis by Flores *et al*[33] performed on 1443 UC patients found that even isolated histologic activity in otherwise endoscopically normal mucosa increased the risk of neoplasia (OR 2.6, 95%CI: 1.49-4.46, $P = 0.01$). In the study by Gupta *et al*[16], the severity of histological inflammation correlated with the risk of progression to an advanced neoplasia (high-grade dysplasia, invasive cancer), with HR being 3.0 (95%CI: 1.4-6.3) for the mean inflammatory score, HR 3.4 (95%CI: 1.1-10.4) for the binary inflammatory score and HR 2.2 [inter-quartile range (IQR) 1.2-4.2] for the maximum inflammatory score. A case-control study of Rutter *et al*[34] included 68 patients with a colorectal neoplasia matched with 136 controls without a neoplasia revealed a highly significant correlation between the histological severity of inflammation and the risk of neoplasia development (OR 4.69, 95%CI: 2.10-10.48, $P < 0.001$). Pai *et al*[35] correlated 52 UC patients with colorectal cancer to 122 patients without cancer. Based on the retrospective re-evaluation of biopsies from the last five years, a mean histological disease activity assessed by two independent histological scores appeared to be a predictor of cancer development, in contrast to endoscopy (HR 7.53, 95%CI: 2.56-12.16, $P < 0.001$ and HR 5.89, 95%CI: 2.18-15.92, $P < 0.001$ respectively). In CD, the predictive value of histology for cancer development is still equivocal. However, in the study by Kirchgesner *et al*[36] assessing a cohort of 398 IBD patients including 237 patients with CD, mean histological disease severity was associated with the risk of cancer development (OR 1.69, 95%CI: 1.29-2.21, $P < 0.001$ per one-unit increase).

In summary, a vast majority of evidence suggests that cessation of microscopic inflammatory activity has a positive impact on the future clinical course of the disease, especially for patients suffering from UC. Assessment of the histological activity should therefore be an integral part of bioptic reports in all

patients with IBD. However, the appropriate extent of the microscopic normalization is still not precisely established. In other words, we still lack a proper definition of histological remission. As a result, establishing it as a primary therapeutic endpoint in clinical practice or clinical trials still lacks validity[6,37,38].

HISTOPATHOLOGIC SCORING INDICES FOR UC

The first histopathological scoring index for UC and the first scoring index for IBD, in general, was established in the 1960s by Truelove and Richards[39]. Since then, up to thirty indices have been proposed according to Cochrane Collaboration review[40], although only a few of them have been fully validated. One of the most widely used remains the Geboes score (GS), established in 2000[41]. This score assesses seven histopathological features including architectural mucosal changes, chronic inflammatory infiltrate, neutrophils and eosinophils in lamina propria, intraepithelial neutrophils, crypt destruction, and mucosal defects. Each of the given variables is further subclassified according to its severity (Table 1). The overall microscopic inflammatory severity should be based on the worst score in the bioptic sample, not on the average grade counted from all samples. Although, such a score may appear overly complicated at the first glance (*i.e.*, grading of the cryptitis severity as < 5%, < 50%, and > 50% of the affected crypts in the sample), it showed surprisingly good interpersonal agreement in preliminary phases of the study, especially when evaluating the presence of disease activity and mucosal defects (Cohen's kappa coefficient κ was above 0.9). A weak agreement was reached for the assessment of an inactive chronic inflammation. The original purpose of the score was a classification scheme, intended to define specific thresholds of the inflammatory severity, such as the presence of the disease activity. In subsequent studies, the score was also used as a continuous scale, assessing treatment efficacy in clinical trials[42,43]. The score seems to have a decent predictive value, being a reliable predictor of a clinical relapse in patients in clinical and endoscopic remission[31,44]. However, it has not been completely validated. In 2017, the Geboes Simplified Score was proposed[45]. The score reduced grading of the inflammatory activity and included the presence of basal plasmacytosis (Table 2). The score shows better overall agreement compared to the original GS (κ 0.56 *vs* 0.4). With regards to individual grades, the best agreement was reached for the detection of the inflammatory activity (κ 0.7). However, the score has not yet been widely used.

Robarts histopathology index (RHI)[46] was established in 2017 and was primarily intended to assess microscopic changes induced by the treatment. The construction process of the index was based on the original GS, from which the histopathological variables with reliable interobserver agreement and good correlation with grades of the inflammatory activity according to Visual Analogue Scale were used and served as a foundation for the final index. The definitive index consists of four histopathological features including chronic inflammatory infiltrate, neutrophils in lamina propria, neutrophils in the epithelium and mucosal defects. Each of the features is further subclassified according to its severity (range 0 to 3), giving the final index range from 0 to 33 points (Table 3). In contrast to GS, RHI exclusively assesses the histologic activity of the disease and excludes the features of chronicity. The agreement among the index grades is very good, with an intraclass correlation coefficient above 0.8. A predictive value of the index is still not fully elucidated. However, the aforementioned study by Pai *et al* [35] showed that a mean index score ≥ 8 during 5 years of observation predicted the development of colorectal cancer.

In the same year, a Nancy histological index (NHI) was proposed[47,48]. It uses five-grade scale based on the presence of chronic and active inflammatory infiltrate and mucosal defects (Table 4 and Figure 1). The final grade is determined by the worst histopathologic feature found in a biopsy sample. Despite the subjective nature of some features making the thresholds between several grades prone to possible higher interobserver variability (*i.e.*, mild *vs* moderate intensity of the chronic inflammatory infiltrate defining grades 0 and 1 respectively), the index shows very good overall interobserver agreement (κ above 0.8) and also a good reciprocal correlation with RHI [49]. The score is fully validated and widely used in clinical practice. With regards to its predictive value, in the study of D'Amico *et al* [49] patients with histologic presence of the inflammation (NHI ≥ 1) had a higher risk of surgical intervention (14% *vs* 0%, $P = 0.01$) and hospitalization (36% *vs* 7.1%, $P = 0.001$) compared to patients in histological remission (NHI grade 0) during a 30-mo median follow-up.

HISTOPATHOLOGIC SCORING INDICES FOR CD

Scoring indices for CD are limited in number. The Cochrane collaboration review mentions 14 indices [50], but the only one used on the larger scale is the Global Histology Activity Score (GHAS)[51]. The score was established by D´Haens *et al* in 1998 with the purpose to assess early postoperative recurrence after ileocecal resection. It includes the following variables: the presence of architectural changes, degree of chronic, neutrophilic and eosinophilic inflammatory infiltration in lamina propria, presence of intraepithelial neutrophils, epithelial damage, mucosal defects, presence of granulomas, and a number of

Table 1 Original Geboes score

Original Geboes score	
Grade 0: Architectural changes	0.0 No abnormality; 0.1 Mild abnormality; 0.2 Mild/moderate diffuse or multifocal abnormalities; 0.3 Severe diffuse or multifocal abnormalities
Grade 1: Chronic inflammatory infiltrate	1.0 No increase; 1.1 Mild but unequivocal increase; 1.2 Moderate increase; 1.3 Marked increase
Grade 2A: Eosinophils in lamina propria	2A.0 No increase; 2A.1 Mild but unequivocal increase; 2A.2 Moderate increase; 2A.3 Marked increase
Grade 2B: Neutrophils in lamina propria	2B.0 No increase; 2B.1 Mild but unequivocal increase; 2B.2 Moderate increase; 2B.3 Marked increase
Grade 3: Neutrophils in epithelium	3.0 None; 3.1 < 5% crypts involved; 3.2 < 50% crypts involved; 3.3 > 50% crypts involved
Grade 4: Crypt destruction	4.0 None; 4.1 Probable: local excess of neutrophils in part of the crypts; 4.2 Probable: marked attenuation; 4.3 Unequivocal crypt destruction
Grade 5: Erosions and ulcerations	5.0 No erosion, ulceration or granulation tissue; 5.1 Recovering epithelium + adjacent inflammation; 5.2 Probable erosion: focally stripped; 5.3 Unequivocal erosion; 5.4 Ulcer or granulation tissue

Table 2 Simplified Geboes score

Simplified Geboes score	
Grade 0: No inflammatory activity	0.0 No abnormalities; 0.1 Presence of architectural changes; 0.2 Presence of architectural changes and chronic mononuclear cell infiltrate
Grade 1: Basal plasma cells	1.0 No increase; 1.1 Mild increase; 1.2 Marked increase
Grade 2A: Eosinophils in lamina propria	2A.0 No increase; 2A.1 Mild increase; 2A.2 Marked increase
Grade 2B: Neutrophils in lamina propria	2B.0 No increase; 2B.1 Mild increase; 2B.2 Marked increase
Grade 3: Neutrophils in epithelium	3.0 None; 3.1 < 50% crypts involved; 3.2 > 50% crypts involved
Grade 4: Epithelial injury (in crypt and surface epithelium)	4.0 None; 4.1 Marked attenuation; 4.2 Probable crypt destruction: probable erosions; 4.3 Unequivocal crypt destruction: unequivocal erosion; 4.4 Ulcer or granulation tissue

Table 3 Robarts histopathology index

Histopathological variable	Grade
Chronic inflammatory infiltrate	0 = No increase; 1 = Mild but unequivocal increase; 2 = Moderate increase; 3 = Marked increase
Lamina propria neutrophils	0 = None; 1 = Mild but unequivocal increase; 2 = Moderate increase; 3 = Marked increase
Neutrophils in epithelium	0 = None; 1 = 50% crypts involved
Erosion or ulceration	0 = No erosion, ulceration or granulation tissue; 1 = Recovering epithelium + adjacent inflammation; 2 = Probable erosion-focally stripped; 3 = Unequivocal erosion; 4 = Ulcer or granulation tissue

affected bowel segments (Table 5). Later on, the score became used separately for terminal ileum and large bowel as Ileal and Colonic GHAS[52]. However, the score is not validated and its utility is limited. Instead of being a continuous scale, it rather represents a sum of present variables, putting minute changes such as architectural distortion or increased mononuclear cells in lamina propria on the same level of importance, for instance mucosal defects. According to a recent multidisciplinary consensus panel[53], the score does not represent a reliable index for the assessment of the inflammatory severity in CD. Its eventual predictive value has not been evidenced.

PRACTICAL ISSUES OF THE MICROSCOPIC ACTIVITY ASSESSMENT

The sole fact that we have been regularly confronted with new indices indirectly implies that we are still struggling to find the perfect one that would satisfy all our demands. A lot of unresolved issues persist

Table 4 Nancy histological index

Grade	Criteria
Grade 0 (no histological significant disease)	No or mild increase in chronic inflammatory infiltrate
Grade 1 (chronic inflammatory infiltrate with no acute inflammatory infiltrate)	Moderate or marked increase in chronic inflammatory infiltrate that is easily apparent. No acute inflammatory infiltrate is present
Grade 2 (mildly active disease)	Few or rare neutrophils in lamina propria or in the epithelium that are difficult to see
Grade 3 (moderately active disease)	Presence of multiple clusters of neutrophils in lamina propria and/or in epithelium that are easily apparent
Grade 4 (severely active disease)	Loss of colonic crypts replaced with "immature" granulation tissue (disorganized blood vessels with extravasated neutrophils) or the presence of fibrinopurulent exudate

Table 5 Global Histology Activity Score

Histopathological variable	Grade
Epithelial damage	0 = Normal; 1 = Focal; 2 = Extensive
Architectural changes	0 = Normal; 1 = Moderate; 2 = Severe
Mononuclear cells in lamina propria	0 = Normal; 1 = Moderate increase; 2 = Severe increase
Neutrophils in lamina propria	0 = Normal; 1 = Moderate increase; 2 = Severe increase
Neutrophils in epithelium	1 = Surface epithelium; 2 = Cryptitis; 3 = Crypt abscess
Erosion or ulceration	0 = No; 1 = Yes
Granuloma	0 = No; 1 = Yes
Number of segmental biopsy specimens affected	1 = < 1/3; 2 = 1/3-2/3; 3 = > 2/3

Each variable is scored independently. The total score is the sum of all individual scores.

throughout the whole diagnostic process, reflecting both the proper biology of the disease and the limitations of given diagnostic modalities.

Segmental and transmural character of the inflammation in CD

A correlation between endoscopic and histologic activity in CD is poor due to the segmental nature of the inflammation on both macroscopic and microscopic levels. Indeed, some degree of discrepancy between endoscopy and histology is desirable since the histology should not only confirm the endoscopic findings but represent an additional value by increasing the sensitivity of the inflammatory activity detection. On the other hand, a focal character of the disease may lead to a false underestimation of the histological activity. It is especially true in patients on therapy since treated IBD typically shows a focal and patchy character of the inflammation, even in UC[54].

In CD, a transmural character of the inflammation is one of the defining features, modifying the overall clinical severity of the disease and eventual development of complications. However, both histology and endoscopy provide information exclusively about the luminal activity of the disease. There is thus an increasing effort to establish a reliable scoring index of transmural severity of the disease. The well-known Lemann index[55] represents a clinical score, assessing the cumulative damage of the intestinal wall according to the presence of strictures, penetrating disease (fistulas or abdominal abscesses), previous surgical interventions, and perianal involvement. The majority of histopathological indices of transmural involvement are aimed at the assessment of resection margins of ileocecal resections. Later on, more complex indices were established, evaluating a full spectrum of transmural CD pathology including a degree of inflammatory intensity, fibrosis, smooth muscle changes, or neuronal hypertrophy[56-58]. However, such scores cannot be applied to endoscopic bioptic samples. In some instances, the sample is so superficial, that the basal portion of the mucosa is missing, precluding the assessment of important predictors such as basal plasmacytosis, which is also included in some scoring indices such as Simplified GS.

Upper GI and small intestinal involvement

Both CD and UC are systemic inflammatory conditions capable of affecting any part of the GI tract. This is especially true for pediatric patients, in which the inflammation in the upper GI is more frequent. As defined by the revised Porto criteria for the diagnosis of IBD in children and adolescents[59], pediatric

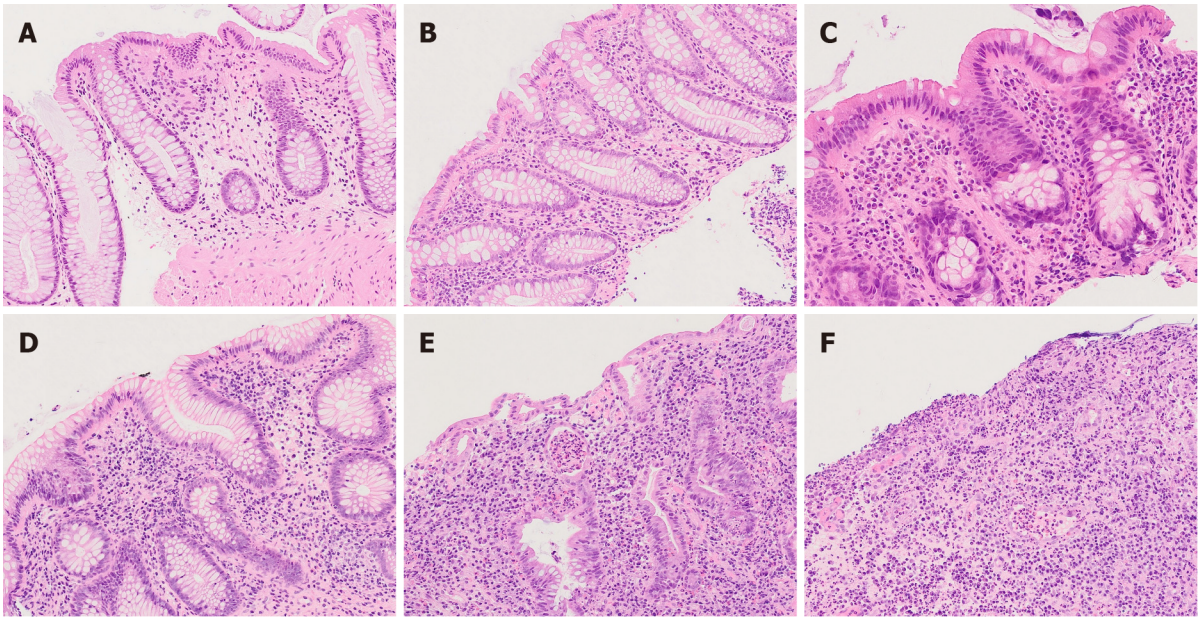

DOI: 10.3748/wjg.v28.i36.5300 **Copyright** ©The Author(s) 2022.

Figure 1 Microphotographs representing individual grades of Nancy Histopathological Index (hematoxylin and eosin, magnification 100×). A: Grade 0 with no increase in inflammatory cells; B: Grade 0 with mild increase in chronic inflammatory cells; C: Grade 1 with moderate increase in chronic inflammatory cells including more numerous eosinophils, but no neutrophils; D: Grade 2 with scarce neutrophils in lamina propria and epithelium; E: Grade 3 with numerous neutrophils including cryptitis and crypt abscess; F: Grade 4 with completely ulcerated colonic mucosa replaced by granulation tissue.

UC with upper GI involvement is even one of the atypical UC subtypes. However, grading of upper GI inflammatory severity is not a part of any available histological scoring index. In adult patients, a routine esophagogastroduodenoscopy is not even a part of the official recommendations for IBD diagnosis[2,3,59]. A subsequent clinical course may also be aggravated by the persisting inflammatory activity in a small bowel. However, an endoscopy can usually assess only its proximal and distal segments, frequently missing jejunum, and a large portion of the ileum. Key modalities for assessment the small bowel involvement are imaging techniques such as magnetic resonance imaging, computer tomography, ultrasonography or other radiologic procedures[60]. Some of them are also accompanied by respective scoring indices such as Simplified Magnetic Resonance Index of Activity for CD[61]. In recent years, scoring indices for capsule endoscopy were established, with Lewis Score[62] and Capsule Endoscopy Crohn Disease Activity Index[63] being among the most frequently used ones, recommended by both European Crohn's and Colitis Organisation (ECCO) and European Society of Gastrointestinal Endoscopy. Currently, there is no feasible way to sample biopsies during capsule endoscopy.

Number of bioptic samples

According to an official recommendation from the European Society of Pathology and ECCO[4,5], a diagnostic endoscopy should include at least two bioptic samples from at least five or six bowel segments including the terminal ileum and rectum. However, there is still no official recommendation for patients on treatment. Many gastroenterologists still prefer to perform an extensive sampling of severely affected regions and avoid normally appearing segments. This may falsely underestimate an overall histological inflammatory severity and negatively affect some scoring indices such as GHAS, which includes the number of affected regions into a final score.

Assessment of the disease activity in pediatric IBD

A Histopathological scoring index primarily designated for the pediatric population has not been established. Adult indices are used instead, but their feasibility for children is not self-evident. Studies aiming at the predictive value of histology in pediatric IBD are still limited in number. A few years ago, our group performed a retrospective analysis of 63 children with CD[64]. The microscopic severity of the inflammation at the time of diagnosis assessed by GHAS showed moderate correlation with endoscopic activity evaluated by Simple Endoscopic Score for Crohn's Disease (r = 0.48, P = 0.0001), no correlation with clinical activity of the disease, and had no predictive value for the development of defined complications [bowel stricture, intraabdominal or perianal abscess or fistula, initiation of anti-tumor necrosis factor (anti-TNF) therapy] during at least one year of follow-up. On the other hand, endoscopic activity appeared to be a predictor of the complications (HR 3.20, IQR 1.04-4.91, P = 0.037). With regards to pediatric UC, our recently conducted retrospective study[65] including 49 children with

UC showed that microscopic activity of the inflammation assessed by NHI and GS had no predictive value for complications development (acute severe colitis, need of colectomy, initiation of anti-TNF therapy, initiation of systemic 5-aminosalicylic therapy and systemic corticosteroid use). By contrast, levels of fecal calprotectin (FCPT) and clinical activity of the disease assessed by Pediatric Ulcerative Colitis Activity Index (PUCAI) showed to be independent predictors of the systemic 5-aminosalicylic acid induction (FCPT: HR 2.42, IQR 1.042-5.631, P = 0.040; PUCAI: HR 2.98, IQR 1.011-8.787, P = 0.048) and systemic corticosteroid use (FCPT: HR 2.517, IQR 1.115-5.681, P = 0.026; PUCAI: HR 2.98, IQR 1.011-8.787, P = 0.048).

ARE WE ASKING THE RIGHT QUESTION?

Histological activity in IBD is defined by the presence of neutrophils. Hence, strictly speaking, the histological index of the disease activity should be based on the extent of neutrophilic infiltration, their localization (lamina propria, superficial epithelium, cryptitis, crypt abscesses), and the presence of mucosal defects. Grading of the microscopic disease activity thus seems to be apparently straightforward. However, such grading per se is of no use if it does not provide any additional value to other means of disease activity assessment such as endoscopy or non-invasive biomarkers. There is thus a fundamental question about whether histological appearance is predictive of subsequent clinical outcomes. As mentioned before, the bulk of evidence suggests that persisting microscopic activity of the disease harbors an increased risk of development of complications. However, disease activity is not the only microscopic variable associated with an adverse clinical course. Other microscopic features such as basal plasmacytosis or granulomas have proven prognostic value. According to Johnson *et al*[66], the presence of granulomas was associated with increased serum levels of C-reactive protein, higher rates of stricturing and penetrating disease, higher rates of steroid, immunomodulators, biological therapy and narcotic use and higher healthcare utilization. With regards to basal plasmacytosis, the aforementioned meta-analysis by Gupta *et al*[8] demonstrated its predictive value for clinical recurrence in UC patients in endoscopic remission, as well. However, these features represent signs of chronicity rather than activity. Apart from that, there is still unresolved issue regarding the contribution of eosinophils, macrophages and other inflammatory cell types. Therefore, it seems to be more convenient to search for a suitable combination of microscopic features, providing the most accurate prediction for the subsequent clinical course of the disease, with a presence of neutrophils as a sign of the disease activity among the assessed variables. Apropos, the very presence of both chronic lymphoplasmacytic and active neutrophilic inflammatory infiltrate in one scoring index of disease activity may not properly reflect the biology of the process. In a majority of the scoring indices, the presence of isolated chronic inflammatory infiltrate is considered a lower grade of the inflammatory activity, aggravating with the increasing presence of neutrophils and eventually with the appearance of mucosal defects. But the lymphoplasmacytic infiltrate reflects rather chronicity of the process than its activity and these two variables don't necessarily represent a continuum. Such a hypothesis was taken into consideration in the recently established scoring index called Inflammatory Bowel Disease-Distribution, Chronicity, Activity (IBD-DCA) score (Table 6)[67]. The score was proposed at Erlangen International Consensus Conference and consists of three parameters - Distribution (D), Chronicity (C) and, Activity (A), which are assessed in this order. Distribution determines the overall extent of the disease, independently of the presence or absence of the activity. Chronicity is represented by the disrupted mucosal architecture, presence of basal plasmacytosis and increased lymphoplasmacytic infiltration in lamina propria. Activity is marked by the presence of neutrophils. The score thus represents not only a scoring index of the histopathological inflammatory activity, but provides information about the overall microscopic severity of the disease. According to the recent evidence[68], it showed moderate inter-rater reliability for parameter D (median intraclass correlation coefficient 0.645), poor to moderate for parameter C (0.568), and moderate to good for parameter A (0.748) for UC and moderate to good for parameter D and A (0.655 and 0.644 respectively) and poor for parameter C (0.303) for CD. The intra-rater agreement was moderate to excellent for D and C parameters (0.894 and 0.798 respectively) and good to excellent for A (0.909) parameter for UC, whilst CD showed moderate to excellent agreement for parameter D (0.854), poor to excellent for parameter C (0.714) and good to excellent for parameter A (0.888). There is a moderate correlation with NHI and Simplified GS. The unique feature of the score is its versatility, which means that it can be used for both CD and UC, as well as for IBDU, which represents 5%-15% of both adult and pediatric IBD[69-71] and in some cases becomes a definite diagnosis. By this, the score questions the necessity of separate scoring indices for CD and UC. Both diseases share a similar pattern of inflammatory activity and the inferior utility of scoring indices for CD stems rather from the segmental and transmural nature of the disease that from inappropriate assessment of its histological activity. Such a hypothesis is also supported by several studies. In the aforementioned study of Kirchgesner *et al*[36] assessing a predictive value of histology for the development of colorectal cancer, the authors used NHI to evaluate microscopic disease severity for the whole IBD cohort. In both UC and CD, the grade of the NHI correlated with the risk of cancer development. In the study by Löwenberg *et al*[72], the authors evaluated the ability of vedolizumab to induce endoscopic and histological remission in patients with

Table 6 Inflammatory Bowel Disease-Distribution, Chronicity, Activity score

Histopathological variable	Grade
Distribution	0 = Normal; 1 = < 50% of tissue affected per same biopsy site; 2 = > 50% of tissue affected per same biopsy
Chronicity	0 = Normal; 1 = Crypt distortion and/or mild lymphoplasmacytosis; 2 = Marked lymphoplasmacytosis and/or basal plasmacytosis
Activity	0 = Normal; 1 = Two or more neutrophils in lamina propria in one high-power field and/or any presence of intraepithelial neutrophils; 2 = Crypt abscesses, erosions, ulcers

Each variable is scored independently.

CD and the microscopic disease activity in the study was assessed by RHI. Using UC scoring indices for CD patients is suggested also by the recent expert consensus panel[53].

STILL FAR FROM THE HISTOLOGICAL REMISSION

Although achieving deeper mucosal healing is presumably associated with improved clinical course, it is far from synonymous with histological remission. However, establishing its proper definition remains challenging. In previous studies, the definition varied from the absence of active inflammation to the complete normalization of bowel mucosa. A recent position paper from ECCO defines histological remission as a "return to normal". Cessation of the microscopic activity undoubtedly correlates with a lower percentage of future complications. But even a mucosa without a presence of neutrophils may display increased chronic lymphoplasmacytic infiltration or architectonic changes that may aggravate the clinical course of the disease. Returning to the meta-analysis by Gupta *et al*[8] once more, their analysis showed that disrupted mucosal architecture was one of the features independently predicting the disease recurrence (OR 2.22). On the other hand, strict adherence to the histological normalization of the mucosa in each patient in endoscopic and clinical remission could lead to an unreasonable burden of aggressive therapy including all possible side effects. More studies need to be performed until a proper degree of histological normalization with an appropriate cost-benefit ratio will be established. One way or another, a complex histopathological scoring index assessing not only a disease activity but rather an overall microscopical severity seems to be necessary before we finally reach a standardized definition of the histological remission in IBD.

CONCLUSION

A proper assessment of the histological disease activity in IBD represents an essential component of the overall disease severity evaluation and provides important data for the subsequent clinical management of the patients. Many histopathological scoring indices exists, especially for UC, and they seem to be useful tools for the proper objectivization of the microscopic activity. However, their broader validation, subsequent implementation in routine bioptic practice and establishing the universally accepted definition of the histological remission are necessary before we could recognize the absence of the microscopic activity as the primary therapeutic target in IBD.

ACKNOWLEDGEMENTS

We would like to thank Drab D for his contribution during the manuscript revision.

FOOTNOTES

Author contributions: Fabian O collected the data, performed the data analysis and wrote the paper; Bajer L participated in the data analysis and wrote the paper.

Supported by Ministry of Health of the Czech Republic, No. NV18-09-00493 and No. NU21J-06-00027.

Conflict-of-interest statement: All the authors report no relevant conflicts of interest for this article.

Country/Territory of origin: Czech Republic

ORCID number: Ondrej Fabian 0000-0002-0393-2415; Lukas Bajer 0000-0002-3815-3120.

S-Editor: Gao CC
L-Editor: A
P-Editor: Gao CC

REFERENCES

1 **Crohn BB**, Ginzburg L, Oppenheimer GD. Regional ileitis; a pathologic and clinical entity. *Am J Med* 1952; **13**: 583-590 [PMID: 12996536 DOI: 10.1016/0002-9343(52)90025-9]
2 **Magro F**, Gionchetti P, Eliakim R, Ardizzone S, Armuzzi A, Barreiro-de Acosta M, Burisch J, Gecse KB, Hart AL, Hindryckx P, Langner C, Limdi JK, Pellino G, Zagórowicz E, Raine T, Harbord M, Rieder F; European Crohn's and Colitis Organisation [ECCO]. Third European Evidence-based Consensus on Diagnosis and Management of Ulcerative Colitis. Part 1: Definitions, Diagnosis, Extra-intestinal Manifestations, Pregnancy, Cancer Surveillance, Surgery, and Ileo-anal Pouch Disorders. *J Crohns Colitis* 2017; **11**: 649-670 [PMID: 28158501 DOI: 10.1093/ecco-jcc/jjx008]
3 **Gomollón F**, Dignass A, Annese V, Tilg H, Van Assche G, Lindsay JO, Peyrin-Biroulet L, Cullen GJ, Daperno M, Kucharzik T, Rieder F, Almer S, Armuzzi A, Harbord M, Langhorst J, Sans M, Chowers Y, Fiorino G, Juillerat P, Mantzaris GJ, Rizzello F, Vavricka S, Gionchetti P; ECCO. 3rd European Evidence-based Consensus on the Diagnosis and Management of Crohn's Disease 2016: Part 1: Diagnosis and Medical Management. *J Crohns Colitis* 2017; **11**: 3-25 [PMID: 27660341 DOI: 10.1093/ecco-jcc/jjw168]
4 **Magro F**, Langner C, Driessen A, Ensari A, Geboes K, Mantzaris GJ, Villanacci V, Becheanu G, Borralho Nunes P, Cathomas G, Fries W, Jouret-Mourin A, Mescoli C, de Petris G, Rubio CA, Shepherd NA, Vieth M, Eliakim R; European Society of Pathology (ESP); European Crohn's and Colitis Organisation (ECCO). European consensus on the histopathology of inflammatory bowel disease. *J Crohns Colitis* 2013; **7**: 827-851 [PMID: 23870728 DOI: 10.1016/j.crohns.2013.06.001]
5 **Annese V**, Daperno M, Rutter MD, Amiot A, Bossuyt P, East J, Ferrante M, Götz M, Katsanos KH, Kießlich R, Ordás I, Repici A, Rosa B, Sebastian S, Kucharzik T, Eliakim R; European Crohn's and Colitis Organisation. European evidence based consensus for endoscopy in inflammatory bowel disease. *J Crohns Colitis* 2013; **7**: 982-1018 [PMID: 24184171 DOI: 10.1016/j.crohns.2013.09.016]
6 **Travis SP**, Higgins PD, Orchard T, Van Der Woude CJ, Panaccione R, Bitton A, O'Morain C, Panés J, Sturm A, Reinisch W, Kamm MA, D'Haens G. Review article: defining remission in ulcerative colitis. *Aliment Pharmacol Ther* 2011; **34**: 113-124 [PMID: 21615435 DOI: 10.1111/j.1365-2036.2011.04701.x]
7 **Peyrin-Biroulet L**, Bressenot A, Kampman W. Histologic remission: the ultimate therapeutic goal in ulcerative colitis? *Clin Gastroenterol Hepatol* 2014; **12**: 929-34.e2 [PMID: 23911875 DOI: 10.1016/j.cgh.2013.07.022]
8 **Gupta A**, Yu A, Peyrin-Biroulet L, Ananthakrishnan AN. Treat to Target: The Role of Histologic Healing in Inflammatory Bowel Diseases: A Systematic Review and Meta-analysis. *Clin Gastroenterol Hepatol* 2021; **19**: 1800-1813.e4 [PMID: 33010406 DOI: 10.1016/j.cgh.2020.09.046]
9 **Chateau T**, Feakins R, Marchal-Bressenot A, Magro F, Danese S, Peyrin-Biroulet L. Histological Remission in Ulcerative Colitis: Under the Microscope Is the Cure. *Am J Gastroenterol* 2020; **115**: 179-189 [PMID: 31809296 DOI: 10.14309/ajg.0000000000000437]
10 **Molander P**, Sipponen T, Kemppainen H, Jussila A, Blomster T, Koskela R, Nissinen M, Rautiainen H, Kuisma J, Kolho KL, Färkkilä M. Achievement of deep remission during scheduled maintenance therapy with TNFα-blocking agents in IBD. *J Crohns Colitis* 2013; **7**: 730-735 [PMID: 23182163 DOI: 10.1016/j.crohns.2012.10.018]
11 **Park S**, Abdi T, Gentry M, Laine L. Histological Disease Activity as a Predictor of Clinical Relapse Among Patients With Ulcerative Colitis: Systematic Review and Meta-Analysis. *Am J Gastroenterol* 2016; **111**: 1692-1701 [PMID: 27725645 DOI: 10.1038/ajg.2016.418]
12 **Bryant RV**, Burger DC, Delo J, Walsh AJ, Thomas S, von Herbay A, Buchel OC, White L, Brain O, Keshav S, Warren BF, Travis SP. Beyond endoscopic mucosal healing in UC: histological remission better predicts corticosteroid use and hospitalisation over 6 years of follow-up. *Gut* 2016; **65**: 408-414 [PMID: 25986946 DOI: 10.1136/gutjnl-2015-309598]
13 **Christensen B**, Hanauer SB, Erlich J, Kassim O, Gibson PR, Turner JR, Hart J, Rubin DT. Histologic Normalization Occurs in Ulcerative Colitis and Is Associated With Improved Clinical Outcomes. *Clin Gastroenterol Hepatol* 2017; **15**: 1557-1564.e1 [PMID: 28238954 DOI: 10.1016/j.cgh.2017.02.016]
14 **Christensen B**, Erlich J, Gibson PR, Turner JR, Hart J, Rubin DT. Histologic Healing Is More Strongly Associated with Clinical Outcomes in Ileal Crohn's Disease than Endoscopic Healing. *Clin Gastroenterol Hepatol* 2020; **18**: 2518-2525.e1 [PMID: 31812654 DOI: 10.1016/j.cgh.2019.11.056]
15 **Rubin DT**, Huo D, Kinnucan JA, Sedrak MS, McCullom NE, Bunnag AP, Raun-Royer EP, Cohen RD, Hanauer SB, Hart J, Turner JR. Inflammation is an independent risk factor for colonic neoplasia in patients with ulcerative colitis: a case-

control study. *Clin Gastroenterol Hepatol* 2013; **11**: 1601-8.e1 [PMID: 23872237 DOI: 10.1016/j.cgh.2013.06.023]
16 **Gupta RB**, Harpaz N, Itzkowitz S, Hossain S, Matula S, Kornbluth A, Bodian C, Ullman T. Histologic inflammation is a risk factor for progression to colorectal neoplasia in ulcerative colitis: a cohort study. *Gastroenterology* 2007; **133**: 1099-105; quiz 1340 [PMID: 17919486 DOI: 10.1053/j.gastro.2007.08.001]
17 **Murasugi S**, Ito A, Omori T, Nakamura S, Tokushige K. Clinical Characterization of Ulcerative Colitis in Patients with Primary Sclerosing Cholangitis. *Gastroenterol Res Pract* 2020; **2020**: 7969628 [PMID: 33224192 DOI: 10.1155/2020/7969628]
18 **Soetikno RM**, Lin OS, Heidenreich PA, Young HS, Blackstone MO. Increased risk of colorectal neoplasia in patients with primary sclerosing cholangitis and ulcerative colitis: a meta-analysis. *Gastrointest Endosc* 2002; **56**: 48-54 [PMID: 12085034 DOI: 10.1067/mge.2002.125367]
19 **Pai RK**, Lauwers GY, Pai RK. Measuring Histologic Activity in Inflammatory Bowel Disease: Why and How. *Adv Anat Pathol* 2022; **29**: 37-47 [PMID: 34879037 DOI: 10.1097/PAP.0000000000000326]
20 **Abraham C**, Cho JH. Inflammatory bowel disease. *N Engl J Med* 2009; **361**: 2066-2078 [PMID: 19923578 DOI: 10.1056/NEJMra0804647]
21 **Conner JR**, Kirsch R. The pathology and causes of tissue eosinophilia in the gastrointestinal tract. *Histopathology* 2017; **71**: 177-199 [PMID: 28370248 DOI: 10.1111/his.13228]
22 **Matsushita T**, Maruyama R, Ishikawa N, Harada Y, Araki A, Chen D, Tauchi-Nishi P, Yuki T, Kinoshita Y. The number and distribution of eosinophils in the adult human gastrointestinal tract: a study and comparison of racial and environmental factors. *Am J Surg Pathol* 2015; **39**: 521-527 [PMID: 25581733 DOI: 10.1097/PAS.0000000000000370]
23 **Polydorides AD**, Banner BF, Hannaway PJ, Yantiss RK. Evaluation of site-specific and seasonal variation in colonic mucosal eosinophils. *Hum Pathol* 2008; **39**: 832-836 [PMID: 18430454 DOI: 10.1016/j.humpath.2007.10.012]
24 **Pascal RR**, Gramlich TL, Parker KM, Gansler TS. Geographic variations in eosinophil concentration in normal colonic mucosa. *Mod Pathol* 1997; **10**: 363-365 [PMID: 9110299]
25 **Villanacci V**, Antonelli E, Reboldi G, Salemme M, Casella G, Bassotti G. Endoscopic biopsy samples of naïve "colitides" patients: role of basal plasmacytosis. *J Crohns Colitis* 2014; **8**: 1438-1443 [PMID: 24931895 DOI: 10.1016/j.crohns.2014.05.003]
26 **Moore M**, Feakins RM, Lauwers GY. Non-neoplastic colorectal disease biopsies: evaluation and differential diagnosis. *J Clin Pathol* 2020; **73**: 783-792 [PMID: 32737191 DOI: 10.1136/jclinpath-2020-206794]
27 **Freeman HJ**. Granuloma-positive Crohn's disease. *Can J Gastroenterol* 2007; **21**: 583-587 [PMID: 17853953 DOI: 10.1155/2007/917649]
28 **Rubio CA**, Orrego A, Nesi G, Finkel Y. Frequency of epithelioid granulomas in colonoscopic biopsy specimens from paediatric and adult patients with Crohn's colitis. *J Clin Pathol* 2007; **60**: 1268-1272 [PMID: 17293387 DOI: 10.1136/jcp.2006.045336]
29 **Yoon H**, Jangi S, Dulai PS, Boland BS, Prokop LJ, Jairath V, Feagan BG, Sandborn WJ, Singh S. Incremental Benefit of Achieving Endoscopic and Histologic Remission in Patients With Ulcerative Colitis: A Systematic Review and Meta-Analysis. *Gastroenterology* 2020; **159**: 1262-1275.e7 [PMID: 32585306 DOI: 10.1053/j.gastro.2020.06.043]
30 **Hefti MM**, Chessin DB, Harpaz NH, Steinhagen RM, Ullman TA. Severity of inflammation as a predictor of colectomy in patients with chronic ulcerative colitis. *Dis Colon Rectum* 2009; **52**: 193-197 [PMID: 19279411 DOI: 10.1007/DCR.0b013e31819ad456]
31 **Azad S**, Sood N, Sood A. Biological and histological parameters as predictors of relapse in ulcerative colitis: a prospective study. *Saudi J Gastroenterol* 2011; **17**: 194-198 [PMID: 21546723 DOI: 10.4103/1319-3767.80383]
32 **Brennan GT**, Melton SD, Spechler SJ, Feagins LA. Clinical Implications of Histologic Abnormalities in Ileocolonic Biopsies of Patients With Crohn's Disease in Remission. *J Clin Gastroenterol* 2017; **51**: 43-48 [PMID: 26927490 DOI: 10.1097/MCG.0000000000000507]
33 **Flores BM**, O'Connor A, Moss AC. Impact of mucosal inflammation on risk of colorectal neoplasia in patients with ulcerative colitis: a systematic review and meta-analysis. *Gastrointest Endosc* 2017; **86**: 1006-1011.e8 [PMID: 28750838 DOI: 10.1016/j.gie.2017.07.028]
34 **Rutter M**, Saunders B, Wilkinson K, Rumbles S, Schofield G, Kamm M, Williams C, Price A, Talbot I, Forbes A. Severity of inflammation is a risk factor for colorectal neoplasia in ulcerative colitis. *Gastroenterology* 2004; **126**: 451-459 [PMID: 14762782 DOI: 10.1053/j.gastro.2003.11.010]
35 **Pai RK**, Hartman DJ, Leighton JA, Pasha SF, Rivers CR, Regueiro M, Binion DG, Pai RK. Validated Indices for Histopathologic Activity Predict Development of Colorectal Neoplasia in Ulcerative Colitis. *J Crohns Colitis* 2021; **15**: 1481-1490 [PMID: 33687061 DOI: 10.1093/ecco-jcc/jjab042]
36 **Kirchgesner J**, Svrcek M, Le Gall G, Landman C, Dray X, Bourrier A, Nion-Larmurier I, Hoyeau N, Sokol H, Seksik P, Cosnes J, Fléjou JF, Beaugerie L; Saint-Antoine Inflammatory Bowel Disease Network. Nancy Index Scores of Chronic Inflammatory Bowel Disease Activity Associate With Development of Colorectal Neoplasia. *Clin Gastroenterol Hepatol* 2020; **18**: 150-157.e1 [PMID: 31085339 DOI: 10.1016/j.cgh.2019.05.002]
37 **D'Haens G**, Sandborn WJ, Feagan BG, Geboes K, Hanauer SB, Irvine EJ, Lémann M, Marteau P, Rutgeerts P, Schölmerich J, Sutherland LR. A review of activity indices and efficacy end points for clinical trials of medical therapy in adults with ulcerative colitis. *Gastroenterology* 2007; **132**: 763-786 [PMID: 17258735 DOI: 10.1053/j.gastro.2006.12.038]
38 **Peyrin-Biroulet L**, Sandborn W, Sands BE, Reinisch W, Bemelman W, Bryant RV, D'Haens G, Dotan I, Dubinsky M, Feagan B, Fiorino G, Gearry R, Krishnareddy S, Lakatos PL, Loftus EV Jr, Marteau P, Munkholm P, Murdoch TB, Ordás I, Panaccione R, Riddell RH, Ruel J, Rubin DT, Samaan M, Siegel CA, Silverberg MS, Stoker J, Schreiber S, Travis S, Van Assche G, Danese S, Panes J, Bouguen G, O'Donnell S, Pariente B, Winer S, Hanauer S, Colombel JF. Selecting Therapeutic Targets in Inflammatory Bowel Disease (STRIDE): Determining Therapeutic Goals for Treat-to-Target. *Am J Gastroenterol* 2015; **110**: 1324-1338 [PMID: 26303131 DOI: 10.1038/ajg.2015.233]
39 **Truelove SC**, Richards WC. Biopsy studies in ulcerative colitis. *Br Med J* 1956; **1**: 1315-1318 [PMID: 13316140 DOI: 10.1136/bmj.1.4979.1315]
40 **Mosli MH**, Parker CE, Nelson SA, Baker KA, MacDonald JK, Zou GY, Feagan BG, Khanna R, Levesque BG, Jairath V.

Histologic scoring indices for evaluation of disease activity in ulcerative colitis. *Cochrane Database Syst Rev* 2017; **5**: CD011256 [PMID: 28542712 DOI: 10.1002/14651858.CD011256.pub2]

41 **Geboes K**, Riddell R, Ost A, Jensfelt B, Persson T, Löfberg R. A reproducible grading scale for histological assessment of inflammation in ulcerative colitis. *Gut* 2000; **47**: 404-409 [PMID: 10940279 DOI: 10.1136/gut.47.3.404]

42 **Lemmens B**, Arijs I, Van Assche G, Sagaert X, Geboes K, Ferrante M, Rutgeerts P, Vermeire S, De Hertogh G. Correlation between the endoscopic and histologic score in assessing the activity of ulcerative colitis. *Inflamm Bowel Dis* 2013; **19**: 1194-1201 [PMID: 23518809 DOI: 10.1097/MIB.0b013e318280e75f]

43 **Jairath V**, Peyrin-Biroulet L, Zou G, Mosli M, Vande Casteele N, Pai RK, Valasek MA, Marchal-Bressenot A, Stitt LW, Shackelton LM, Khanna R, D'Haens GR, Sandborn WJ, Olson A, Feagan BG. Responsiveness of histological disease activity indices in ulcerative colitis: a post hoc analysis using data from the TOUCHSTONE randomised controlled trial. *Gut* 2019; **68**: 1162-1168 [PMID: 30076171 DOI: 10.1136/gutjnl-2018-316702]

44 **Zenlea T**, Yee EU, Rosenberg L, Boyle M, Nanda KS, Wolf JL, Falchuk KR, Cheifetz AS, Goldsmith JD, Moss AC. Histology Grade Is Independently Associated With Relapse Risk in Patients With Ulcerative Colitis in Clinical Remission: A Prospective Study. *Am J Gastroenterol* 2016; **111**: 685-690 [PMID: 26977756 DOI: 10.1038/ajg.2016.50]

45 **Jauregui-Amezaga A**, Geerits A, Das Y, Lemmens B, Sagaert X, Bessissow T, Lobatón T, Ferrante M, Van Assche G, Bisschops R, Geboes K, De Hertogh G, Vermeire S. A Simplified Geboes Score for Ulcerative Colitis. *J Crohns Colitis* 2017; **11**: 305-313 [PMID: 27571771 DOI: 10.1093/ecco-jcc/jjw154]

46 **Mosli MH**, Feagan BG, Zou G, Sandborn WJ, D'Haens G, Khanna R, Shackelton LM, Walker CW, Nelson S, Vandervoort MK, Frisbie V, Samaan MA, Jairath V, Driman DK, Geboes K, Valasek MA, Pai RK, Lauwers GY, Riddell R, Stitt LW, Levesque BG. Development and validation of a histological index for UC. *Gut* 2017; **66**: 50-58 [PMID: 26475633 DOI: 10.1136/gutjnl-2015-310393]

47 **Marchal-Bressenot A**, Salleron J, Boulagnon-Rombi C, Bastien C, Cahn V, Cadiot G, Diebold MD, Danese S, Reinisch W, Schreiber S, Travis S, Peyrin-Biroulet L. Development and validation of the Nancy histological index for UC. *Gut* 2017; **66**: 43-49 [PMID: 26464414 DOI: 10.1136/gutjnl-2015-310187]

48 **Marchal-Bressenot A**, Scherl A, Salleron J, Peyrin-Biroulet L. A practical guide to assess the Nancy histological index for UC. *Gut* 2016; **65**: 1919-1920 [PMID: 27566129 DOI: 10.1136/gutjnl-2016-312722]

49 **D'Amico F**, Guillo L, Baumann C, Danese S, Peyrin-Biroulet L. Histological Disease Activity Measured by the Nancy Index Is Associated with Long-term Outcomes in Patients with Ulcerative Colitis. *J Crohns Colitis* 2021; **15**: 1631-1640 [PMID: 33822915 DOI: 10.1093/ecco-jcc/jjab063]

50 **Novak G**, Parker CE, Pai RK, MacDonald JK, Feagan BG, Sandborn WJ, D'Haens G, Jairath V, Khanna R. Histologic scoring indices for evaluation of disease activity in Crohn's disease. *Cochrane Database Syst Rev* 2017; **7**: CD012351 [PMID: 28731502 DOI: 10.1002/14651858.CD012351.pub2]

51 **D'Haens GR**, Geboes K, Peeters M, Baert F, Penninckx F, Rutgeerts P. Early lesions of recurrent Crohn's disease caused by infusion of intestinal contents in excluded ileum. *Gastroenterology* 1998; **114**: 262-267 [PMID: 9453485 DOI: 10.1016/s0016-5085(98)70476-7]

52 **De Cruz P**, Kamm MA, Prideaux L, Allen PB, Moore G. Mucosal healing in Crohn's disease: a systematic review. *Inflamm Bowel Dis* 2013; **19**: 429-444 [PMID: 22539420 DOI: 10.1002/ibd.22977]

53 **Almradi A**, Ma C, D'Haens GR, Sandborn WJ, Parker CE, Guizzetti L, Borralho Nunes P, De Hertogh G, Feakins RM, Khanna R, Lauwers GY, Mookhoek A, Pai RK, Peyrin-Biroulet L, Riddell R, Rosty C, Schaeffer DF, Valasek MA, Singh S, Crowley E, Feagan BG, Jairath V. An expert consensus to standardise the assessment of histological disease activity in Crohn's disease clinical trials. *Aliment Pharmacol Ther* 2021; **53**: 784-793 [PMID: 33410551 DOI: 10.1111/apt.16248]

54 **MATTS SG**. The value of rectal biopsy in the diagnosis of ulcerative colitis. *Q J Med* 1961; **30**: 393-407 [PMID: 14471445]

55 **Pariente B**, Mary JY, Danese S, Chowers Y, De Cruz P, D'Haens G, Loftus EV Jr, Louis E, Panés J, Schölmerich J, Schreiber S, Vecchi M, Branche J, Bruining D, Fiorino G, Herzog M, Kamm MA, Klein A, Lewin M, Meunier P, Ordas I, Strauch U, Tontini GE, Zagdanski AM, Bonifacio C, Rimola J, Nachury M, Leroy C, Sandborn W, Colombel JF, Cosnes J. Development of the Lémann index to assess digestive tract damage in patients with Crohn's disease. *Gastroenterology* 2015; **148**: 52-63.e3 [PMID: 25241327 DOI: 10.1053/j.gastro.2014.09.015]

56 **Schaeffer DF**, Walsh JC, Kirsch R, Waterman M, Silverberg MS, Riddell RH. Distinctive histopathologic phenotype in resection specimens from patients with Crohn's disease receiving anti-TNF-α therapy. *Hum Pathol* 2014; **45**: 1928-1935 [PMID: 25022570 DOI: 10.1016/j.humpath.2014.05.016]

57 **Chen W**, Lu C, Hirota C, Iacucci M, Ghosh S, Gui X. Smooth Muscle Hyperplasia/Hypertrophy is the Most Prominent Histological Change in Crohn's Fibrostenosing Bowel Strictures: A Semiquantitative Analysis by Using a Novel Histological Grading Scheme. *J Crohns Colitis* 2017; **11**: 92-104 [PMID: 27364949 DOI: 10.1093/ecco-jcc/jjw126]

58 **Pennington L**, Hamilton SR, Bayless TM, Cameron JL. Surgical management of Crohn's disease. Influence of disease at margin of resection. *Ann Surg* 1980; **192**: 311-318 [PMID: 6998388 DOI: 10.1097/00000658-198009000-00006]

59 **Levine A**, Koletzko S, Turner D, Escher JC, Cucchiara S, de Ridder L, Kolho KL, Veres G, Russell RK, Paerregaard A, Buderus S, Greer ML, Dias JA, Veereman-Wauters G, Lionetti P, Sladek M, Martin de Carpi J, Staiano A, Ruemmele FM, Wilson DC; European Society of Pediatric Gastroenterology, Hepatology, and Nutrition. ESPGHAN revised porto criteria for the diagnosis of inflammatory bowel disease in children and adolescents. *J Pediatr Gastroenterol Nutr* 2014; **58**: 795-806 [PMID: 24231644 DOI: 10.1097/MPG.0000000000000239]

60 **Panes J**, Bouhnik Y, Reinisch W, Stoker J, Taylor SA, Baumgart DC, Danese S, Halligan S, Marincek B, Matos C, Peyrin-Biroulet L, Rimola J, Rogler G, van Assche G, Ardizzone S, Ba-Ssalamah A, Bali MA, Bellini D, Biancone L, Castiglione F, Ehehalt R, Grassi R, Kucharzik T, Maccioni F, Maconi G, Magro F, Martín-Comín J, Morana G, Pendsé D, Sebastian S, Signore A, Tolan D, Tielbeek JA, Weishaupt D, Wiarda B, Laghi A. Imaging techniques for assessment of inflammatory bowel disease: joint ECCO and ESGAR evidence-based consensus guidelines. *J Crohns Colitis* 2013; **7**: 556-585 [PMID: 23583097 DOI: 10.1016/j.crohns.2013.02.020]

61 **Ordás I**, Rimola J, Alfaro I, Rodríguez S, Castro-Poceiro J, Ramírez-Morros A, Gallego M, Giner À, Barastegui R, Fernández-Clotet A, Masamunt M, Ricart E, Panés J. Development and Validation of a Simplified Magnetic Resonance

Index of Activity for Crohn's Disease. *Gastroenterology* 2019; **157**: 432-439.e1 [PMID: 30953614 DOI: 10.1053/j.gastro.2019.03.051]

62 **Gralnek IM**, Defranchis R, Seidman E, Leighton JA, Legnani P, Lewis BS. Development of a capsule endoscopy scoring index for small bowel mucosal inflammatory change. *Aliment Pharmacol Ther* 2008; **27**: 146-154 [PMID: 17956598 DOI: 10.1111/j.1365-2036.2007.03556.x]

63 **Gal E**, Geller A, Fraser G, Levi Z, Niv Y. Assessment and validation of the new capsule endoscopy Crohn's disease activity index (CECDAI). *Dig Dis Sci* 2008; **53**: 1933-1937 [PMID: 18034304 DOI: 10.1007/s10620-007-0084-y]

64 **Fabian O**, Hradsky O, Potuznikova K, Kalfusova A, Krskova L, Hornofova L, Zamecnik J, Bronsky J. Low predictive value of histopathological scoring system for complications development in children with Crohn's disease. *Pathol Res Pract* 2017; **213**: 353-358 [PMID: 28216137 DOI: 10.1016/j.prp.2017.01.009]

65 **Fabian O**, Hradsky O, Lerchova T, Mikus F, Zamecnik J, Bronsky J. Limited clinical significance of tissue calprotectin levels in bowel mucosa for the prediction of complicated course of the disease in children with ulcerative colitis. *Pathol Res Pract* 2019; **215**: 152689 [PMID: 31679791 DOI: 10.1016/j.prp.2019.152689]

66 **Johnson CM**, Hartman DJ, Ramos-Rivers C, Rao BB, Bhattacharya A, Regueiro M, Schwartz M, Swoger J, Al Hashash J, Barrie A, Pfanner TP, Dunn M, Koutroubakis IE, Binion DG. Epithelioid Granulomas Associate With Increased Severity and Progression of Crohn's Disease, Based on 6-Year Follow-Up. *Clin Gastroenterol Hepatol* 2018; **16**: 900-907.e1 [PMID: 29277619 DOI: 10.1016/j.cgh.2017.12.034]

67 **Lang-Schwarz C**, Agaimy A, Atreya R, Becker C, Danese S, Fléjou JF, Gaßler N, Grabsch HI, Hartmann A, Kamarádová K, Kühl AA, Lauwers GY, Lugli A, Nagtegaal I, Neurath MF, Oberhuber G, Peyrin-Biroulet L, Rath T, Riddell R, Rubio CA, Sheahan K, Tilg H, Villanacci V, Westerhoff M, Vieth M. Maximizing the diagnostic information from biopsies in chronic inflammatory bowel diseases: recommendations from the Erlangen International Consensus Conference on Inflammatory Bowel Diseases and presentation of the IBD-DCA score as a proposal for a new index for histologic activity assessment in ulcerative colitis and Crohn's disease. *Virchows Arch* 2021; **478**: 581-594 [PMID: 33373023 DOI: 10.1007/s00428-020-02982-7]

68 **Lang-Schwarz C**, Angeloni M, Agaimy A, Atreya R, Becker C, Dregelies T, Danese S, Fléjou JF, Gaßler N, Grabsch HI, Hartmann A, Kamarádová K, Kühl AA, Lauwers GY, Lugli A, Nagtegaal I, Neurath MF, Oberhuber G, Peyrin-Biroulet L, Rath T, Riddell R, Rubio CA, Sheahan K, Siegmund B, Tilg H, Villanacci V, Westerhoff M, Ferrazzi F, Vieth M. Validation of the 'Inflammatory Bowel Disease-Distribution, Chronicity, Activity [IBD-DCA] Score' for Ulcerative Colitis and Crohn´s Disease. *J Crohns Colitis* 2021; **15**: 1621-1630 [PMID: 33773497 DOI: 10.1093/ecco-jcc/jjab055]

69 **Winter DA**, Karolewska-Bochenek K, Lazowska-Przeorek I, Lionetti P, Mearin ML, Chong SK, Roma-Giannikou E, Maly J, Kolho KL, Shaoul R, Staiano A, Damen GM, de Meij T, Hendriks D, George EK, Turner D, Escher JC; Paediatric IBD Porto Group of ESPGHAN. Pediatric IBD-unclassified Is Less Common than Previously Reported; Results of an 8-Year Audit of the EUROKIDS Registry. *Inflamm Bowel Dis* 2015; **21**: 2145-2153 [PMID: 26164665 DOI: 10.1097/MIB.0000000000000483]

70 **Rinawi F**, Assa A, Eliakim R, Mozer-Glassberg Y, Nachmias Friedler V, Niv Y, Rosenbach Y, Silbermintz A, Zevit N, Shamir R. The natural history of pediatric-onset IBD-unclassified and prediction of Crohn's disease reclassification: a 27-year study. *Scand J Gastroenterol* 2017; **52**: 558-563 [PMID: 28128677 DOI: 10.1080/00365521.2017.1282008]

71 **Guindi M**, Riddell RH. Indeterminate colitis. *J Clin Pathol* 2004; **57**: 1233-1244 [PMID: 15563659 DOI: 10.1136/jcp.2003.015214]

72 **Löwenberg M**, Vermeire S, Mostafavi N, Hoentjen F, Franchimont D, Bossuyt P, Hindryckx P, Rispens T, de Vries A, van der Woude CJ, Berends S, Ambarus CA, Mathot R, Clasquin E, Baert F, D'Haens G. Vedolizumab Induces Endoscopic and Histologic Remission in Patients With Crohn's Disease. *Gastroenterology* 2019; **157**: 997-1006.e6 [PMID: 31175865 DOI: 10.1053/j.gastro.2019.05.067]

World Journal of Gastroenterology

Submit a Manuscript: https://www.f6publishing.com

World J Gastroenterol 2022 September 28; 28(36): 5313-5323

DOI: 10.3748/wjg.v28.i36.5313

ISSN 1007-9327 (print) ISSN 2219-2840 (online)

ORIGINAL ARTICLE

Basic Study

Esophageal magnetic compression anastomosis in dogs

Xiang-Hua Xu, Yi Lv, Shi-Qi Liu, Xiao-Hai Cui, Rui-Yang Suo

Specialty type: Gastroenterology and hepatology

Provenance and peer review: Unsolicited article; Externally peer reviewed.

Peer-review model: Single blind

Peer-review report's scientific quality classification
Grade A (Excellent): 0
Grade B (Very good): B, B
Grade C (Good): 0
Grade D (Fair): 0
Grade E (Poor): 0

P-Reviewer: Abass M, Egypt; Tré bol J, Spain

Received: July 14, 2022
Peer-review started: July 14, 2022
First decision: July 31, 2022
Revised: August 11, 2022
Accepted: September 9, 2022
Article in press: September 9, 2022
Published online: September 28, 2022

Xiang-Hua Xu, Yi Lv, Department of Hepatobiliary Surgery, The First Affiliated Hospital of Xi'an Jiaotong University, Xi'an 710061, Shaanxi Province, China

Xiang-Hua Xu, Yi Lv, National Local Joint Engineering Research Center for Precision Surgery and Regenerative Medicine, The First Affiliated Hospital of Xi'an Jiaotong University, Xi'an 710061, Shaanxi Province, China

Shi-Qi Liu, Department of Pediatric Surgery, Xi'an Children's Hospital, Xi'an 710003, Shaanxi Province, China

Xiao-Hai Cui, Department of Thoracic Surgery, The First Affiliated Hospital of Xi'an Jiaotong University, Xi'an 710061, Shaanxi Province, China

Rui-Yang Suo, Zonglian College, Xi'an Jiaotong University Health Science Center, Xi'an 710061, Shaanxi Province, China

Corresponding author: Yi Lv, MD, PhD, Professor, Department of Hepatobiliary Surgery, The First Affiliated Hospital of Xi'an Jiaotong University, No. 277 West Yanta Road, Xi'an 710061, Shaanxi Province, China. luyi169@126.com

Abstract

BACKGROUND

Magnetic compression anastomosis (MCA) is a novel suture-free reconstruction of the digestive tract. It has been used in gastrointestinal anastomosis, jejunal anastomosis, cholangioenteric anastomosis and so on. The traditional operative outcomes of congenital esophageal atresia and benign esophageal stricture are poor, and there are too many complications postoperatively.

AIM

To test MCA technology to reconstruct the esophagus in dogs, prior to studying the feasibility and safety of MCA in humans.

METHODS

Thirty-six dogs were randomized into either the study or control group (n = 18 per group). The dogs in the study group were subjected to end-to-end esophageal anastomosis with the magnetic compression device, while those in the control group underwent hand-sewn anastomosis with 4-0 absorbable multifilament Vicryl. We used interrupted single-layer inverting sutures. The anastomosis time, gross appearance, weight and pathology of the anastomosis were evaluated at one month, three months and six months postoperatively.

RESULTS

The anastomosis time of the MCA group was shorter than that of the hand-sewn group (7.5 ± 1.0 min *vs* 12.5 ± 1.8 min, $P < 0.01$). In the MCA group, X-ray examination was performed every day to locate the magnetic device in the esophagus before the magnetic device fell off from the esophagus. In the hand-sewn group, dogs did not undergo X-ray examination. One month after the surgeries, the mean weight of the dogs in the hand-sewn group had decreased more than that of the dogs in the MCA group (11.63 ± 0.71 kg *vs* 12.73 ± 0.80 kg, $P < 0.05$). At 3 mo and 6 mo after the operation, the dogs' weights were similar between the two groups (13.75 ± 0.84 kg *vs* 14.03 ± 0.82 kg, 14.93 ± 0.80 kg *vs* 15.44 ± 0.47 kg). The number of inflammatory cells in MCA group was lower than that in hand-sewn group on 1 mo after operation.

CONCLUSION

MCA is an effective and safe method for esophageal reconstruction. The anastomosis time of the MCA group was less than that of the hand-sewn group. This study shows that MCA technology may be applied to human esophageal reconstruction, provided these favorable results are confirmed by more publications.

Key Words: Magnetic; Anastomosis; Esophagus; Reconstruction; Hand sewn; Dog

Core Tip: We used magnetic compression anastomosis (MCA) technology to reconstruct the esophagus. The anastomosis time of the MCA group was shorter than that of the hand-sewn group (7.5 ± 1.0 min *vs* 12.5 ± 1.8 min, $P < 0.01$). One month after the surgeries, the mean weight of the dogs in the hand-sewn group had decreased more than that of the dogs in the MCA group (11.63 ± 0.71 kg *vs* 12.73 ± 0.80 kg, $P < 0.05$). At 3 mo and 6 mo after the operation, the dogs' weights were similar between the two groups. MCA is an effective and safe method for esophageal reconstruction. This study shows that MCA technology may be applied to human esophageal reconstruction, provided these favorable results are confirmed by more publications.

Citation: Xu XH, Lv Y, Liu SQ, Cui XH, Suo RY. Esophageal magnetic compression anastomosis in dogs. *World J Gastroenterol* 2022; 28(36): 5313-5323
URL: https://www.wjgnet.com/1007-9327/full/v28/i36/5313.htm
DOI: https://dx.doi.org/10.3748/wjg.v28.i36.5313

INTRODUCTION

Esophageal atresia (EA) is a serious and fatal gastrointestinal developmental malformation in the neonatal period. It has a worldwide prevalence of 2.4 to 3.8 per 10000 newborns[1-4]. Because of the development of surgical and good neonatal intensive care, the survival is about 90% in those born with EA with severe associated anomalies and is even higher in those born with EA alone[5]. However, the postoperative complications of traditional hand-sewn anastomosis are numerous, and the therapeutic effect is not good. The primary complications during the postoperative period are leakage (incidence 15%-20%), stenosis of the anastomosis (30%-40%), gastroesophageal reflux (40%-65%), esophageal dysmotility, fistula recurrence, scoliosis, deformities of the thoracic wall and respiratory disorders[6-8]. After surgery, children suffer from various complications, which seriously affect their development and quality of life.

Magnetic compression anastomosis (MCA) is a novel suture-free reconstruction of the digestive tract. Since Kanshin *et al*[9] reported using a magnetic device to anastomose gastroduodenal and cecojejunal in dogs in 1978, there have been many reports of this technique using animal experiments and regarding its clinical applications. At present, clinically, it has been used in gastrointestinal anastomosis[10,11], jejunal anastomosis[12,13], cholangioenteric anastomosis[14-16] and so on. Fourteen patients underwent MCA for gastrointestinal anastomosis, and the technical success of MCA was achieved in 100% of the cases. Two patients underwent anastomotic restenosis, and 1 patient had an anastomotic perforation due to balloon dilatation to prevent restenosis. Fifteen patients underwent MCA for jejunal anastomosis, of which five patients had severe systemic disease and underwent complex open urinary reconstruction procedures. The device was successfully placed and effectively formed a side-to-side, functional end-to-end jejunal anastomosis. Forty-seven patients underwent MCA for cholangioenteric anastomosis. Thirty-eight patients had a malignant primary disease, while nine had benign disease. With a median

follow-up of 547.5 d (range 223-1042 d), no patients had biliary fistula, while two developed anastomotic stricture at 4 mo and 14 mo after surgery. Magnetic materials have noncontact suction characteristics that will greatly simplify the process of gastrointestinal anastomosis, especially in the case of gastrointestinal stenosis or atresia. Recently, Kamada *et al*[10] reported that MCA without general anesthesia is a valuable alternative to surgery for gastrointestinal obstruction. Some patients with biliary obstruction are not eligible for conventional endoscopic procedures or are unsuitable for surgery. The MCA technique is an available method for performing choledochocholedochostomy and choledochoenterostomy interventionally[16]. The mean age of the patients in these two reports was above 60 years. Therefore, MCA technology can be designed as a minimally invasive technique and is tolerated by elderly patients.

Because of the many complications of traditional operations and the ability to obtain minimally invasive surgery by MCA, MCA could be a superior method to treat congenital EA. There have been several clinical reports on esophageal reconstruction using MCA[17-19]. Muensterer *et al*[17] reported that they used esophageal MCA for staged EA repair in 3 patients (Gross type A, B, and C) at high risk for conventional surgical repair. Surgeries were all successful, and there were no perioperative complications. Liu *et al*[18] reported that two patients who had severe stricture after simultaneous EA and duodenal obstruction repair underwent magnetic compression stricturoplasty. Magnetic compression stricturoplasty successfully established the patency of the esophagus in these two patients with refractory EA stricture. These two cases required multiple additional procedures, but durable esophageal patency with absence of dysphagia was achieved at 15 or 10 mo after magnetic compression stricturoplasty. Dorman *et al*[19] reported a case in which EA was repaired with a proximal fistula using endoscopic MCA after staged lengthening. Magnetic coupling occurred at 4 d, and after magnet removal at 13 d, an esophagram demonstrated a 10 French channel without leakage. A series of studies on MCA technology have been carried out in our laboratory. The technology has been used in choledochojejunostomy, rectovaginal fistula repair, laparoscopic pancreatoduodenectomy (LPD) and liver transplantation. Twenty-six mongrel dogs underwent choledochojejunostomy magnamosis with different magnetic pressure magnets. The surgical procedures were all successful[20]. There was a comparative study with 12 pigs for rectovaginal fistula repair. Eight animals were in the MCA group, and four animals were in the hand-sewn group. The rectovaginal fistula site was smooth, and healing was complete. This technology was used in one case clinically and achieved success[21]. Seven patients received MCA technology in LPD. LPD was successfully completed in all seven patients, of which seven underwent laparoscopic magnetic compression choledochojejunostomy and two received laparoscopic magnetic compression pancreatojejunostomy. No leakages were observed after the operation. After a median follow-up period of 11 mo (range 4-18 mo), there was no incidence of anastomotic stricture[22]. We also used MCA to reconstruct vessels in liver transplantation. In pig liver transplantation, we used MCA to reconstruct the suprahepatic vena cava, infrahepatic vena cava and portal vein. They were all successful, and the pig lived for over one month[23]. Currently, we want to use MCA technology to treat EA, but there is a paucity of published research data and animal studies. Therefore, the purpose of this study was to study the difference between MCA and hand-sewn anastomosis of the esophagus in dogs.

MATERIALS AND METHODS

Animals

The protocol of the animal study was reviewed and approved by the committee for Ethics of Animal Experiments of Xi'an Jiaotong University (No. XJTULAC2020-1441). Thirty-six mongrel dogs (male = 18, female = 18) with body weights of 10-15 kg were provided by the Laboratory Animal Center of Xi'an Jiaotong University. Dogs were acclimatized to laboratory conditions (23 °C, ad libitum access to food and water) for 2 wk prior to experimentation. In this study, we selected mongrel dogs because the esophagus in the neck is long enough for reconstruction. This purpose is to avoid performing surgery in the thoracic cavity and to improve the survival rate.

Study design

Thirty-six dogs were randomized into either the MCA group or the hand-sewn group, n = 18 per group, with the same male to female ratio. The dogs in the MCA group were subjected to end-to-end esophageal anastomosis with the magnetic device, while those in the hand-sewn group underwent hand-sewn anastomosis with 4-0 absorbable multifilament Vicryl. We used interrupted single-layer sutures. In both groups, there was no surgical left in place. Postoperative complications and weight were observed. The anastomosis time, gross appearance and pathology of the anastomoses were evaluated at one month, three months and six months after the operation.

Magnetic anastomosis device

The magnetic anastomosis device used in the study possessed a parent magnetic ring (PMR) and daughter magnetic ring (DMR), which were made of rare earth neodymium iron boron (NdFeB, N40) and plated with nickel from Northwest Institute for Nonferrous Metal Research, Xi'an, China. A special

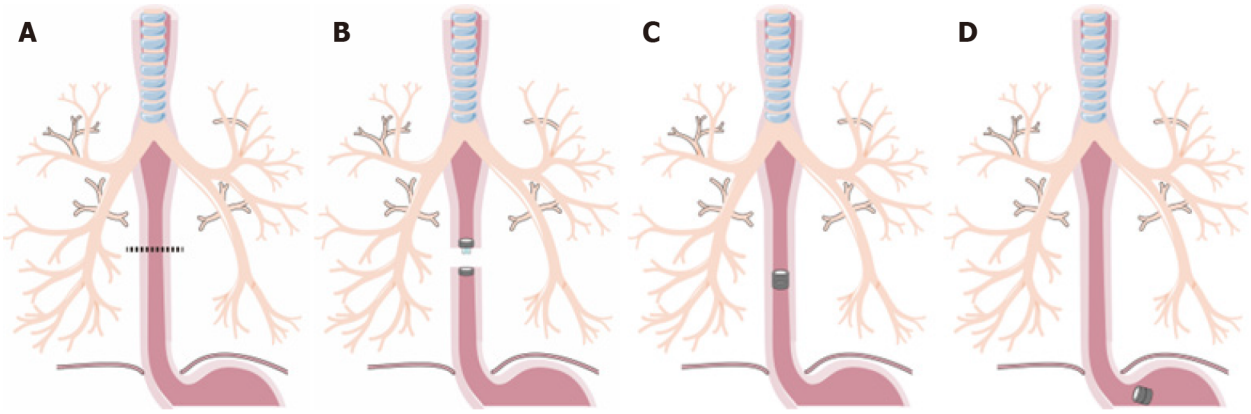

DOI: 10.3748/wjg.v28.i36.5313 **Copyright** ©The Author(s) 2022.

Figure 1 Surgical procedures of magnetic compress esophagus anastomosis. A: Transecting the esophagus at the diseased region; B: Placing the parent magnetic ring (PMR) and daughter magnetic ring (DMR) on the upper and lower ends of esophagus; C: The PMR and DMR attract each other and create the anastomosis, and the esophagus reconstruction is complete, the dispositive allows food passage; D: The magnetic devices fall off the esophagus into the stomach, and the esophagus lumen is completely open.

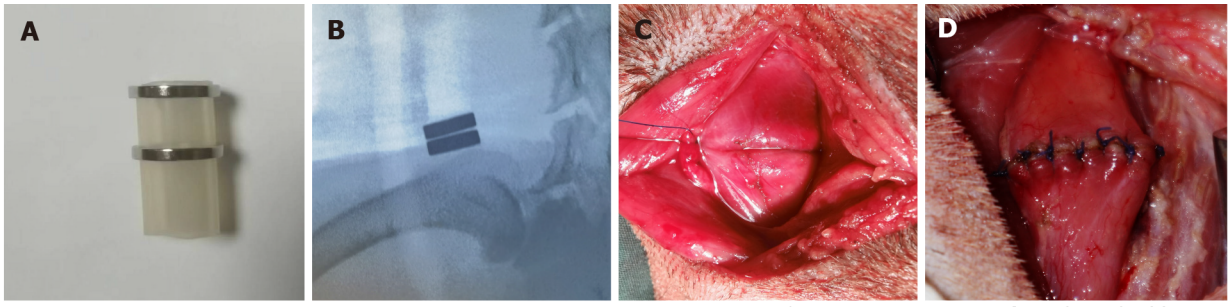

DOI: 10.3748/wjg.v28.i36.5313 **Copyright** ©The Author(s) 2022.

Figure 2 The magnetic device and the appearance on X-ray, the esophageal anastomosis of magnetic compression anastomosis and hand-sewn suture. A: The magnetic device, composed of two magnetic rings and one special catheter; B: The magnetic ring position on X-ray postoperatively, and the anastomosis face is smooth; C: Using the magnetic compression anastomosis technology to finish the esophageal anastomosis; D: The anastomosis by hand-sewn suture.

drainage tube was placed between the PMR and DMR, and both the PMR and DMR had outer diameters of 20 mm, inner diameters of 14 mm, and thicknesses of 2 mm. The magnetic force between the PMR and DMR is 30 Newton at zero distance with a magnetic density of 8000 GS.

Surgical procedures

The dogs were first anesthetized with an intraperitoneal injection of 30 mg/kg pentobarbital sodium solution. The dogs were anesthetized and then placed in the right lateral position on a temperature-controlled operating table with their cervical region shaved and sterilized. The experimental process is shown in Figure 1. A 5 cm incision was made along the anterior edge of the sternocleidomastoid muscle in the neck. Then, the muscle was separated layer by layer, and a 3 cm long portion of the esophagus was found. Next, the esophagus was transected.

In the MCA group, the PMR and DMR were placed in the upper and lower esophagus, respectively, after transecting the esophagus (Figure 1A). The magnetic anastomosis device was shown in Figure 2A. The upper and lower ends of the esophageal anastomosis were sutured with 4-0 silk thread and tightened to the position of the special drainage tube. Under the action of attraction, the magnetic rings at both ends are attracted to each other automatically and press the anastomotic tissue together, and the esophageal anastomosis is then completed (Figure 2C). When the anastomotic tissue is necrotic and falls off, the magnetic device is discharged into the stomach with the digesta and is discharged out of the body. In the control group, the operation was the same as that in the study group, except that end-to-end anastomosis was performed with 4-0 absorbable sutures (Figure 2D).

Postoperative care

An X-ray (Perlove Medical Equipment incorporated company, Nanjing, China) was performed on the dogs in the study group to confirm the target location and precise mating of the magnetic compression rings (Figure 2B). X-ray was performed every day before the magnets fell off the esophagus. Postoper-

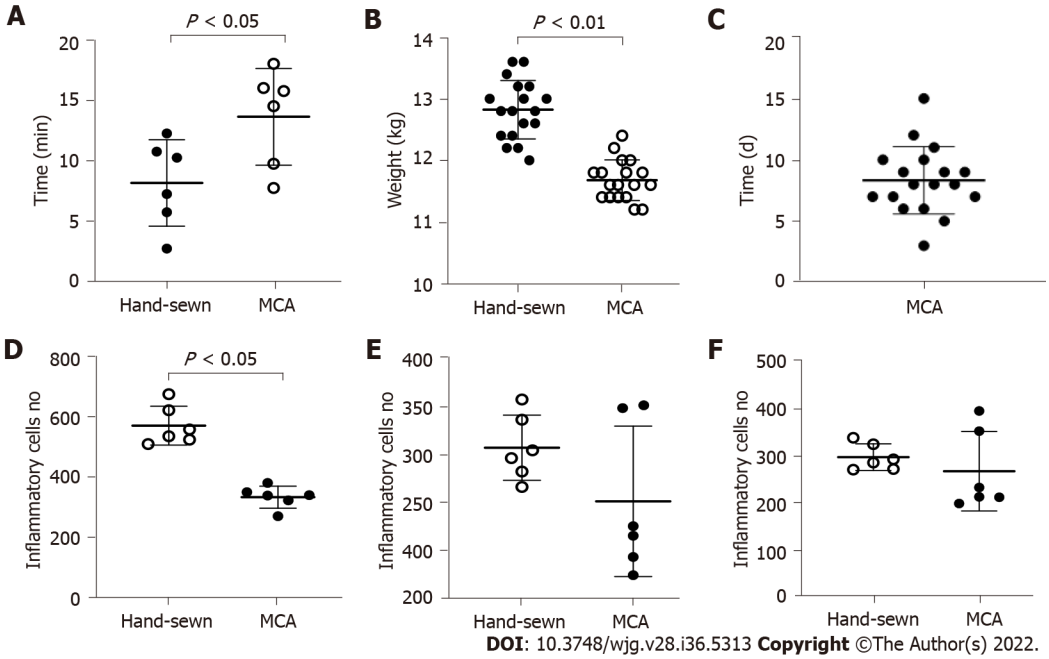

DOI: 10.3748/wjg.v28.i36.5313 **Copyright** ©The Author(s) 2022.

Figure 3 The analysis about anastomosis time, weight changes, the time of the magnetic device fell and the number of inflammatory cells between two groups. A: The anastomosis time of the magnetic compression anastomosis group and hand-sewn group. There were 18 dogs in each group; B: The dogs were weighed at 1 mo, and every group contained 6 dogs. There was a significant difference between the two groups; C: The time when the magnetic device had fallen into the stomach of 18 dogs; D-F: The number of inflammatory cells respectively at 1 mo, 3 mo and 6 mo. MCA: Magnetic compression anastomosis.

atively, every dog was kept in a cage. After the surgery, the dogs in the two groups were fasted for two days and then started on enteral nutrition. However, in the hand-sewn group, dogs generally showed poor appetite and even refused to eat. They started enteral nutrition at 4 d, 5 d, or even longer. During this period, we can only keep them alive with parenteral nutrition. The dogs in the MCA group started enteral nutrition earlier than those in the hand-sewn group. All dogs in both groups were given cefazolin sodium intramuscularly for 3 d postoperatively to prevent infection. Intramuscular injection (0.5 g) was administered twice a day. After a week, dogs were given enteral nutrition, a liquid diet, a semiliquid diet, and a normal diet according to their recovery. Six dogs were randomly selected in each group at 1 mo, 3 mo and 6 mo after the operation. They were weighed and intravenously injected with an overdose of anesthetic.

Specimen collection and histological analysis

All anastomosis segments with a sufficient length were harvested. The anastomotic stoma was found and severed 2 cm above and below the anastomosis. The gross information was observed, and all samples were immersed in 10% buffered formalin overnight. The samples were embedded in paraffin after fixation. Four-micrometer-thick sections were cut at the anastomosis site. Sections were stained with hematoxylin and eosin and Masson's trichrome dye. Then, we observed the changes in the tissue and cells under a light microscope.

Statistical analysis

Data were analyzed using GraphPad Prism v8 software (GraphPad, La Jolla, CA, United States). Quantitative data are expressed as the mean ± SD, and differences between the two groups were analyzed with the independent samples *t* test. The anastomosis time and weight data conformed to a normal distribution and homogeneity of variance. Statistical significance was set at $P < 0.05$.

RESULTS

Procedural parameters

Anastomosis was successfully created in all dogs. The anastomosis time of the MCA group was shorter than that of the hand-sewn group (7.5 ± 1.0 *vs* 12.5 ± 1.8, $P < 0.01$) (Figure 3A). X-ray examinations showed that the esophagi were all unobstructed and that the contrast agent could pass through the anastomosis in the MCA group. All dogs survived. There was one dog in the hand-sewn group and one dog in the MCA group with stenosis after the operation. These were found when we obtained

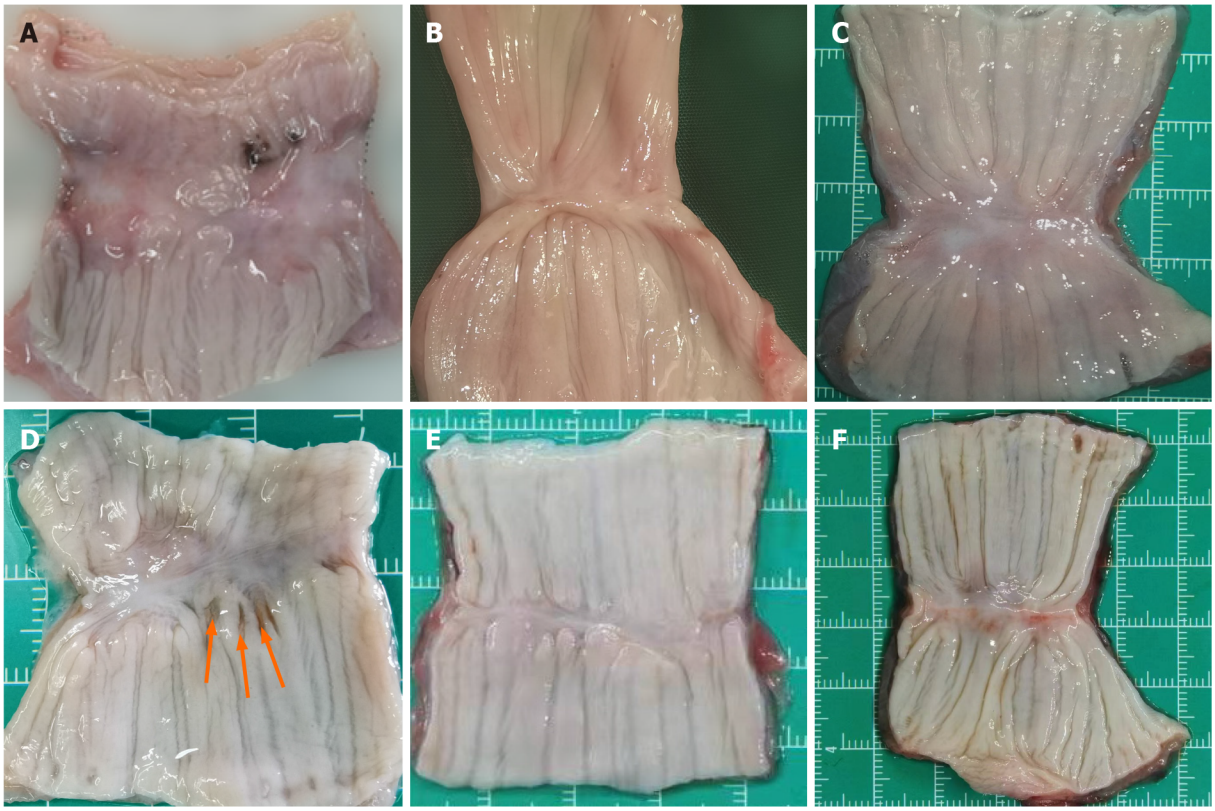

DOI: 10.3748/wjg.v28.i36.5313 **Copyright** ©The Author(s) 2022.

Figure 4 Gross appearance of the anastomosis in magnetic compression anastomosis and hand-sewn group. A: The tissue of magnetic compression anastomosis (MCA) group is thin at 1 mo, but the mucous membrane is intact; B: Anastomotic tissue of the MCA group at 3 mo; C: At 6 mo, the tissue becomes smooth and flat in the MCA group. There is little difference from normal tissue; D: The tissue of the hand-sewn anastomotic stoma is incomplete, and the mucous membrane has a small pinhole at 1 mo, which was caused by the suture needle. Red arrow indicates; E: Anastomotic tissue of the hand-sewn group at 3 mo; F: Anastomotic tissue of the hand-sewn group at 6 mo.

anastomotic stoma tissue. We observed one dog in the hand-sewn group who suddenly refused to eat, and the incision skin was red, swollen and purulent 8 d after the operation. We performed surgical exploration and performed a second esophageal reconstruction.

Expulsion time of the magnetic compression rings and weight changes

We observed how long the magnetic rings took to fall off into the stomach. The mean time was 8.3 ± 2.7 d (range 3-15 d) (Figure 3C). The weights of dogs in the MCA group (13.87 ± 0.63 kg) and the hand-sewn group (13.98 ± 0.80 kg) were similar at the beginning of the experiment. The difference in weight between the two groups was not statistically significant. However, the weights decreased more in the hand-sewn group than in the MCA group 1 mo after the operation. The mean weight of the MCA group was 12.73 ± 0.80 kg, while the mean weight of the hand-sewn group was 11.63 ± 0.71 kg, $P < 0.05$. At 3 mo and 6 mo after the operation, the dog weights were similar between the two groups (13.75 ± 0.84 kg *vs* 14.03 ± 0.82 kg, 14.93 ± 0.80 kg *vs* 15.44 ± 0.47 kg).

Gross appearance of the anastomosis

The esophagi grew well, and there were no ulcerations or fistulas. The mucosa layers were intact. However, the anastomotic stomas were slightly thinner than the peripheral tissue at 1 mo. We could see that the muscle layer tissues were not completely covered. In the hand-sewn anastomosis group, the suture plots were still visible 1 mo after the operation (Figure 4D). With the passage of time, the submucosa and muscle layers were gradually covered, and the anastomoses became increasingly smooth and flat. However, at 1 mo, 3 mo and 6 mo, the anastomoses of the MCA group were smoother than those of the hand-sewn group.

Histological appearance of the anastomosis

Light microscopy showed that the anastomotic mucosa of the MCA group had grown well during the first month after surgery, while the submucosal and muscular layers were still fractured (Figure 5A). Three months after the operation, the submucosal and muscular layers had completely covered the anastomoses, and the anastomotic tissue was similar to the normal esophageal tissue under light microscopy (Figure 5C). In the hand-sewn group, the mucosa was continuous one month after surgery,

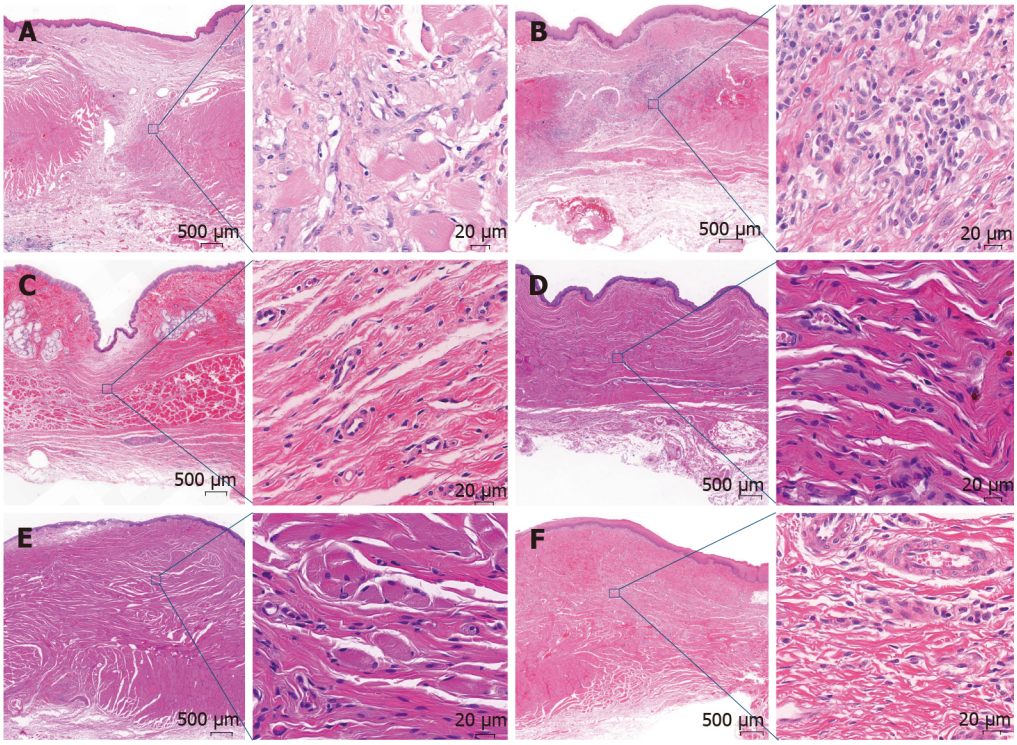

DOI: 10.3748/wjg.v28.i36.5313

Figure 5 Hematoxylin and eosin dye of the anastomotic tissue in magnetic compression anastomosis and hand-sewn group. Each image consists of two parts, one with a 2 × objective view and the other with a 40 × objective view. A: The anastomotic tissue of the magnetic compression anastomosis (MCA) group at 1 mo. The mucous membrane was intact, but the muscularis was separated; B: The anastomotic tissue of the hand-sewn group at 1 mo. There were more inflammatory cells in the tissue of the hand-sewn group than that of the MCA group; C: The anastomotic tissue of the MCA group at 3 mo. The muscularis became continuous; D: The anastomotic tissue of the hand-sewn group at 3 mo; E: The anastomotic tissue of the MCA group at 6 mo; F: The anastomotic tissue of the hand-sewn group at 6 mo.

but the submucosa and muscle layers were still broken, similar to the findings in the MCA group at one month (Figure 5B). At 3 mo postoperatively, the anastomotic site was covered by the submucosa and muscularis (Figure 5D). The number of inflammatory cells in the hand-sewn group was greater than that in the MCA group at 1 mo (Figures 5A and B). We counted the number of inflammatory cells in one high-power field (40 ×) in both groups (334 ± 37 *vs* 572 ± 65, $P < 0.01$). At 3 mo and 6 mo, the number of inflammatory cells was less than that at 1 mo. Between the two groups, the number of inflammatory cells was equal at 3 mo and 6 mo (Figures 5C-F). Masson staining showed that the number of collagen fibers in the hand-sewn group was greater than that in the MCA group. The blue fibers are collagen fibers (Figures 6A-F).

DISCUSSION

We studied the tissue status of the anastomotic esophagus after esophageal reconstruction by magnetic anastomosis technology and clarified the safety of MCA surgery. A comparative study was conducted between magnetic anastomosis and hand-sewn anastomosis for esophageal reconstruction to determine whether the effects of MCA were superior to those of the hand-sewn method.

By observing gross specimens and tissue sections at different time periods in the MCA and hand-sewn groups, we found that in both the MCA group and the hand-sewn anastomosis group, the anastomotic tissues were not completely healed at 1 mo after surgery. The mucosal surface of the two groups was smooth without ischemia or necrosis, while some submucosa and muscularis were still missing. After 3 mo, the anastomotic sites of the two groups had healed well, and the mucosal layer, submucosal layer and muscular layer were continuous. Liquid food is still the main diet in the early stage to reduce the stimulation of esophageal mucosa and prevent the occurrence of ulcers. Based on the results of the experiment, we suggest that MCA patients should consume a liquid diet or a semiliquid diet for at least one month.

The tissue healing of the MCA group was faster and better than that of the hand-sewn group. Six months after the operation, the specimens of the MCA group were smoother than those in the hand-sewn group, and a slight amount of scar tissue was observed in the hand-sewn group. There are several reasons for this. Magnetic anastomosis technology applies the mutual attraction between magnetic rings

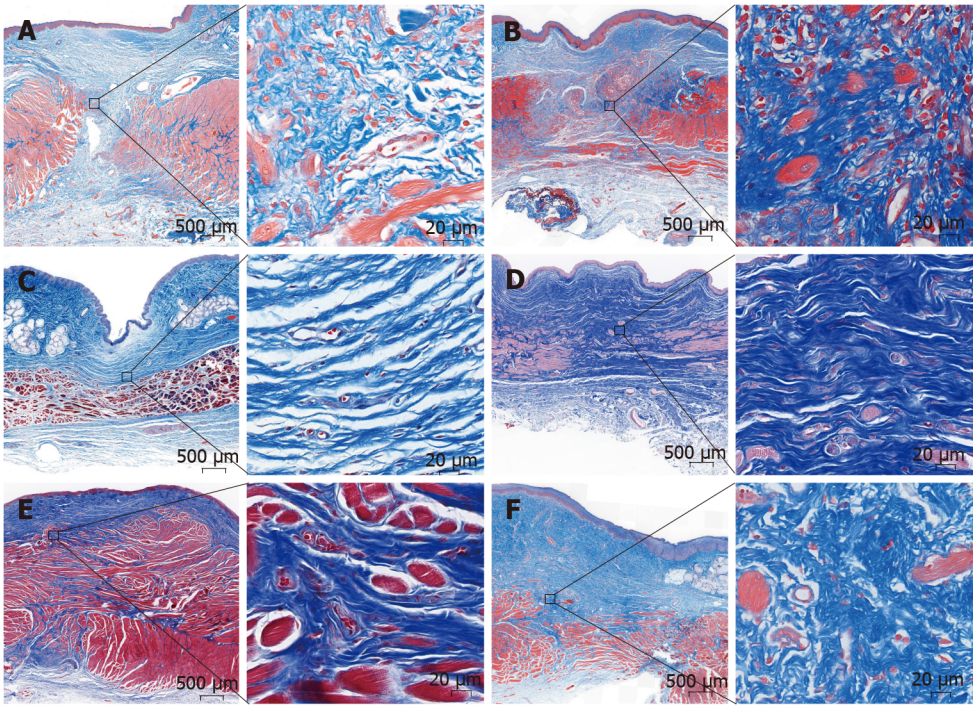

DOI: 10.3748/wjg.v28.i36.5313

Figure 6 Masson Thrichrome dye staining of the anastomotic tissue in magnetic compression anastomosis and hand-sewn group. Each image consists of two parts, one with a 2 × objective view and the other with a 40 × objective view. A: The anastomotic tissue of the magnetic compression anastomosis (MCA) group at 1 mo. The mucous membrane was intact, but the muscularis was separated at 1 mo, and the appearance was similar to that of hematoxylin and eosin staining; B: The anastomotic tissue of the hand-sewn group at 1 mo. There were more collagenous fibers than that in MCA group; C: The anastomotic tissue of the MCA group at 3 mo. The muscularis became continuous; D: The anastomotic tissue of the hand-sewn group at 3 mo; E: The anastomotic tissue of the MCA group at 6 mo; F: The anastomotic tissue of the hand-sewn group at 6 mo.

to maintain a constant and balanced pressure on the tissues at the anastomosis, resulting in slow ischemic necrosis of the tissues between the magnetic rings and the growth and healing of the surrounding tissues. This is a slow process that allows time for esophageal compensation to grow. Hand-sewn sutures use Vicryl to quickly tighten the tissues at both ends of the esophagus. There is a certain tension at both ends of the esophagus, which may lead to shearing forces placed on the esophageal tissue from Vicryl. Second, Vicryl, as an absorbable thread, will exist in the tissue for a long time as a foreign body, which may cause infection and scar hyperplasia. The suture material could play an important role in the healing of esophageal anastomosis. Vicryl is an absorbable material, but the time of absorption is more than 1 mo. During this period, Vicryl may act as a foreign body, leading to foreign body granuloma or anastomosis edema. Braided sutures are more prone to infection than monofilament sutures. Vicryl is the braided suture and perhaps in this study Vicryl is not the best selection.

At six months postoperatively, the magnetic anastomosis group grew slightly better than the hand-sewn group. Before surgery, the weights of the dogs in both groups were the same. One month after surgery, the body weight of the hand-sewn group was significantly lower than that of the magnetic anastomosis group. Three months after surgery, the weights of the dogs were similar in both groups. This suggests that MCA may contribute to enhanced recovery after esophageal reconstruction. There are two reasons that may contribute to the enhanced recovery with MCA technology: (1) The magnetic device has a gap in the middle, through which the liquid can enter the stomach, while it will not contact the anastomotic tissue. It may relieve pain and reduce the incidence of infection; and (2) The shedding time of the magnetic device is shorter than the time of the suture being discharged or absorbed by the tissues. The absorbable time of Vicryl RapideR is approximately 40 d[24], while the magnetic device discharge time is approximately 8 d. We observed that the dogs in the MCA group could feed earlier than those in the hand-sewn group. The MCA group of dogs recovered faster and better than the dogs in the hand-sewn group.

During 6 mo of observation, there was 1 stenosis in the MCA group and 1 stenosis and 1 Leakage in the hand-sewn group. Because the sample size was small, there was no statistically significant difference between the two groups. The rate of stenosis and leakage of anastomosis using the traditional hand-sewn operation is high. This has seriously affected the postoperative growth of children. We hope that this novel MCA technology can improve EA. The complication rate needs to be verified by more animal experiments and clinical case reports.

One clinical report showed that anastomosis was achieved in an average of 6 d (range 3 to 7 d) in 5 patients (age 6 mo to 5.9 years) with severe recurrent postsurgical esophageal stenosis refractory to dilatation[25]. Another MCA was achieved on day 36[26]. Clinical reports have shown that the anastomosis time ranges from 3 d to 36 d[26-28]. It involves many factors, such as the age of the child, type of EA, size of the magnetic ring and field strength of the magnetic device. This will be our next experimental purpose. Based on a large amount of experimental and clinical data, a model was established to estimate various parameters of magnetic devices preoperatively.

There are also some limitations of the study. First, our surgery location was on the dog's neck, not in the thoracic cavity. This is not consistent with the clinicopathology. The position of EA is generally flush with the bifurcation of the main bronchus and may have a tracheoesophageal fistula. Second, in this study, we did not consider the effect of different structural sutures on the anastomosis. Does monofilament have less effect on anastomotic healing than multifilament? Third, this is a model of esophageal anastomosis, and not of anastomosis in the setting of an atresia, there are several differences.

CONCLUSION

MCA is an effective and safe method for esophageal reconstruction in dogs. The anastomosis with MCA is faster than the hand-sewn anastomosis. Postoperatively, some aspects of the recovery of the MCA group were faster and better than those of the hand-sewn group. We provide some information useful for the future clinical application of the device in selected cases.

ARTICLE HIGHLIGHTS

Research background

Magnetic compression anastomosis (MCA) is a novel suture-free reconstruction of the digestive tract. It has been used in gastrointestinal anastomosis, jejunal anastomosis, cholangioenteric anastomosis and so on. The traditional operative outcomes of congenital esophageal atresia and benign esophageal stricture are poor, and there are too many complications postoperatively.

Research motivation

There are several case reports of using MCA to treat esophageal stenosis. However, systematic animal experimental studies are scarce. This has restricted further clinical application of MCA.

Research objectives

This study was conducted to demonstrate the feasibility and safety of MCA for esophageal reconstruction and studied the difference between MCA and hand-sewn esophageal reconstruction.

Research methods

Thirty-six dogs were randomized into either the study or control group (n = 18 per group). The dogs in the study group were subjected to end-to-end esophageal anastomosis with the magnetic compression device, while those in the control group underwent hand-sewn anastomosis with 4-0 absorbable multifilament Vicryl. We used interrupted single-layer sutures. The anastomosis time, gross appearance, weight and pathology of the anastomosis were evaluated at one month, three months and six months postoperatively.

Research results

The anastomosis time of the MCA group was shorter than that of the hand-sewn group (7.5 ± 1.0 min *vs* 12.5 ± 1.8 min, $P < 0.01$). One month after the surgeries, the mean weight of the dogs in the hand-sewn group had decreased more than that of the dogs in the MCA group (11.63 ± 0.71 kg *vs* 12.73 ± 0.80 kg, $P < 0.05$). At 3 mo and 6 mo after the operation, the dogs' weights were similar between the two groups (13.75 ± 0.84 kg *vs* 14.03 ± 0.82 kg, 14.93 ± 0.80 kg *vs* 15.44 ± 0.47 kg). Under an optical microscope, the number of inflammatory cells in MCA group was lower than that in hand-sewn group on 1 mo after operation.

Research conclusions

MCA is an effective and safe method for esophageal reconstruction. The anastomosis time of the MCA was less than that of the hand-sewn group. This study shows that MCA technology may be applied to human esophageal reconstruction, provided these favorable results are confirmed by more publications.

Research perspectives

MCA for esophageal reconstruction in the thoracic cavity needs to be tested, and further clinical trials

are needed to test its safety and guide its clinical application.

ACKNOWLEDGEMENTS

The authors would like to acknowledge the Laboratory Animal Center of Xi'an Jiaotong University for skillful technical assistance.

FOOTNOTES

Author contributions: Xu XH, Liu SQ, Lv Y designed and coordinated the study; Xu XH, Liu SQ, Cui XH and Suo RY performed the experiments and acquired and analyzed the data; XH Xu and Lv Y wrote the manuscript; and all authors approved the final version of the article.

Supported by the National Natural Science Foundation of China, No. 82170676; and Natural Science Foundation of Shaanxi Provincial Key Industries Innovation Chain (Cluster)-Social Development Project, No. 2020ZDLSF02-03.

Institutional animal care and use committee statement: All experimental protocols were approved by the Committee on the Ethics of Animal Experiments of Xi'an Jiaotong University (Permit Number: XJTULAC2020-1441).

Conflict-of-interest statement: All the authors report no relevant conflicts of interest for this article.

Data sharing statement: No additional data are available.

ARRIVE guidelines statement: The authors read the ARRIVE guidelines, and the manuscript was prepared and revised according to the ARRIVE guidelines.

Country/Territory of origin: China

ORCID number: Xiang-Hua Xu 0000-0001-6144-3938; Yi Lv 0000-0003-3636-6664; Shi-Qi Liu 0000-0002-2274-7880; Xiao-Hai Cui 0000-0002-7856-7117; Rui-Yang Suo 0000-0003-3622-958X.

S-Editor: Wang JJ
L-Editor: A
P-Editor: Wang JJ

REFERENCES

1 **Comella A**, Tan Tanny SP, Hutson JM, Omari TI, Teague WJ, Nataraja RM, King SK. Esophageal morbidity in patients following repair of esophageal atresia: A systematic review. *J Pediatr Surg* 2021; **56**: 1555-1563 [PMID: 33051081 DOI: 10.1016/j.jpedsurg.2020.09.010]
2 **Nassar N**, Leoncini E, Amar E, Arteaga-Vázquez J, Bakker MK, Bower C, Canfield MA, Castilla EE, Cocchi G, Correa A, Csáky-Szunyogh M, Feldkamp ML, Khoshnood B, Landau D, Lelong N, López-Camelo JS, Lowry RB, McDonnell R, Merlob P, Métneki J, Morgan M, Mutchinick OM, Palmer MN, Rissmann A, Siffel C, Sipek A, Szabova E, Tucker D, Mastroiacovo P. Prevalence of esophageal atresia among 18 international birth defects surveillance programs. *Birth Defects Res A Clin Mol Teratol* 2012; **94**: 893-899 [PMID: 22945024 DOI: 10.1002/bdra.23067]
3 **Oddsberg J**, Lu Y, Lagergren J. Aspects of esophageal atresia in a population-based setting: incidence, mortality, and cancer risk. *Pediatr Surg Int* 2012; **28**: 249-257 [PMID: 22020495 DOI: 10.1007/s00383-011-3014-1]
4 **Pedersen RN**, Calzolari E, Husby S, Garne E; EUROCAT Working group. Oesophageal atresia: prevalence, prenatal diagnosis and associated anomalies in 23 European regions. *Arch Dis Child* 2012; **97**: 227-232 [PMID: 22247246 DOI: 10.1136/archdischild-2011-300597]
5 **Smith N**. Oesophageal atresia and tracheo-oesophageal fistula. *Early Hum Dev* 2014; **90**: 947-950 [PMID: 25448787 DOI: 10.1016/j.earlhumdev.2014.09.012]
6 **Pinheiro PF**, Simões e Silva AC, Pereira RM. Current knowledge on esophageal atresia. *World J Gastroenterol* 2012; **18**: 3662-3672 [PMID: 22851858 DOI: 10.3748/wjg.v18.i28.3662]
7 **van Lennep M**, Singendonk MMJ, Dall'Oglio L, Gottrand F, Krishnan U, Terheggen-Lagro SWJ, Omari TI, Benninga MA, van Wijk MP. Oesophageal atresia. *Nat Rev Dis Primers* 2019; **5**: 26 [PMID: 31000707 DOI: 10.1038/s41572-019-0077-0]

8 **Schmedding A**, Wittekindt B, Schloesser R, Hutter M, Rolle U. Outcome of esophageal atresia in Germany. *Dis Esophagus* 2021; **34** [PMID: 32995846 DOI: 10.1093/dote/doaa093]

9 **Kanshin NN**, Permiakov NK, Dzhalagoniia RA, Nikulin BI, Kuznetsov AA. [Sutureless anastomoses in gastrointestinal surgery with and without steady magnetic field (experimental study)]. *Arkh Patol* 1978; **40**: 56-61 [PMID: 365148]

10 **Kamada T**, Ohdaira H, Takeuchi H, Takahashi J, Ito E, Suzuki N, Narihiro S, Yoshida M, Yamanouchi E, Suzuki Y. New Technique for Magnetic Compression Anastomosis Without Incision for Gastrointestinal Obstruction. *J Am Coll Surg* 2021; **232**: 170-177.e2 [PMID: 33190786 DOI: 10.1016/j.jamcollsurg.2020.10.012]

11 **Marrache MK**, Itani MI, Farha J, Fayad L, Sharara SL, Kalloo AN, Khashab MA, Kumbhari V. Endoscopic gastrointestinal anastomosis: a review of established techniques. *Gastrointest Endosc* 2021; **93**: 34-46 [PMID: 32593687 DOI: 10.1016/j.gie.2020.06.057]

12 **Graves CE**, Co C, Hsi RS, Kwiat D, Imamura-Ching J, Harrison MR, Stoller ML. Magnetic Compression Anastomosis (Magnamosis): First-In-Human Trial. *J Am Coll Surg* 2017; **225**: 676-681.e1 [PMID: 28843832 DOI: 10.1016/j.jamcollsurg.2017.07.1062]

13 **Machytka E**, Bužga M, Zonca P, Lautz DB, Ryou M, Simonson DC, Thompson CC. Partial jejunal diversion using an incisionless magnetic anastomosis system: 1-year interim results in patients with obesity and diabetes. *Gastrointest Endosc* 2017; **86**: 904-912 [PMID: 28716404 DOI: 10.1016/j.gie.2017.07.009]

14 **Liu XM**, Li Y, Xiang JX, Ma F, Lu Q, Guo YG, Yan XP, Wang B, Zhang XF, Lv Y. Magnetic compression anastomosis for biliojejunostomy and pancreaticojejunostomy in Whipple's procedure: An initial clinical study. *J Gastroenterol Hepatol* 2019; **34**: 589-594 [PMID: 30278106 DOI: 10.1111/jgh.14500]

15 **Liu XM**, Yan XP, Zhang HK, Ma F, Guo YG, Fan C, Wang SP, Shi AH, Wang B, Wang HH, Li JH, Zhang XG, Wu R, Zhang XF, Lv Y. Magnetic Anastomosis for Biliojejunostomy: First Prospective Clinical Trial. *World J Surg* 2018; **42**: 4039-4045 [PMID: 29947988 DOI: 10.1007/s00268-018-4710-y]

16 **Itoi T**, Kasuya K, Sofuni A, Itokawa F, Tsuchiya T, Kurihara T, Ikeuchi N, Takeuchi M, Nagano T, Iwamoto H, Yamanouchi E, Shimazu M, Tsuchida A. Magnetic compression anastomosis for biliary obstruction: review and experience at Tokyo Medical University Hospital. *J Hepatobiliary Pancreat Sci* 2011; **18**: 357-365 [PMID: 21127913 DOI: 10.1007/s00534-010-0350-9]

17 **Muensterer OJ**, Evans LL, Sterlin A, Sahlabadi M, Aribindi V, Lindner A, König T, Harrison MR. Novel Device for Endoluminal Esophageal Atresia Repair: First-in-Human Experience. *Pediatrics* 2021; **148** [PMID: 34615695 DOI: 10.1542/peds.2020-049627]

18 **Liu S**, Fang Y, Lv Y, Zhao J, Luo R, Cheng J, Yang H, Zhang A, Shen Y, Jiang N. Magnetic compression stricturoplasty in patients with severe stricture after simultaneous esophageal atresia and duodenal obstruction repair: A case report. *Exp Ther Med* 2022; **23**: 93 [PMID: 34976135 DOI: 10.3892/etm.2021.11016]

19 **Dorman RM**, Vali K, Harmon CM, Zaritzky M, Bass KD. Repair of esophageal atresia with proximal fistula using endoscopic magnetic compression anastomosis (magnamosis) after staged lengthening. *Pediatr Surg Int* 2016; **32**: 525-528 [PMID: 27012861 DOI: 10.1007/s00383-016-3889-y]

20 **Xue F**, Guo HC, Li JP, Lu JW, Wang HH, Ma F, Liu YX, Lv Y. Choledochojejunostomy with an innovative magnetic compressive anastomosis: How to determine optimal pressure? *World J Gastroenterol* 2016; **22**: 2326-2335 [PMID: 26900294 DOI: 10.3748/wjg.v22.i7.2326]

21 **She ZF**, Yan XP, Ma F, Wang HH, Yang H, Shi AH, Wang L, Qi X, Xiao B, Zou YL, Lv Y. Treatment of rectovaginal fistula by magnetic compression. *Int Urogynecol J* 2017; **28**: 241-247 [PMID: 27530520 DOI: 10.1007/s00192-016-3097-2]

22 **Li Y**, Liu XM, Zhang HK, Zhang XF, Tang B, Ma F, Lv Y. Magnetic Compression Anastomosis in Laparoscopic Pancreatoduodenectomy: A Preliminary Study. *J Surg Res* 2021; **258**: 162-169 [PMID: 33011447 DOI: 10.1016/j.jss.2020.08.044]

23 **Liu K**, Yang H, Huang G, Shi A, Lu Q, Wang S, Qiao W, Wang H, Ke M, Ding H, Li T, Zhang Y, Yu J, Ren B, Wang R, Wang K, Feng H, Suo Z, Tang J, Lv Y. Adhesive anastomosis for organ transplantation. *Bioact Mater* 2022; **13**: 260-268 [PMID: 35224307 DOI: 10.1016/j.bioactmat.2021.11.003]

24 **Al-Qattan MM**. Vicryl Rapide versus Vicryl suture in skin closure of the hand in children: a randomized prospective study. *J Hand Surg Br* 2005; **30**: 90-91 [PMID: 15620501 DOI: 10.1016/j.jhsb.2004.08.005]

25 **Zaritzky M**, Ben R, Johnston K. Magnetic gastrointestinal anastomosis in pediatric patients. *J Pediatr Surg* 2014; **49**: 1131-1137 [PMID: 24952802 DOI: 10.1016/j.jpedsurg.2013.11.002]

26 **Liu SQ**, Lv Y, Fang Y, Luo RX, Zhao JR, Luo RG, Li YM, Zhang J, Zhang PF, Guo JZ, Li QH, Han MX. Magnetic compression for anastomosis in treating an infant born with long-gap oesophageal atresia: A case report. *Medicine (Baltimore)* 2020; **99**: e22472 [PMID: 33080683 DOI: 10.1097/MD.0000000000022472]

27 **Slater BJ**, Borobia P, Lovvorn HN, Raees MA, Bass KD, Almond S, Hoover JD, Kumar T, Zaritzky M. Use of Magnets as a Minimally Invasive Approach for Anastomosis in Esophageal Atresia: Long-Term Outcomes. *J Laparoendosc Adv Surg Tech A* 2019; **29**: 1202-1206 [PMID: 31524560 DOI: 10.1089/lap.2019.0199]

28 **Woo R**, Wong CM, Trimble Z, Puapong D, Koehler S, Miller S, Johnson S. Magnetic Compression Stricturoplasty For Treatment of Refractory Esophageal Strictures in Children: Technique and Lessons Learned. *Surg Innov* 2017; **24**: 432-439 [PMID: 28745145 DOI: 10.1177/1553350617720994]

World Journal of Gastroenterology

Submit a Manuscript: https://www.f6publishing.com

World J Gastroenterol 2022 September 28; 28(36): 5324-5337

DOI: 10.3748/wjg.v28.i36.5324

ISSN 1007-9327 (print) ISSN 2219-2840 (online)

ORIGINAL ARTICLE

Retrospective Cohort Study

Impact of sarcopenia on tumor response and survival outcomes in patients with hepatocellular carcinoma treated by trans-arterial (chemo)-embolization

Gael Roth, Yann Teyssier, Maxime Benhamou, Mélodie Abousalihac, Stefano Caruso, Christian Sengel, Olivier Seror, Julien Ghelfi, Arnaud Seigneurin, Nathalie Ganne-Carrie, Elia Gigante, Lorraine Blaise, Olivier Sutter, Thomas Decaens, Jean-Charles Nault

Specialty type: Gastroenterology and hepatology

Provenance and peer review: Unsolicited article; Externally peer reviewed.

Peer-review model: Single blind

Peer-review report's scientific quality classification

Grade A (Excellent): 0
Grade B (Very good): 0
Grade C (Good): C, C, C
Grade D (Fair): 0
Grade E (Poor): 0

P-Reviewer: Posa A, Italy; Xi D, China; Zhao G, China

Received: May 2, 2022
Peer-review started: May 2, 2022
First decision: June 19, 2022
Revised: June 22, 2022
Accepted: August 30, 2022
Article in press: August 30, 2022
Published online: September 28, 2022

Gael Roth, Yann Teyssier, Julien Ghelfi, Arnaud Seigneurin, Thomas Decaens, Univ. Grenoble-Alpes, Grenoble 38058, France

Gael Roth, Mélodie Abousalihac, Thomas Decaens, Department of Hepatology, Gastroenterology and Digestive Oncology, CHU Grenoble Alpes, Grenoble 38043, France

Gael Roth, Julien Ghelfi, Thomas Decaens, Institute for Advanced Biosciences, INSERM U1209/CNRS UMR 5309, Grenoble 38043, France

Yann Teyssier, Christian Sengel, Julien Ghelfi, Department of Radiology, CHU Grenoble Alpes, Grenoble 38043, France

Maxime Benhamou, Olivier Seror, Olivier Sutter, Department of Radiology, CHU Avicenne-APHP, Bobigny 93000, France

Stefano Caruso, Olivier Seror, Nathalie Ganne-Carrie, Jean-Charles Nault, Functional Genomics of Solid Tumors Laboratory, Centre de Recherche des Cordeliers-INSERM UMR 1138, Inserm, Université Paris, Paris 75006, France

Olivier Seror, Nathalie Ganne-Carrie, Jean-Charles Nault, Unité de Formation et de Recherche Santé Médecine et Biologie Humaine, Université Paris Nord, Paris 93430, France

Arnaud Seigneurin, Service d'Epidémiologie et Evaluation Médicale, CHU Grenoble Alpes, Grenoble 38043, France

Nathalie Ganne-Carrie, Elia Gigante, Lorraine Blaise, Jean-Charles Nault, Department of Hepatology, CHU Avicenne-APHP, Bobigny 93000, France

Corresponding author: Jean-Charles Nault, MD, PhD, Full Professor, Department of Hepatology, CHU Avicenne-APHP, 125 Rue de Stalingrad, Bobigny 93000, France.
naultjc@gmail.com

Abstract

BACKGROUND

At the diagnosis of hepatocellular carcinoma (HCC), more than 90% of HCC patients present cirrhosis, a clinical condition often associated to malnutrition. Sarcopenia is an indirect marker of malnutrition assessable on computed tomography (CT).

AIM

To evaluate the prognostic value of sarcopenia in patients with HCC treated by trans-arterial (chemo)-embolization.

METHODS

Patients with HCC treated by a first session of trans-arterial (chemo)embolization and an available CT scan before treatment were included. Sarcopenia was assessed using skeletal muscle index at baseline and at the first radiological assessment. Radiological response was recorded after the first session of treatment using mRECIST.

RESULTS

Of 225 patients treated by trans-arterial bland embolization (n = 71) or trans-arterial chemoembolization (n = 154) for HCC between 2007 and 2013, Barcelona Clinic of Liver Cancer stage was A, B, and C in 27.5%, 55%, and 16.8% of cases, respectively. Sarcopenia was present in 57.7% of the patients. Patients with sarcopenia presented a higher rate of progressive disease (19% *vs* 8%, P = 0.0236), a shorter progression-free survival (8.3 *vs* 13.2 mo, P = 0.0035), and a shorter median overall survival (19.4 mo *vs* 35.5 mo, P = 0.0149) compared with non-sarcopenic patients. Finally, patients whose sarcopenia appeared after first transarterial treatment had the worst prognosis (P = 0.0004).

CONCLUSION

Sarcopenia is associated with tumor progression and poor survival outcomes after trans-arterial (chemo)-embolization for HCC.

Key Words: Hepatocellular carcinoma; Transarterial chemoembolization; Bland embolization; Sarcopenia; Skeletal muscle index

Core Tip: This work evaluated the predictive value of sarcopenia for tumor response and survival outcomes in hepatocellular carcinoma patients treated by transarterial chemoembolization or transarterial embolization. In this study, sarcopenia at imaging was observed in 57.7% of patients. It was associated with a higher rate of progressive disease and a decreased overall survival after adjustment with usual risk factors of death. Sarcopenia is an easy-to-assess radiological biomarker of poor prognosis that should be measured in order to assess prognosis and test a targeted intervention mixing nutritional support and physical activity.

Citation: Roth G, Teyssier Y, Benhamou M, Abousalihac M, Caruso S, Sengel C, Seror O, Ghelfi J, Seigneurin A, Ganne-Carrie N, Gigante E, Blaise L, Sutter O, Decaens T, Nault JC. Impact of sarcopenia on tumor response and survival outcomes in patients with hepatocellular carcinoma treated by trans-arterial (chemo)-embolization. *World J Gastroenterol* 2022; 28(36): 5324-5337

URL: https://www.wjgnet.com/1007-9327/full/v28/i36/5324.htm

DOI: https://dx.doi.org/10.3748/wjg.v28.i36.5324

INTRODUCTION

Liver cancer is the second cause of cancer-related deaths worldwide[1], mostly represented by hepatocellular carcinoma (HCC). At the diagnosis, 70% of HCC patients have only access to palliative treatments, and among intermediate HCC, classified as Barcelona Clinic of Liver Cancer (BCLC)-B[2], transarterial chemoembolization (TACE) and transarterial embolization (TAE) are the best therapeutic options to offer[3-5]. Nonetheless, despite a good level of tumor response, around 50%-55% of patients receiving these treatments suffer from a high level of relapse[6]. It is well demonstrated that TACE presents the best results on patients with a good general status and a low level of liver insufficiency[7], but additional reliable predictive markers are needed to better define which patients will take full benefit of this procedure, and which ones present an increased risk of low efficacy and liver deterioration. At the diagnosis, more than 90% of HCC patients present with cirrhosis, a clinical condition

often associated to malnutrition with sarcopenia. Indeed, sarcopenia, defined as the "progressive loss of muscle mass and strength with a risk of adverse outcomes such as disability, poor quality of life, and death"[8], is a consequence of chronic inflammation, hypercatabolism, and anorexia found in cirrhosis and advanced tumor stages. Sarcopenia has already been described as a poor prognostic factor in HCC patients undergoing surgical resection or treated by systemic therapies[9-12]. Further studies are needed to clarify the predictive value of sarcopenia in other HCC treatment settings, such as TAE or TACE. Indeed, several studies with small numbers of patients showed interesting results on the predictive value of sarcopenia regarding survival outcomes of patients treated by TACE but without clear impact on tumor response[13]. This study aimed to evaluate the predictive value of sarcopenia for tumor response and survival outcomes in a bicentric cohort of HCC patients treated by TACE or TAE.

MATERIALS AND METHODS

Patient selection

Patients were retrospectively included from December 1, 2007 to November 1, 2013 in Jean Verdier Hospital and from June 1, 2011 to December 1, 2014 in Grenoble-Alpes University Hospital. The inclusion criteria were as follow: Age > 18 years, HCC diagnosed by histology or non-invasive criteria [7], first treatment using TAE or TACE, and available pre- and post-therapeutic computed tomography (CT) scan. Transarterial procedures performed for acute bleeding of HCC were excluded.

Transarterial procedures

Patients were treated with transarterial therapy following standard local protocol[14]. Each indication of TACE or TAE was validated during multidisciplinary tumor board including a hepatologist, an interventional radiologist, and a liver surgeon. In case of TACE, chemotherapy was either doxorubicin or idarubicin according to institutional standards of care, as previously described[15]. The choice of chemotherapy was left to the investigator's discretion. Every TACE or TAE was performed by an expert interventional radiologist.

As recommended by European guidelines, TACE could be repeated 2 mo after the first treatment in case of partial response on postoperative scan and preserved liver function after rediscussion in multidisciplinary tumor board[7].

Ethical approval

Written consent was obtained for every patient before transarterial procedures and the study protocol respects the ethical guidelines of the 1975 Declaration of Helsinki (6th revision, 2008). Study ethics was also approved by the independent French ethic committee CERIM (*Comité d'éthique de la recherche en imagerie médicale;* No. CRM-2004-084).

Clinical and paraclinical data collection

Clinical and biological data were recorded before the treatment: Demographic data, body mass index, liver function, platelets, presence of cirrhosis, etiology of the underlying liver disease, alpha-fetoprotein (AFP) level, tumor size, number of nodules, tumor portal invasion, and esophageal varices at the last upper endoscopy.

After the first treatment, all patients were prospectively followed until death or the last recorded visit until June 30, 2018.

Anthropometric measurements

Anthropometric measurements were assessed on the pre-therapeutic CT scan and the first follow-up CT scan realized 1-3 mo after the transarterial treatment by two radiologists (OSu and YT) using the software Image J®. Skeletal muscle and psoas muscle area were measured on a cross-sectional CT image at the level of the 3rd lumbar vertebra. Skeletal muscle index (SMI) was calculated using the total muscle area on the L3 CT slice divided by squared height as previously described[16]. Sarcopenia was defined by SMI < 50 cm^2/m^2 in male and < 39 cm^2/m^2 in female patients as defined by the North American expert statement on sarcopenia in liver transplantation[17]. Psoas muscle index (PMI) defined as the psoas muscle area on height ratio was also assessed as previously described[17].

The following data were recorded on imaging: Liver volume, spleen volume, presence of ascites at imaging, presence of para-umbilical vein, presence of esophageal varices, and presence of splenomegaly defined by a spleen's cranio-caudal diameter superior to 12 cm.

Assessment of tumor response and survival outcomes

All imaging examinations were archived in a picture archiving and communication system and blindly read by two radiologists (OSu and YT). Clinical and paraclinical parameters were extracted from the patient's electronic medical records.

Radiological response was assessed by two radiologists (OSu and YT) comparing the baseline imaging and the imaging available 1-3 mo after the first session of trans-arterial treatment as recommended[7]. Radiological response was classified into complete response, partial response, stable disease, and progressive disease as defined by the modified RECIST criteria[7].

Progression-free survival was defined as the time between the date of the first treatment and the date of death, radiological progression, or the last recorded visit. Patients were censured at the date of liver transplantation. Overall survival (OS) was defined as the time between the date of the first treatment and the date of death or the last recorded visit, with censoring at the date of liver transplantation in transplanted patients.

Statistical analysis

Categorical variables were compared using the Fisher exact test for two groups and Chi squared test for three groups and more. Continuous variables were compared using the Mann-Whitney test. Logistic regression was used to compare the association with radiological response and baseline variables.

Survival outcomes as OS and progression free survival (PFS) were computed using the Kaplan-Meier method, and the Log-rank test was used to compare survival rates. The association between baseline variable and OS and PFS was assessed in univariate analysis using the Cox model. Variables with a P value < 0.05 in the univariate analysis were computed in multivariate analysis using the Cox model. Statistical analyses were performed using Graph Pad (PRISM) and R software.

RESULTS

Description of the population

A total of 225 patients were included in the analysis, including 93 from Jean Verdier Hospital and 132 from Grenoble-Alpes University Hospital (Figure 1). Patients were mainly male (88.8%) with a median age of 65 (58-75) years old. The underlying liver diseases were mainly related to chronic alcohol intake (61%), hepatitis C (28%), and non-alcoholic steatohepatitis (29%) with 81.6% of patients classified as Child-Pugh A.

HCCs were classified as BCLC-A in 27.5%, BCLC-B in 55.5%, and BCLC-C due to segmental portal vein thrombosis in 16.8% of patients. One hundred and fifty-four (68.4%) of the patients were treated by TACE (127 with doxorubicin and 27 with idarubicin; including 87 by lipiodol TACE and 40 by TACE using drug eluting beads). Seventy-one (31.5%) patients were treated by TAE using lipiodol with gelatin sponge. Patients' characteristics are detailed in Table 1.

Anthropometric and portal hypertension assessment at imaging

Anthropometric measurements including the value of total muscle area in L3 and psoas area in L3 are detailed in Table 1. Ascites was identified in 23.5% of the cases at imaging as well as splenomegaly in 57% of the cases, umbilical vein repermeabilization in 36.4%, and esophageal varices in 71.1%. About 57.7% (n = 130) of the patients had sarcopenia based on the SMI. The value of psoas area/squared height (cm^2/m^2) was significantly positively associated with body mass index (BMI), liver volume, albumin, alcohol intake, male, and non-alcoholic steatohepatitis (NASH), and negatively associated with age and hepatitis C virus (Figure 2A). Sarcopenia at imaging (defined by SMI < 50 cm^2/m^2 in male and < 39 cm^2/m^2 in female patients) was observed in 130 (57.7%) patients.

Sarcopenic patients were significantly older (67.5 years old *vs* 62.5 years old; P = 0.0338), with a lower BMI (24.3 *vs* 28.7 P < 0.0001) and a higher median serum AFP level (11.5 ng/mL *vs* 7.7 ng/mL; P = 0.0152) compared to non-sarcopenic patients at imaging (Table 1 and Figure 2B). Sarcopenia was also associated with a higher tumor burden (sum of the size of the 2 main tumors) and a lower BMI, ALAT level, and spleen volume, and was less frequent in alcohol-related cirrhosis and in NASH patients (Figure 2B). At the first radiological assessment, 28.7% of the patients with sarcopenia harbored an increase in Child-Pugh Class (A to B/C or B to C) compared to 24.53% of patients without sarcopenia (P = 0.6862, Fisher exact test). Patients' baseline features as well as treatments following TACE or TAE, according to the presence or not of sarcopenia, are detailed in Table 1.

Relationship between sarcopenia and radiological response

At the first radiological evaluation after TACE or TAE, 23% (n = 52) of patients harbored a complete response, 39% a partial response (n = 88), 23% a stable disease (n = 52), and 15% (n = 33) a progressive disease based on mRECIST criteria. Presence of portal hypertension signs on endoscopy or imaging was not encountered as predictive markers of radiological response. Presence of sarcopenia had a significant impact on progression proportions after TACE (P = 0.0084, Chi square test Figure 3A). Whereas objective tumor response (complete and partial radiological response) was not statistically different in sarcopenic (64%) compared to non-sarcopenic patients (67%, P = 0.66, Fisher exact test), a higher rate of progressive disease was observed in patients with sarcopenia compared to patients without (19% *vs* 8%, P = 0.0236, Fisher exact Test, Figure 3B). In univariate analysis, sarcopenia [odds ratio (OR): 2.59; 95%CI:

Table 1 Description of population features according to presence of sarcopenia or not

	Overall cohort (*n* = 225)	Sarcopenia (*n* = 130)	No sarcopenia (*n* = 95)	*P* value
Clinical and biological features				
Age (years old)[1]	65 (58-75)	67.5 (59.25-76)	62.5 (57-72.5)	0.0338
Gender[2]	200 (88.8%)	120 (92%)	80 (84%)	0.0841
Alcohol[2]	138 (61%)	72 (55%)	66 (69%)	0.04
NASH[2]	66 (29%)	28 (22%)	38 (40%)	0.003
HCV[2]	64 (28%)	42 (32%)	22 (23%)	0.14
HBV[2]	21 (9%)	11 (8%)	10 (11%)	0.65
Cirrhosis[2]	206 (91.5%)	116 (89.2%)	90 (94.7%)	0.1554
Platelets (10^3/mm^3)[1]	123 (83-180)	131 (83.5-198.3)	113 (82-169)	0.1561
Creatinine (μmol/L)	77 (64-89)	77 (64-90)	77 (65-89)	0.93
Total bilirubin (μmol/L)	16 (9.9-22)	15.8 (9-22)	16 (10-22)	0.55
Albumin (g/dL)	36 (32-39)	35 (32-38)	36 (32-40)	0.11
AFP (ng/mL)[1]	10 (4.3-49)	11.5 (5.135-76.5)	7.7 (4-25.5)	0.0152
Child-Pugh A[2]	184 (81.57%)	105 (80.7%)	79 (83.2%)	0.728
MELD	8.7 (7-11)	8.5 (7.6-10)	9.1 (7.3-11)	0.53
BCLC-A[2]	62 (27.5%)	33 (25.3%)	29 (30.5%)	0.1796
BCLC-B[2]	125 (55.5%)	70 (53.8%)	55 (57.89%)	
BCLC-C[2]	38 (16.8%)	27 (20.76%)	11 (11.57%)	
Segmental portal vein thrombosis[2]	34 (15.1%)	24 (18.46%)	10 (10.5%)	0.1314
Type of treatment				
TACE[2]	154 (68.4%)	86 (66.6%)	68 (71.5%)	0.4681
Bland embolization[2]	71 (31.5%)	43 (33.3%)	27 (28.4%)	0178
Number of procedures *per* patient[1]	2 (1-3)	2 (1-2)	2 (1-3)	0.0178
Body mass index[1]	26.4 (23.5-29.18)	24.3 (22.3-26.9)	28.7 (26.4-32.33)	< 0.0001
Oesophageal varices[2]	107 (49.3%)	61 (48.4%)	46 (50.5%)	0.784
Radiological features				
Size of the largest nodule (mm)[1]	37 (24-61)	40 (24-70)	34 (23-53)	0.0665
Multiples nodules[2]	169 (75.1%)	99 (76.1%)	70 (73.7%)	0.7552
Skeletal muscle index (cm^2/m^2)[1]	47.12 (41.75-53.2)	42.85 (38.61-46.79)	54.19 (51.38-58.27)	< 0.0001
Psoas muscle index (cm^2/m^2)[1]	10 (8.575-11.94)	9.205. (8.087-10.97)	11.51 (9.679-14.26)	< 0.0001
Psoas L3 (cm^2)[1]	17 (14.72-37.27)	15.95 (13.95-18.7)	19.8 (16.6-23.8)	< 0.0001
Muscle L3 (cm^2)[1]	137 (119.3-155.4)	125.8 (113.8-138.1)	156.2 (145-176)	< 0.0001
Umbilical vein repermeabilization[2]	82 (36.4%)	51 (39.2%)	31 (32.6%)	0.3292
Oesophageal varices[2]	160 (71.1%)	91 (70%)	69 (72%)	0.7661
Ascites[2]	53 (23.5%)	29 (22.3%)	24 (25.2%)	0.6355
Liver/spleen volume ratio[1]	4.346 (2.885-6.798)	4.562 (2.927-7.205)	3.797 (2.605-6.187)	0.1085
Liver volume (cm^3)[1]	1715 (1430-2071)	1701 (1407-1978)	1800 (1461-2142)	0.0833
Spleen volume (cm^3)[1]	414 (252-606)	382 (230.5-573.3)	480 (308-634)	0.0283
Splenomegaly[2]	129 (57.6%)	71 (55%)	58 (61%)	0.4127
Treatments following TAE/TACE				

Curative-intent			
Liver resection	2 (0.9%)	1 (0.8%)	1 (1.1%)
RFA/Microwaves/Alcoholization	27 (12.0%)	14 (10.8%)	13 (13.7%)
Liver transplantation	46 (20.4%)	19 (14.6%)	27 (28.4%)
Palliative-intent			
SIRT	2 (0.9%)	2 (1.5%)	0
Sorafenib	44 (19.6%)	28 (21.5%)	16 (16.8%)
Other systemic treatments	8 (3.6%)	4 (3.1%)	4 (4.2%)
No additional treatment	82 (36.4%)	50 (38.5%)	32 (33.7%)

[1]Median (25^{th}-75^{th} percentiles).
[2]Numbers (percentages).
AFP: Alpha-fetoprotein; BCLC: Barcelona clinic liver cancer staging system; HCV: Hepatitis C virus; HBV: Hepatitis B virus; NASH: Non-alcoholic steatohepatitis; RFA: Radiofrequency ablation; SIRT: Selective internal radiation therapy; TACE: Trans-arterial chemoembolization.

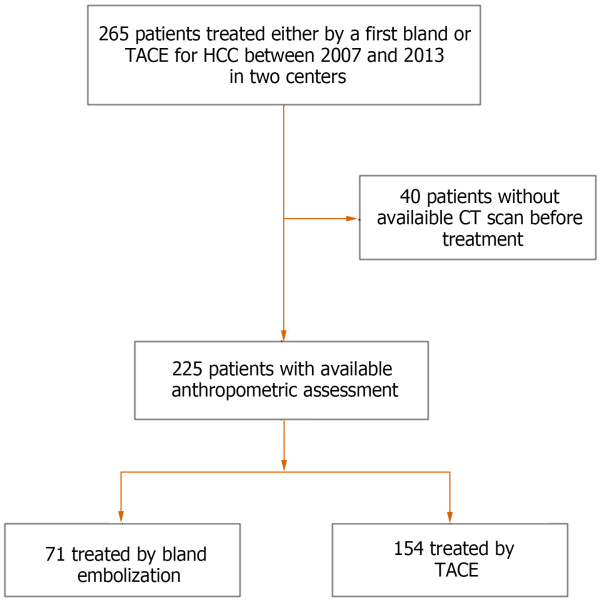

DOI: 10.3748/wjg.v28.i36.5324 **Copyright** ©The Author(s) 2022.

Figure 1 Flowchart of the study. TACE: Transarterial chemoembolization; CT: Computed tomography; HCC: Hepatocellular carcinoma.

1.16-6.40, P = 0.0274], serum AFP level (OR: 1.00029; 95%CI: 1.00008-1.0006, P = 0.0226), and BCLC-C stage (OR: 2.22; 95%CI: 1.25-4.05; P = 0.00758) were related to progressive disease at imaging. In multivariate analysis, only BCLC-C stage (OR: 1.98; 95%CI: 1.038-3.88, P = 0.0416) remained independently associated with a higher rate of progressive disease.

Relationship between sarcopenia before TACE and survival

The median progression-free survival was 9.4 mo. Patients with sarcopenia had a lower median PFS compared to patients without (8.3 mo *vs* 13.2 mo, P = 0.0035, log rank test, Figure 4A). In univariate analysis, sarcopenia, tumor portal vein thrombosis, size of the largest nodule, serum AFP level, and platelet level were significantly associated with a lower PFS (Table 2). In multivariate analysis, sarcopenia [hazard ratio (HR): 1.62; 95%CI: 1.15-2.28], tumor portal vein thrombosis (HR: 1.77; 95%CI: 1.11-2.83), size of the largest nodule (HR: 1.008; 95%CI: 1.002-1.013), and platelet level (HR: 1.002; 95%CI: 1.002; 95%CI: 1.0001-1.005) remained independently associated with a lower PFS (Table 2).

The median OS was 24.3 mo. OS was shorter in patients with sarcopenia compared to patients without (19.4 mo *vs* 35.5 mo, P = 0.0149, log rank test, Figure 4B). Sarcopenia, ascites at imaging, size of the largest nodule, serum AFP level, Child-Pugh score, and BMI were associated with OS at univariate analysis (Table 3). In multivariate analysis, sarcopenia (HR: 1.68; 95%CI: 1.04-2.72), AFP level (HR: 1.0001; 95%CI: 1.00001-1.002), and size of the largest nodule (HR: 1.007, 95%CI: 1.0015-1.013) were independently associated with a higher risk of death (Table 3).

Table 2 Univariate and multivariate Cox analyses of baseline variables associated with progression-free survival

Variable	Univariate analysis			Multivariate analysis		
	HR	95%CI	*P* value	HR	95%CI	*P* value
Sarcopenia (yes *vs* no, imaging)	1.58	1.17-2.15	0.003	1.62	1.15-2.28	0.006
Skeletal muscle index (imaging)[1]	0.91	0.98-1.01	0.306			
Psoas muscle index (imaging)[1]	0.97	0.92-1.02	0.18			
Paraombilical vein (imaging)	1.21	0.88-1.65	0.24			
Esophageal varices (imaging)	0.94	0.68-1.30	0.72			
Ascites (imaging)	1.38	0.97-1.97	0.07			
Liver/spleen ratio (imaging)[1]	1.02	0.98-1.07	0.21			
Liver volume (imaging)[1]	1.00	1.00-1.00	0.062			
Spleen volume (imaging)[1]	0.99	0.99-1.00	0.54			
Splenomegaly (imaging)	1.18	0.87-1.60	0.28			
BCLC stage	1.24	0.98-1.58	0.068			
Multiple nodules	1.03	0.73-1.45	0.88			
Portal vein thrombosis	1.58	1.05-2.39	0.03	1.77	1.11-2.83	0.02
Size of the largest nodule[1]	1.01	1.00-1.01	0.0003	1.008	1.002-1.013	0.006
Esophageal varices at endoscopy	0.98	0.72-1.33	0.88			
Serum AFP[1]	1.00	1.00-1.00	0.0007	1.0001	1.00001-1.00002	0.07
Platelets[1]	1.00	1.00-1.01	0.002	1.002	1.0001-1.005	0.04
Child Pugh B7	1.02	0.67-1.56	0.93			
Creatinin[1]	1.00	0.99-1.01	0.097			
Prothrombin time[1]	1.00	0.99-1.01	0.68			
Total bilirubin[1]	0.99	0.99-1.01	0.99			
Albumin[1]	0.99	0.97-1.03	0.84			
Clinical ascites	1.00	0.63-1.59	0.99			
Cirrhosis	0.87	0.53-1.45	0.60			
NASH	1.21	0.60-1.14	0.24			
HCV	0.85	0.61-1.18	0.32			
HBV	0.73	0.41-1.28	0.27			
Alcohol intake	1.013	0.75-1.37	0.93			
Body mass index[1]	0.98	0.95-1.01	0.21			
Gender (Male)	1.37	0.86-2.19	0.19			
Age (years old)[1]	1.00	0.99-1.02	0.68			

[1]Parameters expressed as continuous variables.
Sarcopenia was analyzed as a categoric factor (yes *vs* no). AFP: Alpha-fetoprotein; BCLC: Barcelona clinic liver cancer; HCV: Hepatitis C virus; HBV: Hepatitis B virus; NASH: Non alcoholic steatohepatitis.

Evolution of sarcopenia after TACE and its impact on OS

Post-TACE SMI was assessed by CT scan at the first radiological assessment in 218 patients in order to assess the evolution of sarcopenia after treatment. Among the patients without sarcopenia at baseline, 71 were still non-sarcopenic, and 22 became sarcopenic. Among the 22 patients who became sarcopenic, 19 had a progressive disease at the first radiological assessment.

Patients with post-TACE sarcopenia presented a shorter median OS (n = 147, 18.15 mo) compared with non-sarcopenic patients (n = 71, 35.7 mo, P = 0.0019) (Figure 4C).

Table 3 Univariate and multivariate Cox analyses of baseline variables associated with overall survival

Variable	Univariate analysis			Multivariate analysis		
	HR	95%CI	*P* value	HR	95%CI	*P* value
Sarcopenia (yes *vs* no, imaging)	1.57	1.09-2.27	0.016	1.68	1.04- 2.72	0.03
Skeletal muscle index (imaging)[1]	0.99	0.97-1.01	0.19			
Psoas muscle index (imaging)[1]	0.95	0.89-1.01	0.14			
Paraombilical vein (imaging)	1.16	0.80-1.66	0.43			
Esophageal varices (imaging)	1.09	0.75-1.61	0.63			
Ascites (imaging)	1.74	1.16-2.60	0.007	1.59	0.97-2.60	0.07
Liver/spleen ratio (imaging)[1]	1.03	0.98-1.08	0.13			
Liver volume (imaging)[1]	1.00	0.99-1.00	0.86			
Spleen volume (imaging)[1]	0.99	0.99-1.00	0.19			
Splenomegaly (imaging)	0.95	0.66-1.35	0.77			
BCLC stage	1.28	0.97-1.68	0.08			
Multiple nodule	0.83	0.56-1.22	0.34			
Portal vein thrombosis	1.52	0.98-2.38	0.06			
Size of the largest nodule[1]	1.01	1.00-1.01	0.003	1.007	1.0015-1.013	0.014
Esophageal varices (endoscopy)	1.17	0.82-1.69	0.38			
AFP[1]	1.00	1.00-1.00	0.00018	1.0001	1.00001-1.0002	0.006
Platelet[1]	1.00	0.99-1.00	0.170			
Child-Pugh B7	2.04	1.21-3.45	0.007	1.59	0.86-2.96	0.14
Creatinin[1]	1.00	0.99-1.00	0.18			
Prothrombin time[1]	1.01	0.98-1.01	0.45			
Total bilirubin[1]	1.02	1.00-1.03	0.035			
Albumin[1]	0.94	0.91-0.98	0.003			
Clinical ascites	1.46	0.88-2.42	0.143			
Cirrhosis	1.27	0.71-2.26	0.42			
NASH	0.70	0.47- 1.04	0.075			
HCV	1.32	0.89-1.95	0.17			
HBV	0.71	0.33-1.54	0.39			
Alcohol intake	1.05	0.67-1.37	0.80			
Age (years old)[1]	1.00	0.99-1.02	0.79			
BMI[1]	0.96	0.93-0.99	0.026	0.99	0.95-1.040	0.75
Gender (Male)	1.08	0.63-1.85	0.79			

[1]Parameters expressed as continuous variables.
Sarcopenia was analyzed as a categoric factor (yes *vs* no). AFP: Alpha-fetoprotein; BCLC: Barcelona clinic liver cancer; HCV: Hepatitis C virus; HBV: Hepatitis B virus; NASH: Non alcoholic steatohepatitis; BMI: Body mass index.

In non-sarcopenic patients at baseline, emergence of a post-TACE sarcopenia was associated with a significant shorter median OS of 17 mo when compared with already sarcopenic patients before TACE (19.3 mo) and patients who stayed non-sarcopenic along TACE procedure (36.43 mo, P = 0.0004) (Figure 4D).

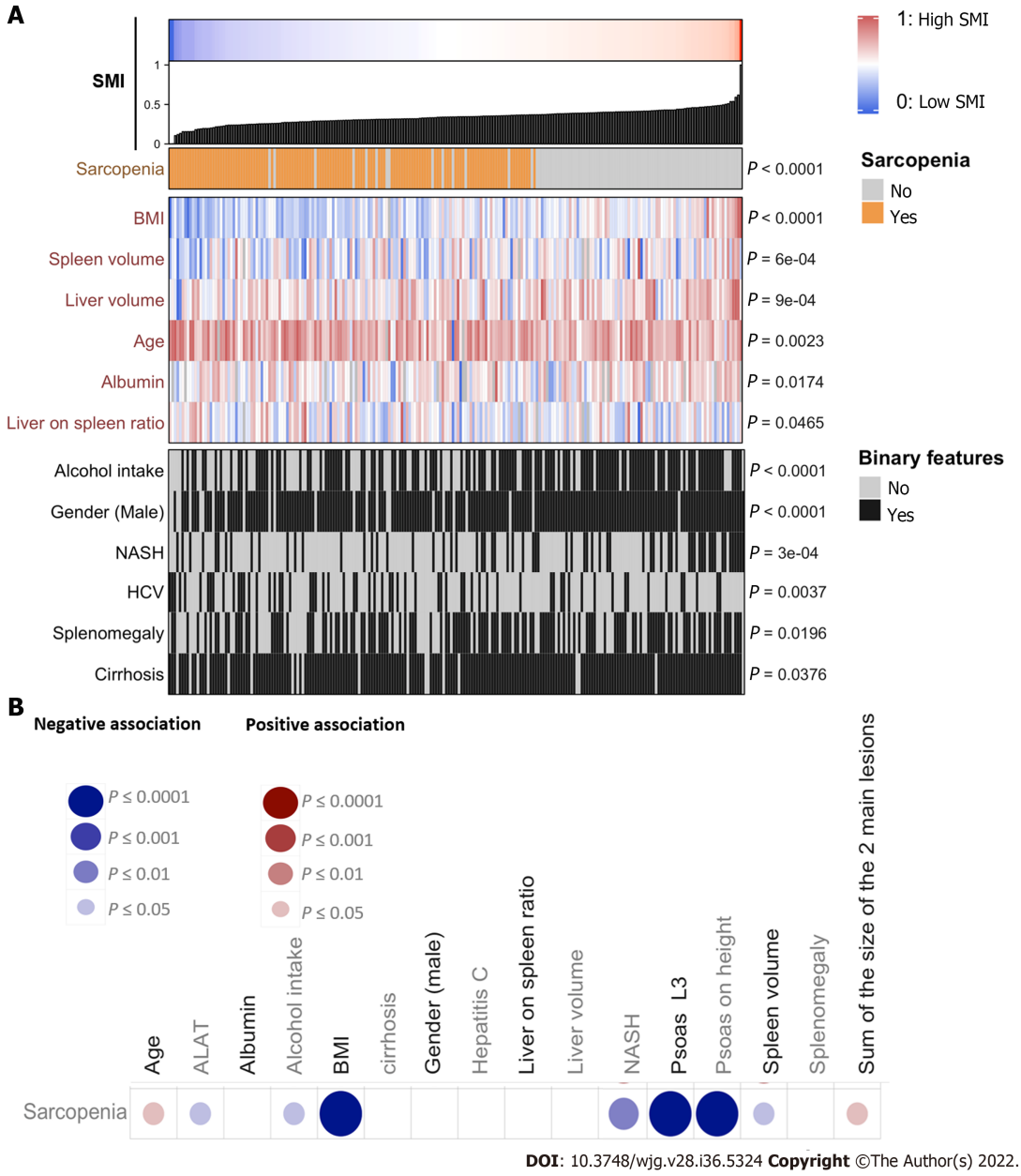

DOI: 10.3748/wjg.v28.i36.5324

Figure 2 Correlation of biological and clinical features with sarcopenia. A: Association of clinical, biological, and radiological features with skeletal muscle index expressed as a continuous variable; B: Association of clinical, biological, and radiological features with the presence or not of sarcopenia. Comparison of a continuous variable in two or more than two groups was performed using Wilcoxon signed-rank test or Kruskal-Wallis test, respectively. Qualitative data were compared using the Fisher's exact test. Correlation analysis between continuous variables was performed using Spearman's rank-order correlation. All tests were two-tailed and a *P*-value < 0.05 was considered significant. BMI: Body mass index; HCV: Hepatitis C virus; NASH: Non-alcoholic steatohepatitis; SMI: Skeletal muscle index.

DISCUSSION

This study is the largest multicentric cohort study exploring the impact of sarcopenia on tumor response and survival outcomes in patients with HCC treated by TACE or TAE. Sarcopenia represents a major challenge in chronic diseases and especially in the treatment of cancers in which the general status is classically altered, and aggressive treatments with poor tolerance profiles are frequent. Sarcopenia in cirrhosis has already been described as impacting survival, confirming the need of a global approach with a close nutritional support of these patients. Sarcopenia measures were assessed on the open-access software Image J®, which has been proved as equivalently efficient as other commercial programs, meaning that radiological assessment of sarcopenia is accessible to every center[18]. The use of SMI was preferred to methods only based on the measurement of PMI or the transverse psoas muscle thickness. Even though the two latter are simple to assess and showed interesting results in term of survival in HCC patients treated by TACE in previous studies, SMI seems to offer a more robust and complete measurement of the muscle mass in cirrhotic patients. Besides, PMI may identify fewer patients at risk of an increased mortality and presents a higher inter-observer variability. To finish, SMI is easy to use

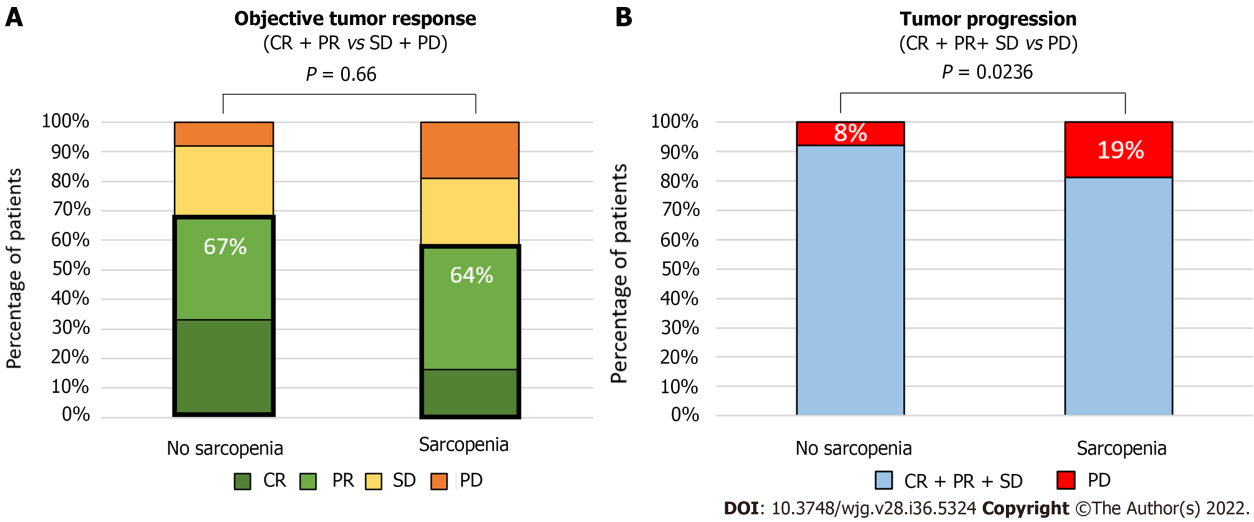

DOI: 10.3748/wjg.v28.i36.5324 **Copyright** ©The Author(s) 2022.

Figure 3 Radiological response according to presence of sarcopenia. A: Complete response *vs* partial response *vs* stable disease *vs* progressive disease assessed using the mRECIST criteria after the first session of treatment; B: Complete and partial response and stable disease *vs* progressive disease assessed using the mRECIST criteria after the first session of treatment. Statistical analysis was performed using the chi square test. CR: Complete response; PR: Partial response; SD: Stable disease; PD: Progressive disease; TACE: Trans-arterial chemoembolization.

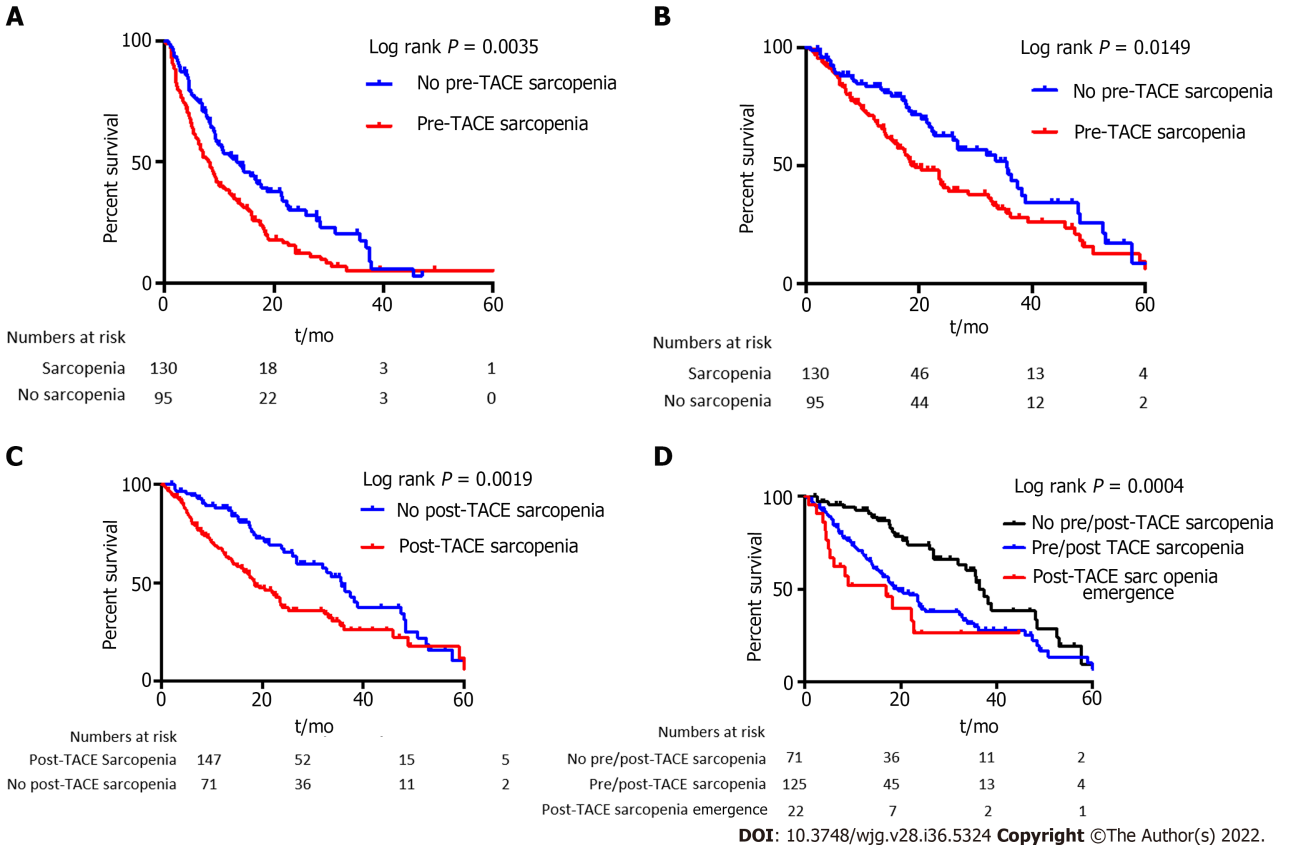

DOI: 10.3748/wjg.v28.i36.5324 **Copyright** ©The Author(s) 2022.

Figure 4 Survival according to presence of sarcopenia before and after trans-arterial chemoembolization. A and B: Progression free survival (A) and overall survival (OS) (B) according to the presence or not of sarcopenia before trans-arterial chemoembolization (TACE); C: OS according to presence or not of sarcopenia after TACE; D: OS according to the presence or not of sarcopenia before TACE, and appearance of sarcopenia after TACE designated as post-TACE sarcopenia. Results were computed using the Kaplan-Meier method and compared by the log rank test. The patients at risk are represented under the x-axis.

and recommended by the North American Expert Opinion Statement on Sarcopenia in Liver Transplantation[17,19,20]. In this study, measures were performed by only one radiologist *per* center, which limits bias induced by potential interobserver variability. This also constitutes a limit as interobserver variability should be studied to improve result exportability and better evaluate their reproducibility.

In this study, a high prevalence of sarcopenia (57%) in patients with HCC treated by transarterial treatment was observed despite the predominance of Child-Pugh A patients and intermediate stage tumors (BCLC-B). This is consistent with a recent HCC cohort study exploring the impact of sarcopenia on survival in patients treated by hepatectomy where 54% of patients were sarcopenic, as well as published data in liver transplantation[17]. Even if patients with sarcopenia have a lower BMI than patients without, most of patients with sarcopenia harbored a normal BMI (median value of 24). Moreover, with the increase of overweight and obesity which represents 15%-20% of the worldwide population[21], BMI is even less sensitive to detect malnutrition in patients with chronic diseases and especially liver diseases. These elements suggest that sarcopenia measured by performant radiological methods reflect more precisely the nutritional state and the protein catabolism of these patients. Nonetheless, other markers that could impact the outcomes after trans-arterial (chemo)embolization such as patient's daily activities and diet are not collected in this study due to its retrospective character. As well, this study lacked of other frailty parameters such as grip strength or walking speed. It constitutes another limit that cannot be addressed due to the retrospective character of the study.

One of the main strengths of this study is the radiological reviewing of radiological response using mRECIST criteria. This analysis revealed that sarcopenia was associated with a higher risk of progressive disease after trans-arterial treatment but without any difference on objective tumor response. Nevertheless, in multivariate analysis, only BCLC-C (segmental portal thrombosis) was independently associated with progressive disease. Sarcopenia was also associated with a shorter PFS together with tumor size in multivariate analysis. These data suggest that a subgroup of patients with advanced tumor stage and sarcopenia have a more aggressive disease which is more prone to resist to trans-arterial treatments. Indeed, sarcopenia may reflect the consequences of an intense hypercatabolism due to a particularly aggressive disease. In these patients, transarterial treatment may be deleterious in addition to be less effective as it could lead to liver failure and decrease the possibility of using systemic treatments after progression. Besides, the increased rate of radiological response obtained with the recent combination atezolizumab-bevacizumab forces us to better select the optimal treatment for patients between TACE and systemic treatments[22]. However, as sarcopenia has also been associated with poorer survival outcomes in patients under systemic therapies[10], it remains to be studied if sarcopenic patients with a high tumor burden benefit more from systemic treatments than trans-arterial procedures. In any case, sarcopenia needs to be detected as early as possible to initiate a medical intervention using nutritional support and physical activity to reverse sarcopenia and potentially improve survival. Indeed, muscle restoration before starting these treatments showed interesting results in terms of survival[10,23], and this type of intervention should be tested in a randomized controlled trial as up to 60% of patients treated by TACE harbored sarcopenia.

Sarcopenia was also associated with a shorter OS independently of tumor burden, suggesting that undernutrition and loss of muscle are key prognostic factors in patients with HCC treated by TACE or TAE. As sarcopenia is easily assessable using a CT scan in clinical practice, it could be useful to stratify patients in clinical trials. This study showed that sarcopenia assessed at the first radiological evaluation after TACE was also associated with a shorter OS, underlying the robustness of this association. Moreover, a subset of patients rapidly developed sarcopenia at the first radiological assessment which was particularly associated with a poor OS. Almost all these patients presented a progressive disease at the first evaluation, suggesting that they harbored an aggressive tumoral disease potentially responsible for the fast development of sarcopenia.

CONCLUSION

In conclusion, sarcopenia is associated with a higher rate of tumor progression and shorter survival in patients with HCC treated by TACE or TAE. Moreover, sarcopenia is an easy-to-assess radiological biomarker of poor prognosis that should be measured in order to better estimate prognosis and test a targeted intervention mixing nutritional support and physical activity.

ARTICLE HIGHLIGHTS

Research background

At the diagnosis of hepatocellular carcinoma (HCC), more than 90% of HCC patients present a cirrhosis, a clinical condition often associated to malnutrition. Sarcopenia has been associated with a lower tumor response or poorer survival of patients undergoing various treatments such as surgery or systemic therapies. Transarterial chemoembolization is the treatment of choice for intermediate HCC and is largely used worldwide, but the impact of sarcopenia on its results was poorly studied.

Research motivation

Finding easy ways to detect sarcopenia within daily practice should benefit to patients by better charac-

terizing their prognosis and taking their nutritional status into account in therapeutic decisions.

Research objectives

This study aimed to evaluate the prognostic value of sarcopenia in patients with HCC treated by transarterial (chemo)-embolization based on baseline computed tomography (CT) findings and study its impact on objective tumor response and survival outcomes.

Research methods

Sarcopenia is easy to assess on CT by measuring the skeletal muscle index. A skeletal muscle index (SMI) < 50 cm^2/m^2 in male and < 39 cm^2/m^2 in female patients corresponding to sarcopenia was observed in 57.7% of the patients.

Research results

Based on SMI analysis measured on baseline imaging, sarcopenia was observed in 57.7% of the patients. After full review of radiological response using mRECIST criteria, sarcopenia was associated with a higher rate of progressive disease. It was also associated with a decrease overall survival even after adjustment with usual risk factors of death.

Research conclusions

Sarcopenia is an easy-to-assess radiological biomarker of poor prognosis that should be measured in order to better assess prognosis of HCC patients.

Research perspectives

Sarcopenia should be systematically detected at baseline, and induce a targeted intervention mixing nutritional support and physical activity. Further studies are needed to assess the benefit of these strategies in HCC patients.

FOOTNOTES

Author contributions: Roth G, Teyssier Y, Decaens T, and Nault JC equivalently contributed to this work; Roth G, Decaens T, and Nault JC contributed to the conceptualization; Roth G and Nault JC contributed to the methodology; Roth G, Teyssier Y, Benhamou M, Abousalihac M, Sengel C, Seror O, Ghelfi J, Ganne-Carrié N, Gigante E, Blaise L, Sutter O, Decaens T, and Nault JC contributed to the investigation; Roth G, Benhamou M, Teyssier Y, Abousalihac M, and Nault JC contributed to the formal analysis; Roth G, Nault JC, Seigneurin A, and Caruso S contributed to the data curation; Nault JC, Seigneurin A, and Caruso S contributed to the statistical analysis; Roth G, Teyssier Y, Benhamou M, Caruso S, Seigneurin A, Abousalihac M, Sengel C, Seror O, Ghelfi J, Ganne-Carrié N, Gigante E, Blaise L, Sutter O, Decaens T, and Nault JC contributed to the validation; Decaens T and Nault JC contributed to the resources; Roth G and Nault JC wrote the original draft; Roth G, Teyssier Y, Benhamou M, Seigneurin A, Abousalihac M, Sengel C, Seror O, Ghelfi J, Ganne-Carrié N, Gigante E, Blaise L, Sutter O, Decaens T, and Nault JC reviewed and edited the manuscript; Roth G, Decaens T, and Nault JC contributed to the supervision; all authors have read and approved the manuscript.

Institutional review board statement: The study was conducted according to the guidelines of the Declaration of Helsinki. Study ethics was approved by the independent French ethic committee CERIM (Comité d'éthique de la recherche en imagerie médicale) (approval date May 25 2020; No. CRM-2004-084).

Informed consent statement: Patients gave their written consent before TACE procedures as in routine care practice. No specific consent statement was required regarding the retrospective analysis of data as they were anonymously used.

Conflict-of-interest statement: All the authors report no relevant conflicts of interest for this article.

Data sharing statement: No additional data are available.

STROBE statement: The authors have read the STROBE Statement—checklist of items, and the manuscript was prepared and revised according to the STROBE Statement—checklist of items.

Country/Territory of origin: France

ORCID number: Gael Roth 0000-0001-5822-4320; Yann Teyssier 0000-0002-9785-8729; Maxime Benhamou 0000-0002-8590-5161; Mélodie Abousalihac 0000-0002-0661-1684; Stefano Caruso 0000-0002-6319-3642; Christian Sengel 0000-0001-9004-256X; Olivier Seror 0000-0001-6680-8991; Julien Ghelfi 0000-0002-9039-6488; Arnaud Seigneurin 0000-0002-2168-1672; Nathalie Ganne-Carrie 0000-0002-7351-5027; Elia Gigante 0000-0002-5455-2308; Lorraine Blaise 0000-0001-5344-1625; Olivier Sutter 0000-0002-2802-9652; Thomas Decaens 0000-0003-0928-0048; Jean-Charles Nault 0000-0002-4875-9353.

S-Editor: Fan JR
L-Editor: Wang TQ
P-Editor: Cai YX

REFERENCES

1 **Bray F**, Ferlay J, Soerjomataram I, Siegel RL, Torre LA, Jemal A. Global cancer statistics 2018: GLOBOCAN estimates of incidence and mortality worldwide for 36 cancers in 185 countries. *CA Cancer J Clin* 2018; **68**: 394-424 [PMID: 30207593 DOI: 10.3322/caac.21492]
2 **Reig M**, Forner A, Rimola J, Ferrer-Fàbrega J, Burrel M, Garcia-Criado Á, Kelley RK, Galle PR, Mazzaferro V, Salem R, Sangro B, Singal AG, Vogel A, Fuster J, Ayuso C, Bruix J. BCLC strategy for prognosis prediction and treatment recommendation: The 2022 update. *J Hepatol* 2022; **76**: 681-693 [PMID: 34801630 DOI: 10.1016/j.jhep.2021.11.018]
3 **Llovet JM**, Bruix J. Systematic review of randomized trials for unresectable hepatocellular carcinoma: Chemoembolization improves survival. *Hepatology* 2003; **37**: 429-442 [PMID: 12540794 DOI: 10.1053/jhep.2003.50047]
4 **Sieghart W**, Hucke F, Peck-Radosavljevic M. Transarterial chemoembolization: modalities, indication, and patient selection. *J Hepatol* 2015; **62**: 1187-1195 [PMID: 25681552 DOI: 10.1016/j.jhep.2015.02.010]
5 **Blanc JF**, Debaillon-Vesque A, Roth G, Barbare JC, Baumann AS, Boige V, Boudjema K, Bouattour M, Crehange G, Dauvois B, Decaens T, Dewaele F, Farges O, Guiu B, Hollebecque A, Merle P, Selves J, Aparicio T, Ruiz I, Bouché O; Thésaurus National de Cancérologie Digestive (TNCD); Société Nationale Française de Gastroentérologie (SNFGE); Fédération Francophone de Cancérologie Digestive (FFCD); Groupe Coopérateur multidisciplinaire en Oncologie (GERCOR); Fédération Nationale des Centres de Lutte Contre le Cancer (UNICANCER); Société Française de Chirurgie Digestive (SFCD); Société Française d'Endoscopie Digestive (SFED); Société Française de Radiothérapie Oncologique (SFRO); Association Française pour l'Etude du Foie (AFEF). Hepatocellular carcinoma: French Intergroup Clinical Practice Guidelines for diagnosis, treatment and follow-up (SNFGE, FFCD, GERCOR, UNICANCER, SFCD, SFED, SFRO, AFEF, SIAD, SFR/FRI). *Clin Res Hepatol Gastroenterol* 2021; **45**: 101590 [PMID: 33780876 DOI: 10.1016/j.clinre.2020.101590]
6 **Lencioni R**, de Baere T, Soulen MC, Rilling WS, Geschwind JF. Lipiodol transarterial chemoembolization for hepatocellular carcinoma: A systematic review of efficacy and safety data. *Hepatology* 2016; **64**: 106-116 [PMID: 26765068 DOI: 10.1002/hep.28453]
7 **European Association for the Study of the Liver**. EASL Clinical Practice Guidelines: Management of hepatocellular carcinoma. *J Hepatol* 2018; **69**: 182-236 [PMID: 29628281 DOI: 10.1016/j.jhep.2018.03.019]
8 **Fielding RA**, Vellas B, Evans WJ, Bhasin S, Morley JE, Newman AB, Abellan van Kan G, Andrieu S, Bauer J, Breuille D, Cederholm T, Chandler J, De Meynard C, Donini L, Harris T, Kannt A, Keime Guibert F, Onder G, Papanicolaou D, Rolland Y, Rooks D, Sieber C, Souhami E, Verlaan S, Zamboni M. Sarcopenia: an undiagnosed condition in older adults. Current consensus definition: prevalence, etiology, and consequences. International working group on sarcopenia. *J Am Med Dir Assoc* 2011; **12**: 249-256 [PMID: 21527165 DOI: 10.1016/j.jamda.2011.01.003]
9 **Voron T**, Tselikas L, Pietrasz D, Pigneur F, Laurent A, Compagnon P, Salloum C, Luciani A, Azoulay D. Sarcopenia Impacts on Short- and Long-term Results of Hepatectomy for Hepatocellular Carcinoma. *Ann Surg* 2015; **261**: 1173-1183 [PMID: 24950264 DOI: 10.1097/SLA.0000000000000743]
10 **Nishikawa H**, Nishijima N, Enomoto H, Sakamoto A, Nasu A, Komekado H, Nishimura T, Kita R, Kimura T, Iijima H, Nishiguchi S, Osaki Y. Prognostic significance of sarcopenia in patients with hepatocellular carcinoma undergoing sorafenib therapy. *Oncol Lett* 2017; **14**: 1637-1647 [PMID: 28789390 DOI: 10.3892/ol.2017.6287]
11 **Fujiwara N**, Nakagawa H, Kudo Y, Tateishi R, Taguri M, Watadani T, Nakagomi R, Kondo M, Nakatsuka T, Minami T, Sato M, Uchino K, Enooku K, Kondo Y, Asaoka Y, Tanaka Y, Ohtomo K, Shiina S, Koike K. Sarcopenia, intramuscular fat deposition, and visceral adiposity independently predict the outcomes of hepatocellular carcinoma. *J Hepatol* 2015; **63**: 131-140 [PMID: 25724366 DOI: 10.1016/j.jhep.2015.02.031]
12 **Marasco G**, Serenari M, Renzulli M, Alemanni LV, Rossini B, Pettinari I, Dajti E, Ravaioli F, Golfieri R, Cescon M, Festi D, Colecchia A. Clinical impact of sarcopenia assessment in patients with hepatocellular carcinoma undergoing treatments. *J Gastroenterol* 2020; **55**: 927-943 [PMID: 32748172 DOI: 10.1007/s00535-020-01711-w]
13 **Loosen SH**, Schulze-Hagen M, Bruners P, Tacke F, Trautwein C, Kuhl C, Luedde T, Roderburg C. Sarcopenia Is a Negative Prognostic Factor in Patients Undergoing Transarterial Chemoembolization (TACE) for Hepatic Malignancies. *Cancers (Basel)* 2019; **11** [PMID: 31597337 DOI: 10.3390/cancers11101503]
14 **Roth GS**, Benhamou M, Teyssier Y, Seigneurin A, Abousalihac M, Sengel C, Seror O, Ghelfi J, Ganne-Carrié N, Blaise L, Sutter O, Decaens T, Nault JC. Comparison of Trans-Arterial Chemoembolization and Bland Embolization for the Treatment of Hepatocellular Carcinoma: A Propensity Score Analysis. *Cancers (Basel)* 2021; **13** [PMID: 33672012 DOI: 10.3390/cancers13040812]
15 **Roth GS**, Teyssier Y, Abousalihac M, Seigneurin A, Ghelfi J, Sengel C, Decaens T. Idarubicin *vs* doxorubicin in transarterial chemoembolization of intermediate stage hepatocellular carcinoma. *World J Gastroenterol* 2020; **26**: 324-334 [PMID: 31988592 DOI: 10.3748/wjg.v26.i3.324]
16 **Prado CM**, Lieffers JR, McCargar LJ, Reiman T, Sawyer MB, Martin L, Baracos VE. Prevalence and clinical implications

of sarcopenic obesity in patients with solid tumours of the respiratory and gastrointestinal tracts: a population-based study. *Lancet Oncol* 2008; **9**: 629-635 [PMID: 18539529 DOI: 10.1016/S1470-2045(08)70153-0]

17 **Carey EJ**, Lai JC, Sonnenday C, Tapper EB, Tandon P, Duarte-Rojo A, Dunn MA, Tsien C, Kallwitz ER, Ng V, Dasarathy S, Kappus M, Bashir MR, Montano-Loza AJ. A North American Expert Opinion Statement on Sarcopenia in Liver Transplantation. *Hepatology* 2019; **70**: 1816-1829 [PMID: 31220351 DOI: 10.1002/hep.30828]

18 **Long DE**, Villasante Tezanos AG, Wise JN, Kern PA, Bamman MM, Peterson CA, Dennis RA. A guide for using NIH Image J for single slice cross-sectional area and composition analysis of the thigh from computed tomography. *PLoS One* 2019; **14**: e0211629 [PMID: 30730923 DOI: 10.1371/journal.pone.0211629]

19 **Lanza E**, Masetti C, Messana G, Muglia R, Pugliese N, Ceriani R, Lleo de Nalda A, Rimassa L, Torzilli G, Poretti D, D'Antuono F, Politi LS, Pedicini V, Aghemo A; Humanitas HCC Multidisciplinary Group. Sarcopenia as a predictor of survival in patients undergoing bland transarterial embolization for unresectable hepatocellular carcinoma. *PLoS One* 2020; **15**: e0232371 [PMID: 32555707 DOI: 10.1371/journal.pone.0232371]

20 **Beer L**, Bastati N, Ba-Ssalamah A, Pötter-Lang S, Lampichler K, Bican Y, Lauber D, Hodge J, Binter T, Pomej K, Simbrunner B, Semmler G, Trauner M, Mandorfer M, Reiberger T. MRI-defined sarcopenia predicts mortality in patients with chronic liver disease. *Liver Int* 2020; **40**: 2797-2807 [PMID: 32816394 DOI: 10.1111/liv.14648]

21 **Tao W**, Lagergren J. Clinical management of obese patients with cancer. *Nat Rev Clin Oncol* 2013; **10**: 519-533 [PMID: 23856746 DOI: 10.1038/nrclinonc.2013.120]

22 **Finn RS**, Qin S, Ikeda M, Galle PR, Ducreux M, Kim TY, Kudo M, Breder V, Merle P, Kaseb AO, Li D, Verret W, Xu DZ, Hernandez S, Liu J, Huang C, Mulla S, Wang Y, Lim HY, Zhu AX, Cheng AL; IMbrave150 Investigators. Atezolizumab plus Bevacizumab in Unresectable Hepatocellular Carcinoma. *N Engl J Med* 2020; **382**: 1894-1905 [PMID: 32402160 DOI: 10.1056/NEJMoa1915745]

23 **Cheng TY**, Lee PC, Chen YT, Chao Y, Hou MC, Huang YH. Pre-sarcopenia determines post-progression outcomes in advanced hepatocellular carcinoma after sorafenib failure. *Sci Rep* 2020; **10**: 18375 [PMID: 33110117 DOI: 10.1038/s41598-020-75198-z]

World Journal of Gastroenterology

Submit a Manuscript: https://www.f6publishing.com

World J Gastroenterol 2022 September 28; 28(36): 5338-5350

DOI: 10.3748/wjg.v28.i36.5338

ISSN 1007-9327 (print) ISSN 2219-2840 (online)

ORIGINAL ARTICLE

Retrospective Cohort Study

Machine learning-based gray-level co-occurrence matrix signature for predicting lymph node metastasis in undifferentiated-type early gastric cancer

Xin Wei, Xue-Jiao Yan, Yu-Yan Guo, Jie Zhang, Guo-Rong Wang, Arsalan Fayyaz, Jiao Yu

Specialty type: Gastroenterology and hepatology

Provenance and peer review: Unsolicited article; Externally peer reviewed.

Peer-review model: Single blind

Peer-review report's scientific quality classification

Grade A (Excellent): A, A
Grade B (Very good): B
Grade C (Good): 0
Grade D (Fair): 0
Grade E (Poor): 0

P-Reviewer: He D, China; Pantelis AG, Greece; Toyoshima O, Japan

Received: July 20, 2022
Peer-review started: July 20, 2022
First decision: August 6, 2022
Revised: August 14, 2022
Accepted: September 6, 2022
Article in press: September 6, 2022
Published online: September 28, 2022

Xin Wei, Department of Oncology, Shaanxi Provincial People's Hospital, Xi'an 710068, Shaanxi Province, China

Xue-Jiao Yan, Department of Magnetic Resonance, Shaanxi Provincial People's Hospital, Xi'an 710068, Shaanxi Province, China

Yu-Yan Guo, Department of Radiotherapy, The Second Affiliated Hospital of Xi'an Jiaotong University, Xi'an 710004, Shaanxi Province, China

Jie Zhang, Department of Gastrointestinal Surgery, Shaanxi Provincial Tumour Hospital, Xi'an 710068, Shaanxi Province, China

Guo-Rong Wang, Department of General Surgery, Shaanxi Provincial People's Hospital, Xi'an 710068, Shaanxi Province, China

Arsalan Fayyaz, School of Management, Northwestern Polytechnical University, Xi'an 710072, Shaanxi Province, China

Jiao Yu, Department of Radiotherapy, Shaanxi Provincial People's Hospital, Xi'an 710068, Shaanxi Province, China

Corresponding author: Jiao Yu, MD, Radiologist, Department of Radiotherapy, Shaanxi Provincial People's Hospital, No. 256 Youyi West Road, Beilin District, Xi'an 710068, Shaanxi Province, China. shawn170215@163.com

Abstract

BACKGROUND

The most important consideration in determining treatment strategies for undifferentiated early gastric cancer (UEGC) is the risk of lymph node metastasis (LNM). Therefore, identifying a potential biomarker that predicts LNM is quite useful in determining treatment.

AIM

To develop a machine learning (ML)-based integral procedure to construct the LNM gray-level co-occurrence matrix (GLCM) prediction model.

METHODS

We retrospectively selected 526 cases of UEGC confirmed through pathological examination after radical gastrectomy without endoscopic treatment in four tertiary hospitals between January 2015 to December 2021. We extracted GLCM-based features from grayscale images and applied ML to the classification of candidate predictive variables. The robustness and clinical utility of each model were evaluated based on the following factors: Receiver operating characteristic curve (ROC), decision curve analysis, and clinical impact curve.

RESULTS

GLCM-based feature extraction significantly correlated with LNM. The top 7 GLCM-based factors included inertia value 0° (IV_0), inertia value 45° (IV_45), inverse gap 0° (IG_0), inverse gap 45° (IG_45), inverse gap full angle (IG_all), Haralick 30° (Haralick_30), Haralick full angle (Haralick_all), and Entropy. The areas under the ROC curve (AUCs) of the random forest classifier (RFC) model, support vector machine, eXtreme gradient boosting, artificial neural network, and decision tree ranged from 0.805 [95% confidence interval (CI): 0.258-1.352] to 0.925 (95%CI: 0.378-1.472) in the training set and from 0.794 (95%CI: 0.237-1.351) to 0.912 (95%CI: 0.355-1.469) in the testing set, respectively. The RFC (training set: AUC: 0.925, 95%CI: 0.378-1.472; testing set: AUC: 0.912, 95%CI: 0.355-1.469) model that incorporates Entropy, Haralick_all, Haralick_30, IG_all, IG_45, IG_0, and IV_45 had the highest predictive accuracy.

CONCLUSION

The evaluation results indicate that the method of selecting radiological and textural features becomes more effective in the LNM discrimination against UEGC patients. Additionally, the ML-based prediction model developed using the RFC can be used to derive treatment options and identify LNM, which can hence improve clinical outcomes.

Key Words: Undifferentiated early gastric cancer; Machine learning; Lymph node metastasis; Gray-level co-occurrence matrix; Feature selection; Prediction

Core Tip: Gray-level co-occurrence matrix-based feature extraction can be a robust and promising tool to improve the efficiency in predicting lymph node metastasis of individual undifferentiated early gastric cancer patients. Additionally, machine learning adopts more optimized algorithms and more clear feature extraction. Models developed using random forest classifier have the highest predictive accuracy in terms of Entropy, Haralick full angle, Haralick 30°, inverse gap full angle, inverse gap 45°, inverse gap 0°, and inertia value 45°. Further research is required to develop these models for clinical practice.

Citation: Wei X, Yan XJ, Guo YY, Zhang J, Wang GR, Fayyaz A, Yu J. Machine learning-based gray-level co-occurrence matrix signature for predicting lymph node metastasis in undifferentiated-type early gastric cancer. *World J Gastroenterol* 2022; 28(36): 5338-5350

URL: https://www.wjgnet.com/1007-9327/full/v28/i36/5338.htm

DOI: https://dx.doi.org/10.3748/wjg.v28.i36.5338

INTRODUCTION

Gastric cancer (GC) is one of the most common and fatal malignancies worldwide and is an important part of the global cancer burden[1,2]. In GC, undifferentiated early GC (UEGC) differs from differentiated-type GC in terms of clinical features and disease state, and their treatment and prognosis vary[3]. Therefore, UEGC should be identified and diagnosed early.

The incidence of lymphatic vessel invasion and risk of lymph node metastasis (LNM) in UEGC are high in surgical specimens of GC[4,5]. Endoscopic resection (ER), including endoscopic mucosal resection (EMR) and endoscopic submucosal dissection (ESD), has been considered a minimally invasive treatment option for early GC with negligible risk of LNM[6,7]. Nevertheless, indication or curability evaluation has not been conducted for ESD of undifferentiated GC (*e.g.*, poorly differentiated adenocarcinoma, signet ring cell carcinoma, or mucinous adenocarcinoma) due to the potential risk of LNM. Although ER can be used as painless treatment, the LNM incidence after non-curative ER can be as low as 5.1% and as high as 12.2%[8-10]. Additionally, ESD is only applicable to intramucosal cancer with a tumor diameter of ≤ 20 mm and without ulcer lesions; thus, treating lesions that meet the ESD indications through surgery is unnecessary[11,12]. That is, when resection beyond the expanded

standard is considered ineffective, the potential risk of LNM cannot be ignored. Hence, additional surgical resection and lymph node dissection should be performed. Unlike differentiated early GC, ER indications of UEGC are limited. Therefore, to address this challenging problem, a precise tool that can predict LNM must be explored.

Previous studies have mainly focused on risk factors for LNM or distant metastasis of differentiated-type early GC[13-15]. However, for UEGC, LNM has different risk factors. Thus, objective and universal evaluation indicators for evaluating its risk are lacking. In this study, we clarified the LNM risk factors of patients with UEGC who underwent surgical resection. Subsequently, we analyzed clinical-pathological factors by introducing gray-level co-occurrence matrix (GLCM) image feature extraction mining to classify LNM risk groups according to the combination of risk factors. This study aims to provide a reference for clinical diagnosis and treatment.

MATERIALS AND METHODS

Patient selection

The clinical records of 526 patients who were diagnosed with UEGC were confirmed through pathological examination after radical gastrectomy without endoscopic treatment at four tertiary hospitals. These hospitals are Shaanxi Provincial People's Hospital, Shaanxi Provincial Tumour Hospital, the First Affiliated Hospital of Xi'an Jiaotong University, and the Second Affiliated Hospital of Xi'an Jiaotong University. The clinical records were between January 2015 to December 2021 and were retrospectively reviewed. The following were the inclusion criteria: (1) Imaging examination was performed; (2) Patients have a complete set of medical data; (3) Primary lesion was resected either *via* open surgery or laparoscopic surgery and not *via* EMR or ESD; and (4) The status of infiltrating lymph nodes was assessed through routine hematoxylin-eosin staining. To minimize the confounding effect of unnecessary variables, the following were the exclusion criteria: (1) Sufficient information cannot be extracted or mismatched clinical data of patients; and (2) Patients without complete magnetic resonance imaging (MRI) plain scan or the MRI image quality being unacceptable. This study complies with the provisions of the Helsinki Declaration (revised in 2013) and was approved by the Institutional Review Committee of Shaanxi Provincial People's Hospital (2021-Y024). Figure 1 presents in detail the patient screening steps and modeling process.

Construction strategy of the GLCM

All texture parameter post-processing was conducted on Omni dynamics software (GE pharmaceuticals, Shanghai). Two radiologists who have vast experience in gastrointestinal diagnosis referred to the MRI images to sketch the lesions on the ADC map. First, they manually sketch the entire area with cancer on each layer of the map, avoiding the gas in the intestine, until the whole tumor volume was cut out. Second, the software automatically generates the texture features. In this study, the following are the selected texture parameters of the GLCM: Total frequency, energy value, entropy, inertia value, correlation coefficient, inverse moment, cluster shadow, and cluster prominence.

Data extraction and quality assessment

For variables with missing values (often this missing value is less than 10%), the variable's mean value should be filled. If ≥ 10% of the given variables are missing, this value is excluded from the variable screening of the final model. Similarly, this study adopted unit feature interpolation for the missing values that meet the interpolation requirements. That is, the missing values can be interpolated using the constant values provided or using the statistical data of each column where these missing values are located (*e.g.*, average value, median value, or the most frequently occurring value)[16,17].

Construction and effectiveness evaluation of the LNM model

Based on the machine learning (ML) algorithm, the commonly used iterative algorithm models are included: Random forest classifier (RFC), decision tree (DT), support vector machine (SVM), eXtreme gradient boosting (XGBoost), and artificial neural network (ANN). The RFC is an integrated method that forms a cumulative effect by integrating multiple relatively simple evaluators. Random forest is an integrated learning tool based on DT. The SVM is a type of a generalized linear classifier that categorizes data binary through supervised learning. The ANN is a nonlinear equation transformation output algorithm comprising input, hidden, and output layers. Finally, XGBoost is an additive model. In each iteration, only the sub-models in the current step are optimized. In this study, we refer to the guide proposed by Luo *et al*[18] for the best use of prediction models in biomedical research, that is, the Delphi method, which is used to generate the list of reported items.

For the screening of candidate variables, we mainly rely on the principle of "bag repeatedly put back and extract", sort according to variables' weight, and finally obtain the final predictor of the prediction model from the top 10 variables[19]. For the effectiveness evaluation of the prediction model, the receiver operating characteristic (ROC) curve is used to evaluate the accuracy of the model. Meanwhile,

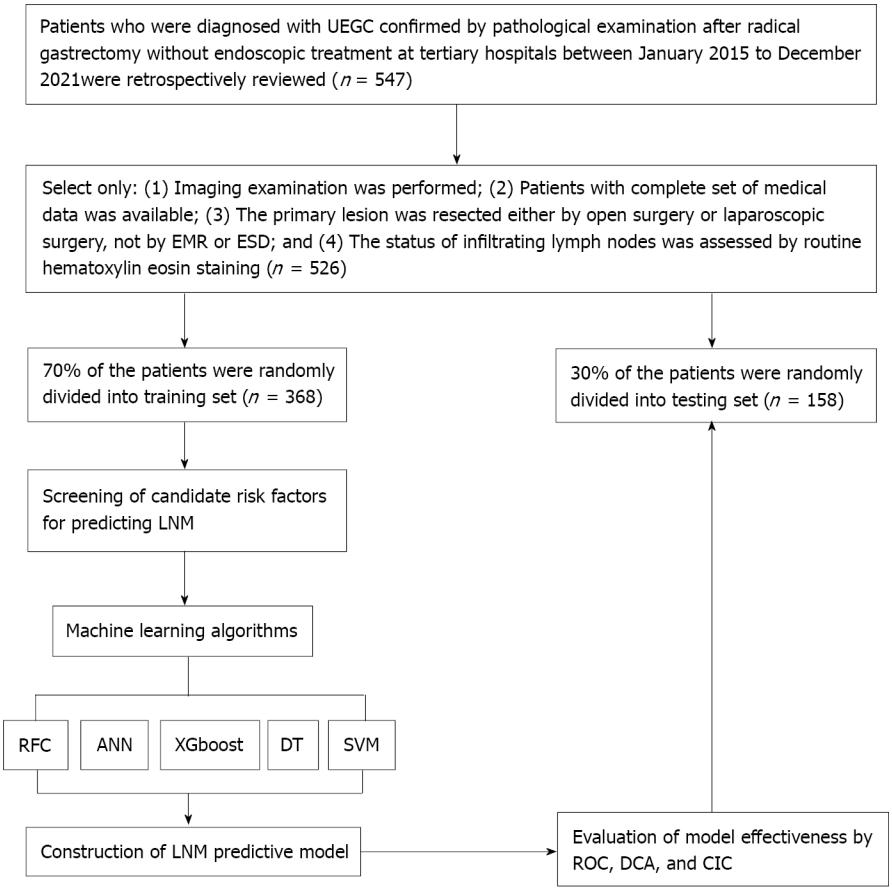

DOI: 10.3748/wjg.v28.i36.5338 **Copyright** ©The Author(s) 2022.

Figure 1 Flowchart of patient selection and data processing. UEGC: Undifferentiated early gastric cancer; EMR: Endoscopic mucosal resection; ESD: Endoscopic submucosal dissection; RFC: Random forest classifier; SVM: Support vector machine; DT: Decision tree; ANN: Artificial neural network; XGboost: Extreme gradient boosting; ROC: Receiver operating characteristic; DCA: Decision curve analysis; CIC: Clinical impact curve; LNM: Lymph node metastasis.

the decision curve analysis and clinical impact curve (CIC) were used to evaluate the model's robustness and differentiation, respectively.

Statistical analysis

The measurement and counting data in this study are expressed by interquartile spacing (25%, 75%) and percentage (%), respectively. For the comparison between groups, the continuous variables adopt the *t*-test or Mann-Whitney *U* test of independent samples (provided that it does not conform to the normal distribution). The counting data adopt the chi-square goodness-of-fit test. Values of Bonferroni corrected probability are used to compare the qualitative data[20]. The prediction model visualization and other data analysis are performed using R software (version 4.0.4, http://www.r-project.org/). For the comparison between groups, P value < 0.05 is considered statistically significant and vice versa.

RESULTS

Comparison of baseline data between LNM and non-LNM queues

Table 1 summarizes the baseline characteristics of 526 hospitalized patients with UEGC. For internal validation, the patients were randomly divided into two sets using the caret package: Training set (n = 368, 70%) and validation set (n = 158, 30%). Regarding the LNM rate, the training and validation cohorts were 62 (16.85%) and 29 (18.35%), respectively. In addition to the previously reported clinical-related indicators (*e.g.*, tumor size, infiltration depth, vascular_invasion, and vascular tumor thrombus), significant differences exist between the LNM and non-LNM groups. We found that GLCM-based texture acquisition features also have significant statistical differences between the two groups.

Feature correlation and potential predictors

We conducted a correlation analysis on the variables with significant differences based on the statistical difference analysis of baseline data. As shown in Figure 2A, the correlation matrix (based on Pearson

Table 1 Patient baseline population and image index characteristic

Variables	Training set				Testing set			
	Overall (*n* = 368)	Yes (*n* = 62)	No (*n* = 306)	*P* value	Overall (*n* = 158)	Yes (*n* = 29)	No (*n* = 129)	*P* value
Age (median, IQR), yr	51.00 (40.75, 61.00)	52.50 (40.25, 64.50)	51.00 (41.00, 60.00)	0.185	47.00 (37.25, 58.75)	53.00 (39.00, 63.00)	46.00 (37.00, 57.00)	0.215
Sex (%)								
Male	266 (72.3)	48 (77.4)	218 (71.2)	0.404	123 (77.8)	21 (72.4)	102 (79.1)	0.594
Female	102 (27.7)	14 (22.6)	88 (28.8)		35 (22.2)	8 (27.6)	27 (20.9)	
Site (%)								
Nearly 1/3	81 (22.0)	10 (16.1)	71 (23.2)	0.384	37 (23.4)	9 (31.0)	28 (21.7)	0.138
Medium 1/3	73 (19.8)	15 (24.2)	58 (19.0)		23 (14.6)	1 (3.4)	22 (17.1)	
Far 1/3	214 (58.2)	37 (59.7)	177 (57.8)		98 (62.0)	19 (65.5)	79 (61.2)	
Ulcer (%)								
Yes	103 (28.0)	21 (33.9)	82 (26.8)	0.329	45 (28.5)	11 (37.9)	34 (26.4)	0.308
No	265 (72.0)	41 (66.1)	224 (73.2)		113 (71.5)	18 (62.1)	95 (73.6)	
Gross_type (%)								
Uplift	98 (26.6)	14 (22.6)	84 (27.5)	0.587	56 (35.4)	8 (27.6)	48 (37.2)	0.227
Flat	72 (19.6)	11 (17.7)	61 (19.9)		27 (17.1)	8 (27.6)	19 (14.7)	
Sunken	198 (53.8)	37 (59.7)	161 (52.6)		75 (47.5)	13 (44.8)	62 (48.1)	
Tumor_size (%)								
≤ 2 cm	296 (80.4)	18 (29.0)	278 (90.8)	< 0.001	120 (75.9)	6 (20.7)	114 (88.4)	< 0.001
> 2 cm	72 (19.6)	44 (71.0)	28 (9.2)		38 (24.1)	23 (79.3)	15 (11.6)	
Infiltration_depth (%)								
Mucosal layer	267 (72.6)	12 (19.4)	255 (83.3)	< 0.001	113 (71.5)	9 (31.0)	104 (80.6)	< 0.001
Submucosa	101 (27.4)	50 (80.6)	51 (16.7)		45 (28.5)	20 (69.0)	25 (19.4)	
Vascular_invasion (%)								
Yes	124 (33.7)	42 (67.7)	82 (26.8)	< 0.001	56 (35.4)	21 (72.4)	35 (27.1)	< 0.001
No	244 (66.3)	20 (32.3)	224 (73.2)		102 (64.6)	8 (27.6)	94 (72.9)	
VTT (%)								
Yes	124 (33.7)	45 (72.6)	79 (25.8)	< 0.001	44 (27.8)	23 (79.3)	21 (16.3)	< 0.001
No	244 (66.3)	17 (27.4)	227 (74.2)		114 (72.2)	6 (20.7)	108 (83.7)	
TF (median, IQR)	3.78 (3.56, 3.99)	4.13 (3.97, 4.27)	3.70 (3.51, 3.90)	< 0.001	3.79 (3.52, 4.01)	4.16 (4.00, 4.31)	3.70 (3.49, 3.93)	< 0.001
EV (median, IQR)	0.88 (0.64, 1.12)	0.60 (0.49, 0.68)	0.98 (0.72, 1.20)	< 0.001	0.85 (0.65, 1.09)	0.64 (0.54, 0.70)	0.92 (0.72, 1.16)	< 0.001
Entropy (median, IQR)	8.68 (8.37, 8.98)	10.51 (10.07, 10.88)	8.57 (8.33, 8.83)	< 0.001	8.79 (8.43, 9.02)	10.44 (10.16, 10.96)	8.65 (8.38, 8.89)	< 0.001
IG_all (median, IQR)	2.16 (1.76, 2.47)	3.04 (2.64, 3.62)	2.03 (1.69, 2.30)	< 0.001	2.12 (1.75, 2.47)	2.94 (2.70, 3.54)	1.97 (1.64, 2.31)	< 0.001
IG_0 (median, IQR)	2.26 (1.75, 2.66)	3.34 (2.72, 3.80)	2.10 (1.69, 2.48)	< 0.001	2.41 (1.90, 2.79)	3.70 (3.16, 4.18)	2.22 (1.77, 2.62)	< 0.001
IG_45 (median, IQR)	1.88 (1.54, 2.18)	2.85 (2.32, 3.26)	1.78 (1.47, 2.04)	< 0.001	1.85 (1.48, 2.18)	2.73 (2.31, 3.11)	1.74 (1.40, 2.03)	< 0.001
IG_90 (median, IQR)	2.34 (1.85, 2.85)	3.36 (2.89, 3.84)	2.20 (1.75, 2.63)	< 0.001	2.42 (1.94, 2.78)	3.27 (3.03, 3.61)	2.25 (1.75, 2.61)	< 0.001
IV_all (median, IQR)	176.90 (148.98, 207.25)	134.80 (109.30, 163.02)	182.00 (156.00, 210.75)	< 0.001	175.50 (143.25, 200.75)	133.50 (105.80, 155.70)	183.00 (154.00, 206.00)	< 0.001
IV_all_SD (median, IQR)	4584.00 (3148.00, 6602.50)	2166.50 (1340.50, 3535.00)	5025.00 (3747.00, 7011.75)	< 0.001	4940.50 (2987.25, 6682.00)	2849.00 (1841.00, 3428.00)	5618.00 (3813.00, 6897.00)	< 0.001

IV_0 (median, IQR)	149.85 (122.75, 186.75)	96.40 (78.95, 125.82)	163.20 (134.00, 195.65)	< 0.001	146.70 (112.78, 185.57)	74.10 (65.60, 90.60)	158.40 (131.40, 196.20)	< 0.001
IV_45 (median, IQR)	239.55 (201.40, 284.75)	164.40 (123.83, 188.62)	254.30 (220.67, 290.60)	< 0.001	226.25 (201.25, 266.67)	157.40 (133.90, 193.80)	243.90 (214.30, 273.50)	< 0.001
IV_90 (median, IQR)	129.00 (103.00, 154.00)	101.00 (77.75, 119.00)	134.00 (109.25, 159.00)	< 0.001	124.50 (109.00, 150.75)	105.00 (77.00, 118.00)	133.00 (117.00, 156.00)	< 0.001
Haralick_all (median, IQR)	0.10 (0.09, 0.10)	0.12 (0.11, 0.13)	0.09 (0.09, 0.10)	< 0.001	0.10 (0.09, 0.10)	0.12 (0.12, 0.14)	0.09 (0.09, 0.10)	< 0.001
Haralick_30 (median, IQR)	0.10 (0.09, 0.11)	0.14 (0.12, 0.15)	0.10 (0.09, 0.11)	< 0.001	0.10 (0.09, 0.11)	0.14 (0.13, 0.15)	0.10 (0.09, 0.11)	< 0.001
Haralick_45 (median, IQR)	0.09 (0.08, 0.10)	0.11 (0.10, 0.12)	0.09 (0.08, 0.10)	< 0.001	0.09 (0.08, 0.10)	0.11 (0.10, 0.13)	0.09 (0.08, 0.10)	< 0.001
Haralick_90 (median, IQR)	0.11 (0.10, 0.13)	0.14 (0.12, 0.16)	0.11 (0.09, 0.12)	< 0.001	0.12 (0.10, 0.13)	0.15 (0.12, 0.16)	0.11 (0.09, 0.13)	< 0.001
CSV (median, IQR)	106.00 (102.00, 111.00)	108.00 (105.00, 111.00)	106.00 (101.00, 111.00)	0.001	107.00 (102.25, 111.00)	109.00 (105.00, 113.00)	107.00 (102.00, 111.00)	0.007
CP (median, IQR)	65.50 (60.00, 70.00)	68.00 (66.00, 71.00)	64.00 (59.00, 70.00)	< 0.001	64.00 (60.00, 68.00)	67.00 (64.00, 68.00)	63.00 (59.00, 68.00)	0.002

IQR: Interquartile range; TF: Total frequency; EV: Energy value; IV_0: Inertia value 0°; IV_45: Inertia value 45°; IV_90: Inertia value 90°; IG_0: Inverse gap 0°; IG_45: Inverse gap 45°; IG_90: Inverse gap 90°; IG_all: Inverse gap full angle; Haralick_30: Haralick 30°; Haralick_45: Haralick 45°; Haralick_90: Haralick 90°; Haralick_all: Haralick full angle; CSV: Cluster shadow value; CP: Cluster prominence.

correlation analysis) indicates that the characteristic variables in the GLCM and LNM had a strong correlation degree ($r > 0.6$). For example, Entropy, Haralick full angle (Haralick_all), Haralick 30° (Haralick_30), Inverse gap full angle (IG_all), Inverse gap 45° (IG_45), Inverse gap 0° (IG_0), *etc.* were highly correlated with LNM. This suggests that these potential candidate variables can be used as LNM predictors and for the construction of subsequent models. Interestingly, in the subsequent models developed based on ML algorithms, we found that Entropy, Haralick_all, Haralick_30, IG_all, IG_45, IG_0, and Inertia value 45° (IV_45) occupied high weights as the top 7 GLCM-based factors (Figure 2B). Specifically, Entropy has the largest weight among these factors.

Establishment and performance evaluation of the LNM prediction model

When constructing the RFC model [training set: Areas under the ROC curve (AUC): 0.925, 95% confidence interval (CI): 0.378-1.472; testing set: AUC: 0.912, 95%CI: 0.355-1.469], we repeatedly randomly selected *N* samples from the original training set *N* to generate the new training set DT and then generate *M* DTs to form a random forest according to the above steps. As shown in Figure 3A and Supplementary Table 1, the smallest Gini index after splitting was selected, including that for Entropy, Haralick_all, Haralick_30, IG_all, IG_45, IG_0, and IV_45. Similarly, Haralick_30 and IG_all served as important weight at DT branches (training set: AUC: 0.856, 95%CI: 0.309-1.403; testing set: AUC: 0.813, 95%CI: 0.256-1.370) (Figure 3B). In the ANN model (Figure 4), the accuracy of the prediction model developed using the prediction variables in the GLCM can also reach 0.887 (95%CI: 0.340-1.434) and 0.837 (95%CI: 0.280-1.394) in the training and verification sets, respectively. Although this accuracy is slightly inferior to that of the RFC model, it is better than those of other prediction models (*i.e.*, DT, XGBoost, and SVM). Table 2, Supplementary Table 1, and Figure 5 summarize the predictive performance of ML-based models. In general, the prediction model constructed by using any ML algorithm was better than the logistic regression algorithm in predicting LNM, further confirming the superiority of ML algorithm, especially the robustness of the RFC.

Internal validation of the optimal RFC predictive model

The prediction efficiency of the RFC model was the best in the process of precise stratification of LNM patients. To further evaluate the "stratification effect" of the RFC, results of CIC analysis indicate that high-risk LNM was accurately distinguished using the RFC model, and "cross-linking" did not occur in the stratification process. The results of this model for the validation and training sets were consistent (Supplementary Table 2), implying that the robustness and LNM discrimination of the RFC model were satisfactory.

DISCUSSION

The standard treatment for early GC is surgery. However, recently, ER has become the standard local

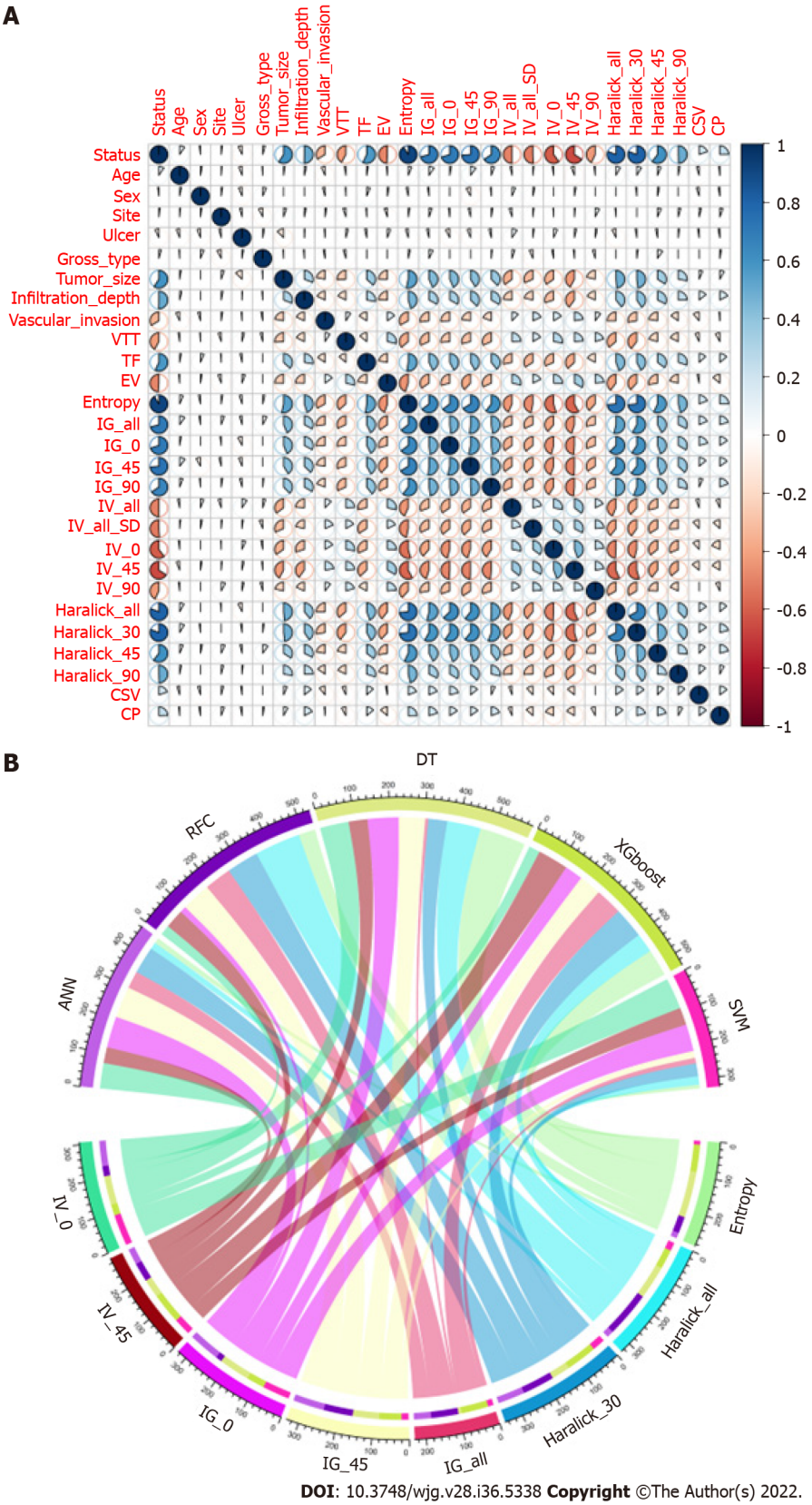

DOI: 10.3748/wjg.v28.i36.5338 **Copyright** ©The Author(s) 2022.

Figure 2 Variable screening and weight allocation. A: Correlation matrix analysis of candidate features; B: Weight distribution of candidate variables for each mL based model. RFC: Random forest classifier; SVM: Support vector machine; DT: Decision tree; ANN: Artificial neural network; XGboost: Extreme gradient boosting.

treatment for some patients with early GC without LNM[21]. For a long time, it has been used to treat differentiated-type early GC limited to the mucosa, with a diameter of < 2 cm[22,23]. Recent studies have shown that ER indications have been expanded in many studies, even including UEGC and ≤ 2 cm diameter, without ulcer or lymphatic vessel invasion[24]. However, whether UEGC can accept the

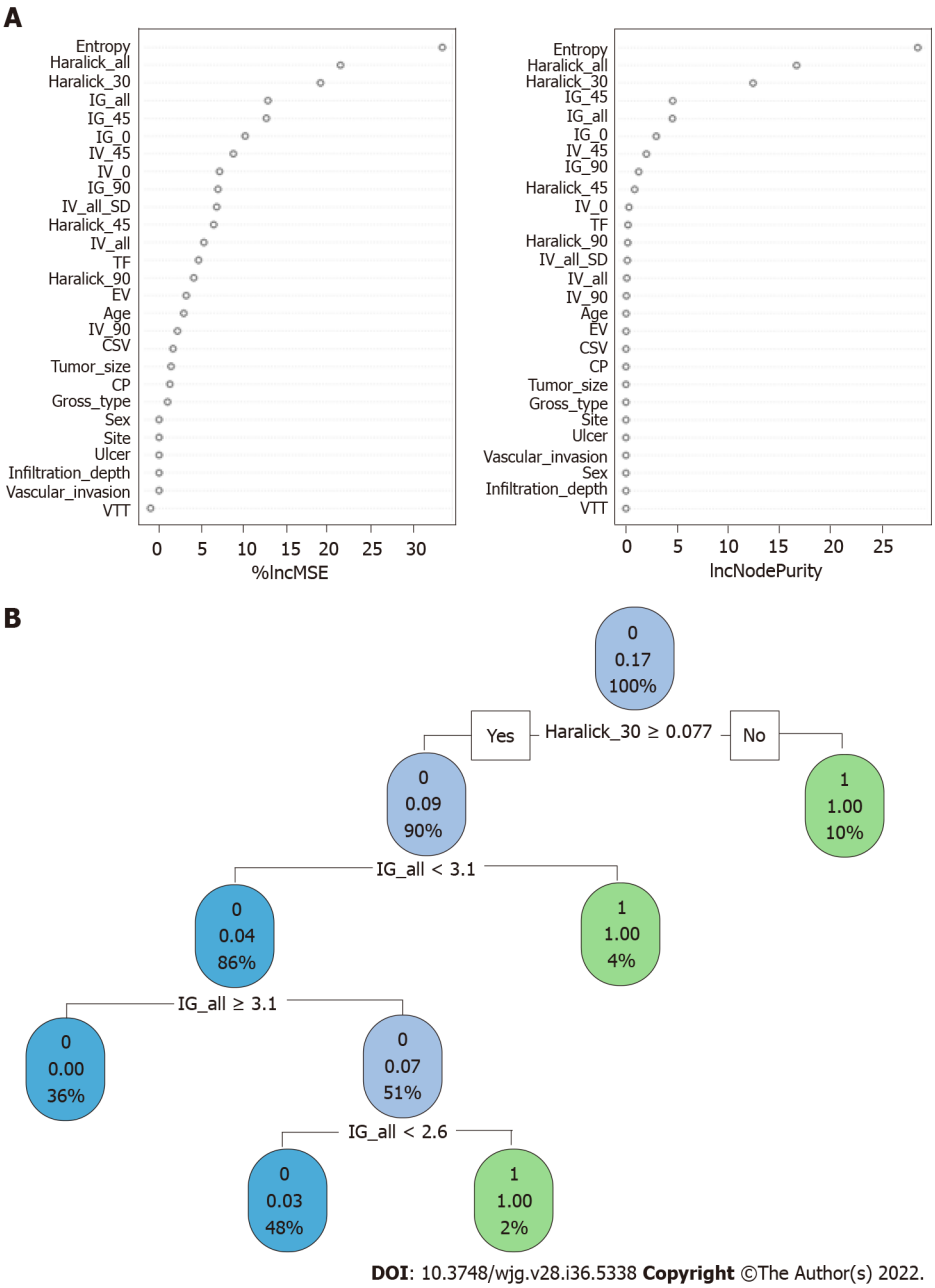

DOI: 10.3748/wjg.v28.i36.5338

Figure 3 Visualization model prediction based on machine learning based algorithm. A: Random forest classifier model; B: Decision tree model. Candidate factors associated with fracture risk are named through random forest classifier algorithm, and prediction nodes and weights are assigned by the decision tree algorithm.

standard treatment of ER remains a subject of debate. That is, additional surgery should be performed if curability is considered questionable. Given this situation, the risk factors of LNM or distant metastasis and mortality after non-curative ER of UEGC should be investigated. Previous studies have also shown that patients with two or more risk factors (*e.g.*, ulcer, submucosal invasion, and positive vertical margin) benefit greatly from surgical resection after ER that cannot be cured by UEGC[14,25]. However, due to the heterogeneity of clinical characteristics, risk stratification based on these predictions provides a simple prediction, which is challenging to apply in clinical practice.

The potential application of the GLCM in the prediction of LNM of UEGC has not been systematically explored thus far. In this study, GLCM-based features were extracted from underlying grayscale images collected through MRI. We developed an LNM risk prediction model for patients with UEGC using an ML-based algorithm. The following are the two important findings of our study. First, the accurate risk stratification of UEGC patients who should undergo additional surgery depends on the added value of the GLCM. Second, a new ML-based prediction model was used to identify patients and whether they have LNM. According to previous studies[26], texture analysis can quantify the spatial differences of pixels and the subtle differences reflected in gray values, which is consistent with the conclusion of this study. To some extent, we used GLCM features to gather spatial information and reduced the

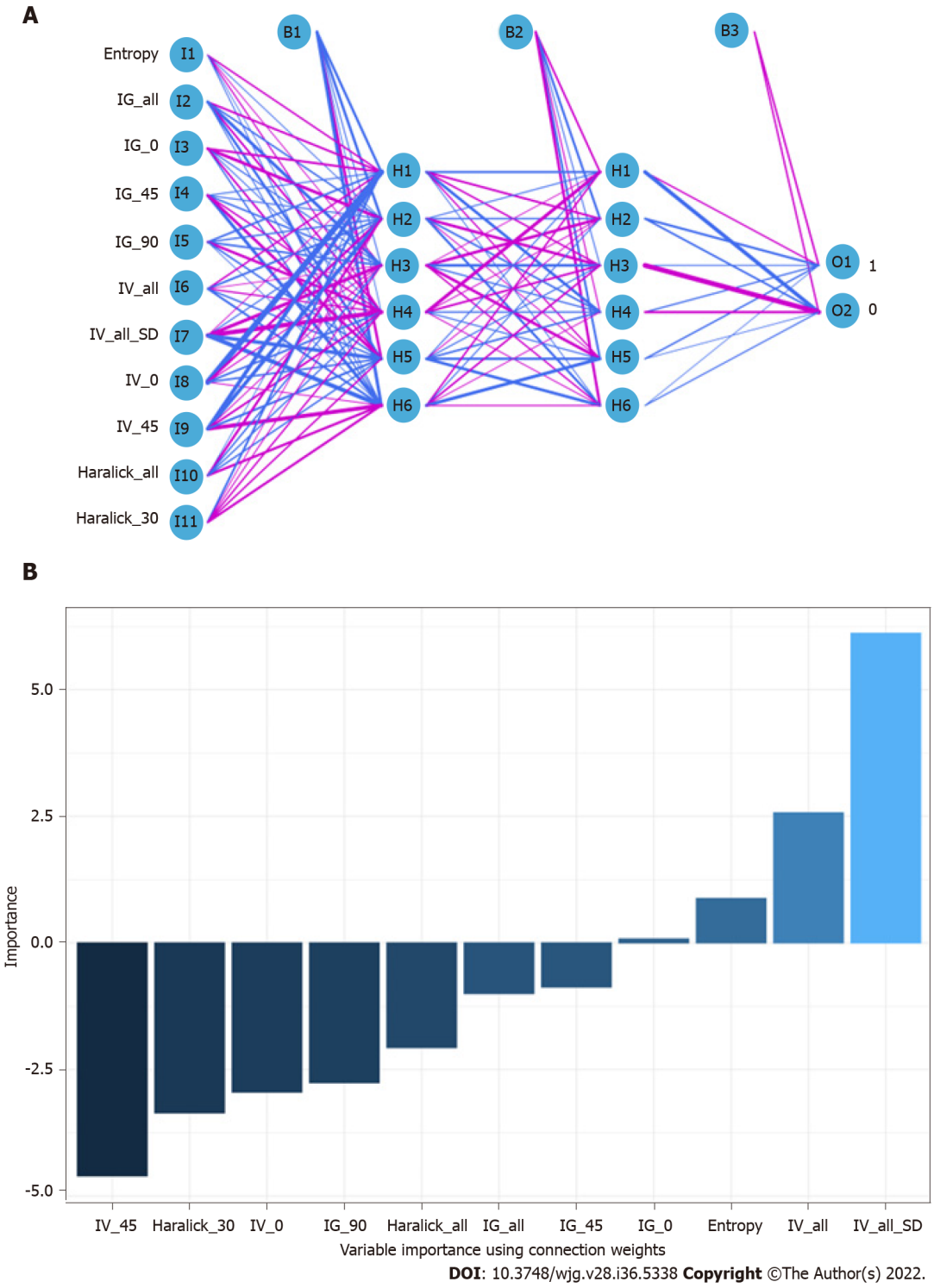

DOI: 10.3748/wjg.v28.i36.5338

Figure 4 Visualization of prediction models based on artificial neural network algorithm. A: Artificial neural network model; B: Importance of variables using connection weights. Candidate factors associated with lymph node metastasis are ordered *via* artificial neural network (ANN) algorithm and prediction nodes, and weights are assigned *via* an ANN algorithm. IV_0: Inertia value 0°; IV_45: Inertia value 45°; IG_0: Inverse gap 0°; IG_45: Inverse gap 45°; IG_all: Inverse gap full angle; Haralick_30: Haralick 30°; Haralick_all: Haralick full angle.

overfitting effect by replacing the softmax layer with the ML-based algorithm.

In this study, we created five types of ML-based models (*i.e.*, RFC, ANN, DT, XGBoost, and SVM), which used GLCM features to predict LNM. Interestingly, there were differences in the prediction efficiency obtained by ML-based models of different algorithms. For example, the RFC model had the highest predictive accuracy, which was achieved by incorporating Entropy, Haralick_all, Haralick_30, IG_all, IG_45, IG_0, and IV_45. Meanwhile, the ANN, DT, XGBoost, and SVM exhibited an inferior performance compared with the RFC. This suggests that the accuracy of the RFC in predicting LNM is superior to that of the ML model. A previous study indicated that a random forest algorithm is more

Table 2 Receiver operating characteristic curve analysis of lymph node metastasis in each mL based model

Model	Training set		Testing set		Variables[1]
	AUC mean	AUC 95%CI	AUC mean	AUC 95%CI	
RFC	0.925	0.378-1.472	0.912	0.355-1.469	Entropy, Haralick_all, Haralick_30, IG_all, IG_45, IG_0, IV_45
ANN	0.887	0.340-1.434	0.837	0.280-1.394	Entropy, IG_all, IG_0, IG_45, IG_90, IV_all, IV_all_SD, IV_0, IV_45, Haralick_all, Haralick_30
DT	0.856	0.309-1.403	0.813	0.256-1.370	Entropy, Haralick_all, Haralick_30, IG_all, IG_45, IG_0, IV_45
XGboost	0.814	0.267-1.361	0.807	0.250-1.364	Entropy, Haralick_all, Haralick_30, IG_all, IG_45, IG_0, IV_45, IG_90
SVM	0.805	0.258-1.352	0.794	0.237-1.351	Entropy, Haralick_all, Haralick_30, IG_all, IG_45, IG_0, IV_45
GLM	0.796	0.229-1.362	0.799	0.233-1.365	Entropy, Haralick_all, Haralick_30, IG_all, IG_45, IG_0, IV_45
Radiologist	0.789	0.242-1.336	0.801	0.254-1.348	-

[1]Variables are included in the model.

RFC: Random forest classifier; SVM: Support vector machine; DT: Decision tree; ANN: Artificial neural network; XGboost: Extreme gradient boosting; GLM; Generalized linear model; AUC: Area under the receiver operating characteristic curve; 95%CI: 95% confidence interval; IV_0: Inertia value 0°; IV_45: Inertia value 45°; IV_90: Inertia value 90°; IG_0: Inverse gap 0°; IG_45: Inverse gap 45°; IG_90: Inverse gap 90°; IG_all: Inverse gap full angle; Haralick_30: Haralick 30°.

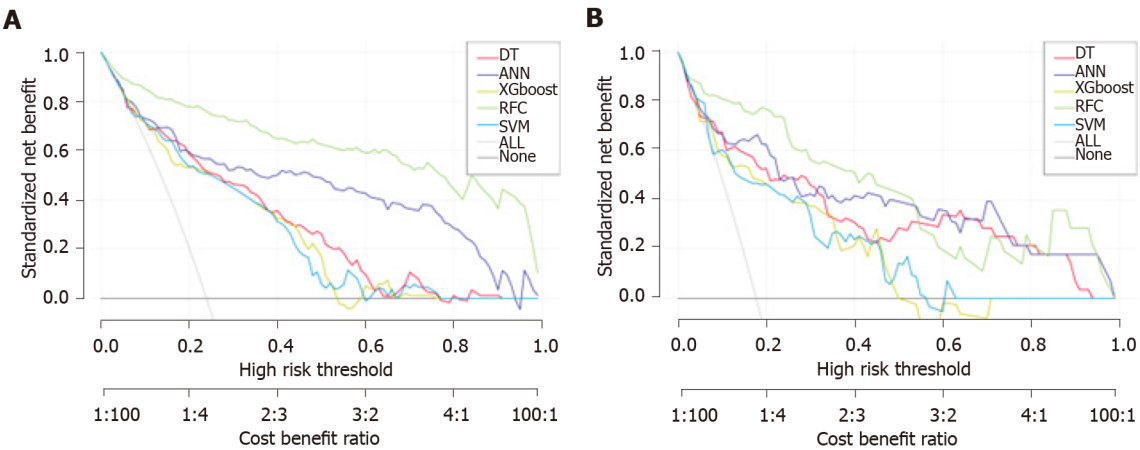

DOI: 10.3748/wjg.v28.i36.5338

Figure 5 Predictive performance of candidate models based on machine learning based algorithm. A: Decision curve analysis (DCA) for five mL based models in training sets; B: DCA for five ml based models in test sets. RFC: Random forest classifier; SVM: Support vector machine; DT: Decision tree; ANN: Artificial neural network; XGboost: Extreme gradient boosting.

efficient in processing classification problems, which is consistent with the results of this study[27]. Meanwhile, DT is not as good as the RFC in terms of fitting, and the low prediction ability of the ANN model indicates that an "overfitting" phenomenon may occur. In general, different ML models show consistent accuracy, indicating that the prediction performance of ML can be improved through data processing.

Our results confirm a GLCM-based LNM classification, which has an ideal predictive effect on the diagnosis and treatment of patients with UEGC. However, the following problems were inevitably encountered in this study. First, because this study involved a retrospective analysis, the case inclusion criteria may have a certain bias on the results, which remains to be confirmed by a large sample of prospective studies in the future. Second, there were relatively few selected cases in this study, and only some parameters of the GLCM were extracted. Thus, the results of its prediction model should be verified by external data. Third, when data from multi-center and large sample studies are available in the future, it is crucial to predict the presence or absence of LNM. Additionally, the GLCM is an important imaging sequence of UEGC, and hence we will further perform other image texture analyses

in subsequent research.

CONCLUSION

GLCM-based feature extraction could, in general, serve as a robust and promising tool to improve predictive efficiency for LNM in individual UEGC patients. ML adopts the algorithm of "classification and pruning" and clearer feature extraction, leading to better data fitting than the conventional prediction model. The model constructed using the RFC had the highest predictive accuracy, with the following being the most important predictors: Entropy, Haralick_all, Haralick_30, IG_all, IG_45, IG_0, and IV_45. In the future, we are still required to validate and optimize these prediction models using datasets of various scenarios to better apply them to clinical practice.

ARTICLE HIGHLIGHTS

Research background

Gray-level co-occurrence matrix (GLCM) based feature extraction could serve as a robust and promising tool to improve the predictive efficiency for lymph node metastasis (LNM) of individual undifferentiated early gastric cancer (UEGC) patients. Additionally, machine learning (ML) adopts more optimized algorithms and more clear feature extraction. Models built using random forest classifier (RFC) have the highest predictive accuracy in Entropy, Haralick full angle (Haralick_all), Haralick 30° (Haralick_30), Inverse gap full angle (IG_all), Inverse gap 45° (IG_45), Inverse gap 0° (IG_0), and Inertia value 45° (IV_45). Further research is needed to develop these models for clinical practice.

Research motivation

The evaluation results indicate that the method of selecting radiological and textural features becomes more effective in the discrimination of LNM from UEGC patients. In addition, an ML-based prediction model developed using RFC can be used to derive treatment options and identify LNM that can improve clinical outcomes.

Research objectives

GLCM based feature extraction significantly correlated with LNM. The top 7 GLCM based factors included Inertia value 0°, IV_45, IG_0, IG_45, IG_all, Haralick_30, Haralick_all, and Entropy. The areas under the receiver operating characteristic (ROC) curve (AUCs) of the RFC model, support vector machine (SVM), eXtreme gradient boosting (XGBoost), artificial neural network (ANN), and decision tree (DT) ranged from 0.805 [95% confidence interval (CI): 0.258-1.352] to 0.925 (95%CI: 0.378-1.472) in the training set and from 0.794 (95%CI: 0.237-1.351) to 0.912 (95%CI: 0.355-1.469) in the testing set, respectively. The RFC (training set: AUC: 0.925, 95%CI: 0.378-1.472; testing set: AUC: 0.912, 95%CI: 0.355-1.469) model incorporating Entropy, Haralick_all, Haralick_30, IG_all, IG_45, IG_0, and IV_45 had the highest predictive accuracy.

Research methods

We retrospectively selected 526 cases of UEGC confirmed by pathological examination after radical gastrectomy without endoscopic treatment in four tertiary hospitals between January 2015 to December 2021. GLCM-based features were extracted from grayscale images and ML was applied to the classification of candidate predictive variables. In order to evaluate robustness and clinical utility of each model, the following were made: ROC, decision curve analysis, and clinical impact curve.

Research results

Identifying a potential biomarker that predicts LNM is proven to be very useful in determining treatment.

Research conclusions

To develop a ML-based integral procedure to construct the LNM gray level co-occurrence matrix (GLCM) prediction model.

Research perspectives

The risk of LNM is the most important consideration in determining treatment strategies for UEGC. Therefore, identifying a potential biomarker that predicts LNM is proven to be very useful in determining treatment.

ACKNOWLEDGEMENTS

The authors thank all study participants for consenting to the use of their medical records.

FOOTNOTES

Author contributions: Yu J and Wei X conceived and designed the study and wrote the manuscript; Yan XJ, Guo YY, Zhang J, Wang GR, and Arsalan F collected the data, performed the data analysis, and interpreted the outcomes; and all authors critically reviewed the content of the manuscript and helped with the drafts.

Supported by the General Project-Social Development Field of Shaanxi Province Science and Technology Department, No. 2021SF-313; and Innovation Capability Support Plan of Shaanxi Science and Technology Department - Science and Technology Innovation Team, No. 2020TD-048.

Institutional review board statement: This study was approved by the Institutional Review Committee of Shaanxi Provincial People's Hospital (2021-Y024).

Informed consent statement: Written informed consent was not required given the retrospective nature of the study from chart review.

Conflict-of-interest statement: All the authors report no relevant conflicts of interest for this article.

Data sharing statement: No additional data are available.

STROBE statement: The authors have read the STROBE Statement-a checklist of items is provided. The manuscript was prepared and revised according to the STROBE Statement-a checklist of items is provided.

Country/Territory of origin: China

ORCID number: Jiao Yu 0000-0002-8707-8606.

S-Editor: Wang JJ
L-Editor: A
P-Editor: Wang JJ

REFERENCES

1 **Puliga E**, Corso S, Pietrantonio F, Giordano S. Microsatellite instability in Gastric Cancer: Between lights and shadows. *Cancer Treat Rev* 2021; **95**: 102175 [PMID: 33721595 DOI: 10.1016/j.ctrv.2021.102175]
2 **Karimi P**, Islami F, Anandasabapathy S, Freedman ND, Kamangar F. Gastric cancer: descriptive epidemiology, risk factors, screening, and prevention. *Cancer Epidemiol Biomarkers Prev* 2014; **23**: 700-713 [PMID: 24618998 DOI: 10.1158/1055-9965.EPI-13-1057]
3 **Lee A**, Chung H. Endoscopic Resection of Undifferentiated-type Early Gastric Cancer. *J Gastric Cancer* 2020; **20**: 345-354 [PMID: 33425437 DOI: 10.5230/jgc.2020.20.e37]
4 **Horiuchi Y**, Fujisaki J, Yamamoto N, Ishizuka N, Ishiyama A, Yoshio T, Hirasawa T, Yamamoto Y, Nagahama M, Takahashi H, Tsuchida T. Undifferentiated-type predominant mixed-type early gastric cancer is a significant risk factor for requiring additional surgeries after endoscopic submucosal dissection. *Sci Rep* 2020; **10**: 6748 [PMID: 32317768 DOI: 10.1038/s41598-020-63781-3]
5 **Ono H**, Kondo H, Gotoda T, Shirao K, Yamaguchi H, Saito D, Hosokawa K, Shimoda T, Yoshida S. Endoscopic mucosal resection for treatment of early gastric cancer. *Gut* 2001; **48**: 225-229 [PMID: 11156645 DOI: 10.1136/gut.48.2.225]
6 **Lee JH**, Kim JJ. Endoscopic mucosal resection of early gastric cancer: Experiences in Korea. *World J Gastroenterol* 2007; **13**: 3657-3661 [PMID: 17659722 DOI: 10.3748/wjg.v13.i27.3657]
7 **Ohkuwa M**, Hosokawa K, Boku N, Ohtu A, Tajiri H, Yoshida S. New endoscopic treatment for intramucosal gastric tumors using an insulated-tip diathermic knife. *Endoscopy* 2001; **33**: 221-226 [PMID: 11293753 DOI: 10.1055/s-2001-12805]
8 **Zhao X**, Cai A, Xi H, Chen L, Peng Z, Li P, Liu N, Cui J, Li H. Predictive Factors for Lymph Node Metastasis in Undifferentiated Early Gastric Cancer: a Systematic Review and Meta-analysis. *J Gastrointest Surg* 2017; **21**: 700-711 [PMID: 28120275 DOI: 10.1007/s11605-017-3364-7]

9 **Kato M**, Nishida T, Yamamoto K, Hayashi S, Kitamura S, Yabuta T, Yoshio T, Nakamura T, Komori M, Kawai N, Nishihara A, Nakanishi F, Nakahara M, Ogiyama H, Kinoshita K, Yamada T, Iijima H, Tsujii M, Takehara T. Scheduled endoscopic surveillance controls secondary cancer after curative endoscopic resection for early gastric cancer: a multicentre retrospective cohort study by Osaka University ESD study group. *Gut* 2013; **62**: 1425-1432 [PMID: 22914298 DOI: 10.1136/gutjnl-2011-301647]

10 **Hahn KY**, Park JC, Kim EH, Shin S, Park CH, Chung H, Shin SK, Lee SK, Lee YC. Incidence and impact of scheduled endoscopic surveillance on recurrence after curative endoscopic resection for early gastric cancer. *Gastrointest Endosc* 2016; **84**: 628-638.e1 [PMID: 26996290 DOI: 10.1016/j.gie.2016.03.1404]

11 **Nasu J**, Doi T, Endo H, Nishina T, Hirasaki S, Hyodo I. Characteristics of metachronous multiple early gastric cancers after endoscopic mucosal resection. *Endoscopy* 2005; **37**: 990-993 [PMID: 16189772 DOI: 10.1055/s-2005-870198]

12 **Nakajima T**, Oda I, Gotoda T, Hamanaka H, Eguchi T, Yokoi C, Saito D. Metachronous gastric cancers after endoscopic resection: how effective is annual endoscopic surveillance? *Gastric Cancer* 2006; **9**: 93-98 [PMID: 16767364 DOI: 10.1007/s10120-006-0372-9]

13 **Kawata N**, Kakushima N, Takizawa K, Tanaka M, Makuuchi R, Tokunaga M, Tanizawa Y, Bando E, Kawamura T, Sugino T, Kusafuka K, Shimoda T, Nakajima T, Terashima M, Ono H. Risk factors for lymph node metastasis and long-term outcomes of patients with early gastric cancer after non-curative endoscopic submucosal dissection. *Surg Endosc* 2017; **31**: 1607-1616 [PMID: 27495338 DOI: 10.1007/s00464-016-5148-7]

14 **Suzuki H**, Oda I, Abe S, Sekiguchi M, Nonaka S, Yoshinaga S, Saito Y, Fukagawa T, Katai H. Clinical outcomes of early gastric cancer patients after noncurative endoscopic submucosal dissection in a large consecutive patient series. *Gastric Cancer* 2017; **20**: 679-689 [PMID: 27722825 DOI: 10.1007/s10120-016-0651-z]

15 **Hirasawa T**, Gotoda T, Miyata S, Kato Y, Shimoda T, Taniguchi H, Fujisaki J, Sano T, Yamaguchi T. Incidence of lymph node metastasis and the feasibility of endoscopic resection for undifferentiated-type early gastric cancer. *Gastric Cancer* 2009; **12**: 148-152 [PMID: 19890694 DOI: 10.1007/s10120-009-0515-x]

16 **Donders AR**, van der Heijden GJ, Stijnen T, Moons KG. Review: a gentle introduction to imputation of missing values. *J Clin Epidemiol* 2006; **59**: 1087-1091 [PMID: 16980149 DOI: 10.1016/j.jclinepi.2006.01.014]

17 **Carpenter JR**, Smuk M. Missing data: A statistical framework for practice. *Biom J* 2021; **63**: 915-947 [PMID: 33624862 DOI: 10.1002/bimj.202000196]

18 **Luo W**, Phung D, Tran T, Gupta S, Rana S, Karmakar C, Shilton A, Yearwood J, Dimitrova N, Ho TB, Venkatesh S, Berk M. Guidelines for Developing and Reporting Machine Learning Predictive Models in Biomedical Research: A Multidisciplinary View. *J Med Internet Res* 2016; **18**: e323 [PMID: 27986644 DOI: 10.2196/jmir.5870]

19 **Fan J**, Lv J. A Selective Overview of Variable Selection in High Dimensional Feature Space. *Stat Sin* 2010; **20**: 101-148 [PMID: 21572976]

20 **Armstrong RA**. When to use the Bonferroni correction. *Ophthalmic Physiol Opt* 2014; **34**: 502-508 [PMID: 24697967 DOI: 10.1111/opo.12131]

21 **Goto O**, Fujishiro M, Kodashima S, Ono S, Omata M. Outcomes of endoscopic submucosal dissection for early gastric cancer with special reference to validation for curability criteria. *Endoscopy* 2009; **41**: 118-122 [PMID: 19214889 DOI: 10.1055/s-0028-1119452]

22 **Gotoda T**, Yanagisawa A, Sasako M, Ono H, Nakanishi Y, Shimoda T, Kato Y. Incidence of lymph node metastasis from early gastric cancer: estimation with a large number of cases at two large centers. *Gastric Cancer* 2000; **3**: 219-225 [PMID: 11984739 DOI: 10.1007/pl00011720]

23 **Kojima T**, Parra-Blanco A, Takahashi H, Fujita R. Outcome of endoscopic mucosal resection for early gastric cancer: review of the Japanese literature. *Gastrointest Endosc* 1998; **48**: 550-4; discussion 554 [PMID: 9831855 DOI: 10.1016/s0016-5107(98)70108-7]

24 **Soetikno R**, Kaltenbach T, Yeh R, Gotoda T. Endoscopic mucosal resection for early cancers of the upper gastrointestinal tract. *J Clin Oncol* 2005; **23**: 4490-4498 [PMID: 16002839 DOI: 10.1200/JCO.2005.19.935]

25 **Kim ER**, Lee H, Min BH, Lee JH, Rhee PL, Kim JJ, Kim KM, Kim S. Effect of rescue surgery after non-curative endoscopic resection of early gastric cancer. *Br J Surg* 2015; **102**: 1394-1401 [PMID: 26313295 DOI: 10.1002/bjs.9873]

26 **Naik A**, Edla DR, Dharavath R. Prediction of Malignancy in Lung Nodules Using Combination of Deep, Fractal, and Gray-Level Co-Occurrence Matrix Features. *Big Data* 2021; **9**: 480-498 [PMID: 34191590 DOI: 10.1089/big.2020.0190]

27 **Li J**, Tian Y, Zhu Y, Zhou T, Li J, Ding K. A multicenter random forest model for effective prognosis prediction in collaborative clinical research network. *Artif Intell Med* 2020; **103**: 101814 [PMID: 32143809 DOI: 10.1016/j.artmed.2020.101814]

World Journal of Gastroenterology

Submit a Manuscript: https://www.f6publishing.com

World J Gastroenterol 2022 September 28; 28(36): 5351-5363

DOI: 10.3748/wjg.v28.i36.5351

ISSN 1007-9327 (print) ISSN 2219-2840 (online)

ORIGINAL ARTICLE

Observational Study

Early extrahepatic recurrence as a pivotal factor for survival after hepatocellular carcinoma resection: A 15-year observational study

Jae Hyun Yoon, Sung Kyu Choi, Sung Bum Cho, Hee Joon Kim, Yang Seok Ko, Chung Hwan Jun

Specialty type: Gastroenterology and hepatology

Provenance and peer review: Unsolicited article; Externally peer reviewed.

Peer-review model: Single blind

Peer-review report's scientific quality classification

Grade A (Excellent): 0
Grade B (Very good): B, B
Grade C (Good): C
Grade D (Fair): 0
Grade E (Poor): 0

P-Reviewer: Ding J, China; Manrai M, India; Posa A, Italy

Received: May 11, 2022
Peer-review started: May 11, 2022
First decision: August 1, 2022
Revised: August 11, 2022
Accepted: September 8, 2022
Article in press: September 8, 2022
Published online: September 28, 2022

Jae Hyun Yoon, Sung Kyu Choi, Department of Gastroenterology and Hepatology, Chonnam National University Hospital and College of Medicine, Gwangju 61469, South Korea

Sung Bum Cho, Department of Gastroenterology and Hepatology, Hwasun Chonnam National University Hospital and College of Medicine, Hwasun 58128, South Korea

Hee Joon Kim, Department of Surgery, Chonnam National University Hospital and College of Medicine, Gwangju 61469, South Korea

Yang Seok Ko, Department of Surgery, Hwasun Chonnam National University Hospital and College of Medicine, Hwasun 58128, South Korea

Chung Hwan Jun, Department of Internal Medicine, Mokpo Hankook Hospital, Mokpo 58643, South Korea

Corresponding author: Sung Kyu Choi, MD, PhD, Professor, Department of Gastroenterology and Hepatology, Chonnam National University Hospital and College of Medicine, Jebongroe 42, Gwangju 61469, South Korea. choisk@jnu.ac.kr

Abstract

BACKGROUND

Surgical resection is one of the most widely used modalities for the treatment of hepatocellular carcinoma (HCC). Early extrahepatic recurrence (EHR) of HCC after surgical resection is considered to be closely associated with poor prognosis. However, data regarding risk factors and survival outcomes of early EHR after surgical resection remain scarce.

AIM

To investigate the clinical features and risk factors of early EHR and elucidate its association with survival outcomes.

METHODS

From January 2004 to December 2019, we enrolled treatment-naïve patients who were ≥ 18 years and underwent surgical resection for HCC in two tertiary academic centers. After excluding patients with tumor types other than HCC and/or ineligible data, this retrospective study finally included 779 patients. Surgical resection of HCC was performed according to the physicians' decisions and the EHR was diagnosed based on contrast-enhanced computed tomography

or magnetic resonance imaging, and pathologic confirmation was performed in selected patients. Multivariate Cox regression analysis was performed to identify the variables associated with EHR.

RESULTS

Early EHR within 2 years after surgery was diagnosed in 9.5% of patients during a median follow-up period of 4.4 years. The recurrence-free survival period was 5.2 mo, and the median time to EHR was 8.8 mo in patients with early EHR. In 52.7% of patients with early EHR, EHR occurred as the first recurrence of HCC after surgical resection. On multivariate analysis, serum albumin < 4.0 g/dL, serum alkaline phosphatase > 100 U/L, surgical margin involvement, venous and/or lymphatic involvement, satellite nodules, tumor necrosis detected by pathology, tumor size ≥ 7 cm, and macrovascular invasion were determined as risk factors associated with early EHR. After sub-categorizing the patients according to the number of risk factors, the rates of both EHR and survival showed a significant correlation with the risk of early EHR. Furthermore, multivariate analysis revealed that early EHR was associated with substantially worse survival outcomes (Hazard ratio, 6.77; 95% confidence interval, 4.81-9.52; $P < 0.001$).

CONCLUSION

Early EHR significantly deteriorates the survival of patients with HCC, and our identified risk factors may predict the clinical outcomes and aid in postoperative strategies for improving survival.

Key Words: Early extrahepatic recurrence; Hepatocellular carcinoma; Prognosis; Surgery; Survival

Core Tip: Surgical resection of hepatocellular carcinoma is effective and curative treatment modality. However, early extrahepatic recurrence (EHR) after resection is related to poor prognosis. This study indicates the close correlation between the early EHR and survival outcome (hazard ratio 6.77, 95% confidence interval 4.81-9.52). The time to EHR was 8.8 mo and in 52.7% of early EHR group, EHR occurred as the first recurrence. On multivariate analysis, serum albumin < 4.0 g/dL, serum alkaline phosphatase > 100 U/L, surgical margin involvement, venous and/or lymphatic involvement, satellite nodules, tumor necrosis, tumor size ≥ 7 cm, and macrovascular invasion were associated risk factors with early EHR.

Citation: Yoon JH, Choi SK, Cho SB, Kim HJ, Ko YS, Jun CH. Early extrahepatic recurrence as a pivotal factor for survival after hepatocellular carcinoma resection: A 15-year observational study. *World J Gastroenterol* 2022; 28(36): 5351-5363

URL: https://www.wjgnet.com/1007-9327/full/v28/i36/5351.htm

DOI: https://dx.doi.org/10.3748/wjg.v28.i36.5351

INTRODUCTION

Surgical resection remains one of the best options for treating early hepatocellular carcinoma (HCC), along with liver transplantation and radiofrequency ablation[1-3]. With the development of surgical techniques and medical devices, surgical resection of tumors has been performed for a wide spectrum of patients with HCC. Nonetheless, HCC recurrence after surgery leads to an unfavorable prognosis and is still a major issue, with the 2-year recurrence rate ranging from 30.0% to 43.0%[4,5].

HCC recurrence after surgical resection mostly occurs inside the liver (intrahepatic), but recurrence outside the liver (extrahepatic) can also occur[2,6]. Most cases of extrahepatic recurrence (EHR) of HCC generally have an aggressive phenotype, and this contributes to poor survival outcomes[7]. Taketomi *et al*[6] reported the 3-, 5-, and 10-year cumulative survival rates of EHR as 60.3%, 24.0%, and 6.0%, respectively, which were lower than those in patients with intrahepatic recurrence (IHR) (74.5%, 57.7%, and 23.1%, respectively; $P = 0.004$). Although IHR of HCC can be managed by various loco-regional treatment modalities and systemic therapies, there are only limited methods for the treatment of EHR. However, despite an expected poor prognosis, favorable outcomes in selected patients with limited EHR have been reported with treatment modalities, such as metastasectomy[8]. Therefore, predicting the risk of EHR is essential, and better outcomes can be accomplished by predicting high-risk patients and monitoring these patients with close follow-up surveillance for early detection of EHR and/or timely postoperative adjuvant therapy.

We have reported simple parameters for predicting EHR after hepatectomy[9], and in that study, approximately 49.2% of the patients with EHR (31 of 63 patients) showed early EHR and demonstrated poorer recurrence-free survival (RFS) and overall survival rates. There have been many reports regarding the risk factors and predictive models for early recurrence mostly concerning IHR of HCC after surgery[10-12]; however, there are limited data regarding the risk factors and survival outcomes related to early EHR after surgical resection of HCC. Moreover, the clinical characteristics and survival outcomes of patients with early EHR in comparison with those with a later onset of EHR have not been examined. Hence, we aimed to investigate the characteristics and potential risk factors of early EHR after curative surgical resection for HCC and explore the relationship between early EHR and survival outcomes.

MATERIALS AND METHODS

Patients

This study enrolled 890 patients who underwent surgery for HCC from January 2004 to December 2019 at two tertiary hospitals. Patients with tumor types other than HCC, previous treatment experience, and ineligible data were excluded. Finally, 779 patients were enrolled for this study and were analyzed. Surgical resection of HCC was determined by a physician's decision regarding the tumor stage, liver function, and the patient's physical status. There had been no changes in the keynote of surgical resection during the study period in both centers. To exclude potential bias regarding surgical technique and concentrate on EHR development and survival rate based on tumor findings, patients who developed EHR prior to the completion of the post-surgical duration of 60 d were excluded.

Baseline HCC staging, surgical resection, and follow-up

HCC was diagnosed according to the guidelines of the Korean Liver Cancer Study Group and the National Cancer Center[13]. HCC staging at the time of diagnosis was determined using the modified Union for International Cancer Control (mUICC) staging system[14] and the Barcelona Clinic Liver Cancer (BCLC) classification system[3]. Milan criteria were based on radiologic findings at initial the diagnosis of HCC[15]. Abdominal computed tomography (CT) or magnetic resonance imaging (MRI) and assessment of serological tumor markers were routinely performed 1 mo after surgical resection and at each 3-6-month follow-up visit.

The tumor sizes were measured by radiologic modalities with CT or MRI. The histological differentiation of HCC was graded according to the criteria of Edmondson and Steiner[16]. The presence of macrovascular invasion was defined as vascular invasion of HCC detected on CT imaging or MRI while microvascular invasion was defined as invasion of vascular structures on microscopic analysis of resected tumor specimens. Lymph node metastasis, serosal invasion, bile duct invasion, capsule formation, multicentricity, satellite nodule, intrahepatic metastasis, tumor necrosis, tumor hemorrhage, and fatty changes within tumors were all confirmed from pathological findings of resected specimens. Overall survival was defined as the time interval in days between the date of diagnosis of HCC and the date of death or last follow-up examination. The cause of death of each patient is presented in Supplementary Table 1.

Diagnosis of recurrence and EHR

The diagnosis of EHR was confirmed by contrast-enhanced CT or MRI, and pathological examination was performed only for selected patients as decided by the physician. In addition, chest radiographs, bone scintigraphy, positron emission tomography-CT, and brain MR or CT imaging were used when new signs suggesting tumor metastasis manifested. Early EHR was defined as EHR that developed within 2 years after initial surgical resection. Most cases of EHR were diagnosed during the routine follow-up studies, with a few cases diagnosed during the evaluation of new-onset symptoms or based on significant elevation in alpha-fetoprotein (AFP) or serial AFP elevation without definite intra-hepatic lesions.

Ethics statement

This study was approved by the Institutional Review Board of Chonnam National University Hospital (IRB No. CNUH-2019-203). Because of the retrospective design of our study and the use of de-identified data, the requirement for informed consent was waived under the approval of the Institutional Review Board of Chonnam National University Hospital. The study was performed in compliance with the tenets of the 1975 Helsinki Declaration.

Statistical analysis

The data are presented as means ± SD or as medians and ranges, as appropriate, for the data type and distribution. Univariate analyses were performed using the chi-squared test or Student's *t*-test, as appropriate. Variables with a P value of < 0.05 on univariate analyses were included in a multivariate

logistic regression analysis to identify factors predictive of EHR. A multivariate Cox regression model was built using a stepwise backward selection of variables, and variables with a P value of < 0.05 were retained as predictive factors. The risk levels of EHR were defined based on the number of risk factors present, and Kaplan-Meier survival curves were constructed for each risk level. All statistical analyses were performed using SPSS software version 27.0 (IBM Corp., Armonk, NY, United States). The statistical methods of this study were reviewed by Cho Hee Hwang from the Biomedical research institute of Chonnam National University Hospital.

RESULTS

Baseline characteristics of the enrolled patients

The baseline characteristics of patients with early EHR were assessed (Table 1). These patients were younger, had lower serum albumin levels, and higher initial serum AFP concentration > 400 (IU/mL) than those without early EHR. Additionally, patients with early EHR showed more advanced tumor stage with respect to tumor size, BCLC stage, mUICC stage, and beyond Milan criteria. The patients in the early EHR group presented higher rates of macrovascular invasion and longer duration of hospital stay after liver resection. Furthermore, when we subdivided the patients into those without EHR, those with non-early EHR, and those with early EHR, the following factors exhibited a close relationship to the interval of EHR development: younger age, ALP levels, albumin levels, preoperative serum AFP > 1500 IU/mL, tumor size, tumor numbers, tumor stages, and the presence of macrovascular invasion (Supplementary Table 2).

Comparison of clinicopathological findings and clinical outcomes

We analyzed the surgical findings of tumor specimens categorized by the presence of early EHR (Table 2). Patients with early EHR had more metastatic lymph nodes, microvascular invasion, and satellite nodules (0.1% *vs* 4.1%, 16.3% *vs* 44.6%, and 12.2% *vs* 23.0%, respectively). Furthermore, the tumor specimens in the early EHR group showed a higher probability of tumor necrosis, hemorrhages, and absence of fatty changes (41.5% *vs* 82.4%, 43.0% *vs* 62.2%, and 36.0% *vs* 20.5%, respectively). On subgroup analysis stratifying patients with EHR into the early EHR and non-early EHR groups, microvascular invasion, serosal invasion, presence of satellite nodules, tumor necrosis, hemorrhages, and absence of fatty changes still showed consistent significance (Supplementary Table 3).

When comparing the findings on the first recurrence between the early and non-early EHR groups, the proportion of patients with serum AFP > 400 IU/mL was higher (10.2% *vs* 31.0%, P < 0.001) (Table 2) and the RFS was shorter (32.4 *vs* 5.21 mo, P < 0.001) in the early EHR group. These trends for serum AFP and RFS also showed consistency when we compared all patients with non-early EHR and early EHR (Supplementary Table 1). Furthermore, the mUICC stage at first recurrence was more advanced in the early EHR group (38.7% *vs* 75.7% with mUICC stage ≥ 3, P < 0.001), and 52.7% of patients developed EHR as the first recurrence after surgical resection.

Analysis of factors associated with early EHR

We performed Cox regression analysis to assess multiple factors relevant to EHR after surgical resection of HCC (Table 3). Among various risk factors, eight were proven to be closely associated with EHR, including serum albumin < 4.0 g/dL [Hazard ratio (HR), 2.12; P < 0.001], serum ALP > 100 U/L (HR, 1.586; P = 0.018), surgical margin involvement (HR, 2.53; P = 0.032), venous and/or lymphatic involvement (HR, 1.900; P = 0.002), satellite nodules (HR, 1.73; P = 0.011), tumor necrosis (HR, 1.92; P = 0.001), sum of tumor size ≥ 7 cm (HR, 1.84; P = 0.004), and macrovascular invasion (HR, 2.30; P = 0.008).

Analysis of factors associated with overall survival

We conducted Cox regression analysis to determine the risk factors associated with survival after surgical resection of HCC and to assess the relationship between early EHR and survival. On multivariate analysis, serum albumin < 4.0 g/dL (HR, 2.44; P < 0.001), serum ALP > 100 U/L (HR, 1.61; P = 0.001), major Edmondson-Steiner grade ≥ 3 (HR, 1.45; P = 0.008), pathological mUICC stage III or IVa (HR, 1.63; P = 0.002), satellite nodules (HR, 1.92; P < 0.011), tumor necrosis (HR, 1.35; P = 0.030), and early EHR (HR, 6.77; P < 0.001) were identified as factors related to survival outcome.

Cumulative rates of early EHR and overall survival

Among the 779 patients enrolled, 136 (17.5%) developed EHR during a median follow-up period of 4.41 years, and 74 (54.4%) exhibited early EHR after surgical resection of HCC. Both the cumulative rates of recurrence and the overall survival rates after surgical resection of HCC showed stepwise correlations with the interval to EHR (Figure 1). The 1-, 3-, 5-, and 10-year cumulative rates of recurrence were 15.8%, 35.4%, 46.5%, and 60.1% in the non-EHR group and were 32.3%, 64.5%, 85.5%, and 100.0% in the non-early EHR group. The early EHR group had a 1-year recurrence rate of 83.8% and 100.0% from the 2nd year after surgical resection (Figure 1A). The 1-, 3-, 5-, and 10-year cumulative rates of overall

Table 1 Baseline characteristics of the enrolled patients

	Patients without early EHR (*n* = 705)	Patients with early EHR (*n* = 74)	*P* value
Age (yr)	59.49 ± 10.08	56.51 ± 10.37	**0.020**
Male sex (*n*, %)	603 (85.5)	64 (86.5)	0.824
BMI (kg/m^2)	23.89 ± 3.03	24.10 ± 2.98	0.790
Etiology of hepatitis, *n* (%)			0.569
HBV/HCV	425 (63.2)/55 (8.2)	53 (73.6)/8 (11.1)	
Alcohol/combined	40 (10.4)/49 (7.0)	5 (6.9)/2 (2.8)	
NASH/unknown	1 (0.1)/73 (10.8)	0/4 (5.6)	
ALP (U/L)	89.25 ± 44.04	113.23 ± 106.76	0.059
Albumin (mg/dL)	4.36 ± 0.45	4.19 ± 0.48	**0.002**
ALBI grade ≥ 2, *n* (%)	97 (13.8)	16 (21.9)	0.063
ICG R15	12.02 ± 7.29	12.58 ± 7.62	0.566
Preoperative serum AFP > 400 (IU/mL)	127 (18.6)	24 (32.9)	**0.004**
Sum of tumor size	4.17 ± 2.44	6.06 ± 3.38	**< 0.001**
Tumor numbers	1.19 ± 0.54	1.32 ± 0.82	0.176
BCLC stage, *n* (%)			**< 0.001**
0/A/≥ B	89 (12.7)/491 (69.9)/122 (17.4)	3 (4.1)/44 (59.5)/27 (36.5)	
Pathological mUICC stage, *n* (%)			**< 0.001**
I/II/≥ III	111 (15.8)/431 (61.4)/160 (22.8)	2 (2.7)/32 (43.2)/40 (54.1)	
Radiological mUICC stage, *n* (%)			**< 0.001**
I/II/≥ III	112 (15.9%)/463 (66.0%)/127 (18.1%)	4 (5.4)/43 (58.1)/27 (36.5)	
Beyond Milan criteria, *n* (%)	179 (25.4)	40 (54.1)	**< 0.001**
Macrovascular invasion, *n* (%)	32 (4.6)	11 (14.9)	**< 0.001**
Hospital stay, days (median, range)	13.3 ± 7.1	15.6 ± 75.6	**0.049**
Follow-up duration, years (median, range)	4.8 (0.23-15.36)	1.8 (0.31-1.43)	**< 0.001**

Values are presented as mean ± SD. SD: Standard deviation; EHR: Extrahepatic recurrence; BMI: Body mass index; HBV: Hepatitis B virus; HCV: Hepatitis C virus; AST: Aspartate transaminase; ALT: Alanine transaminase; ALP: Alkaline phosphatase; AFP: Alpha-fetoprotein; BCLC: Barcelona Clinic Liver Cancer; mUICC: Modified Union for International Cancer Control.

survival were as follows: 97.8%, 90.2%, 80.9%, and 66.8% for the non-EHR group; 100.0%, 90.3%, 67.2%, and 9.9% for the non-early EHR group; and 74.9%, 23.0%, 15.2%, and 10.8% for the early EHR group (Figure 1B).

Cumulative rates of early EHR and survival categorized by risk factors

Depending on the eight factors proven to be associated with early EHR, we categorized the patients according to the number of risk factors. The cumulative rates of early EHR onset and survival were analyzed in the sub-categorized patients, and both rates showed stepwise correlations according to the number of risk factors (Figure 2A and B). Consequently, we stratified the patients into three categories: a low-risk group with 0-1 risk factor, an intermediate-risk group with 2-3 risk factors, and a high-risk group with ≥ 4 risk factors. The rates of EHR and survival exhibited a significant correlation with the risk stratification model (Figure 2C and D). The 1-, 2-, 3-, 5-, and 10-year cumulative rates of EHR in each group were as follows: 0.5%, 2.0%, 3.4%, 6.2%, and 16.8% in the low-risk group; 10.3%, 16.1%, 18.6%, 23.8%, and 42.8% in the intermediate-risk group; and 31.7%, 44.0%, 50.2%, 66.2%, and 77.5% in the high-risk group. The 1-, 3-, 5-, and 10-year overall survival rates in each group were as follows: 98.9%, 94.7%, 89.5%, and 70.0% in the low-risk group; 93.9%, 75.7%, 59.3%, and 38.1% in the intermediate-risk group; and 78.8%, 47.7%, 31.2%, and 12.5% in the high-risk group.

Table 2 Comparison of surgical findings and clinical outcomes in patients with and without extrahepatic recurrence

	Patients without early EHR (*n* = 705)	Patients with early EHR (*n* = 74)	*P* value
Margin involvement, *n* (%)	16 (2.3%)	4 (5.5%)	0.104
Metastatic lymph nodes, *n* (%)	1 (0.1)	3 (4.1)	**< 0.001**
Microvascular invasion, *n* (%)	114 (16.3)	33 (44.6)	**< 0.001**
Serosal invasion, *n* (%)	13 (1.9)	4 (5.4)	0.052
Bile duct invasion, *n* (%)	9 (1.3)	1 (1.4)	0.975
Capsule formation, *n* (%)	456 (66.7)	53 (71.6)	0.389
Multicentricity, *n* (%)	54 (7.8)	8 (10.8)	0.372
Satellite nodule, *n* (%)	84 (12.2)	17 (23.0)	**0.009**
Intrahepatic metastasis, *n* (%)	8 (1.2)	2 (2.7)	0.268
Necrosis, *n* (%)	286 (41.5)	61 (82.4)	**< 0.001**
Haemorrhage, *n* (%)	296 (43.0)	46 (62.2)	**0.002**
Fatty change, *n* (%)	246 (36.0)	15 (20.5)	**0.008**
Major Edmondson-Steiner grade, *n* (%)			0.243
1/2	30 (4.4)/352 (51.8)	2 (2.7)/30 (41.1)	
3/4	274 (40.3)/24 (3.5)	38 (52.1)/3 (4.1)	
Worst Edmondson-Steiner grade, *n* (%)			0.094
1/2	8 (1.1)/130 (18.9)	1 (1.4)/5 (6.8)	
3/4	357 (51.8)/194 (28.2)	40 (54.1)/28 (37.8)	
Serum AFP > 400 IU/mL on first recurrence	34 (10.2)	22 (31.0)	**< 0.001**
Recurrence-free survival, mo (median, range)	32.4 (2.24-177.34)	5.21 (2.04-20.28)	**< 0.001**
mUICC T stage on first recurrence, *n* (%)			**< 0.001**
0/1	6 (1.8)/144 (43.6)	10 (13.7)/23 (31.5)	
2/3	131 (39.7)/39 (11.8)	14 (19.2)/20 (27.4)	
4	10 (3.0)	6 (8.2)	
Second treatment modality			0.070
Surgery/RFA	46 (6.5)/95 (13.5)	9 (12.2)/10 (13.5)	
TACE/RFA + TACE	156(22.1)/14 (2.0)	13 (17.6)/6 (8.1)	
RT/systemic chemotherapy/BSC	20 (2.8)/11 (1.5)/20 (2.8)	3 (4.1)/1 (1.4)	

AFP: Alpha-fetoprotein; mUICC: Modified Union for International Cancer Control stage; RFA: Radiofrequency ablation; TACE: Trans-arterial chemoembolization; RT: Radiotherapy; BSC: Best supportive care.

DISCUSSION

EHR of HCC is a well-known predictive marker of poor survival outcomes, and EHR after surgical resection of HCC is deemed to be a pivotal factor for grave prognosis[7,9,17,18]. In this large-scale 15-year observational study conducted at two academic tertiary hospitals, EHR and early EHR occurred in 17.5% and 9.5% of 779 patients with HCC, respectively. Patients with early EHR had a rapid recurrence of HCC after surgical resection and poor survival outcomes. Furthermore, we elucidated the potential risk factors for early EHR after curative surgical resection of HCC.

Since the proportion of IHR cases is higher than that of EHR cases after surgical resection of HCC, previous studies have analyzed various risk factors associated with IHR alone, previous studies have analyzed various risk factors associated with IHR. Portolani *et al*[19] examined the early and late recurrence of HCC after liver resection and showed that the survival rates in the early recurrence group were significantly lower than those in the late recurrence group (25.7% *vs* 4.5% at 5 years). Moreover, similar results were demonstrated in a large-scale multicenter study conducted in China by Yan *et al*[20] comprising 1426 patients, where patients in the early recurrence group showed poor post-recurrence

Table 3 Univariate and multivariate analyses of factors associated with early extrahepatic recurrence

	Univariate analysis		Multivariate analysis	
	HR (95%CI)	*P* value	HR (95%CI)	*P* value
Serum albumin < 4.0 g/dL	2.27 (1.56-3.29)	< 0.001	**2.19 (1.45-3.31)**	**< 0.001**
Serum ALP > 100 U/L	1.76 (1.24-2.52)	0.002	**1.59 (1.08-2.32)**	**0.018**
ALBI grade ≥ 2	1.71 (1.12-2.59)	0.012		
Surgical margin involvement	2.30 (1.07-4.93)	0.032	**2.53 (1.09-5.90)**	**0.032**
Pathological mUICC stage (III, IVa)	2.94 (2.09-4.12)	< 0.001		
Multiple tumors[1]	3.21 (1.57-6.56)	0.002		
Venous/lymphatic involvement[2]	2.98 (2.09-4.25)	< 0.001	**1.90 (1.28-2.83)**	**0.002**
Serosa invasion	2.86 (1.33-6.12)	0.007		
Bile duct invasion	3.25 (1.20-8.83)	0.020		
Satellite nodule	2.69 (1.83-3.94)	< 0.001	**1.73 (1.14-2.63)**	**0.011**
Intrahepatic metastasis	2.99 (1.10-8.09)	0.032		
Tumor necrosis	3.18 (2.20-4.61)	<0.001	**1.92 (1.29-2.79)**	**0.001**
Tumor hemorrhage	1.81 (1.28-2.55)	0.001		
Sum of tumor size ≥ 7 cm	3.25 (2.23-4.73)	< 0.001	**1.84 (1.21-2.77)**	**0.004**
Macrovascular invasion	2.48 (1.37-4.50)	0.003	**2.30 (1.24-4.26)**	**0.008**
Serum AFP > 1500 IU/mL	1.99 (1.27-3.12)	0.003		

[1]Number of tumors examined during pathological evaluation.
[2]Confirmed findings during pathological evaluation.
HR: Hazards ratio; CI: Confidence interval; ALP: Alkaline phosphatase; ALBI: Albumin-bilirubin; mUICC: Modified Union for International Cancer Control; AFP: Alpha-fetoprotein.

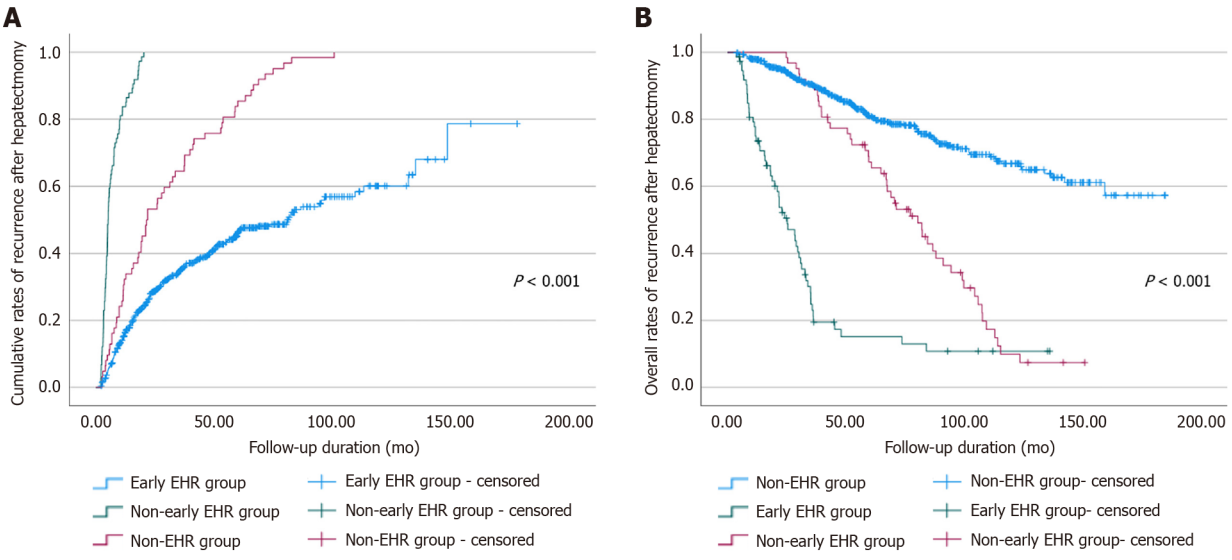

Figure 1 Both the cumulative rates of recurrence and the overall survival rates after surgical resection of hepatocellular carcinoma showed stepwise correlations with the interval to extrahepatic recurrence. A: Cumulative rate of the first recurrence of hepatocellular carcinoma after curative surgical resection; B: Overall survival rates stratified by the characteristics of extrahepatic recurrence. EHR: Extrahepatic recurrence.

survival (13.5 *vs* 36.6 mo, $P < 0.001$). Furthermore, Yang *et al*[21] stated that recurrent HCC cases with multicentric recurrence may have had greater survival than intrahepatic metastasis cases. In contrast, Byeon *et al*[22] compared the outcomes of 111 patients with IHR and 41 patients with EHR who had undergone surgical resection for HCC and found that patients in the EHR group showed significantly lower 5-year survival rates than those in the IHR group (21.5% *vs* 36.3%, $P < 0.001$). Considering the

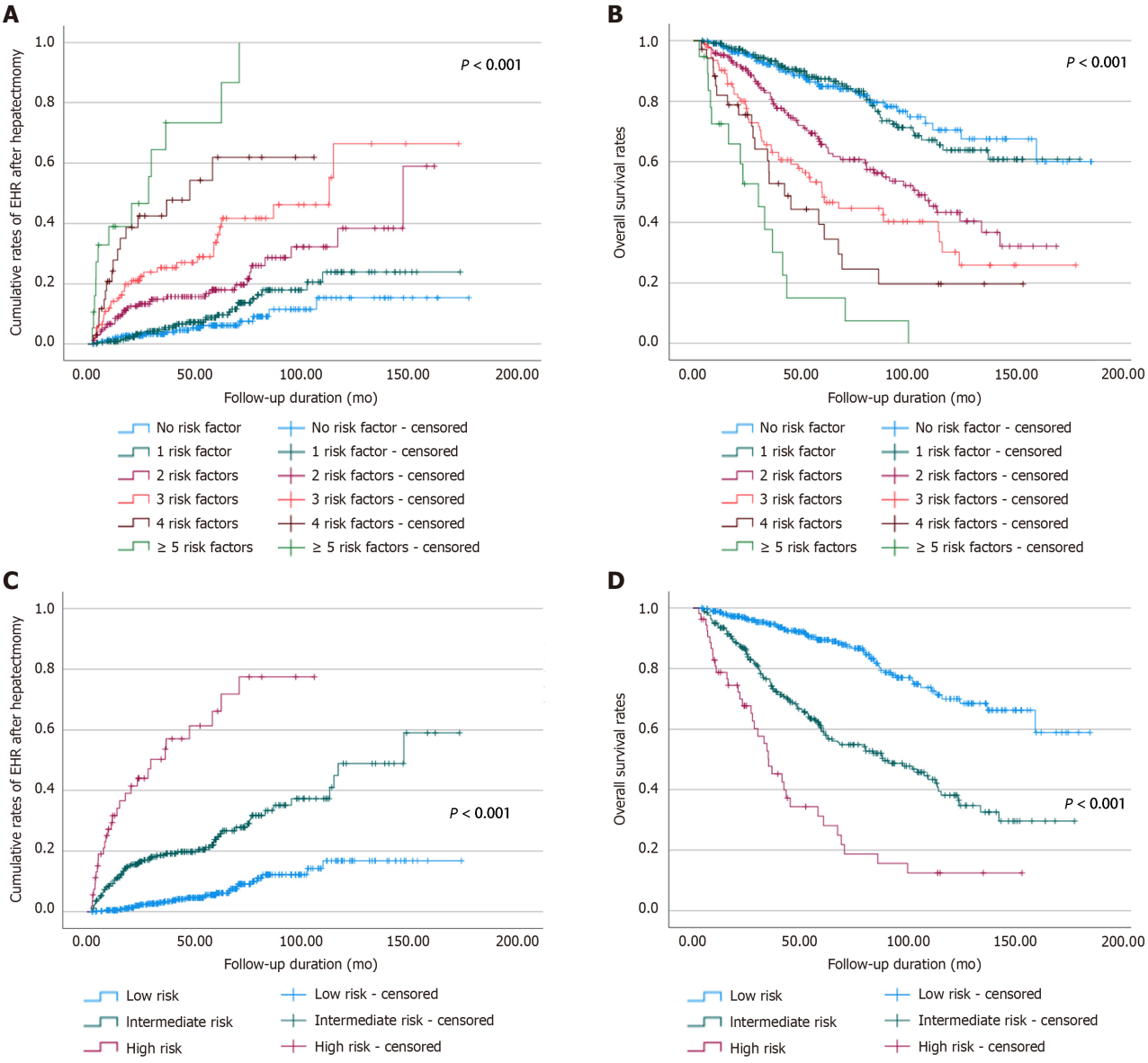

Figure 2 Patients were classified according to the number of eight risk factors related to early extrahepatic recurrence, and the probability of extrahepatic recurrence and overall survival rate was evaluated. A: Cumulative rates of extrahepatic recurrence; B: Cumulative rates of overall survival after surgical resection; C: The cumulative rates of extrahepatic recurrence; D: The cumulative rates of overall survival. EHR: Extrahepatic recurrence.

non-negligible rates of EHR after surgical resection of HCC and the dismal prognosis of patients with EHR, risk stratification and prediction of early EHR may have been of great importance in improving the clinical outcome.

In 52.7% of the patients with early EHR, EHR was the first recurrence of HCC after surgical resection (Supplementary Table 1), and both interval to first recurrence and EHR were significantly shorter in the early EHR group compared with that in the non-early EHR group (5.2 *vs* 21.6 mo, $P < 0.001$; and 8.81 *vs* 58.57 mo, $P < 0.001$). Moreover, a higher proportion of patients with early EHR showed an advanced stage at first recurrence (mUICC stage ≥ 3, 75.7% *vs* 38.7%, $P < 0.001$), and 43.2% of patients had no intrahepatic HCC (mUICC T stage 0) at EHR. This suggests that EHR may occur within a very short interval after surgical resection of HCC with an advanced tumor stage while intrahepatic HCC is not exhibited. Considering the aggressive nature of the tumors in patients with early EHR, adjuvant therapy after surgical resection or meticulous postoperative surveillance may be highly required in a specific group of patients to prompt detection of EHR. In addition, with respect to the high proportion of patients with EHR as their first recurrence (52.7%), pre- and/or peri-operative factors are considered to play critical roles in predicting early EHR.

Among the several factors associated with early EHR, serum albumin < 4.0 g/dL, serum ALP > 100 U/L, surgical margin involvement, venous and/or lymphatic involvement, satellite nodules, tumor necrosis, tumor size ≥ 7 cm, and the presence of macrovascular invasion confirmed on radiologic examination were identified as risk factors related to early EHR, as determined by multivariate Cox regression analysis (Table 3). The concentrations of albumin and/or ALP alone or in combination with

other parameters have been proposed as useful markers for predicting recurrence after surgical removal of HCC in previous studies[23-26]. Li *et al*[27] showed the prognostic value of the albumin-to-ALP ratio in patients with HCC who received liver transplants, whereas Yu *et al*[26] determined ALP concentration as an independent factor influencing disease-free survival and overall survival that aids in the prediction of recurrence in high-risk patients with HCC. Additionally, involvement of the surgical margins was related to poor clinical outcomes, as shown by a previous study[28] and a meta-analysis conducted by Zhong *et al*[29], which is consistent with the findings of our study. Chen *et al*[30] reported a poorer prognosis related to microvascular invasion in solitary small HCC in their meta-analysis, while Hasegawa *et al*[31] reported the association between lymphatic system involvement and patient survival after surgical resection of HCC, which are consistent with our findings. In a large-scale study of 734 patients who underwent surgery for HCC, satellite nodules, tumor size (> 5 cm), and the presence of macrovascular invasion were closely related to late recurrence of HCC in multivariate analysis (HR, 1.59, 1.49, and 4.63, respectively), and these findings are concordant with our study[32]. A recent study by Wei *et al*[33] reported that tumor necrosis was associated with the prognosis of patients undergoing surgery for HCC with regard to overall survival and RFS and advanced tumor characteristics, and Ling *et al*[34] also reported tumor necrosis as a potential parameter of the aggressiveness of HCC. Concordant with these previous study results, our study also demonstrated a significant association between tumor necrosis and early EHR.

In addition, we analyzed multiple factors associated with overall survival after surgical resection of HCC and identified that serum albumin < 4.0 g/dL, serum ALP > 100 U/L, major Edmondson-Steiner grade ≥ 3, pathological mUICC stage III or IVa, satellite nodules, tumor necrosis, and early EHR were related to survival (Table 4). Most risk factors exhibited similar results in the multivariate analysis of factors associated with early EHR (serum albumin < 4.0 g/dL, serum ALP > 100 U/L, satellite nodules, and tumor necrosis). The Edmondson-Steiner grade has been previously reported as a crucial predictor of recurrence and survival by Zhou *et al*[31] and Martins-Filho *et al*[32], and our study also showed poor survival outcomes in patients with major Edmondson-Steiner grade ≥ 3. Finally, early EHR showed a significant association with poor survival and increased the risk of death more than six times (HR, 6.77; 95%CI, 4.81-9.52; $P < 0.001$).

The cumulative rates of first recurrence and overall survival were correlated with the development of EHR and the interval to EHR (Figure 1). In particular, patients with early EHR showed substantially worse survival outcomes (HR, 6.77; 95%CI, 4.81-9.52; $P < 0.001$). Furthermore, considering the heterogeneity of patient characteristics regarding the tumor nature, degree of liver cirrhosis, and diverse disease courses after surgical resection, predictive markers of early EHR within 2 years after surgical resection with preoperative and/or operative factors may well reflect the initial state of the tumor.

We categorized the patients by the number of eight risk factors associated with early EHR and assessed the probability rates of EHR and overall survival. As demonstrated in Figure 2, there was a significant relationship between the number of the risk factors and the cumulative rates of both EHR and overall survival ($P < 0.001$). For a simple and intuitive predictive model of EHR, we subgrouped the patients into three categories: a low-risk group with 0-1 risk factor, an intermediate-risk group with 2-3 risk factors, and a high-risk group with ≥ 4 risk factors. The rates of both EHR and survival showed a substantial correlation with these risk stratifications. Hence, the prediction of early EHR after surgical resection of HCC may be regarded as essential, especially for high-risk patients.

Our study had several limitations. First, this study was retrospective and included patients with heterogenous clinical courses and outcomes. The postoperative surveillance methods, schedule, and treatment methods for recurrence of HCC were not fully standardized. To minimize the potential bias owing to the design of this study, we strived to enroll a large number of patients in multiple tertiary academic hospitals. Furthermore, the fact that more than half of the patients (52.7%) developed EHR as their first recurrence highlighted the importance of preoperative and operative factors. Second, although pathological confirmation of EHR was performed for a few patients, most instances of EHR were solely identified at the physician's discretion using imaging diagnostic modalities. Finally, owing to patient geographic characteristics, the majority of patients had chronic hepatitis B as the etiology of liver cirrhosis and HCC. Further studies are warranted to investigate characteristics and risk factors for early EHR in patients with diverse chronic hepatitis by using a standardized study protocol. Especially, the use of radiomic tumor features for the prediction of recurrence after HCC treatment can be considered as an additional tool for prompt detection of early EHR[35,36]. Using an accurate tool for the prediction of early EHR, the prognosis of patients with a high risk of early EHR may be improved with the utilization of adjunctive post-operative therapy.

CONCLUSION

Patients with early EHR showed rapid recurrence of HCC after surgical resection and significantly worse survival outcomes. . We derived several risk factors associated with early EHR and the numbers of risk factors correlated with not only with cumulative rates of EHR but also with survival rates. In terms of poor prognosis associated with early EHR, patients who undergo surgical resection for HCC

Table 4 Univariate and multivariate analysis of factors associated with overall survival

	Univariate analysis		Multivariate analysis	
	HR (95%CI)	*P* value	HR (95%CI)	*P* value
Serum albumin < 4.0 g/dL	2.14 (1.61-2.85)	< 0.001	**2.44 (1.79-3.32)**	**< 0.001**
ALBI grade ≥ 2	1.84 (1.36-2.51)	< 0.001		
Serum ALP > 100 U/L	1.84 (1.41-2.41)	< 0.001	**1.62 (1.22-2.16)**	**0.001**
Single tumor[1]	1.87 (1.21-2.91)	0.005		
Major Edmondson-Steiner grade ≥ 3	1.64 (1.26-2.13)	< 0.001	**1.45 (1.10-1.90)**	**0.008**
Venous/lymphatic involvement[2]	2.44 (1.84-3.22)	< 0.001		
Pathological mUICC stage (III, IVa)	2.59 (2.00-3.35)	< 0.001	**1.63 (1.21-2.22)**	**0.002**
Bile duct invasion	2.72 (1.21-6.13)	0.016		
Intrahepatic metastasis	3.66 (1.72-7.77)	0.001		
Multicentricity	1.91 (1.29-2.82)	0.001		
Satellite nodule	2.45 (1.82-3.30)	< 0.001	**1.92 (1.38-2.69)**	**< 0.001**
Tumor necrosis	2.12 (1.63-2.77)	< 0.001	**1.35 (1.030-1.78)**	**0.030**
Tumor hemorrhage	1.58 (1.21-2.05)	0.001		
Sum of tumor size ≥ 7 cm	2.21 (1.63-3.00)	< 0.001		
Beyond Milan criteria	1.79 (1.38-2.33)	< 0.001		
Serum AFP > 1500 IU/mL	1.47 (1.01-2.15)	0.046		
Early extrahepatic recurrence	7.72 (5.67-10.51)	< 0.001	**6.77 (4.81-9.52)**	**< 0.001**

[1]Number of tumors examined during pathological evaluation.
[2]Confirmed findings during pathological evaluation.
HR: Hazards ratio; CI: Confidence interval; ALBI: Albumin-bilirubin; ALP: Alkaline phosphatase; mUICC: Modified Union for International Cancer Control; AFP: Alpha-fetoprotein.

can be stratified by the risk of EHR with our model, and meticulous postoperative surveillance and adjuvant therapies may be required for timely EHR detection and positive clinical outcomes.

ARTICLE HIGHLIGHTS

Research background

Surgical resection is one of the most widely used modalities for the treatment of hepatocellular carcinoma (HCC). Early extrahepatic recurrence (EHR) of HCC after surgical resection is considered to be closely associated with poor prognosis.

Research motivation

Data regarding risk factors and survival outcomes of early EHR after surgical resection remain scarce.

Research objectives

We decided to investigate the clinical features and risk factors of early EHR and elucidate its association with survival outcomes.

Research methods

From January 2004 to December 2019, we enrolled treatment-naïve patients who were ≥ 18 years and underwent surgical resection for HCC in two tertiary academic centers. After excluding patients with tumor types other than HCC and/or ineligible data, this retrospective study finally included 779 patients. Surgical resection of HCC was performed according to the physicians' decisions and the EHR was diagnosed based on contrast-enhanced computed tomography or magnetic resonance imaging, and pathologic confirmation was performed in selected patients. Multivariate Cox regression analysis was performed to identify the variables associated with EHR.

Research results

Early EHR within 2 years after surgery was diagnosed in 9.5% of patients during a median follow-up period of 4.4 years. The recurrence-free survival period was 5.2 mo, and the median time to EHR was 8.8 mo in patients with early EHR. In 52.7% of patients with early EHR, EHR occurred as the first recurrence of HCC after surgical resection. On multivariate analysis, serum albumin < 4.0 g/dL, serum alkaline phosphatase > 100 U/L, surgical margin involvement, venous and/or lymphatic involvement, satellite nodules, tumor necrosis detected by pathology, tumor size ≥ 7 cm, and macrovascular invasion were determined as risk factors associated with early EHR. After sub-categorizing the patients according to the number of risk factors, the rates of both EHR and survival showed a significant correlation with the risk of early EHR. Furthermore, multivariate analysis revealed that early EHR was associated with substantially worse survival outcomes (hazard ratio, 6.77; 95% confidence interval, 4.81-9.52; $P < 0.001$).

Research conclusions

Early EHR significantly deteriorates the survival of patients with HCC, and our identified risk factors may predict the clinical outcomes and aid in postoperative strategies for improving survival.

Research perspectives

Further studies are warranted to investigate characteristics and risk factors for early EHR in patients with diverse chronic hepatitis by using a standardized study protocol. Using an accurate tool for the prediction of early EHR, the prognosis of patients with a high risk of early EHR may be improved with the utilization of adjunctive post-operative therapy.

FOOTNOTES

Author contributions: Yoon JH wrote the manuscript; Choi SK, Cho SB, and Jun CH designed the concept of the study; Yoon JH, Kim HJ, and Ko YS collected and analyzed the data on baseline patient characteristics and recurrence of HCC; Yoon JH interpreted the data; Choi SK, Cho SB, and Jun CH supervised the project.

Supported by Research Supporting Program of the Korean Association for the Study of the Liver and the Korean Liver Foundation, No. KASLKLF2019-06; and Chonnam National University Hospital Biomedical Research Institute, No. BCRI121007.

Institutional review board statement: This study was approved by the Institutional Review Board of Chonnam National University Hospital (IRB No. CNUH-2019-203).

Informed consent statement: Owing to the retrospective design of our study and the use of de-identified data, the requirement for informed consent was waived under the approval of the Institutional Review Board of Chonnam National University Hospital.

Conflict-of-interest statement: The authors declare no competing interests.

Data sharing statement: Data available on additional request.

STROBE statement: The authors have read the STROBE Statement—checklist of items, and the manuscript was prepared and revised according to the STROBE Statement—checklist of items.

Country/Territory of origin: South Korea

ORCID number: Jae Hyun Yoon 0000-0002-4993-2496; Sung Kyu Choi 0000-0002-6878-3385; Sung Bum Cho 0000-0001-9816-3446; Hee Joon Kim 0000-0002-8636-5726; Yang Seok Ko 0000-0000-0368-5389; Chung Hwan Jun 0000-0002-7136-8350.

S-Editor: Wu YXJ
L-Editor: A
P-Editor: Li X

REFERENCES

1 **Villanueva A**. Hepatocellular Carcinoma. *N Engl J Med* 2019; **380**: 1450-1462 [PMID: 30970190 DOI: 10.1056/NEJMra1713263]
2 **Torimura T**, Iwamoto H. Optimizing the management of intermediate-stage hepatocellular carcinoma: Current trends and prospects. *Clin Mol Hepatol* 2021; **27**: 236-245 [PMID: 33317248 DOI: 10.3350/cmh.2020.0204]
3 **Reig M**, Forner A, Rimola J, Ferrer-Fàbrega J, Burrel M, Garcia-Criado Á, Kelley RK, Galle PR, Mazzaferro V, Salem R, Sangro B, Singal AG, Vogel A, Fuster J, Ayuso C, Bruix J. BCLC strategy for prognosis prediction and treatment recommendation: The 2022 update. *J Hepatol* 2022; **76**: 681-693 [PMID: 34801630 DOI: 10.1016/j.jhep.2021.11.018]
4 **Chan AWH**, Zhong J, Berhane S, Toyoda H, Cucchetti A, Shi K, Tada T, Chong CCN, Xiang BD, Li LQ, Lai PBS, Mazzaferro V, García-Fiñana M, Kudo M, Kumada T, Roayaie S, Johnson PJ. Development of pre and post-operative models to predict early recurrence of hepatocellular carcinoma after surgical resection. *J Hepatol* 2018; **69**: 1284-1293 [PMID: 30236834 DOI: 10.1016/j.jhep.2018.08.027]
5 **Kim J**, Kang W, Sinn DH, Gwak GY, Paik YH, Choi MS, Lee JH, Koh KC, Paik SW. Substantial risk of recurrence even after 5 recurrence-free years in early-stage hepatocellular carcinoma patients. *Clin Mol Hepatol* 2020; **26**: 516-528 [PMID: 32911589 DOI: 10.3350/cmh.2020.0016]
6 **Taketomi A**, Toshima T, Kitagawa D, Motomura T, Takeishi K, Mano Y, Kayashima H, Sugimachi K, Aishima S, Yamashita Y, Ikegami T, Gion T, Uchiyama H, Soejima Y, Maeda T, Shirabe K, Maehara Y. Predictors of extrahepatic recurrence after curative hepatectomy for hepatocellular carcinoma. *Ann Surg Oncol* 2010; **17**: 2740-2746 [PMID: 20411432 DOI: 10.1245/s10434-010-1076-2]
7 **Uka K**, Aikata H, Takaki S, Shirakawa H, Jeong SC, Yamashina K, Hiramatsu A, Kodama H, Takahashi S, Chayama K. Clinical features and prognosis of patients with extrahepatic metastases from hepatocellular carcinoma. *World J Gastroenterol* 2007; **13**: 414-420 [PMID: 17230611 DOI: 10.3748/wjg.v13.i3.414]
8 **Wang L**, Ye G, Zhan C, Sun F, Lin Z, Jiang W, Wang Q. Clinical Factors Predictive of a Better Prognosis of Pulmonary Metastasectomy for Hepatocellular Carcinoma. *Ann Thorac Surg* 2019; **108**: 1685-1691 [PMID: 31445050 DOI: 10.1016/j.athoracsur.2019.06.086]
9 **Yoon JH**, Lee WJ, Kim SM, Kim KT, Cho SB, Kim HJ, Ko YS, Kook HY, Jun CH, Choi SK, Kim BS, Cho SY, You HS, Lee Y, Son S. Simple parameters predicting extrahepatic recurrence after curative hepatectomy for hepatocellular carcinoma. *Sci Rep* 2021; **11**: 12984 [PMID: 34155324 DOI: 10.1038/s41598-021-92503-6]
10 **Li WF**, Yen YH, Liu YW, Wang CC, Yong CC, Lin CC, Cheng YF, Wang JH, Lu SN. Preoperative predictors of early recurrence after resection for hepatocellular carcinoma. *Am J Surg* 2022; **223**: 945-950 [PMID: 34399978 DOI: 10.1016/j.amjsurg.2021.08.012]
11 **Beumer BR**, Takagi K, Vervoort B, Buettner S, Umeda Y, Yagi T, Fujiwara T, Steyerberg EW, IJzermans JNM. Prediction of Early Recurrence After Surgery for Liver Tumor (ERASL): An International Validation of the ERASL Risk Models. *Ann Surg Oncol* 2021; **28**: 8211-8220 [PMID: 34235600 DOI: 10.1245/s10434-021-10235-3]
12 **Saito A**, Toyoda H, Kobayashi M, Koiwa Y, Fujii H, Fujita K, Maeda A, Kaneoka Y, Hazama S, Nagano H, Mirza AH, Graf HP, Cosatto E, Murakami Y, Kuroda M. Prediction of early recurrence of hepatocellular carcinoma after resection using digital pathology images assessed by machine learning. *Mod Pathol* 2021; **34**: 417-425 [PMID: 32948835 DOI: 10.1038/s41379-020-00671-z]
13 **Llovet JM**, Di Bisceglie AM, Bruix J, Kramer BS, Lencioni R, Zhu AX, Sherman M, Schwartz M, Lotze M, Talwalkar J, Gores GJ; Panel of Experts in HCC-Design Clinical Trials. Design and endpoints of clinical trials in hepatocellular carcinoma. *J Natl Cancer Inst* 2008; **100**: 698-711 [PMID: 18477802 DOI: 10.1093/jnci/djn134]
14 **Kudo M**, Kitano M, Sakurai T, Nishida N. General Rules for the Clinical and Pathological Study of Primary Liver Cancer, Nationwide Follow-Up Survey and Clinical Practice Guidelines: The Outstanding Achievements of the Liver Cancer Study Group of Japan. *Dig Dis* 2015; **33**: 765-770 [PMID: 26488173 DOI: 10.1159/000439101]
15 **Mazzaferro V**, Regalia E, Doci R, Andreola S, Pulvirenti A, Bozzetti F, Montalto F, Ammatuna M, Morabito A, Gennari L. Liver transplantation for the treatment of small hepatocellular carcinomas in patients with cirrhosis. *N Engl J Med* 1996; **334**: 693-699 [PMID: 8594428 DOI: 10.1056/NEJM199603143341104]
16 **EDMONDSON HA**, STEINER PE. Primary carcinoma of the liver: a study of 100 cases among 48,900 necropsies. *Cancer* 1954; **7**: 462-503 [PMID: 13160935 DOI: 10.1002/1097-0142(195405)7:3<462::aid-cncr2820070308>3.0.co;2-e]
17 **Yoon JH**, Goo YJ, Lim CJ, Choi SK, Cho SB, Shin SS, Jun CH. Features of extrahepatic metastasis after radiofrequency ablation for hepatocellular carcinoma. *World J Gastroenterol* 2020; **26**: 4833-4845 [PMID: 32921960 DOI: 10.3748/wjg.v26.i32.4833]
18 **Natsuizaka M**, Omura T, Akaike T, Kuwata Y, Yamazaki K, Sato T, Karino Y, Toyota J, Suga T, Asaka M. Clinical features of hepatocellular carcinoma with extrahepatic metastases. *J Gastroenterol Hepatol* 2005; **20**: 1781-1787 [PMID: 16246200 DOI: 10.1111/j.1440-1746.2005.03919.x]
19 **Portolani N**, Coniglio A, Ghidoni S, Giovanelli M, Benetti A, Tiberio GA, Giulini SM. Early and late recurrence after liver resection for hepatocellular carcinoma: prognostic and therapeutic implications. *Ann Surg* 2006; **243**: 229-235 [PMID: 16432356 DOI: 10.1097/01.sla.0000197706.21803.a1]
20 **Yan WT**, Li C, Yao LQ, Qiu HB, Wang MD, Xu XF, Zhou YH, Wang H, Chen TH, Gu WM. Predictors and long-term prognosis of early and late recurrence for patients undergoing hepatic resection of hepatocellular carcinoma: a large-scale multicenter study. *Hepatobiliary Surg Nutr* 2021 [DOI: 10.21037/hbsn-21-288]
21 **Yang SL**, Luo YY, Chen M, Zhou YP, Lu FR, Deng DF, Wu YR. A systematic review and meta-analysis comparing the prognosis of multicentric occurrence and vs. intrahepatic metastasis in patients with recurrent hepatocellular carcinoma after hepatectomy. *HPB (Oxford)* 2017; **19**: 835-842 [PMID: 28734693 DOI: 10.1016/j.hpb.2017.06.002]
22 **Byeon J**, Cho EH, Kim SB, Choi DW. Extrahepatic recurrence of hepatocellular carcinoma after curative hepatic resection. *Korean J Hepatobiliary Pancreat Surg* 2012; **16**: 93-97 [PMID: 26388915 DOI: 10.14701/kjhbps.2012.16.3.93]
23 **He W**, Peng B, Tang Y, Yang J, Zheng Y, Qiu J, Zou R, Shen J, Li B, Yuan Y. Nomogram to Predict Survival of Patients With Recurrence of Hepatocellular Carcinoma After Surgery. *Clin Gastroenterol Hepatol* 2018; **16**: 756-764.e10 [PMID:

29246702 DOI: 10.1016/j.cgh.2017.12.002]

24 **Jeng LB**, Li TC, Hsu SC, Chan WL, Teng CF. Association of Low Serum Albumin Level with Higher Hepatocellular Carcinoma Recurrence in Patients with Hepatitis B Virus Pre-S2 Mutant after Curative Surgical Resection. *J Clin Med* 2021; **10** [PMID: 34575311 DOI: 10.3390/jcm10184187]

25 **Ekpanyapong S**, Philips N, Loza BL, Abt P, Furth EE, Tondon R, Khungar V, Olthoff K, Shaked A, Hoteit MA, Reddy KR. Predictors, Presentation, and Treatment Outcomes of Recurrent Hepatocellular Carcinoma After Liver Transplantation: A Large Single Center Experience. *J Clin Exp Hepatol* 2020; **10**: 304-315 [PMID: 32655233 DOI: 10.1016/j.jceh.2019.11.003]

26 **Yu MC**, Chan KM, Lee CF, Lee YS, Eldeen FZ, Chou HS, Lee WC, Chen MF. Alkaline phosphatase: does it have a role in predicting hepatocellular carcinoma recurrence? *J Gastrointest Surg* 2011; **15**: 1440-1449 [PMID: 21541770 DOI: 10.1007/s11605-011-1537-3]

27 **Li H**, Wang L, Chen L, Zhao H, Cai J, Yao J, Zheng J, Yang Y, Wang G. Prognostic Value of Albumin-to-Alkaline Phosphatase Ratio in Hepatocellular Carcinoma Patients Treated with Liver Transplantation. *J Cancer* 2020; **11**: 2171-2180 [PMID: 32127944 DOI: 10.7150/jca.39615]

28 **Wang H**, Yu H, Qian YW, Cao ZY, Wu MC, Cong WM. Impact of Surgical Margin on the Prognosis of Early Hepatocellular Carcinoma (≤5 cm): A Propensity Score Matching Analysis. *Front Med (Lausanne)* 2020; **7**: 139 [PMID: 32478080 DOI: 10.3389/fmed.2020.00139]

29 **Zhong FP**, Zhang YJ, Liu Y, Zou SB. Prognostic impact of surgical margin in patients with hepatocellular carcinoma: A meta-analysis. *Medicine (Baltimore)* 2017; **96**: e8043 [PMID: 28906395 DOI: 10.1097/MD.0000000000008043]

30 **Chen ZH**, Zhang XP, Wang H, Chai ZT, Sun JX, Guo WX, Shi J, Cheng SQ. Effect of microvascular invasion on the postoperative long-term prognosis of solitary small HCC: a systematic review and meta-analysis. *HPB (Oxford)* 2019; **21**: 935-944 [PMID: 30871805 DOI: 10.1016/j.hpb.2019.02.003]

31 **Hasegawa K**, Makuuchi M, Kokudo N, Izumi N, Ichida T, Kudo M, Ku Y, Sakamoto M, Nakashima O, Matsui O, Matsuyama Y; Liver Cancer Study Group of Japan. Impact of histologically confirmed lymph node metastases on patient survival after surgical resection for hepatocellular carcinoma: report of a Japanese nationwide survey. *Ann Surg* 2014; **259**: 166-170 [PMID: 23532111 DOI: 10.1097/SLA.0b013e31828d4960]

32 **Xu XF**, Xing H, Han J, Li ZL, Lau WY, Zhou YH, Gu WM, Wang H, Chen TH, Zeng YY, Li C, Wu MC, Shen F, Yang T. Risk Factors, Patterns, and Outcomes of Late Recurrence After Liver Resection for Hepatocellular Carcinoma: A Multicenter Study From China. *JAMA Surg* 2019; **154**: 209-217 [PMID: 30422241 DOI: 10.1001/jamasurg.2018.4334]

33 **Wei T**, Zhang XF, Bagante F, Ratti F, Marques HP, Silva S, Soubrane O, Lam V, Poultsides GA, Popescu I, Grigorie R, Alexandrescu S, Martel G, Workneh A, Guglielmi A, Hugh T, Aldrighetti L, Endo I, Pawlik TM. Tumor Necrosis Impacts Prognosis of Patients Undergoing Curative-Intent Hepatocellular Carcinoma. *Ann Surg Oncol* 2021; **28**: 797-805 [PMID: 33249525 DOI: 10.1245/s10434-020-09390-w]

34 **Ling YH**, Chen JW, Wen SH, Huang CY, Li P, Lu LH, Mei J, Li SH, Wei W, Cai MY, Guo RP. Tumor necrosis as a poor prognostic predictor on postoperative survival of patients with solitary small hepatocellular carcinoma. *BMC Cancer* 2020; **20**: 607 [PMID: 32600297 DOI: 10.1186/s12885-020-07097-5]

35 **Wang F**, Chen Q, Zhang Y, Chen Y, Zhu Y, Zhou W, Liang X, Yang Y, Hu H. CT-Based Radiomics for the Recurrence Prediction of Hepatocellular Carcinoma After Surgical Resection. *J Hepatocell Carcinoma* 2022; **9**: 453-465 [PMID: 35646748 DOI: 10.2147/JHC.S362772]

36 **Iezzi R**, Casà C, Posa A, Cornacchione P, Carchesio F, Boldrini L, Tanzilli A, Cerrito L, Fionda B, Longo V, Miele L, Lancellotta V, Cellini F, Tran HE, Ponziani FR, Giuliante F, Rapaccini GL, Grieco A, Pompili M, Gasbarrini A, Valentini V, Gambacorta MA, Tagliaferri L, Manfredi R. Project for interventional Oncology LArge-database in liveR Hepatocellular carcinoma - Preliminary CT-based radiomic analysis (POLAR Liver 1.1). *Eur Rev Med Pharmacol Sci* 2022; **26**: 2891-2899 [PMID: 35503635 DOI: 10.26355/eurrev_202204_28620]

World Journal of Gastroenterology

Submit a Manuscript: https://www.f6publishing.com

World J Gastroenterol 2022 September 28; 28(36): 5364-5379

DOI: 10.3748/wjg.v28.i36.5364

ISSN 1007-9327 (print) ISSN 2219-2840 (online)

ORIGINAL ARTICLE

Observational Study

Atherogenic index of plasma combined with waist circumference and body mass index to predict metabolic-associated fatty liver disease

Shao-Jie Duan, Zhi-Ying Ren, Tao Zheng, Hong-Ye Peng, Zuo-Hu Niu, Hui Xia, Jia-Liang Chen, Yuan-Chen Zhou, Rong-Rui Wang, Shu-Kun Yao

Specialty type: Gastroenterology and hepatology

Provenance and peer review: Unsolicited article; Externally peer reviewed.

Peer-review model: Single blind

Peer-review report's scientific quality classification

Grade A (Excellent): 0
Grade B (Very good): 0
Grade C (Good): C, C
Grade D (Fair): 0
Grade E (Poor): 0

P-Reviewer: Cumhur Cure M, Turkey; Lin WR, Taiwan

Received: June 26, 2022
Peer-review started: June 26, 2022
First decision: August 1, 2022
Revised: August 9, 2022
Accepted: September 8, 2022
Article in press: September 8, 2022
Published online: September 28, 2022

Shao-Jie Duan, Zhi-Ying Ren, Tao Zheng, Hong-Ye Peng, Zuo-Hu Niu, Hui Xia, Rong-Rui Wang, Graduate School, Beijing University of Chinese Medicine, Beijing 100029, China

Jia-Liang Chen, Center of Integrative Medicine, Beijing Ditan Hospital, Capital Medical University, Beijing 100015, China

Yuan-Chen Zhou, Graduate school, Peking University China-Japan Friendship School of Clinical Medicine, Beijing 100029, China

Shu-Kun Yao, Department of Gastroenterology, China-Japan Friendship Hospital, Beijing 100029, China

Corresponding author: Shu-Kun Yao, MD, Professor, Department of Gastroenterology, China-Japan Friendship Hospital, No. 2 Yinghua East Street, Chaoyang District, Beijing 100029, China. shukunyao@126.com

Abstract

BACKGROUND

Early identification of metabolic-associated fatty liver disease (MAFLD) is urgent. Atherogenic index of plasma (AIP) is a reference predictor of obesity-related diseases, but its predictive value for MAFLD remains unclear. No studies have reported whether its combination with waist circumference (WC) and body mass index (BMI) can improve the predictive performance for MAFLD.

AIM

To systematically explore the relationship between AIP and MAFLD and evaluate its predictive value for MAFLD and to pioneer a novel noninvasive predictive model combining AIP, WC, and BMI while validating its predictive performance for MAFLD.

METHODS

This cross-sectional study consecutively enrolled 864 participants. Multivariate logistic regression analysis and receiver operating characteristic curve were used to evaluate the relationship between AIP and MAFLD and its predictive power for MAFLD. The novel prediction model A-W-B combining AIP, WC, and BMI to

predict MAFLD was established, and internal verification was completed by magnetic resonance imaging diagnosis.

RESULTS

Subjects with higher AIP exhibited a significantly increased risk of MAFLD, with an odds ratio of 12.420 (6.008-25.675) for AIP after adjusting for various confounding factors. The area under receiver operating characteristic curve of the A-W-B model was 0.833 (0.807-0.858), which was significantly higher than that of AIP, WC, and BMI (all $P < 0.05$). Subgroup analysis illustrated that the A-W-B model had significantly higher area under receiver operating characteristic curves in female, young and nonobese subgroups (all $P < 0.05$). The best cutoff values for the A-W-B model to predict MAFLD in males and females were 0.5932 and 0.4105, respectively. Additionally, in the validation set, the area under receiver operating characteristic curve of the A-W-B model to predict MAFLD was 0.862 (0.791-0.916). The A-W-B level was strongly and positively associated with the liver proton density fat fraction ($r = 0.630$, $P < 0.001$) and significantly increased with the severity of MAFLD ($P < 0.05$).

CONCLUSION

AIP was strongly and positively associated with the risk of MAFLD and can be a reference predictor for MAFLD. The novel prediction model A-W-B combining AIP, WC, and BMI can significantly improve the predictive ability of MAFLD and provide better services for clinical prediction and screening of MAFLD.

Key Words: Atherogenic index of plasma; Metabolic-associated fatty liver disease; Receiver operating characteristic curve; Predictor

Core Tip: Metabolic-associated fatty liver disease (MAFLD) is the most common chronic liver disease, and early identification of MAFLD is urgent. This study demonstrated that the atherogenic index of plasma was strongly and positively associated with the risk of MAFLD, and it can be a reference predictor for MAFLD. Then, we pioneered a novel noninvasive prediction model, A-W-B, combining atherogenic index of plasma, waist circumference, and body mass index and validated its excellent predictive performance for MAFLD. Furthermore, we also pointed out the optimal cutoff values of the A-W-B model to predict MAFLD in males and females, which will facilitate early clinical identification of MAFLD in different sex populations. This study is highly innovative, and the noninvasive prediction model, A-W-B, is convenient, affordable, and easy to obtain, which can provide better services for clinical prediction and screening of MAFLD and metabolic-related diseases.

Citation: Duan SJ, Ren ZY, Zheng T, Peng HY, Niu ZH, Xia H, Chen JL, Zhou YC, Wang RR, Yao SK. Atherogenic index of plasma combined with waist circumference and body mass index to predict metabolic-associated fatty liver disease. *World J Gastroenterol* 2022; 28(36): 5364-5379
URL: https://www.wjgnet.com/1007-9327/full/v28/i36/5364.htm
DOI: https://dx.doi.org/10.3748/wjg.v28.i36.5364

INTRODUCTION

Metabolic-associated fatty liver disease (MAFLD), formerly known as nonalcoholic fatty liver disease, is a common disease closely related to genetic, obesity, and metabolic abnormalities and has become a global public health problem[1,2]. In recent decades, obesity has become increasingly widespread owing to huge changes in dietary structure and living habits[3,4]. The prevalence of MAFLD has risen rapidly, and patients tend to be younger[5]. Notably, MAFLD can not only progress to hepatitis, liver cirrhosis, and liver cancer[6] but also increase the occurrence and development of diabetes[7] and cardiovascular diseases[8,9], which seriously endangers individual health and increases the social and medical economic burden[10]. Therefore, it is necessary to predict and screen MAFLD at an early stage to intervene in a timely manner.

The occurrence and development of MAFLD are closely related to lipid metabolism disorders and dyslipidemia caused by the accumulation of visceral fat[11]. Patients with fatty liver usually have elevated triglycerides (TG) and generally lower high-density lipoprotein cholesterol (HDL-C) than healthy people[12]. Waist circumference (WC) and body mass index (BMI) are commonly used as

indicators to assess obesity, and it has been shown that elevated WC and BMI can significantly increase the risk of fatty liver disease. However, they have certain limitations in accurately reflecting the accumulation of visceral fat[13].

Recently, the atherogenic index of plasma (AIP), calculated from the logarithm of the ratio of TG to HDL-C[14], has been proven to be closely related to abdominal obesity, and it can sensitively reflect the accumulation of visceral fat and effectively predict the risk of atherosclerosis and cardiovascular disease [15,16]. Previous studies indicate that AIP is significantly higher in patients with fatty liver and may be a potential indicator for identifying fatty liver disease[17]. However, few studies have systematically reported the predictive value of AIP for MAFLD and whether AIP combined with WC and BMI can improve the predictive ability for MAFLD is unclear.

Therefore, the two main objectives of this study were: (1) To systematically assess the relationship between AIP and MAFLD and evaluate its predictive value for MAFLD; and (2) To establish a novel noninvasive prediction model combining AIP, WC and BMI and validate its predictive performance for MAFLD.

MATERIALS AND METHODS

Study design and participants

This study was conducted in Beijing, China. Among the adults who underwent a physical examination for health at China-Japan Friendship Hospital in Beijing from September 2018 to October 2021, we consecutively recruited 943 participants who completed the standardized questionnaire, finished anthropometric and laboratory tests, and underwent liver ultrasonography. All subjects agreed to participate in this study voluntarily and submitted informed consent forms.

According to quality control, after excluding pregnant and lactating women, subjects who had a history of any severe brain, heart, lung, kidney, or blood diseases, mental illness, infectious diseases, malignant tumors, *etc* as well as the subjects with incomplete data, a total of 864 subjects were finally included (Figure 1), with 624 males and 240 females, aged from 20-years-old to 78-years-old.

This study was approved by the Clinical Research Ethics Committee of China-Japan Friendship Hospital (2018-110-K79-1).

Data collection and definition

The physical examination was performed in the morning in a fasting state. Anthropometric indicators were measured by professionally trained doctors. Height, weight, and waist circumference were measured while subjects were naturally standing barefoot with lightweight clothes. After 10 min of rest, the blood pressure was measured with an upper arm electronic sphygmomanometer. Peripheral blood was drawn into an EDTA-containing tube and subjected to biochemical experiments within 2 h. The relevant laboratory indicators were obtained through the electronic database of this physical examination center, including alanine aminotransferase (ALT), aspartate aminotransferase (AST), total cholesterol, TG, HDL-C, low-density lipoprotein cholesterol, fasting blood glucose (FBG), serum uric acid (SUA) and so on.

BMI was calculated as the body weight (in kilograms) divided by the square of the height (in meters). WC referred to the waist circumference at the level of the flat navel. AIP was calculated as the logarithmic transformation of the ratio of TG to HDL-C [log (TG/HDL-C)].

Diagnostic criteria and detection methods of MAFLD

The diagnostic criteria of MAFLD refer to the consensus of international experts in 2020 that in addition to the evidence of hepatic steatosis[18], one of the following three criteria, namely, overweight/obesity, type 2 diabetes, or metabolic dysregulation, needs to be met[19,20]. Among them, metabolic dysregulation refer to the existence of at least two of the following metabolic risk criteria: (1) Waist circumference ≥ 102/88 cm in Caucasian males and females, respectively, or ≥ 90/80 cm in Asian males and females; (2) Blood pressure ≥ 130/85 mmHg or specific drug treatment; (3) Plasma TG ≥ 1.70 mmol/L or specific drug treatment; (4) Plasma HDL-C < 1.0 mmol/L for males and < 1.3 mmol/L for females or specific drug treatment; (5) Prediabetes (*i.e.* fasting glucose levels 5.6 to 6.9 mmol/L or 2-h post load glucose levels 7.8 to 11.0 mmol or glycated hemoglobin 5.7% to 6.4%; (6) Homeostasis model assessment-insulin resistance score ≥ 2.5; and (7) Plasma high-sensitivity C-reactive protein level > 2 mg/L.

In the training set, fatty liver (hepatic steatosis) was defined by liver ultrasound examination based on at least two of the following three abnormal findings: (1) Diffusely increased echogenicity of the liver relative to the kidney or spleen; (2) Ultrasound beam attenuation; and (3) Poor visualization of intrahepatic structures.

In the validation set, the proton density fat fraction (PDFF) based on magnetic resonance spectroscopy and magnetic resonance imaging (MRI) was used to diagnose fatty liver and to evaluate the severity of MAFLD[21]. PDFF < 5% was defined as no fatty liver, PDFF 5.0%-14.0% was defined as mild MAFLD, and PDFF > 14.0% was defined as moderate to severe MAFLD.

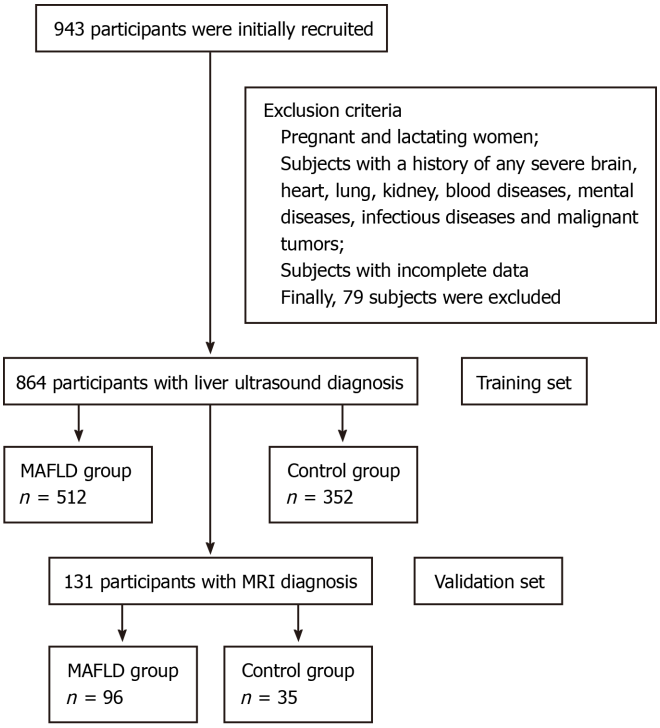

DOI: 10.3748/wjg.v28.i36.5364

Figure 1 Flow chart of the study subjects. MAFLD: Metabolic-associated fatty liver disease; MRI: Magnetic resonance imaging.

Statistical analysis

First, the baseline characteristics of the MAFLD and non-MAFLD groups were compared. The independent samples *t* test was used for comparing normally or approximately normally distributed quantitative data between groups, expressed as the mean and standard deviation (SD). The Mann-Whitney *U* test was used for comparing nonnormally distributed quantitative data between groups, represented as medians and quartiles. The χ^2 test was used for comparing categorical data between groups, represented as numbers and percentages.

Then, multivariate logistic regression analysis was conducted to calculate the odds ratios (ORs) and 95% confidence intervals of AIP for MAFLD under different adjustment conditions. The logistic regression prediction model A-W-B combining AIP, WC, and BMI was established. The Hosmer-Lemeshow test and the receiver operating characteristic (ROC) curve were used to evaluate the calibration and discrimination of this model. The DeLong test was used to compare the predictive ability of the AIP, WC, BMI, and A-W-B model for MAFLD. Spearman's correlation analysis was used to explore the correlation between parameters. Finally, the internal verification was completed with MRI as the diagnostic standard.

All statistical tests were two-tailed and were considered significant for *P* less than 0.05 ($P < 0.05$). Statistical analyses were performed using Statistical Package for the Sciences (SPSS, version 25.0) and MedCalc statistical software (version 19.6.4).

RESULTS

Characteristics of participants

The demographics, anthropometrics, and laboratory test characteristics of 864 subjects are presented in Table 1. The prevalence of male and young patients (age < 40-years-old) and the percentage of smoking history, drinking history, overweight, obesity, elevated ALT, and elevated ALT in MAFLD subjects were significantly higher than those in the non-MAFLD subjects (all $P < 0.05$). Participants with MAFLD had dramatically higher WC, BMI, SBP, DBP, ALT, AST, total cholesterol, TG, low-density lipoprotein cholesterol, FBG, and SUA and significantly lower AST/ALT and HDL-C (all $P < 0.05$). In addition, a significant association between AIP and MAFLD was initially demonstrated.

Multivariate logistic regression analysis of AIP on the risk of MAFLD

Multivariate logistic regression analyses were conducted to further explore the relationship between AIP and MAFLD, and the results are shown in Table 2. AIP had a strong association with the risk of MAFLD, and the OR for a 1-SD increase in AIP was 50.286 (26.953-93.819) without adjustment (Model

Table 1 Baseline characteristics of the study subjects

Variable	Non-MAFLD, *n* = 352	MAFLD, *n* = 512	Statistics[1]	*P* value
Demographics				
Sex			χ^2 = 14.020	< 0.001
Male	230 (65.3)	394 (77.0)		
Female	122 (34.7)	118 (23.0)		
Age in yr	37.750 ± 10.736	41.240 ± 10.852	*t* = -4.634	< 0.001
Age ≥ 40 yr	115 (32.7)	254 (49.6)	χ^2 = 24.461	< 0.001
Age < 40 yr	237 (67.3)	258 (40.4)		
Smoking history	81 (23.0)	174 (34.0)	χ^2= 12.073	< 0.001
Drinking history	76 (21.6)	145 (28.3)	χ^2= 4.962	0.027
Anthropometrics				
WC in cm	86.240 ± 9.893	96.790 ± 8.618	*t* = -16.219	< 0.001
BMI in kg/m^2	24.436 ± 3.169	28.028 ± 3.221	*t* = -16.228	< 0.001
SBP in mmHg	125.880 ± 14.883	133.610 ± 16.859	*t* = -6.908	< 0.001
DBP in mmHg	77.500 ± 11.658	82.950 ± 12.525	*t* = -6.461	< 0.001
Laboratory tests				
ALT in U/L	21.0 (15.0, 30.0)	34.0 (24.0, 54.0)	*Z* = -12.276	< 0.001
AST in U/L	19.0 (17.0, 23.0)	23.0 (19.0, 29.0)	*Z* = -9.058	< 0.001
TC in mmol/L	4.539 ± 0.847	4.783 ± 0.902	*t* = -4.104	< 0.001
TG in mmol/L	1.1 (0.7, 1.5)	1.8 (1.3, 2.6)	*Z* = -13.650	< 0.001
HDL-C in mmol/L	1.351 ± 0.283	1.191 ± 0.256	*t* = 8.321	< 0.001
LDL-C in mmol/L	2.645 ± 0.708	2.906 ± 0.884	*t* = -4.568	< 0.001
FBG in mmol/L	5.2 (4.9, 5.4)	5.4 (5.1, 5.9)	*Z* = -7.637	< 0.001
SUA in μmol/L	332.722 ± 86.289	377.836 ± 85.859	*t* = -7.590	< 0.001
AIP	-0.11 (-0.30, 0.08)	0.20 (0.03, 0.39)	*Z* = -14.006	< 0.001

[1]Comparison of significant differences between the two groups; χ2 value calculated by the χ2 test; *Z* value calculated by the Mann-Whitney *U* test; *t* value calculated by the independent samples *t* test. Data are presented as median and interquartile range, mean and standard deviation or frequency (percentage). MAFLD: Metabolic-associated fatty liver disease; WC: Waist circumference; BMI: Body mass index; SBP: Systolic blood pressure; DBP: Diastolic blood pressure; ALT: Alanine aminotransferase; AST: Aspartate aminotransferase; TC: Total cholesterol; TG: Triglyceride; HDL-C: High-density lipoprotein cholesterol; LDL-C: Low-density lipoprotein cholesterol; FBG: Fasting blood glucose; SUA: Serum uric acid; AIP: Atherogenic index of plasma.

1). After adjusting for sex and age, the OR for a 1-SD increase in AIP was 48.874 (26.087-91.569) (Model 2). After further adjusting for smoking history, drinking history, WC, and BMI, the degree of this association changed but was still strong; the OR for a 1-SD increase in AIP was 16.184 (7.961-32.902) (Model 3). Further adjusting for SBP, DBP, ALT, AST, total cholesterol, TG, HDL-C, low-density lipoprotein cholesterol, FBG, and SUA attenuated the association but only slightly; there was still a 12.420-fold (6.008-25.675) higher risk for MAFLD with a 1-SD increase in AIP (Model 4).

After dividing AIP into quartiles, the risk of MAFLD increased robustly with higher AIP quartiles. When comparing the top quartiles with the bottom categories, the risk of MAFLD increased 16.882-fold to 7.160-fold from Model 1 to Model 4. The *P* values for the linear trend were less than 0.01, signifying that linear trends from the lowest to the highest quartiles were eminent.

Predictive ability of AIP for MAFLD in different subgroups

The ROC curve of AIP for predicting MAFLD in different sex, age, and weight subgroups was plotted, and the DeLong test was used to compare the area under the ROC curve (AUC) between the subgroups. As shown in Figure 2, the AUC of AIP for MAFLD in the young was significantly higher than that in middle-age and elderly subjects [0.816 (0.779-0.849) *vs* 0.726 (0.678-0.771), $P < 0.05$]. The AUC of AIP for MAFLD in nonobese subjects was significantly higher than that in obese subjects [0.783 (0.747-0.816) *vs* 0.579 (0.519-0.638), $P < 0.0001$]. However, there was no significant difference between males and females

Table 2 Multivariate logistic regression of atherogenic index of plasma for the risk of metabolic-associated fatty liver disease

Variable		β	SE	Wald χ^2	*P* value	OR (95%CI)
Model 1	AIP level (per change in SD)	3.918	0.318	151.599	< 0.001	50.286 (26.953-93.819)
	Quartiles of AIP					
	A1 (≤ -0.1265)	-	-	-	-	1 (Ref)
	A2 (-0.1265-0.0947)	1.241	0.209	35.108	< 0.001	3.460 (2.295-5.217)
	A3 (0.0947-0.3023)	2.323	0.226	105.794	< 0.001	10.204 (6.554-15.885)
	A4 (> 0.3022)	2.826	0.245	132.611	< 0.001	16.882 (10.436-27.311)
Model 2	AIP level (per change in SD)	3.889	0.32	147.414	< 0.001	48.874 (26.087-91.569)
	Quartiles of AIP					
	A1 (≤ -0.1265)	-	-	-	-	1 (Ref)
	A2 (-0.1265-0.0947)	0.847	0.241	12.347	< 0.001	3.218 (2.124-4.876)
	A3 (0.0947-0.3023)	1.690	0.260	42.107	< 0.001	9.774 (6.256-15.270)
	A4 (> 0.3022)	2.103	0.281	55.913	< 0.001	16.514 (10.176-26.799)
Model 3	AIP level (per change in SD)	2.784	0.362	59.147	< 0.001	16.184 (7.961-32.902)
	Quartiles of AIP					
	A1 (≤ -0.1265)	-	-	-	-	1 (Ref)
	A2 (-0.1265-0.0947)	0.847	0.241	12.347	< 0.001	2.334 (1.455-3.744)
	A3 (0.0947-0.3023)	1.690	0.260	42.107	< 0.001	5.421 (3.253-9.032)
	A4 (> 0.3022)	2.103	0.281	55.913	< 0.001	8.194 (4.721-14.22)
Model 4	AIP level (per change in SD)	2.519	0.371	46.230	< 0.001	12.420 (6.008-25.675)
	Quartiles of AIP					
	A1 (≤ -0.1265)	-	-	-	-	1 (Ref)
	A2 (-0.1265-0.0947)	0.828	0.249	11.088	0.001	2.288 (1.4063-725)
	A3 (0.0947-0.3023)	1.642	0.268	37.636	< 0.001	5.167 (3.058-8.732)
	A4 (> 0.3022)	1.969	0.289	46.343	< 0.001	7.160 (4.062-12.62)

Model 1: Unadjusted. Model 2: Adjusted for age and sex. Model 3: Adjusted for age, sex, smoking history, drinking history, waist circumference and body mass index. Model 4: Adjusted for age, sex, smoking history, drinking history, waist circumference, body mass index, systolic blood pressure, diastolic blood pressure, alanine aminotransferase, aspartate aminotransferase, total cholesterol, triglyceride, high-density lipoprotein cholesterol, low-density lipoprotein cholesterol, fasting blood glucose, and serum uric acid. AIP: Atherogenic index of plasma; SE: Standard error; OR: Odds ratio; CI: Confidence interval; SD: Standard deviation.

(P = 0.0639).

In addition, the best cutoff values for AIP to predict MAFLD in males and females were 0.0821 and -0.1390, respectively. The AUCs of AIP, WC, and BMI for predicting total MAFLD were 0.780 (0.751-0.807), 0.790 (0.761-0.817), and 0.788 (0.759-0.814), respectively, with no significant difference among the three (Table 3).

Establishment of the A-W-B model for better predicting MAFLD

To further improve the predictive ability of MAFLD, we combined AIP, WC, and BMI and put them into the binary logistic regression model to construct a new logistic regression prediction model, A-W-B. The regression equation was logit (A-W-B) = -8.782 + 2.560 × AIP + 0.049 × WC + 0.170 × BMI (Table 4).

The Hosmer-Lemeshow test and ROC curve analysis were used to evaluate the calibration and discrimination of the A-W-B model. Figure 3A illustrated the calibration line graph of the A-W-B model, and the result of the Hosmer-Lemeshow test showed that χ^2 = 8.5901, P = 0.3780 > 0.05, indicating that the A-W-B model had a good calibration ability for MAFLD. Figure 3B illustrated the ROC curve of the A-W-B model, with the AUC of 0.833 (0.807-0.858), indicating that the A-W-B model had a good

Table 3 Results analysis of the receiver operating characteristic curves

Variable	AUC (95%CI)	*P* value	Sensitivity (%)	Specificity (%)	Youden index	Cutoff value
Total						
AIP	0.780 (0.751-0.807)	< 0.0001	75.20	69.89	0.4508	0.0340
WC in cm	0.790 (0.761-0.817)	< 0.0001	85.94	58.52	0.4446	88.00
BMI in kg/m^2	0.788 (0.759-0.814)	< 0.0001	83.20	59.09	0.4229	25.10
A-W-B	0.833 (0.807-0.858)[1,2,3]	< 0.0001	86.13	68.47	0.5460	0.5019
Male						
AIP	0.755 (0.719-0.788)	< 0.0001	75.89	64.78	0.4067	0.0821
WC in cm	0.770 (0.735-0.803)	< 0.0001	72.59	67.39	0.3998	92.50
BMI in kg/m^2	0.773 (0.738-0.805)	< 0.0001	72.34	68.70	0.4103	26.32
A-W-B	0.814 (0.781-0.843)[1,2,3]	< 0.0001	82.99	65.65	0.4865	0.5932
Female						
AIP	0.819 (0.764-0.865)	< 0.0001	82.2	70.49	0.5270	-0.1390
WC in cm	0.820 (0.765-0.866)	< 0.0001	81.36	69.67	0.5103	85.50
BMI in kg/m^2	0.804 (0.748-0.852)	< 0.0001	88.98	58.20	0.4718	23.34
A-W-B	0.874 (0.826-0.914)[1,2,3]	< 0.0001	78.81	83.61	0.6242	0.4105
Age ≥ 40 yr						
AIP	0.726 (0.678-0.771)	< 0.0001	71.26	66.96	0.3822	0.0367
WC in cm	0.736 (0.688-0.780)	< 0.0001	82.68	52.17	0.3485	88.00
BMI in kg/m^2	0.736 (0.688-0.780)	< 0.0001	71.26	66.96	0.3822	26.03
A-W-B	0.787 (0.742-0.828)[1,2,3]	< 0.0001	77.56	69.57	0.4712	0.5574
Age < 40 yr						
AIP	0.816 (0.779-0.849)	< 0.0001	73.64	77.22	0.5086	0.0814
WC in cm	0.824 (0.787-0.856)	< 0.0001	89.15	61.60	0.5075	88.00
BMI in kg/m^2	0.820 (0.783-0.853)	< 0.0001	83.72	66.24	0.4997	25.31
A-W-B	0.863 (0.830-0.892)[1,2,3]	< 0.0001	89.92	71.73	0.6165	0.4947
BMI ≥ 28 kg/m^2						
AIP	0.579 (0.519-0.638)	0.0849	25.63	90.91	0.1654	0.4140
WC in cm	0.597 (0.688-0.780)	0.0303	36.97	79.55	0.1652	104.50
BMI in kg/m^2	0.648 (0.589-0.704)	0.0005	65.13	68.18	0.3331	29.38
A-W-B	0.644 (0.585-0.700)[1]	0.0007	43.28	84.09	0.2737	0.9009
BMI < 28 kg/m^2						
AIP	0.783 (0.747-0.816)[3]	< 0.0001	69.71	76.30	0.4601	0.0340
WC in cm	0.754 (0.717-0.789)	< 0.0001	78.1	63.31	0.4141	87.50
BMI in kg/m^2	0.733 (0.695-0.768)	< 0.0001	77.37	59.42	0.3679	24.56
A-W-B	0.822 (0.789-0.852)[1,2,3]	< 0.0001	80.66	72.08	0.5273	0.4531

[1]Indicates significantly larger compared with atherogenic index of plasma.
[2]Indicates significantly larger as compared with waist circumference.
[3]Indicates significantly larger as compared with body mass index.
AUC: Area under the receiver operating characteristic curve; AIP: Atherogenic index of plasma; WC: Waist circumference; BMI: Body mass index; A-W-B: Prediction model combining atherogenic index of plasma, waist circumference, and body mass index; CI: Confidence interval.

Table 4 Establishment of the logistic regression prediction model A-W-B combined with the atherogenic index of plasma, waist circumference, and body mass index

Variable	β	SE	Wald χ^2	*P* value	OR (95%CI)
AIP	2.560	0.345	55.017	< 0.001	12.939 (6.578-25.45)
WC	0.049	0.017	7.951	0.005	1.050 (1.015-1.087)
BMI	0.170	0.051	11.087	0.001	1.186 (1.073-10311)
Constant	-8.782	1.003	76.689		

AIP: Atherogenic index of plasma; WC: Waist circumference; BMI: Body mass index; SE: Standard error; OR: Odds ratio; CI: Confidence interval.

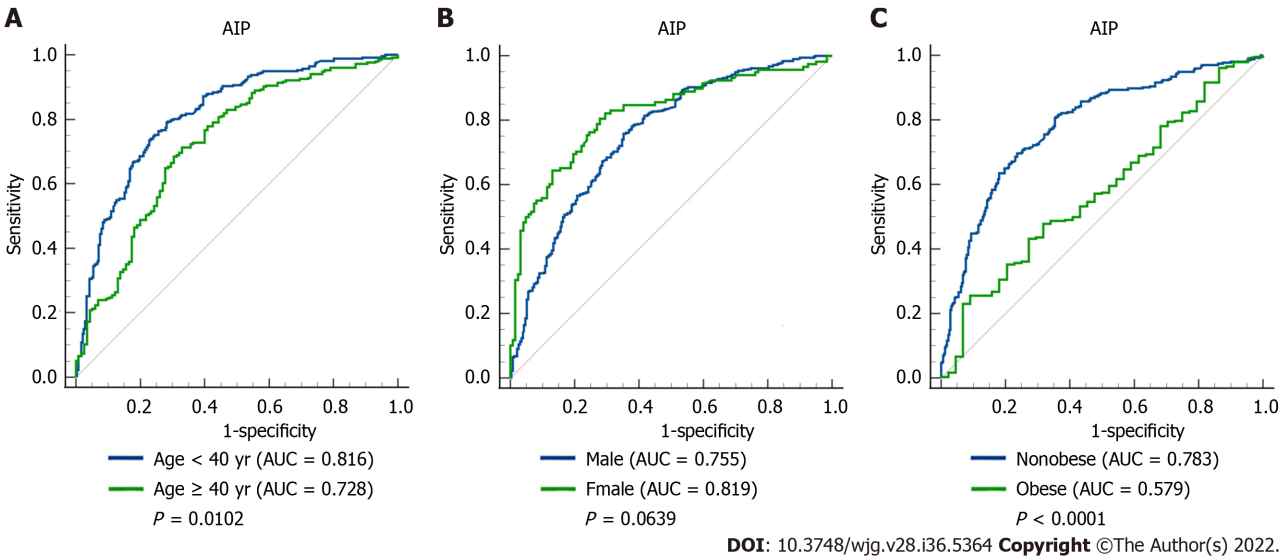

DOI: 10.3748/wjg.v28.i36.5364

Figure 2 Receiver operating characteristic curves of atherogenic index of plasma in predicting metabolic-associated fatty liver disease in different subgroups. A: Comparison between the young (age < 40 years) and middle-age and elderly (age ≥ 40 years) subjects (*P* = 0.0102); B: Comparison between male and female subjects (*P* = 0.0639); C: Comparison between nonobese and obese subjects (*P* < 0.0001). AIP: Atherogenic index of plasma; AUC: Area under the receiver operating characteristic curve.

discrimination ability for MAFLD.

Predictive ability of the A-W-B model for MAFLD in different subgroups

To further evaluate the predictive power of the A-W-B model for MAFLD in different populations, we performed a subgroup analysis. As shown in Figure 4, the AUCs of A-W-B for MAFLD in female, young, and nonobese subjects were 0.874 (0.826-0.914), 0.863 (0.830-0.892), and 0.822 (0.789-0.852), respectively, which were significantly higher than those in male [0.814 (0.781-0.843)], middle-aged and elderly [0.787 (0.742-0.828)], and obese subjects [0.644 (0.585-0.700)] (all $P < 0.05$). These results indicated that the A-W-B model had stronger predictive power for MAFLD in female, young, and nonobese subjects. Furthermore, the results in Table 3 showed that the best cutoff values for A-W-B to predict MAFLD in males and females were 0.5932 and 0.4105, respectively.

Comparison of the A-W-B model and AIP, WC, and BMI for predicting MAFLD

The DeLong test was used to compare the predictive ability of the A-W-B model and AIP, WC, and BMI. The AUC of the A-W-B model for MAFLD was 0.833 (0.807-0.858), which was significantly higher than that of AIP, WC, and BMI ($P < 0.05$). The sensitivity, specificity, Youden index, and cutoff value of the A-W-B model were 86.13%, 68.47%, 0.5460, and 0.5019, respectively (Table 3).

As shown in Figure 5A-E, subgroup analysis showed that the AUCs of the A-W-B model were significantly higher than those of AIP, WC, and BMI in male, female, young, middle-aged and elderly, and nonobese subjects (all $P < 0.01$), demonstrating that the A-W-B model has a higher ability to predict MAFLD than AIP, WC, and BMI in different age, sex, and nonobese subjects. However, as shown in Figure 5F, among obese subjects, the predictive ability of the A-W-B model for MAFLD was only better than that of AIP. In addition, the Z values between the AIP, WC, BMI, and the A-W-B model in different subgroups were illustrated in Supplementary Table 1.

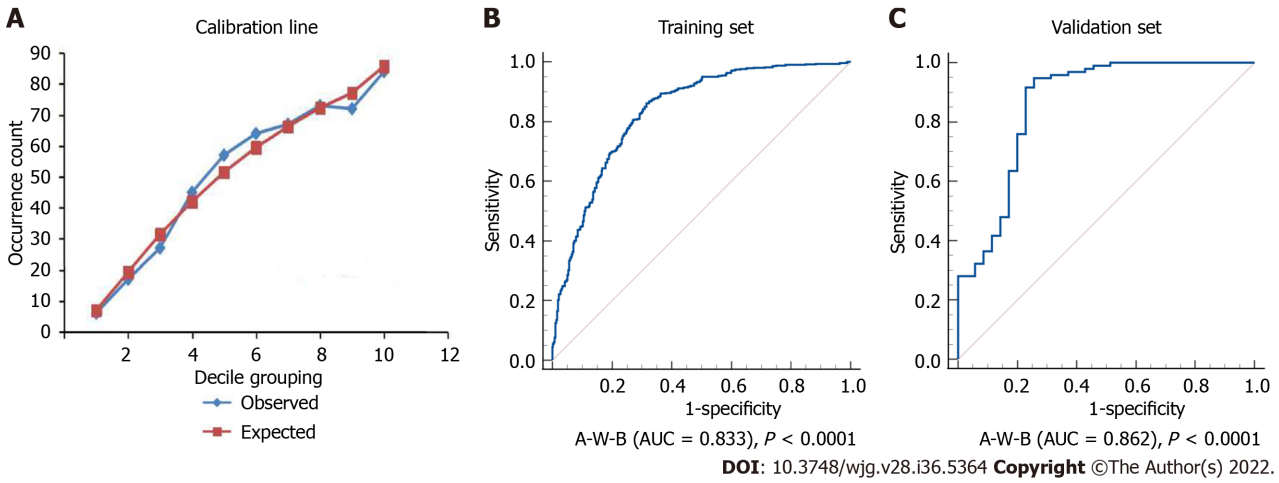

DOI: 10.3748/wjg.v28.i36.5364 **Copyright** ©The Author(s) 2022.

Figure 3 Calibration line and receiver operating characteristic curves of the A-W-B model. A: Calibration line of the prediction model combining atherogenic index of plasma, waist circumference, and body mass index (A-W-B) model (Hosmer-Lemeshow test: χ^2 = 8.5901, P = 0.3780); B: Receiver operating characteristic curve of the A-W-B model in the training set (area under the receiver operating characteristic curve [AUC] = 0.833); C: Receiver operating characteristic curve of the A-W-B model in the validation set (AUC = 0.862).

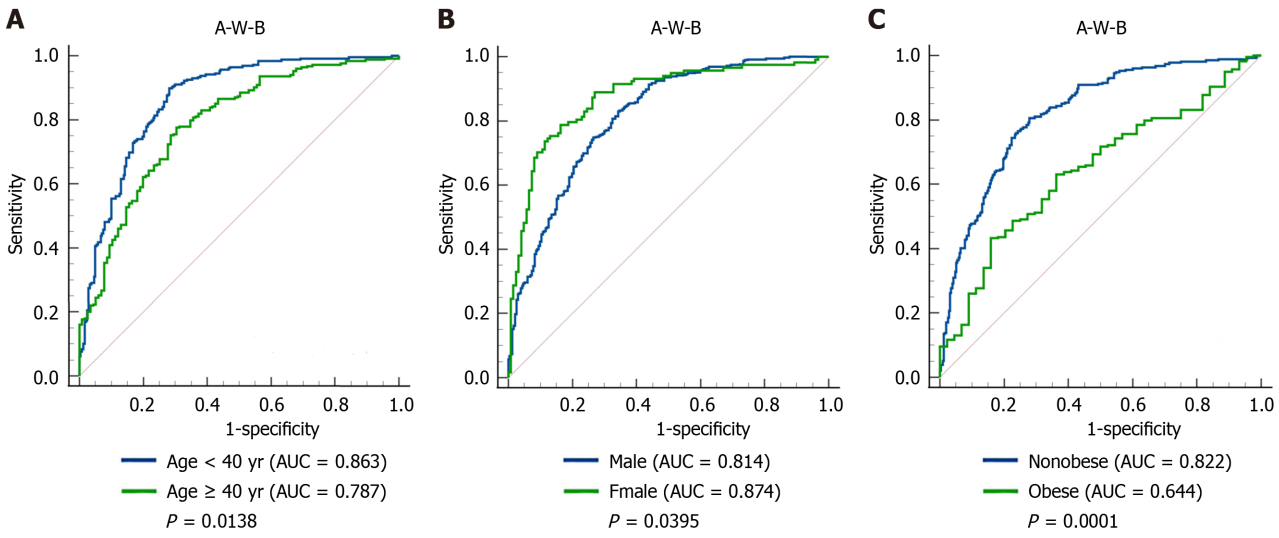

DOI: 10.3748/wjg.v28.i36.5364 **Copyright** ©The Author(s) 2022.

Figure 4 Receiver operating characteristic curves of the A-W-B model to predict metabolic-associated fatty liver disease in different subgroups. A: Comparison between young (age < 40 years) and middle-age and elderly (age ≥ 40 years) subjects (P = 0.0138); B: Comparison between male and female subjects (P = 0.0395); C: Comparison between nonobese and obese subjects (P = 0.0001); AUC: Area under the receiver operating characteristic curve; A-W-B: Prediction model combining atherogenic index of plasma, waist circumference, and body mass index.

The concrete ROC curve results of the AIP, WC, BMI, and A-W-B model for predicting MAFLD in different subgroups were illustrated in Table 3. Compared to AIP, WC, and BMI, the A-W-B model had the best sensitivity in male, young and nonobese subjects, which may be more conducive to identifying patients with positive MAFLD to reduce the missed diagnosis rate. Meanwhile, the A-W-B model had the best specificity in female and middle-aged and elderly subjects, which may be more beneficial to identifying people without MAFLD and reducing the misdiagnosis rate.

Moreover, Spearman's correlations between A-W-B, AIP, WC, BMI, and various physical and chemical indicators are illustrated in Table 5. Compared with AIP, WC, and BMI, the A-W-B model had a higher positive association with SBP, DBP, ALT, AST, FBG, and SUA.

Validation of the A-W-B model

To further validate the diagnostic performance of the A-W-B model for MAFLD, we randomly selected approximately 15% of the subjects (131 cases) from the overall subjects as the validation set and used MRI to diagnose MAFLD. Among them, 35 cases were in the control group, 67 cases were mild MAFLD, and 29 cases were moderate to severe MAFLD. The data comparison between the training set and validation set was shown in Table 6. There was no statistically significant difference in age, sex, and

Table 5 Spearman's correlation analysis results between various indicators (*r* value)

Variable	AIP	WC	BMI	A-W-B
SBP in mmHg	0.299[b]	0.358[b]	0.362[b]	0.392[b]
DBP in mmHg	0.327[b]	0.325[b]	0.315[b]	0.375[b]
ALT in U/L	0.470[b]	0.455[b]	0.451[b]	0.530[b]
AST in U/L	0.306[b]	0.307[b]	0.304[b]	0.351[b]
TC in mmol/L	0.193[b]	0.070[a]	0.056	0.132[b]
TG in mmol/L	0.954[b]	0.455[b]	0.430[b]	0.763[b]
HDL-C in mmol/L	-0.617[b]	-0.365[b]	-0.373[b]	-0.543[b]
LDL-C in mmol/L	0.253[b]	0.128[b]	0.105[b]	0.190[b]
FBG in mmol/L	0.294[b]	0.280[b]	0.274[b]	0.334[b]
SUA in μmol/L	0.462[b]	0.375[b]	0.358[b]	0.469[b]

[a]$P < 0.05$.
[b]$P < 0.01$.
SBP: Systolic blood pressure; DBP: Diastolic blood pressure; ALT: Alanine aminotransferase; AST: Aspartate aminotransferase; TC: Total cholesterol; TG: Triglyceride; HDL-C: High-density lipoprotein cholesterol; LDL-C: Low-density lipoprotein cholesterol; FBG: Fasting blood glucose; SUA: Serum uric acid; AIP: Atherogenic index of plasma; WC: Waist circumference; BMI: Body mass index; A-W-B: Prediction model combining atherogenic index of plasma, waist circumference, and body mass index.

various indicators between the two groups (all $P > 0.05$).

Figure 3C illustrated the ROC curve of the A-W-B model in the validation set, with the AUC of 0.862 (0.791-0.916), indicating that the A-W-B model also exhibited outstanding discrimination for MAFLD in the validation set. In addition, Figure 6 shows that the A-W-B level was strongly and positively associated with the PDFF ($r = 0.630$, $P < 0.001$). With the degree of severity of MAFLD increased, the A-W-B level also increased significantly ($P < 0.05$).

DISCUSSION

In this study, the relationship between AIP and MAFLD was systematically assessed, and it was confirmed that AIP had a strong and positive association with the risk of MAFLD and can be used as a reference predictor for MAFLD. Then, to further improve the predictive power for MAFLD, we combined AIP, WC, and BMI to pioneer a novel noninvasive prediction model, A-W-B, and confirmed that it had a better predictive value for MAFLD than AIP, WC, and BMI. At the same time, we also pointed out the optimal cutoff values of the A-W-B model to predict MAFLD in males and females, which will facilitate early clinical identification of MAFLD in different sex populations. Finally, we internally validated the model with MRI as the diagnostic standard, further affirming its outstanding predictive performance for MAFLD, which provided a new tool for the early prevention and screening of MAFLD.

As a new type of body fat index calculated as the logarithmic transformation of the ratio of TG to HDL-C, AIP is more sensitive to visceral fat accumulation than WC and BMI and has shown predictive potential for fatty liver in previous studies[15]. Xie *et al*[17] found that a higher AIP level was positively associated with fatty liver, which might be a novel and strong predictor associated with fatty liver in the Chinese Han population. In this study, the multivariate logistic regression results showed that the subjects with higher AIP still exhibited a significantly increased risk of MAFLD after adjusting for age, sex, smoking history, drinking history, WC, BMI, and various physical and chemical indicators, indicating that AIP was strongly and positively associated with the risk of MAFLD.

Visceral fat accumulation has been proven to increase the prevalence of a variety of cardiovascular risk factors, including insulin resistance and dyslipidemia, which also play a tremendously crucial role in the pathogenesis of fatty liver disease[16]. It is widely accepted that the increased TG caused by liver lipid accumulation is a prerequisite for MAFLD and that insulin resistance is a key factor during its development. Previous studies demonstrated that increasing levels of TG and decreasing concentrations of HDL-C could reduce sensitivity to insulin, and higher TG/HDL-C usually indicates insulin resistance [22], which may explain the close relationship between AIP and MAFLD. In addition, this study also pointed out the optimal cutoff values of AIP for predicting MAFLD in males and females, which provided a new idea for the early prevention of MAFLD. People with AIP levels above this cutoff point may be at higher risk for MAFLD and require more attention to liver conditions.

Table 6 Data comparison between training set and validation set

Variable	Training set, *n* = 864	Validation set, *n* = 131	*P* value
Sex, female	240 (27.8)	38 (29.0)	0.770
Age in yr	39.820 ± 10.934	39.660 ± 10.861	0.885
Smoking history	255 (29.5)	38 (29.0)	0.906
Drinking history	221 (25.6)	24 (18.3)	0.072
WC in cm	92.490 ± 10.522	93.690 ± 10.759	0.057
BMI in kg/m^2	26.563 ± 3.653	27.055 ± 3.772	0.155
SBP in mmHg	130.460 ± 16.517	129.090 ± 16.822	0.386
DBP in mmHg	80.730 ± 12.464	78.560 ± 12.192	0.063
ALT in U/L	28.0 (19.0, 42.0)	28.0 (19.0, 43.0)	0.837
AST in U/L	21.0 (18.0, 26.0)	22.0 (18.0, 26.0)	0.612
TC in mmol/L	4.683 ± 0.888	4.607 ± 0.865	0.349
TG in mmol/L	1.5 (1.0, 2.2)	1.6 (1.0, 2.5)	0.307
HDL-C in mmol/L	1.256 ± 0.279	1.241 ± 0.293	0.533
LDL-C in mmol/L	2.800 ± 0.826	2.763 ± 0.769	0.651
FBG in mmol/L	5.3 (5.0, 5.7)	5.2 (4.9, 5.8)	0.326
SUA in μmol/L	359.434 ± 88.800	342.901 ± 88.448	0.052
AIP	0.09 (-0.13, 0.30)	0.12 (-0.13, 0.33)	0.306

Data are presented as median and interquartile range, mean ± SD, or *n* (%). WC: Waist circumference; BMI: Body mass index; SBP: Systolic blood pressure; DBP: Diastolic blood pressure; ALT: Alanine aminotransferase; AST: Aspartate aminotransferase; TC: Total cholesterol; TG: Triglyceride; HDL-C: High-density lipoprotein cholesterol; LDL-C: Low-density lipoprotein cholesterol; FBG: Fasting blood glucose; SUA: Serum uric acid; AIP: Atherogenic index of plasma.

Xie *et al*[17] indicated that the ORs of AIP on the risk of fatty liver disease in women and young adults increased faster. This study showed that the AIP had a better predictive ability for MAFLD in young subjects, which may be related to the higher excessive fat accumulation of young people caused by dietary irregularities and insufficient exercise. However, there was no significant difference between males and females. Wang *et al*[23] and Dong *et al*[24] studied the predictive value of AIP for nonalcoholic fatty liver disease in obese and nonobese populations separately, with AUCs of 0.718 and 0.803, respectively. It seems that the predictive ability of AIP in the nonobese population might be better, but no studies have directly compared the ability of AIP in identifying MAFLD between different weights. Fortunately, our study filled this gap, and confirmed that the AIP had a remarkably higher predictive ability for MAFLD in nonobese subjects. A cohort study demonstrated that visceral obesity was dose-dependently associated with nonalcoholic fatty liver disease[25]. It is worth noting that lean people with unhealthy metabolism may have a greater accumulation of visceral fat[26], and nonobese MAFLD patients with unhealthy metabolism usually exhibit higher liver damage and cardiovascular risks[27]. AIP, as a sensitive indicator that reflects the accumulation of visceral fat, might have a stronger association with nonobese MAFLD patients and thus might have a better predictive ability for MAFLD in nonobese populations.

WC and BMI are common indicators for obesity evaluation and have been proven to be good predictors of fatty liver[17]. This study confirmed that they also had good predictive ability for MAFLD, with no significant difference compared to AIP. However, no previous study has assessed the predictive power of AIP combined with WC and BMI for MAFLD. Therefore, another focus of this study was to explore whether AIP combined with WC and BMI can improve the ability to identify MAFLD. The results showed that the logistic regression prediction Model A-W-B established by AIP combined with WC and BMI had excellent calibration and discrimination for MAFLD and had a significantly better ability to identify MAFLD. At the same time, it also had an outstanding ability to identify MAFLD in the validation, further affirming its outstanding predictive performance for MAFLD. Interestingly, we also found that the level of A-W-B was positively correlated with the liver fat content and the degree of severity of MAFLD in the validation, which may be objective evidence explaining the positive association and excellent predictive ability of the A-W-B model for MAFLD.

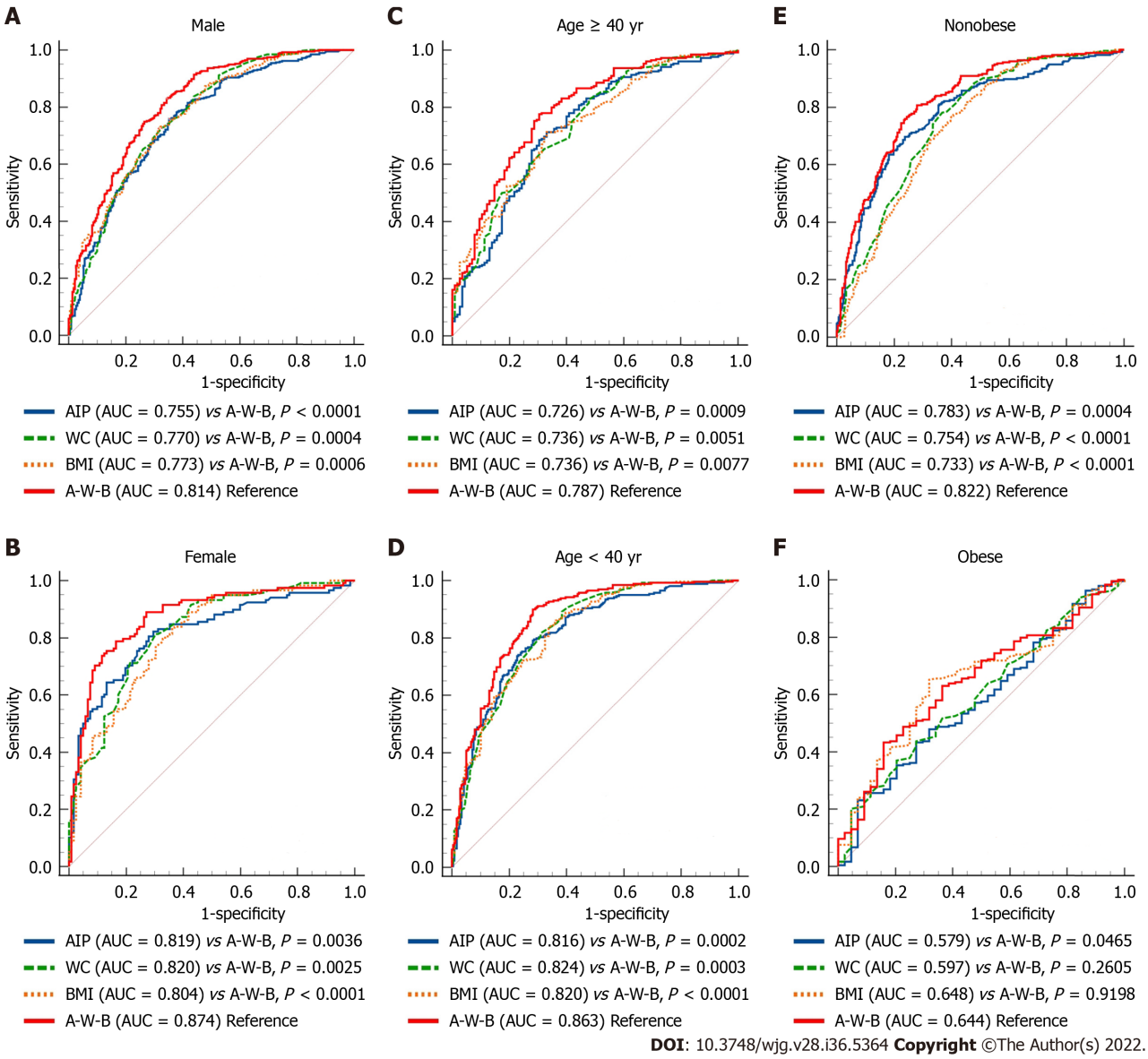

DOI: 10.3748/wjg.v28.i36.5364

Figure 5 Receiver operating characteristic curves of atherogenic index of plasma, waist circumference, body mass index, and A-W-B model to predict metabolic-associated fatty liver disease in different subgroups. A-E: The area under the receiver operating characteristic curve (AUC) of the prediction model combining atherogenic index of plasma, waist circumference (WC), and body mass index (BMI) (A-W-B) model was significantly higher than that of A-W-B in male, female, young, middle-aged and elderly, and nonobese subjects (all $P < 0.01$); F: The AUC of the A-W-B model was only better than atherogenic index of plasma (AIP) in obese subjects ($P = 0.0465$).

The Spearman's correlation analysis showed that AIP, WC, and BMI were all positively associated with SBP, DBP, ALT, AST, FBG, and SUA. Notably, these physical and chemical indicators were also risk factors for MAFLD, and compared with AIP, WC, and BMI, the A-W-B model had a higher correlation with SBP, DBP, ALT, AST, FBG, and SUA, which may indirectly explain the better correlation and predictive ability of the A-W-B model for MAFLD. Furthermore, this study also pointed out that the optimal cutoff values of the A-W-B model to predict MAFLD in males and females were 0.5932 and 0.4105, respectively, which will facilitate early clinical identification of MAFLD in different sex populations. When the A-W-B level of the subject is above the cutoff point, it can be preliminarily identified as MAFLD.

In summary, compared with other studies, this study has the following advantages. First, this study confirmed that AIP was strongly and positively associated with the risk of MAFLD, and it can be a reference predictor for MAFLD and determined the optimal cutoff values of AIP for predicting MAFLD in males and females, providing a new idea for early prevention of MAFLD. Then, we pioneered a novel noninvasive prediction model A-W-B combining AIP, WC, and BMI that can significantly improve the predictive ability for MAFLD and determined its optimal cutoff values of the A-W-B model to predict MAFLD in males and females. Furthermore, we also validated the model with MRI as the diagnostic standard, further affirming its outstanding predictive performance for MAFLD. This study is highly innovative, and this noninvasive prediction model A-W-B is convenient, affordable, and easy to obtain,

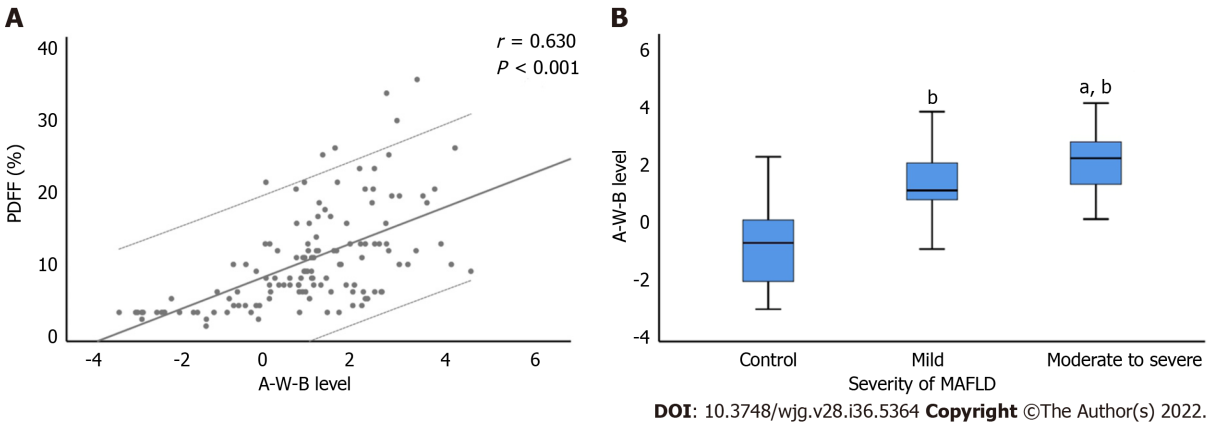

DOI: 10.3748/wjg.v28.i36.5364 **Copyright** ©The Author(s) 2022.

Figure 6 Correlation between A-W-B levels with liver proton density fat fraction and the severity of metabolic-associated fatty liver disease. A: The prediction model combining atherogenic index of plasma, waist circumference, and body mass index (A-W-B) level was strongly and positively associated with liver proton density fat fraction (PDFF) (r = 0.630, P < 0.001); B: Compared with the control group, ^{b}P < 0.001; compared with the mild group, ^{a}P < 0.01. MAFLD: Metabolic-associated fatty liver disease.

which can provide better services for clinical prediction and screening of MAFLD and metabolic-related diseases.

However, there are still some limitations. First, to avoid subject recall bias, this study did not collect confounding factors, such as specific dietary structure and physical activity, and mainly focused on objective laboratory indicators and basic demographic indicators, which may slightly affect the results of multiple logistic regression analysis. Second, the subjects in this study were limited to a single physical examination center, which may cause selection bias. Third, fatty liver in the training set of this study was diagnosed by abdominal ultrasonography, and we did not use ultrasonography to accurately classify the severity of MAFLD. Therefore, the relationship between AIP, A-W-B model, and the severity of fatty liver by ultrasonography was unclear. Notably, we found that the A-W-B levels were positively correlated with MRI-diagnosed MAFLD severity in the validation set. However, due to limited funds, the number of validation sets using MRI as the diagnostic standard was relatively small. Therefore, further multicenter, large-sample prospective cohort studies are needed in the future to verify and explore the predictive value of AIP and A-W-B for MAFLD and differential severity.

CONCLUSION

AIP was strongly and positively associated with MAFLD, and it can be a reference predictor for MAFLD. The novel noninvasive prediction model A-W-B combining AIP, WC, and BMI can significantly improve the predictive ability for MAFLD and provide better services for clinical prediction and screening of MAFLD.

ARTICLE HIGHLIGHTS

Research background

Metabolic-associated fatty liver disease (MAFLD) is the most common chronic liver disease and poses great harm to people's health. Early identification of MAFLD is imminent.

Research motivation

Atherogenic index of plasma (AIP) is a reference predictor of obesity-related diseases, but its predictive value for MAFLD remains unclear. No studies have reported whether its combination with waist circumference (WC) and body mass index (BMI) can improve the predictive performance for MAFLD.

Research objectives

This study had two main objectives: (1) To systematically explore the relationship between AIP and MAFLD and evaluate its predictive value for MAFLD; and (2) To pioneer a novel prediction model combining AIP, WC, and BMI and validate its predictive performance for MAFLD.

Research methods

This cross-sectional study consecutively enrolled 864 participants. Multivariate logistic regression analysis and receiver operating characteristic curve were used to evaluate the relationship between AIP and MAFLD and its predictive power for MAFLD. The novel prediction model A-W-B combining AIP, WC, and BMI to predict MAFLD was established, and internal verification was completed by magnetic resonance imaging diagnosis.

Research results

Subjects with higher AIP exhibited a significantly increased risk of MAFLD, with an odds ratio of 12.420 (6.008-25.675) for AIP after adjusting for various confounding factors. The area under receiver operating characteristic curve of the A-W-B model was 0.833 (0.807-0.858), which was significantly higher than that of AIP, WC, and BMI (all P <0.05). The best cutoff values for the A-W-B model to predict MAFLD in males and females were 0.5932 and 0.4105, respectively. Additionally, in the validation set the area under receiver operating characteristic curve of A-W-B model to predict MAFLD was 0.862 (0.791-0.916). The A-W-B level was strongly and positively associated with the liver proton density fat fraction (r = 0.630, P < 0.001) and significantly increased with the severity of MAFLD (P < 0.05).

Research conclusions

AIP was strongly and positively associated with MAFLD and can be a reference predictor for MAFLD. The novel noninvasive prediction model A-W-B combining AIP, WC, and BMI can significantly improve the predictive ability for MAFLD and provide better services for clinical prediction and screening of MAFLD.

Research perspectives

Studies that may be conducted in the future should further explore the predictive value of AIP and the A-W-B model for different severities of MAFLD and other related metabolic diseases.

ACKNOWLEDGEMENTS

We thank all staff for helping recruit the subjects. We thank English language expert Liang JT for the English language revision.

FOOTNOTES

Author contributions: Duan SJ designed and performed the study, analyzed the data, and drafted the manuscript; Ren ZY, Zheng T, Peng HY, Niu ZH, and Wang RR collected the samples and clinical data of the patients; Xia H, Chen JL, and Zhou YC took part in designing the study and analyzing the data; Yao SK designed the study, supervised the study performance, and revised the manuscript.

Institutional review board statement: This study was approved by the Clinical Research Ethics Committee of China-Japan Friendship Hospital (2018-110-K79-1).

Informed consent statement: All study participants provided informed written consent prior to study enrollment.

Conflict-of-interest statement: All the authors report no relevant conflicts of interest for this article.

Data sharing statement: No additional data are available.

STROBE statement: The authors have read the STROBE Statement checklist of items, and the manuscript was prepared and revised according to the STROBE Statement checklist of items.

Country/Territory of origin: China

ORCID number: Shao-Jie Duan 0000-0002-6022-5039; Zhi-Ying Ren 0000-0001-7834-0556; Tao Zheng 0000-0002-4241-5584; Hong-Ye Peng 0000-0001-7980-683X; Zuo-Hu Niu 0000-0001-5215-8318; Hui Xia 0000-0001-7481-673X; Jia-Liang Chen 0000-0002-3007-0451; Yuan-Chen Zhou 0000-0001-6024-6246; Rong-Rui Wang 0000-0001-5279-5472; Shu-Kun Yao 0000-0002-8512-2589.

S-Editor: Gong ZM
L-Editor: Filipodia
P-Editor: Gong ZM

REFERENCES

1 **Loomba R**, Sanyal AJ. The global NAFLD epidemic. *Nat Rev Gastroenterol Hepatol* 2013; **10**: 686-690 [PMID: 24042449 DOI: 10.1038/nrgastro.2013.171]
2 **Younossi ZM**, Koenig AB, Abdelatif D, Fazel Y, Henry L, Wymer M. Global epidemiology of nonalcoholic fatty liver disease-Meta-analytic assessment of prevalence, incidence, and outcomes. *Hepatology* 2016; **64**: 73-84 [PMID: 26707365 DOI: 10.1002/hep.28431]
3 **Caballero B**. Humans against Obesity: Who Will Win? *Adv Nutr* 2019; **10**: S4-S9 [PMID: 30721956 DOI: 10.1093/advances/nmy055]
4 **Ogden CL**, Fakhouri TH, Carroll MD, Hales CM, Fryar CD, Li X, Freedman DS. Prevalence of Obesity Among Adults, by Household Income and Education - United States, 2011-2014. *MMWR Morb Mortal Wkly Rep* 2017; **66**: 1369-1373 [PMID: 29267260 DOI: 10.15585/mmwr.mm6650a1]
5 **Sarin SK**, Kumar M, Eslam M, George J, Al Mahtab M, Akbar SMF, Jia J, Tian Q, Aggarwal R, Muljono DH, Omata M, Ooka Y, Han KH, Lee HW, Jafri W, Butt AS, Chong CH, Lim SG, Pwu RF, Chen DS. Liver diseases in the Asia-Pacific region: a Lancet Gastroenterology & Hepatology Commission. *Lancet Gastroenterol Hepatol* 2020; **5**: 167-228 [PMID: 31852635 DOI: 10.1016/S2468-1253(19)30342-5]
6 **Dulai PS**, Singh S, Patel J, Soni M, Prokop LJ, Younossi Z, Sebastiani G, Ekstedt M, Hagstrom H, Nasr P, Stal P, Wong VW, Kechagias S, Hultcrantz R, Loomba R. Increased risk of mortality by fibrosis stage in nonalcoholic fatty liver disease: Systematic review and meta-analysis. *Hepatology* 2017; **65**: 1557-1565 [PMID: 28130788 DOI: 10.1002/hep.29085]
7 **Dewidar B**, Kahl S, Pafili K, Roden M. Metabolic liver disease in diabetes - From mechanisms to clinical trials. *Metabolism* 2020; **111S**: 154299 [PMID: 32569680 DOI: 10.1016/j.metabol.2020.154299]
8 **Lee H**, Lee YH, Kim SU, Kim HC. Metabolic Dysfunction-Associated Fatty Liver Disease and Incident Cardiovascular Disease Risk: A Nationwide Cohort Study. *Clin Gastroenterol Hepatol* 2021; **19**: 2138-2147.e10 [PMID: 33348045 DOI: 10.1016/j.cgh.2020.12.022]
9 **Stahl EP**, Dhindsa DS, Lee SK, Sandesara PB, Chalasani NP, Sperling LS. Nonalcoholic Fatty Liver Disease and the Heart: JACC State-of-the-Art Review. *J Am Coll Cardiol* 2019; **73**: 948-963 [PMID: 30819364 DOI: 10.1016/j.jacc.2018.11.050]
10 **Wong MCS**, Huang JLW, George J, Huang J, Leung C, Eslam M, Chan HLY, Ng SC. The changing epidemiology of liver diseases in the Asia-Pacific region. *Nat Rev Gastroenterol Hepatol* 2019; **16**: 57-73 [PMID: 30158570 DOI: 10.1038/s41575-018-0055-0]
11 **Ipsen DH**, Lykkesfeldt J, Tveden-Nyborg P. Molecular mechanisms of hepatic lipid accumulation in non-alcoholic fatty liver disease. *Cell Mol Life Sci* 2018; **75**: 3313-3327 [PMID: 29936596 DOI: 10.1007/s00018-018-2860-6]
12 **Katsiki N**, Mikhailidis DP, Mantzoros CS. Non-alcoholic fatty liver disease and dyslipidemia: An update. *Metabolism* 2016; **65**: 1109-1123 [PMID: 27237577 DOI: 10.1016/j.metabol.2016.05.003]
13 **Eslam M**, Sarin SK, Wong VW, Fan JG, Kawaguchi T, Ahn SH, Zheng MH, Shiha G, Yilmaz Y, Gani R, Alam S, Dan YY, Kao JH, Hamid S, Cua IH, Chan WK, Payawal D, Tan SS, Tanwandee T, Adams LA, Kumar M, Omata M, George J. The Asian Pacific Association for the Study of the Liver clinical practice guidelines for the diagnosis and management of metabolic associated fatty liver disease. *Hepatol Int* 2020; **14**: 889-919 [PMID: 33006093 DOI: 10.1007/s12072-020-10094-2]
14 **Dobiásová M**. Atherogenic index of plasma [log(triglycerides/HDL-cholesterol)]: theoretical and practical implications. *Clin Chem* 2004; **50**: 1113-1115 [PMID: 15229146 DOI: 10.1373/clinchem.2004.033175]
15 **Zhu X**, Yu L, Zhou H, Ma Q, Zhou X, Lei T, Hu J, Xu W, Yi N, Lei S. Atherogenic index of plasma is a novel and better biomarker associated with obesity: a population-based cross-sectional study in China. *Lipids Health Dis* 2018; **17**: 37 [PMID: 29506577 DOI: 10.1186/s12944-018-0686-8]
16 **Shen SW**, Lu Y, Li F, Yang CJ, Feng YB, Li HW, Yao WF, Shen ZH. Atherogenic index of plasma is an effective index for estimating abdominal obesity. *Lipids Health Dis* 2018; **17**: 11 [PMID: 29334966 DOI: 10.1186/s12944-018-0656-1]
17 **Xie F**, Zhou H, Wang Y. Atherogenic index of plasma is a novel and strong predictor associated with fatty liver: a cross-sectional study in the Chinese Han population. *Lipids Health Dis* 2019; **18**: 170 [PMID: 31511022 DOI: 10.1186/s12944-019-1112-6]
18 **Eslam M**, Sanyal AJ, George J; International Consensus Panel. MAFLD: A Consensus-Driven Proposed Nomenclature for Metabolic Associated Fatty Liver Disease. *Gastroenterology* 2020; **158**: 1999-2014.e1 [PMID: 32044314 DOI: 10.1053/j.gastro.2019.11.312]
19 **Shiha G**, Korenjak M, Eskridge W, Casanovas T, Velez-Moller P, Högström S, Richardson B, Munoz C, Sigurðardóttir S, Coulibaly A, Milan M, Bautista F, Leung NWY, Mooney V, Obekpa S, Bech E, Polavarapu N, Hamed AE, Radiani T, Purwanto E, Bright B, Ali M, Dovia CK, McColaugh L, Koulla Y, Dufour JF, Soliman R, Eslam M. Redefining fatty liver disease: an international patient perspective. *Lancet Gastroenterol Hepatol* 2021; **6**: 73-79 [PMID: 33031758 DOI: 10.1016/S2468-1253(20)30294-6]
20 **Eslam M**, Newsome PN, Sarin SK, Anstee QM, Targher G, Romero-Gomez M, Zelber-Sagi S, Wai-Sun Wong V, Dufour JF, Schattenberg JM, Kawaguchi T, Arrese M, Valenti L, Shiha G, Tiribelli C, Yki-Järvinen H, Fan JG, Grønbæk H, Yilmaz Y, Cortez-Pinto H, Oliveira CP, Bedossa P, Adams LA, Zheng MH, Fouad Y, Chan WK, Mendez-Sanchez N, Ahn SH, Castera L, Bugianesi E, Ratziu V, George J. A new definition for metabolic dysfunction-associated fatty liver disease: An international expert consensus statement. *J Hepatol* 2020; **73**: 202-209 [PMID: 32278004 DOI:

10.1016/j.jhep.2020.03.039]
21 **Kromrey ML**, Ittermann T, Berning M, Kolb C, Hoffmann RT, Lerch MM, Völzke H, Kühn JP. Accuracy of ultrasonography in the assessment of liver fat compared with MRI. *Clin Radiol* 2019; **74**: 539-546 [PMID: 30955836 DOI: 10.1016/j.crad.2019.02.014]
22 **Li YW**, Kao TW, Chang PK, Chen WL, Wu LW. Atherogenic index of plasma as predictors for metabolic syndrome, hypertension and diabetes mellitus in Taiwan citizens: a 9-year longitudinal study. *Sci Rep* 2021; **11**: 9900 [PMID: 33972652 DOI: 10.1038/s41598-021-89307-z]
23 **Wang Q**, Zheng D, Liu J, Fang L, Li Q. Atherogenic index of plasma is a novel predictor of non-alcoholic fatty liver disease in obese participants: a cross-sectional study. *Lipids Health Dis* 2018; **17**: 284 [PMID: 30545385 DOI: 10.1186/s12944-018-0932-0]
24 **Dong BY**, Mao YQ, Li ZY, Yu FJ. The value of the atherogenic index of plasma in non-obese people with non-alcoholic fatty liver disease: a secondary analysis based on a cross-sectional study. *Lipids Health Dis* 2020; **19**: 148 [PMID: 32576204 DOI: 10.1186/s12944-020-01319-2]
25 **Kim D**, Chung GE, Kwak MS, Seo HB, Kang JH, Kim W, Kim YJ, Yoon JH, Lee HS, Kim CY. Body Fat Distribution and Risk of Incident and Regressed Nonalcoholic Fatty Liver Disease. *Clin Gastroenterol Hepatol* 2016; **14**: 132-8.e4 [PMID: 26226099 DOI: 10.1016/j.cgh.2015.07.024]
26 **Stefan N**, Schick F, Häring HU. Causes, Characteristics, and Consequences of Metabolically Unhealthy Normal Weight in Humans. *Cell Metab* 2017; **26**: 292-300 [PMID: 28768170 DOI: 10.1016/j.cmet.2017.07.008]
27 **Fracanzani AL**, Petta S, Lombardi R, Pisano G, Russello M, Consonni D, Di Marco V, Cammà C, Mensi L, Dongiovanni P, Valenti L, Craxì A, Fargion S. Liver and Cardiovascular Damage in Patients With Lean Nonalcoholic Fatty Liver Disease, and Association With Visceral Obesity. *Clin Gastroenterol Hepatol* 2017; **15**: 1604-1611.e1 [PMID: 28554682 DOI: 10.1016/j.cgh.2017.04.045]

World Journal of Gastroenterology

Submit a Manuscript: https://www.f6publishing.com

World J Gastroenterol 2022 September 28; 28(36): 5380-5382

DOI: 10.3748/wjg.v28.i36.5380

ISSN 1007-9327 (print) ISSN 2219-2840 (online)

LETTER TO THE EDITOR

Nonalcoholic steatohepatitis and hepatocellular carcinoma: Beyond the boundaries of the liver

Tarana Gupta

Specialty type: Gastroenterology and hepatology

Provenance and peer review: Unsolicited article; Externally peer reviewed.

Peer-review model: Single blind

Peer-review report's scientific quality classification

Grade A (Excellent): 0
Grade B (Very good): 0
Grade C (Good): C, C, C
Grade D (Fair): D
Grade E (Poor): 0

P-Reviewer: Kao JT, Taiwan; Protopapas AA, Greece; Sempokuya T, United States; Tsoulfas G, Greece

Received: May 8, 2022
Peer-review started: May 8, 2022
First decision: June 8, 2022
Revised: June 20, 2022
Accepted: September 12, 2022
Article in press: September 12, 2022
Published online: September 28, 2022

Tarana Gupta, Department of Medicine, Pandit Bhagwat Dayal Sharma Post Graduate Institute of Medical Sciences, Rohtak 124001, Haryana, India

Corresponding author: Tarana Gupta, Doctor, MBBS, MD, DM Hepatology, Professor, Department of Medicine, Pandit Bhagwat Dayal Sharma Post Graduate Institute of Medical Sciences, Medical Mor, Rohtak 124001, Haryana, India. taranagupta@gmail.com

Abstract

The burden of non-alcoholic steatohepatitis (NASH) related hepatocellular carcinoma (HCC) is drawing attention due to the emerging epidemic of obesity and metabolic syndrome and is expected to increase in the near future. Antidiabetic medications, air pollutants, and newer genetic mutations are latest concerns as risk factors for HCC development in patients with NASH. Although molecular signatures are very accurate, they are not cost-effective and cannot be applied in larger population due to logistic issues. We need multicentric longitudinal studies including diverse geographical areas to evaluate the complex interplay of different risk factors and genetics in these patients.

Key Words: Non-alcoholic steatohepatitis; Hepatocellular carcinoma; Cirrhosis; Genetic factors; Lifestyle factors; Surveillance

Core Tip: Nonalcoholic steatohepatitis (NASH) is a metabolic liver disease which also involves multiple organs like the heart, lungs, and kidneys. NASH may arise primarily, followed by involvement of other organs, or it may come late in the course of metabolic syndrome. The multidisciplinary approach is needed towards a patient with diabetes, obesity, and metabolic syndrome to address all issues related to the liver, heart, *etc.* Genetic and molecular signatures have provided a ray of hope for estimating risk in these patients; however, it has many practical issues. The impact of environmental pollutants and toxins as a causative factor in NASH, especially lean patient population, should also be considered. We need population based studies from different geographical areas for estimation of metabolic, environmental, and genetic risk factors.

Citation: Gupta T. Nonalcoholic steatohepatitis and hepatocellular carcinoma: Beyond the boundaries of the liver. *World J Gastroenterol* 2022; 28(36): 5380-5382
URL: https://www.wjgnet.com/1007-9327/full/v28/i36/5380.htm
DOI: https://dx.doi.org/10.3748/wjg.v28.i36.5380

TO THE EDITOR

Chrysavgis *et al*[1] have extensively reviewed the literature on non-alcoholic steatohepatitis (NASH) related hepatocellular carcinoma (HCC) with regard to its risk stratification, screening, and surveillance strategies. Metabolic syndrome is a systemic disease involving the heart, kidneys, lungs, and liver, *etc.* NASH is the liver manifestation of metabolic syndrome. With the emerging epidemic of obesity and metabolic syndrome, NASH is expected to supersede all other etiologies of liver cirrhosis as well as HCC. In various studies as discussed by Chrysavgis *et al*[1], the prevalence of HCC in non-cirrhotic non-alcoholic fatty liver disease (NAFLD) patients ranges from 15%-55%. Factors like age, male sex, concomitant smoking and alcohol intake, obesity, and type 2 diabetes mellitus have been shown to increase the risk of HCC in non-cirrhotic NASH. Recently, use of insulin and sulfonylureas has also been shown to increase the long-term risk of HCC in patients with diabetes. In an Italian study[2], an increased HCC risk with an odds ratio of 3.7 for insulin, 1.3 for sulfonylureas, and 2.1 for repaglinide was found in patients with diabetes. Even the duration of treatment with insulin, though not with other therapies, increased the risk of HCC. The same has also been confirmed in a nationwide nested case-control study[3] in Korea which showed an increased HCC risk with glimepiride instead of other sulfonylureas. And yet we do not have long-term data for GLP-1 agonists and DPP4 inhibitors. Chinese data[4] recently showed an increased association of air pollutants of particulate matter (PM) with an aerodynamic diameter of < 1 (PM_1), < 2.5 ($PM_{2.5}$), and < 10 μm (PM_{10}) with metabolic associated fatty liver disease. The role of intestinal dysbiosis has also been investigated in animal models and found to be associated with an increased risk of NASH and HCC.

In a multicentric trial, Pinyol *et al*[5] collected samples from NASH-HCC and NASH patients, performed expression array and whole exome sequencing, and compared it with HCC from non-NASH etiologies like viral/alcohol. They found *TERT* promoter, *CTNNB1*, *TP53*, and *ACVR2A* most frequently to be present in NASH-HCC patients. The *ACVR2A* (activin type 2 receptor gene) mutation was found in a higher number of patients with NASH-HCC as compared to those with HCC of other etiologies. The molecular signature revealed higher expression of bile acid and fatty acid signaling pathways. The Wnt/TGF-β proliferation subclass was more common in NASH-HCC. The upcoming data suggests that the molecular signature of NASH-HCC is different from that of HCC due to other etiologies. Collectively, the development of NAFLD-HCC results from a complex interplay of multiple factors related to unhealthy life style, environment, and genetics of an individual.

The authors have included abbreviated magnetic resonance imaging (MRI) in their suggested algorithm for HCC surveillance in NAFLD due to a poor window of ultrasound in obese patients. We have concerns regarding this strategy. First, a large number of individuals would need surveillance, so its cost-effectiveness, availability on large scale, and practicality need to be addressed. Second, how frequently MRI would have to be repeated is a practical issue. Third, when during the clinical course of NASH, screening should be performed. Although authors have included HCC risk model as suggested by Ioannou *et al*[6] in their algorithm, we believe that future prospective longitudinal studies are needed to determine the weightage of different risk factors in determining HCC risk in patients with cirrhotic and non-cirrhotic NAFLD, separately. The role of extracellular vesicles (EVs) for molecular characterization of HCC in patients with NASH may further be evaluated for HCC surveillance also. NAFLD is a risk factor not only for HCC but also for colorectal and breast cancers. Instead of screening for each carcinoma separately, we need to have studies on a common platform targeting the molecular signatures in blood for surveillance of different carcinomas in the body which share the pathogenetic mechanisms or pathways. The challenges involved are large population-based studies in different geographical regions, mapping of molecular signatures, and implementation. It has to be cost-effective, easily accessible, and readily available.

In patients with NAFLD, all-cause mortality includes mortality related to issues of the liver, heart, kidneys, lungs, *etc.* It is time to recognise the need for multidisciplinary approach towards a patient with diabetes, obesity, and metabolic syndrome to address all issues related to the liver, heart, kidneys, *etc.* Large prospective, multicentric studies including diverse geographical regions and dietary habits are needed to evaluate for risk stratification in these patients regarding need for HCC surveillance.

FOOTNOTES

Author contributions: Gupta T wrote and critically revised the manuscript.

Conflict-of-interest statement: There are no conflicts of interest to report.

Country/Territory of origin: India

ORCID number: Tarana Gupta 0000-0003-3453-2040.

Corresponding Author's Membership in Professional Societies: American Association for the Study of Liver Diseases, 226223.

S-Editor: Chen YL
L-Editor: Wang TQ
P-Editor: Chen YL

REFERENCES

1 **Chrysavgis L**, Giannakodimos I, Diamantopoulou P, Cholongitas E. Non-alcoholic fatty liver disease and hepatocellular carcinoma: Clinical challenges of an intriguing link. *World J Gastroenterol* 2022; **28**: 310-331 [PMID: 35110952 DOI: 10.3748/wjg.v28.i3.310]

2 **Bosetti C**, Franchi M, Nicotra F, Asciutto R, Merlino L, La Vecchia C, Corrao G. Insulin and other antidiabetic drugs and hepatocellular carcinoma risk: a nested case-control study based on Italian healthcare utilization databases. *Pharmacoepidemiol Drug Saf* 2015; **24**: 771-778 [PMID: 26013675 DOI: 10.1002/pds.3801]

3 **Lee JY**, Jang SY, Nam CM, Kang ES. Incident Hepatocellular Carcinoma Risk in Patients Treated with a Sulfonylurea: A Nationwide, Nested, Case-Control Study. *Sci Rep* 2019; **9**: 8532 [PMID: 31189966 DOI: 10.1038/s41598-019-44447-1]

4 **Guo B**, Guo Y, Nima Q, Feng Y, Wang Z, Lu R, Baimayangji, Ma Y, Zhou J, Xu H, Chen L, Chen G, Li S, Tong H, Ding X, Zhao X; China Multi-Ethnic Cohort (CMEC) collaborative group. Exposure to air pollution is associated with an increased risk of metabolic dysfunction-associated fatty liver disease. *J Hepatol* 2022; **76**: 518-525 [PMID: 34883157 DOI: 10.1016/j.jhep.2021.10.016]

5 **Pinyol R**, Torrecilla S, Wang H, Montironi C, Piqué-Gili M, Torres-Martin M, Wei-Qiang L, Willoughby CE, Ramadori P, Andreu-Oller C, Taik P, Lee YA, Moeini A, Peix J, Faure-Dupuy S, Riedl T, Schuehle S, Oliveira CP, Alves VA, Boffetta P, Lachenmayer A, Roessler S, Minguez B, Schirmacher P, Dufour JF, Thung SN, Reeves HL, Carrilho FJ, Chang C, Uzilov AV, Heikenwalder M, Sanyal A, Friedman SL, Sia D, Llovet JM. Molecular characterisation of hepatocellular carcinoma in patients with non-alcoholic steatohepatitis. *J Hepatol* 2021; **75**: 865-878 [PMID: 33992698 DOI: 10.1016/j.jhep.2021.04.049]

6 **Ioannou GN**, Green P, Kerr KF, Berry K. Models estimating risk of hepatocellular carcinoma in patients with alcohol or NAFLD-related cirrhosis for risk stratification. *J Hepatol* 2019; **71**: 523-533 [PMID: 31145929 DOI: 10.1016/j.jhep.2019.05.008]

Published by **Baishideng Publishing Group Inc**
7041 Koll Center Parkway, Suite 160, Pleasanton, CA 94566, USA
Telephone: +1-925-3991568
E-mail: bpgoffice@wjgnet.com
Help Desk: https://www.f6publishing.com/helpdesk
https://www.wjgnet.com